Stomata operation in halophytes

By

Fatemeh Rasouli

B Sci and MSc in Ag Sci

Shiraz University, Shiraz, Iran

Submitted in fulfilment of the requirements for the degree of

Doctor of Philosophy

University of Tasmania

May 2020

Statements and Declarations

Declarations of Originality

This thesis contains no material which has been accepted for a degree or diploma by the University or any other institution, except by way of background information and duly acknowledged in the thesis, and to the best of my knowledge and belief no material previously published or written by another person except where due acknowledgement is made in the text of the thesis, nor does the thesis contain any material that infringes copyright.

Authority of Access

This thesis is not to be made available for loan or copying for two years following the date this statement was signed. Following that time, the thesis may be made available for loan and limited copying and communication in accordance with the Copyright Act 1968.

Statement Regarding Published Work Contained in Thesis

The publishers of the papers comprising Chapter 2, 4, 5 and 6 hold copyright for that content and access to the material should be sought from the respective publisher and journals. The remaining non published contents of the thesis may be made available for loan and limited copying and communication in accordance with the Copyright Act 1968.

Student Signature

Primary Supervisor Signature

Statement of Co-Authorship

This thesis was completed during the course of my enrolment in a PhD degree in the Tasmanian Institute of Agriculture at the University of Tasmania. This thesis contains no experimental results that have previously presented for any degree at this or other institution.

This thesis contains one literature review chapter, one general discussion chapter and five main research chapters. Results described in the two research chapters (Chapters 3 and 4) have been published in two different journals.

The following people and institutions contributed to the publication of work undertaken as part of this thesis:

Author	Name	Institution
Candidate	Fatemeh Rasouli	Tasmanian Institute of Agriculture University of Tasmania
Author 1	Sergey Shabala	Tasmanian Institute of Agriculture University of Tasmania
Author 2	Heng Zhang	Shanghai Centre for Plant Stress Biology Chinese Academy of Sciences
Author 3	Rainer Hedrich	Institute for Molecular Plant Physiology and Biophysics, University of Wuerzburg
Author 4	Richard Wilson	Central Sciences Laboratory University of Tasmania
Author 5	Leiting Li	Shanghai Centre for Plant Stress Biology Chinese Academy of Sciences
Author 6	Zhong-Hua Chen	School of Science and Health Western Sydney University
Author 7	Ali Kiani-Pouya	Tasmanian Institute of Agriculture University of Tasmania

Author details and their roles:

Paper 1, **Rasouli F.,** Kiani-Pouya A., Zhang H., Shabala S. 2020. Developing and validating protocols for mechanical isolation of guard-cell enriched epidermal peels for omics studies. Functional Plant Biology, accepted. **Located in chapter 3.**

Candidate was the primary author and contributed 80% to the planning, execution and preparation of the work for the paper. Author 1 contributed to the design of the project and wrote the paper. Author 2 critically assessed the data and revised the paper. Author 7 contributed in performing the experiment.

Paper 2, **Rasouli F.,** Kiani-Pouya A., Li L., Zhang H., Chen Z., Hedrich R., Wilson R., Shabala S. 2020. Sugar beet (*Beta vulgaris*) guard cells responses to salinity stress: a proteomic analysis. International Journal of Molecular Sciences 21, 2331. **Located in chapter 4.**

Candidate was the primary author and contributed 80% of the experimental work and wrote the paper. Author 1 contributed to the design of experiments and wrote the paper. Authors 2, 3 and 6 critically assessed the data and revised the paper. Author 4 acquired the proteomics data and critically assessed the data and revised the paper. Author 5 contributed to bioinformatic analysis. Author 6 metabolomics analysis and interpretation of the results. Authors 7 contributed to data collection.

We the undersigned agree with the above stated "proportion of work undertaken" for each of the above published peer-reviewed manuscripts contributing to this thesis:

Signed:

	Fatemeh Rasouli Tasmanian Institute of Agriculture, University of Tasmania	Prof Sergey Shabala Tasmanian Institute of Agriculture, University of Tasmania	Prof Michael Rose Tasmanian Institute of Agriculture, University of Tasmania
Date:	20 May 2020	20 May 2020	20 May 2020

Publications Arising from this Thesis

Rasouli F., Kiani-Pouya A., Zhang H., Shabala S. 2020. Developing and validating protocols for mechanical isolation of guard-cell enriched epidermal peels for omics studies. Functional Plant Biology, 47, 803–814.
https://doi.org/10.1071/FP20085

Rasouli F., Kiani-Pouya A., Li L., Zhang H., Chen Z., Hedrich R., Wilson R., Shabala S. 2020. Sugar beet (*Beta vulgaris*) guard cells responses to salinity stress: a proteomic analysis. International Journal of Molecular Sciences 21, 2331.
https://doi.org/10.3390/ijms21072331

Acknowledgements

It is a pleasure for me to acknowledge individuals who support me to achieve the goal of successful completion of this thesis.

Foremost, I would like to express my sincere gratitude to my main supervisor Professor Sergey Shabala who convincingly and continually conveyed a spirit of excitement and adventure in regard to research. Without his persistence help and guidance, this thesis would not be possible.

I am deeply grateful to my supervisory team member Dr. Richard Wilson who has been journeyed with me as I stepped in a new area of study. I would also like to thank my supervisory team member and laboratory manager, Professor Lana Shabala whose effort for encouraging students scientifically as well as uplifting the spirits of lab members was exemplary.

I am highly indebted to Professor Heng Zhang who hosted and supported me in the Shanghai Centre for Plant Stress Biology (PSC), for learning new techniques. I also owe my immense gratitude to Professor Zhong-Hua Chen in Western Sydney University, and Professor Rainer Hedrich (University of Würzburg) for their help and supports.

I wish to extend my gratitude toward Professor Karen Barry for her time and recurrent assistance and care, and thanks to Professor Calum Wilson, my coordinator in the graduate research office, for his guidance and support.

I also would like to gratefully acknowledge the staff in the University of Tasmania and Tasmanian Institute of Agriculture especially Dr. Adam Smolenski (Molecular Biology Laboratory), Sharee McCammon, Caroline Claye (Field Horticulture Laboratory), Phil Andrews (Horticultural Research Centre), Justin Direen for their scientific and technical supports.

I would like to take this opportunity to thank Ali Kiani-Pouya and his family for their support and care in Australia in absence of my family and thanks to my family who served as an inspiration to peruse this work.

Lastly and most of all, I wish to thank God who is the source of life, wisdom and knowledge.

Table of Contents

List of Figures

List of Supplementary Figures

List of Tables

List of Supplementary Tables

List of Abbreviations

A, CO_2 assimilation rate

AAP, amino acid permease

ABA, abscisic acid

ABC, ATP-binding cassette

ABI, ABA insensitive

ABP, auxin binding protein

ABRE, ABA-responsive element

ANN, annexin

APX, L-ascorbate peroxidase

ASPG, aspartic protease in guard cell

bHLH, basic helix loop helix

BLAST, basic local alignment search tool

bZIP, basic-leucine zipper

CAT, catalase

CDD, conserved domain database

CDK, cyclin-dependent kinase

cDNA, complementary DNA

CDPK, Ca^{2+} dependent protein kinases

C_i, leaf internal CO_2 concentration

COG, clusters of orthologous groups

CPC, caprice

CPK, calcium-dependent protein kinase

DAB, 3,3'-Diaminobenzidine

DDR, DNA damage-responsive protein

DEG, differently expressed gene

DRE, dehydration-responsive element

EBC, epidermal bladder cell

EPF, epidermal patterning factor

ERD, early responsive to dehydration

FACS, fluorescent activated cell sorting

FDR, false discovery rate

FPKM, fragments per kilobase of transcript per million

Fv/Fm, maximal photochemical efficiency of PSII

FW, fresh weight

GC, guard cell

GFP, green fluorescent protein

GHR, guard cell hydrogen peroxide resistance

GMC, guard mother cell

GRP, glycine-rich protein

GO, gene ontology

GORK, gated outward rectifying K^+ channel

g_s, stomatal conductance

HAK, high affinity K^+ transporter

HB, homeobox

HPCA, hydrogen-peroxide-induced Ca^{2+}

HT, high leaf temperature

J, rate of RuBP regeneration via electron transport

JA, jasmonic acid

KEGG, Kyoto Encyclopedia of Genes and Genomes

KT, potassium transporter

LAM, laser assisted microdissection

LEA, late embryogenesis abundant

LFQ, label-free quantification

LTP, lipid transfer protein

MCM, minichromosome maintenance

MMC, meristemoid mother cell

mRNA, messenger RNA

NCED, nine-cis-epoxycarotenoid dioxygenase

NGS, next-generation sequencing

OST, open stomata

PAR, photosynthetic active radiation

PCA, principal component analysis

PHOT, phototropin

PME, pectin methylesterase

POD, peroxidase isoform

PP2C, protein phosphatase 2C

PPase, pyrophosphatase

PR, pathogenesis-related

PYR, pyrabactin resistance

RBOH, respiratory burst oxidases

RCAR, regulatory components of ABA receptors

RIN, RNA integrity number

ROS, reactive oxygen species

RT-PCR, reverse transcription polymerase chain reaction

Rubisco, ribulose-1, 5-bisphosphate carboxylase/oxygenase

SDS-PAGE, SDS-polyacrylamide gel electrophoresis

SKOR, Stelar K^+ outward rectifier

SLAC, S-type anion channel

SnRK2, Sucrose Non-fermenting 1-Related subfamily 2 protein Kinase

SPCH, SPEECHLESS

SOD, super oxide dismutase

SUC, sucrose

T, transpiration rate

TAIR, The Arabidopsis Information Resource

TCA, tricarboxylic acid

TGG, THIOGLUCOSIDE GLUCOHYDROLASE

TRX, thioredoxin H-type

V_{cmax}, the maximum velocity of carboxylation

WUE, water use efficiency

Abstract

The ability of plants to grow under adverse environmental conditions implies optimising the water and gas exchange by controlling operation of stomata, microscopic valves at the leaf surface. Stomata represent approximately 0.5 to 5% of total leaf surface but play a vital role in gas exchange where they are responsible for over 95% of all the water lost by the leaf. Soil salinity is one of the major environmental hurdles and affects stomata operation by imposing osmotic, oxidative and ionic stresses onto stomata operation. This results in reduced growth and yield and associated economic penalties in crop production systems.

While significant advances have been made in our understanding of stomatal function in glycophyte plants, much less is known about stomata operation in halophytes, naturally salt-loving species. Therefore, a comparative analysis of the effects of salinity stress on stomatal operation in both glycophytes and halophytes may be an important step in improving salt stress tolerance in traditional crops.

In light of the above, the major aim of this PhD study was to address the following gaps in our knowledge: (i) investigate stomata patterning and operation in various plant species contrasting in their salinity stress tolerance; (ii) investigate the difference in protein profile of stomata in closely related halophytic (quinoa) and glycophytic (spinach) plant species that might assist plant adaptation and stomata operation under hyperosmotic saline conditions; (iii) to conduct comparative RNA-sequencing analysis of GCs of halophytic quinoa plants under control and saline conditions with the aim of understanding salt-induced transcriptome changes in GC and leaf lamina; and (iv) reveal the molecular identity of proteins and ion transporters that likely are involved in salt stress responses and stomatal movement.

Understanding the adaptive strategies of halophytes to maintain their productivity under saline conditions in comparison to traditional plants is essential for plant breeding programs. Working along these lines, three halophytic species [quinoa (*Chenopodium quinoa* Wild.), sea barley (*Hordeum marinum*), and sea beet (*Beta maritima*)] and their glycophytic relatives [*Chenopodium album*, cultivated barley (*Hordeum vulgare*) and sugar beet (*Beta vulgaris*)] were grown under

control and saline (100, 200, 300, 400 and 500 mM NaCl) conditions. Plant agronomical, ionic, and photosynthetic traits were then determined. Reduction in stomatal conductance decreased in a dose-dependent manner with increasing NaCl concentrations. However, net CO_2 assimilation rates remained constant or displayed higher values at the medium level of salinity in halophytes. Stomatal densities were lower in halophytic species and they increased with increasing salinity levels in the studied species except for *C. album* and quinoa. Stomatal size was reduced with salinity in all studies species. The speed of stomatal response to light and dark was species-specific, with the highest values in the cultivated barley and sea barley and the lowest ones in sugar beet and sea beet. Halophytes exhibited a higher speed of stomatal opening and closure in response to light/dark fluctuations. Fast stomatal responses to internal signals and environmental factors may be essential for synchronization of photosynthetic and stomatal conductance responses, thus optimizing water use efficiency under changing conditions.

To be able to apply transcriptomics and proteomics approaches in stomatal function studies, we then developed and validated protocols for mechanical isolation of GC-enriched epidermal peels for omics studies. Accordingly, we develop and optimised the method for GC isolation from the leaf epidermis of spinach, sugar beet and quinoa under control and salt-stress conditions. The RNA integrity, gene expression and 1D SDS-PAGE tests were performed to validate the suitability of this technique for omics studies. The results confirmed the appropriateness of this method for proteomics analysis as well as the suitability of RNA integrity for gene expression analysis. Transcriptional levels of several GC-specific genes such as *MYB60*, *FAMA*, *ICE1*, *SLAC1* and *PP2CA* were quantified in both leaf and GC samples. A high abundance of transcripts of these genes was observed in GC compared with those in the leaf. Isolated GCs were enriched in GC-specific genes suggesting suitability of this isolation approach for molecular studies.

By successfully validating the aforementioned GC isolation method and in order to better understand the molecular mechanisms underlying stomatal function under saline conditions, we used a proteomics approach to study isolated GCs from the salt-tolerant sugar beet species. Of the 2088 proteins identified in sugar beet

GCs, 82 were differentially regulated by salt treatment. According to bioinformatics analysis (GO enrichment analysis and protein classification), these proteins were involved in lipid metabolism, cell wall modification, ATP biosynthesis, and signalling. Among the significant differentially expressed proteins several proteins classified as "stress proteins" were upregulated, including non-specific lipid transfer proteins, chaperone proteins, heat shock proteins, and inorganic pyrophosphatase 2, responsible for the vacuole membrane for ion transportation. Moreover, several antioxidant enzymes (peroxide, superoxidase dismutase) were highly upregulated. Furthermore, cell wall proteins detected in GCs provided some evidence that GC walls were more flexible in response to salt stress. Proteins such as L-ascorbate oxidase that were constitutively high under both control and high salinity conditions may contribute to the ability of sugar beet GCs to adapt to salinity by mitigating salinity-induced oxidative stress.

We then applied proteomics analyses of GCs in halophyte quinoa under salinity. In total, 2147 proteins were identified, of which 36% were differentially expressed in response to salinity stress in GCs. Up and downregulated proteins included signaling molecules, enzyme modulators, transcription factors and oxidoreductases. Several proteins involved in stress in general and osmotic/salt stresses in particular, were found to be highly abundant in GCs following salinity treatment, including desiccation-responsive protein 29B (50-fold), osmotin-like protein OSML13 (13-fold), PLAT domain-containing protein 3-like (8-fold), and dehydrin ERD14 (8-fold). Ten proteins related to the gene ontology term "response to ABA" were upregulated in quinoa GC such as aspartic protease in guard cell-1, phospholipase D and plastid-lipid-associated protein. In addition, seven proteins in the sucrose-starch pathway were upregulated in the GC in response to salinity stress. Furthermore, the accumulation of two enzymes involved in the amino acid biosynthesis (tryptophan synthase and L-methionine synthase) was observed in the GC under salt stress. Exogenous application of sucrose and amino acids on stomatal conductance showed that tryptophan, L-methionine and sucrose were associated with less stomatal aperture and conductance, which could be advantageous for plants under salt stress.

Given the lack of comparative transcriptomics analysis of GC, we further isolated

GC for RNA-sequencing. We performed comparative transcriptome analysis of halophyte (*Chenopodium quinoa* Wild.) and glycophyte (*Spinacia oleracea*) guard cells in response to salt stress. The RNA-sequencing analysis of mechanically prepared guard cell-enriched epidermal fragments of quinoa and spinach demonstrated that these two plant species had similar responses where in both plants salt-responsive genes were mainly related to biological processes such as protein metabolism, secondary metabolites, signal transduction, and transportation system. On the other hand, genes related to ABA signalling and ABA biosynthesis were strongly induced in quinoa GCs. Furthermore, GCs in quinoa as a halophytic plant showed higher expression levels of amino acids, proline, sugars, sucrose and potassium transporters under saline condition.

This study also shown that one of the main transcriptomic differences between quinoa and spinach was occurred at the cell wall where spinach as a traditional crop plant developed more rigid guard cell wall while quinoa as a halophyte had flexible cell wall upon exposure to salt stress. These differences resulted in higher stomatal movements in response to light and dark in quinoa. Furthermore, genes involving in inhibition of stomata development and differentiation were highly expressed by salt in quinoa but not in spinach. This resulted in lesser stomatal density and index in quinoa leaf while salinity did not alter stomatal formation in the epidermal tissue in spinach. Overall, this comparative transcriptomic analysis revealed that quinoa GCs had better salt-adaptability responses compared to spinach.

Altogether, the results of this project revealed that at the whole plant level, halophytes were superior to glycophytes under saline conditions through higher velocity of carboxylation, higher K^+/Na^+ selectivity and faster stomatal responses to environmental factors. Also, the results of guard cell transcriptomics and proteomics studies demonstrated that many proteins and genes are either expressed constitutively or induced by salt stress which may contribute to the ability of halophytes to adapt to saline conditions.

Chapter 1: Literature Review

1.1 Stomata as mediators of gas exchange between plant and atmosphere

Stomata are tiny pores located on the surface of aerial parts of plants. A stoma is created from two guard cells that control its opening and closure (Franks and Farquhar 2007). Stomatal pores take only a small proportion of total leaf surface (approximately between 0.5 to 5%) but play a vital role in gas exchange, being responsible for over 95% of all water lost by the leaf (Hetherington and Woodward 2003a). Stomatal pores regulate gas exchange between the leaf interior and the external environment and control almost all the water absorbed through these pores through transpiration and thus, adjust stomatal opening and closure in response to environmental factors and internal signals (Roelfsema and Hedrich 2005). This control of gaseous fluxes in and out of the leaf lamina is crucial to control leaf temperature and meet the mesophyll demand for CO_2. Given the importance of stomata and the fact that they are key players of water use in crop plants and thus have a major role in the global water cycle, functions and physical attributes of stomata are very important. These characteristics have the potential to be targeted for manipulation by breeders, with the aim of improving carbon gain and plant productivity of major staple crops.

1.2 Structure and development of stomata

1.2.1 Anatomy and morphology of leaf epidermis

In general, a mature leaf epidermis in plants has three cell types: trichomes (or salt glands/epidermal bladder cells in halophytes), stomatal guard cells and pavement cells. Stomata can develop on both leaf surfaces and be limited to form on one leaf surface only (Serna *et al.* 2002).

With respect to stomatal patterning, their development in the leaf epidermis is species-dependent and in many plant species stomatal density is higher on the abaxial leaf surface (Martin and Glover 2007). Stomatal and pavement cells pattering are also species-dependant and there is difference between monocotyledonous and dicotyledonous plants (McKown and Bergmann 2018; Nunes *et al.* 2019). Stomata and pavement cells are arranged in a regular pattern of alternating cell files in monocotyledonous plants, however stomatal patterning is relatively random in dicotyledonous plants (Bertolino *et al.* 2019). With the

exception of some members of the Selaginellaceae, stomata seldom develop over the major veins of plants (Martin and Glover 2007). This absence of developing stomata over veins may be due to the fact that photosynthetically active mesophyll cells are rarely present in close proximity to vascular bundles (Casson and Gray 2008). This characteristic may also help prevent water loss.

1.2.2 Development and differentiation of stomata

The generation of various cell types is usually linked with asymmetric cell division, which is any cell divisions that produces two daughter cells that can differentiate then to two different cells (Scheres and Benfey 1999). In plants, there are various examples of asymmetric cell divisions, such as division of the zygote cell, male microspore division and asymmetric cell divisions of the cortex (Scheres and Benfey 1999; Lukowitz *et al.* 2004). Stomatal formation is also a result of an asymmetric epidermal cell division. Stomata are formed by two guard cells surrounding a pore through which plants mediate gas exchange with the surrounding atmosphere (Lawson and Vialet-Chabrand 2019). Therefore, stomatal development has a vital role in plant survival and performance under different environmental conditions (Hetherington and Woodward 2003a).

The cellular and molecular bases of stomatal development have been studied in numerous plant species and in this context the model plant Arabidopsis is the best-investigated plant (Scheres and Benfey 1999; Wang *et al.* 2007). As shown in Figure 1.1, the development of stomata in Arabidopsis starts with an asymmetric cell division of meristemoid mother cells (MMCs), which produces two morphologically distinct daughter cells (Serna 2013). As a result of this asymmetric cell division, a small triangular meristemoid cell and a larger neighbouring cell are produced. In Arabidopsis, the meristemoid is able to keep stem cell-like activity and hence could undergo additional rounds of asymmetrical cell division (Fig. 1.1). Each round of an asymmetric cell division results in production of two cells, a smaller meristemoid and a larger neighbour cell (Lau and Bergmann 2012). The meristemoid finally differentiates into a small rounded guard mother cell (GMC) that then divides symmetrically to generate a guard cell pair (Fig. 1.1).

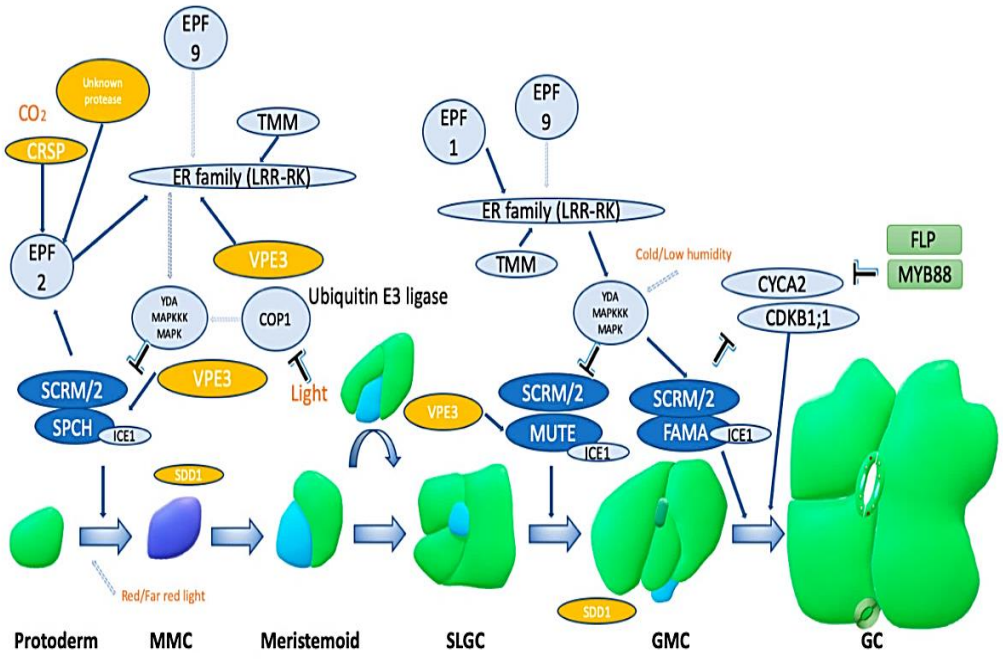

Fig. 1.1 Cell differentiation during development of stomata in Arabidopsis (Fanourakis, *et al*. 2020).

Studies have shown that three basic helix-loop-helix (bHLH) transcription factors including FAMA, MUTE and SPEECHLESS (SPCH) are involved in stomatal development (Ohashi-Ito and Bergmann 2006; MacAlister *et al.* 2007; Pillitteri *et al.* 2007). SPCH which is expressed in MMC and meristemoids, drives the formation of MMC and is also responsible for entry of these cells into an asymmetric division pattern (MacAlister *et al.* 2007). The transcription factor MUTE terminates stem cell characteristic through promoting the differentiation of meristemoid cells into GMCs (Pillitteri *et al.* 2007), while transcription factor FAMA promotes the terminal cell division and differentiation of GMCs into guard cells (Ohashi-Ito and Bergmann 2006). It has been revealed that *MUTE* cannot generate guard cells in the absence of *FAMA* while it can bypass the need for SPCH (MacAlister *et al.* 2007). It is also noteworthy to mention that the activity of these bHLH transcription factors, which act in concert with the bHLH-Leu zipper proteins *SCREAM1* and *SCREAM2*, is regulated by the activity of the mitogen-activated protein kinases in the nucleus, where they finally promote the development of stomata (Wang *et al.* 2007).

1.2.3 Effects of environmental factors on stomatal development

It has long been known that environmental factors such as CO_2 and light affect stomatal density in plants (Woodward 1987; Case *et al.* 1998; Driscoll *et al.* 2006). Increases in CO_2 levels reduces both stomatal density and index in many plant species. Analysis of changes in stomatal density in 100 plant species in response to elevated CO_2 revealed that about 75% of studied plants reduced their stomatal density (Woodward and Kelly 1995). This study also showed that initial stomatal density had a significant role in the subsequent response of the plant to elevated CO_2 level, where plants that initially had higher number of stomata tended to be more responsive to increased CO_2 levels (Woodward and Kelly 1995)

Light intensity may also change the stomatal patterning, with higher light intensity increasing stomatal index (Schoch *et al.* 1980; Thomas *et al.* 2003). For example, it has been shown through shifting between high and low light intensities in cowpea (*Vigna sinensis*) that higher light intensity resulted in higher stomatal density and mature leaves were determinant of stomatal index of leaf (Schoch *et al.* 1980). The light intensity accompanied by the leaf maturity are also determinants of stomatal index in other species.(Thomas *et al.* 2003) showed that exposing developing leaves of tobacco to high-intensity light while shading the mature leaves led to 13% decrease in stomatal index in developing leaves compared with control leaves that only exposed to high-intensity light. In contrary to this result, shading of developing leaves in combination with exposure of the mature leaves to high-intensity light resulted in 24% increase in stomatal index compared with the controls indicating that mature leaves have a primary impact on stomatal index (Thomas *et al.* 2003).

In regards to effects of salinity stress on stomatal development many questions need to be answered in relation to the stomatal development as a component of the salinity tolerance mechanism (Kiani-Pouya *et al.* 2019a). Although salinity stress negatively affects stomatal parameters through toxic levels of Na^+ as well as osmotic stress (Lawson 2009), halophytic plants have been shown to be capable of optimising their stomata performance under saline conditions (Shabala 2013; Hedrich and Shabala 2018). However, the mechanisms behind this have not been well elucidated. In a large-scale study exploring varietal differences in a salinity tolerance of quinoa (*Chenopodium quinoa* Wild.) it has been shown

that stomatal density remained unchanged between salt stress and control conditions while stomatal length was reduced between 3% and 43% amongst accessions (Kiani-Pouya *et al.* 2019a).

1.3 Regulation of stomatal movement

The specific characteristic of stomata is that they are able to rapidly decrease their cell size through efflux of ions from guard cells into their cell wall. Given the fact that mature guard cells do not have plasmodesmata, these volume alterations are accompanied by the reversible fusion of vesicles, where the plasma membrane plays a primary role (Shope *et al.* 2003). Most influx and efflux of solutes necessary for the opening and closing of stomata are facilitated through transporters, ion channels, and pumps that are located in the plasma membrane (Schroeder *et al.* 2001; Roelfsema and Hedrich 2005). As a result, guard cells are able to adjust volume in response to variable environmental conditions as well as plant internal factors, such as hormonal signals (Hetherington and Woodward 2003a; Roelfsema and Hedrich 2005). This characteristic enables guard cells to properly facilitate gas exchange, which in turn prevents excessive water loss.

1.3.1 Stomatal opening

In contrast to stomatal closure, which is stimulated by different factors, stomatal opening is generally provoked by light (Kollist *et al.* 2014). Stomatal opening by light acts through two signalling pathways, where one pathway is particularly sensitive to blue light and the second pathway is stimulated through photosynthetic active radiation (Shimazaki *et al.* 2007), which are discussed in more details in the next sections.

1.3.1.1 Blue light-specific responses in stomata

The specific blue light response of stomata was first reported by (Iino *et al.* 1985). In that study, leaves of *Commelina communis* were kept under high photon flux densities of red light, and then short pulses of blue light were used to trigger stomatal opening (Iino *et al.* 1985).

The light receptor was then identified as phototropins (PHOT), although based on absorption properties, other receptors such as carotenoids, flavins, and pterins also have been suggested as blue-light photoreceptors in plants (Horwitz *et al.* 1997). Phototropins are linked with the plasma membrane and their function to

blue light is activated by protein kinases (Christie 2007) that upon stimulation with blue light become auto-phosphorylated (Inoue *et al.* 2008).

A primary component of the blue-light response in guard cells is H^+ extrusion into the apoplast. While blue light stimulates H^+-ATPases via a signalling pathway, it also inhibits S-type anion channels in guard cells (Marten *et al.* 2007). The loss of protons from the guard cells contributes to hyperpolarization of the plasma membrane, which creates an electrical gradient that provides the driving force for the uptake of positively charged K^+, leading to K^+ uptake into guard cells.

Blue-light-mediated responses of higher plants allow them to efficiently sense light and hence optimize their photosynthesis and growth under different light conditions (Kinoshita *et al.* 2001). Furthermore, blue light is among many environmental stimuli that open stomata (Assmann 1993; Schroeder *et al.* 2001). Several types of blue light receptors are known in plants. In Arabidopsis mutants, four blue light receptors (*cry1*, *cry2*, *phot1* and *phot2*) have been identified (Ahmad and Cashmore 1993; Briggs and Huala 1999; Kagawa *et al.* 2001). The Phot1 protein is a serine/threonine protein kinase (Huala *et al.* 1997) that is considered as a stomatal blue-light receptor (Kinoshita *et al.* 2001). This protein mediates the increase in cytosolic Ca^{2+} in response to blue light (Kinoshita and Shimazaki 1999). Stomatal opening is mediated through accumulation of K^+ in guard cells by a K^+ channel and driven by an inside-negative electrical potential (Schroeder *et al.* 1987). This electrical potential is created by blue light via phosphorylation and activation of the plasma membrane H^+-ATPase (Assmann 1993; Schroeder *et al.* 2001).

1.3.1.2 Photosynthesis and stomatal opening

Although red light triggers opening of stomata, photon flux densities should be high enough to support photosynthesis (Sharkey and Raschke 1981; Roelfsema *et al.* 2006). This fact suggests that a small beam of light directed on the stomata would not be able to trigger stomata opening and only when a larger part of a leaf is illuminated it results in opening of stomata (Mott *et al.* 2008). This finding also suggests that stomata respond to signals they receive from neighbouring mesophyll cells where active photosynthesis processes occur. In this context, it has been shown that in intact leaves, photosynthetic active radiation (PAR) stimulates a

reduction in the CO_2 levels of the substomatal cavity that is sensed by guard cells and leads to stomatal opening (Hanstein *et al.* 2001). This finding suggests that alterations in the CO_2 contents of the substomatal cavity may act as an intermediate signal in the PAR response of guard cells. This result is confirmed by the fact that the activity of plasma membrane anion channels is inhibited by both PAR and CO_2 (Marten *et al.* 2008).

1.3.2 Stomatal closure

Stomatal closure is a rapid response that is controlled through a complex network of signalling pathways, in which the major and the best-known players are phytohormones (Nemhauser *et al.* 2006)). The complexity of the response is primarily dependent on the initial level of stress and it is controlled through positive and negative hormonal regulators. In this context, abscisic acid (ABA) and jasmonic acid (JA) act as positive regulators and increasing their levels results in stomatal closure. Auxin and cytokinins on the other hand act as positive regulators that have a role in stomatal opening (Huang *et al.* 2008).

Stomatal closure needs ion efflux from guard cells that is achieved by the release of osmotically active ions resulting in shrinking of guard cells. Given the fact that transporters and ion channels play central roles in ion efflux, activation and inactivation of these components in the guard cell are the main targets of signalling networks that regulate stomatal closure (Kim *et al.* 2010; Roelfsema *et al.* 2012). In general, darkness, high temperature, high concentration of CO_2 and low humidity are the main environmental parameters promoting the closure of stomata (Assmann 1993).

1.3.2.1 Open stomata 1 plays pivotal role in stomatal closure

Open stomata 1 (OST1) that was first identified in Arabidopsis (Mustilli *et al.* 2002) belongs to the Sucrose Non-fermenting 1-Related protein Kinases (SnRK2) family. Within this group of proteins, OST1 alongside SnRK 2.2 and 2.3 are primary targets of the type 2C protein phosphatases (Fujita *et al.* 2009). OST1 triggers stomatal closure by a direct interaction with anion channels (S-type anion channel SLAC1, as well as the R-type channel ALMT12) (Lee *et al.* 2009b; Imes *et al.* 2013). This is a central molecular switch that triggers stomatal closure in response to stimuli such as water stress, darkness and ABA (Merilo *et al.* 2013). Furthermore, OST1

also phosphorylate plasma membrane respiratory burst oxidases (RBOHs) (Sirichandra *et al.* 2009). RBOHs-triggered reactive oxygen species (ROS) production may then activate Ca^{2+}-permeable channels in guard cells (Murata *et al.* 2001), which consequently leads to an increase in cytosolic Ca^{2+} levels that activates calcium-dependent protein kinases (CPKs) (McAinsh *et al.* 1996). These findings indicate the fundamental effects caused by interaction between OST1 and RBOHs. This interaction could have a primary effect on ROS production by ABA as well as impacts on signals produced by cytosolic Ca^{2+} and the activation of CPKs in guard cells (Song *et al.* 2014).

1.3.2.2 ABA triggers stomatal closure

ABA is a phytohormone that has pivotal roles in plant growth and development as well as plant responses to different unfavourable growth conditions (Wang *et al.* 2011a; Merilo *et al.* 2015). When the plant is exposed to stressful conditions (e.g. salt stress), ABA builds up in the leaves, which triggers a reduction in the stomatal aperture (Merilo *et al.* 2015). This decreasing in stomatal pore width that is a result of reduction of turgor guard cells is beneficial to plant via reduction of the amount of transpirational water loss (Hetherington and Woodward 2003a; Shabala 2013; Hedrich and Shabala 2018).

Upon uptake of ABA via the ABC transporters in guard cells, it is perceived by the ABA receptors ((PYRABACTIN RESISTANCE1 (PYR1)/PYR1-LIKE (PYL)/REGULATORY COMPONENTS OF ABA RECEPTORS (RCAR)) and develops complexes which prevent protein phosphatase 2C (PP2Cs). This complex is the negative regulator of ABA signalling, such as ABA insensitive 1 (ABI1), ABI2, hypersensitive to ABA1 (HAB1) (Park *et al.* 2009). Inactivated PP2Cs triggers phosphorylation of downstream targets and activates SnRK2 (Umezawa *et al.* 2009).

ABA is one of the strongest signals that through activation of S- and R-type ion channels in the plasma membrane trigger stomatal closure (Pei *et al.* 1997; Imes *et al.* 2013). Activation of these ion channels depolarizes the plasma membrane leading to extrusion of anions and K^+ from guard cells. Additionally, ABA also prevents the activity of plasma membrane H^+-ATPases that probably restricts the reopening of stomata (Hayashi *et al.* 2011).

1.3.2.3 The role of cytosolic Ca^{2+} in stomatal closing

The role of Ca^{2+} in stomatal opening was first shown in a study with epidermal peels of *Commelina communis (*De Silva *et al.* 1985*)*. In this experiment it was indicated that, in contrast to K^+ that triggers the opening of stomata, Ca^{2+} stimulated the closure of stomata (De Silva *et al.* 1985). It is now well-known that many stimuli that lead to stomatal aperture employ a signal transduction pathway that is related to alteration of free cytosolic Ca^{2+} concentrations in guard cell (Kollist *et al.* 2019).

High extracellular Ca^{2+} stimulates repetitive rises in the free cytosolic Ca^{2+} level, which in turn activate anion channels, eventually resulting in the closing of stomata (Stange *et al.* 2010; Brandt *et al.* 2015). In this context, other stimuli, such as ABA, also induce repetitive rises of the cytosolic Ca^{2+} contents (Webb *et al.* 1996). For example, external exposure to ABA in *Vicia faba* resulted in transient repetitive increases in the cytosolic free Ca^{2+} levels as well as an increase in inward-directed ion currents (Schroeder and Hagiwara 1990). The results of this study indicated that increase in both cytosolic Ca^{2+} and inward-directed ion currents was terminated by membrane depolarisation, suggesting that ABA-mediated Ca^{2+} transient spikes were generated through passive influx of Ca^{2+} from the extracellular space by Ca^{2+}-permeable channels (Schroeder and Hagiwara 1990). Thus, ABA-activated ion channels allow an increase in free cytosolic Ca^{2+} levels that can regulate cellular responses stimulating stomatal closure.

1.3.2.4 The role of ROS in stomatal closure

While ROS have been known as toxic by-products of aerobic metabolism however, they are now recognized as key players in the complex signalling network of cells (Song *et al.* 2014). As signalling molecules, ROS can regulate different biological processes such as growth, cell cycle, programmed cell death, hormone signalling and particularly biotic and abiotic stresses (Bose *et al.* 2017) . In regards to guard cells, ROS act as signal intermediates in different guard cell signalling pathways that result in stomatal closure (Song *et al.* 2014).

Currently, the important role of H_2O_2 as a key ROS molecule involved in signal transduction of biotic and abiotic clues is widely accepted (Hossain *et al.* 2015). Given that the H_2O_2 signalling kinetics in halophytes is much faster than in traditional plants (Bose *et al.* 2014), it has been concluded that the higher levels of

H_2O_2 upon salinity stress are required to trigger salinity stress signalling and adaptive response in halophytes (Shabala *et al.* 2015). As a small-sized and long-lived ROS, some extracellular H_2O_2 moves from the apoplast into the cytoplasm through aquaporins channels (Rodrigues *et al.* 2017). H_2O_2 then triggers an influx of Ca^{2+} ions into the cell that results in the systemic transmission of signals between cells in waves, facilitating various plant processes, such as stress acclimation or resistance to pathogens (Hossain *et al.* 2015). Specifically for guard cells, it has been reported that H_2O_2 controls the opening and closing of stomata and the mechanism of this process has recently been identified (Wu *et al.* 2020). In the proposed mechanism, hydrogen-peroxide-induced Ca^{2+} 1 (HPCA1), a membrane-spanning enzyme of the leucine-rich repeat receptor kinase protein family, acts as a sensor that detects H_2O_2 at the surface of a cell allowing plant cells to perceive and respond to environmental stress (Wu *et al.* 2020). This study also demonstrated that HPCA1 has two special pairs of cysteine (Cys) amino acid residues in its extracellular domain. The thiol groups of Cys residues are known to be a target for oxidation by H_2O_2 (Paulsen and Carroll 2013). The presence of extracellular H_2O_2 results in the oxidation of extracellular Cys residues of HPCA1, activating the intracellular kinase activity of HPCA1. This triggers activation of Ca^{2+}-channels in guard cells and Ca^{2+} influx that leads to stomatal closure (Wu *et al.* 2020).

Hydrogen peroxide can oxidize cysteine residues and hence directly affect proteins activity. For instance, it has been shown in Arabidopsis that SKOR as a K^+ efflux channel is activated by H_2O_2 (Garcia-Mata and Lamattina 2010). In addition, H_2O_2 restricts K^+ influx channels (Zhang *et al.* 2001) while activating Ca^{2+} influx channels that increases the free Ca^{2+} concentration in the cytosol (Pei *et al.* 2000) thereby activating guard cell anion channels. Thus, ABA and H_2O_2 activation of K^+ and anion efflux from guard cells finally result in stomata closure.

1.3.2.5 Stomatal closure in response to CO_2 and ozone

In addition to the aforementioned roles of OST1 stomatal closure in response to ABA, OST1 is also involved with other signals such as high CO_2 concentrations and a pulse of the air pollutant ozone, which results in stomatal closure (Hu *et al.* 2010; Vahisalu *et al.* 2010; Xue *et al.* 2011).

Increased CO_2 concentration affects plants through stomatal closure. It has been reported that a doubling of atmospheric CO_2 concentration increases stomatal

closure by 20–40% in various plant species (Drake *et al.* 2013). Increased CO_2 concentration enhances K^+ efflux channels as well as S type anion channel activities leading to ion extrusion during stomatal closure (Raschke *et al.* 2003). In association with these results, Cl^- release from guard cells is stimulated by elevated CO_2 concentration (Hanstein *et al.* 2001) and high CO_2 concentration depolarizes guard cells (Roelfsema *et al.* 2002).

A sudden application of ozone triggers a rapid stomatal closure that likely is a result of degradation of ozone into ROS, such as superoxide and hydrogen peroxide within the cell wall (Vahisalu *et al.* 2010). It has been proposed that guard cell hydrogen peroxide resistance 1 (GHR1) protein may play as a receptor of ROS in plasma membrane (Hua *et al.* 2012). In this context, *ghr1* mutants were strongly impaired in stomatal closure in response to different stimuli (Hua *et al.* 2012).

1.4 The metabolism of guard cells

Guard cells need energy source for their movement and during the day, required ATP is provided through photosynthesis of guard cells and mitochondria that maintaining the activity of plasma membrane H^+-ATPases (Cândido-Sobrinho *et al.* 2019). However, contrary to mesophyll cell, guard cell has fewer and smaller chloroplasts which in turns has lower content of chlorophyll and RuBisCO, with less developed thylakoid structures (Willmer and Fricker 1996). With an exception of some plants such as fern (*Polypodium vulgare*), chloroplasts are present in the guard cells in most plant species (Lawson *et al.* 2003). A typical guard cells usually contains 10 to 15 chloroplasts while in the adjacent photosynthetically active mesophyll cells this number is 30 to 70 (Humble and Raschke 1971).

These facts indicating that the CO_2 fixation rate in guard cell is lower than mesophyll cell that results in a limited photosynthetic rate (Gotow *et al.* 1988). This insufficient photosynthesis capacity in guard cell would not be able to sustain its own energetic and metabolic demands (Cândido-Sobrinho *et al.* 2019). Thus, to meet this energetic requirement of guard cells sucrose may be imported from neighbouring mesophyll cells (Fig. 1.2A). This transportation of sucrose to guard cells is facilitated by sucrose transporters or when it is degraded into hexoses it can be transported by hexose transporters (Ritte *et al.* 1999). Furthermore, starch also can be breakdown to sucrose via enzymatic activities within guard cells (Fig. 1.2A).

Sucrose has various roles in guard cells including involvement in stomatal movement (Medeiros *et al.* 2018). Given that sucrose is imported from neighbouring mesophyll cells, it may also operate as a putative signal from mesophyll cells that connects mesophyll photosynthetic process with stomatal opening and closure. As it has shown in Figure 1.2A, sucrose is an energetic source for different processes such as a carbon source for glycolysis, biosynthesis of glutamine and a differential non-cycle mode activity of the tricarboxylic acid cycle (Cândido-Sobrinho *et al.* 2019).

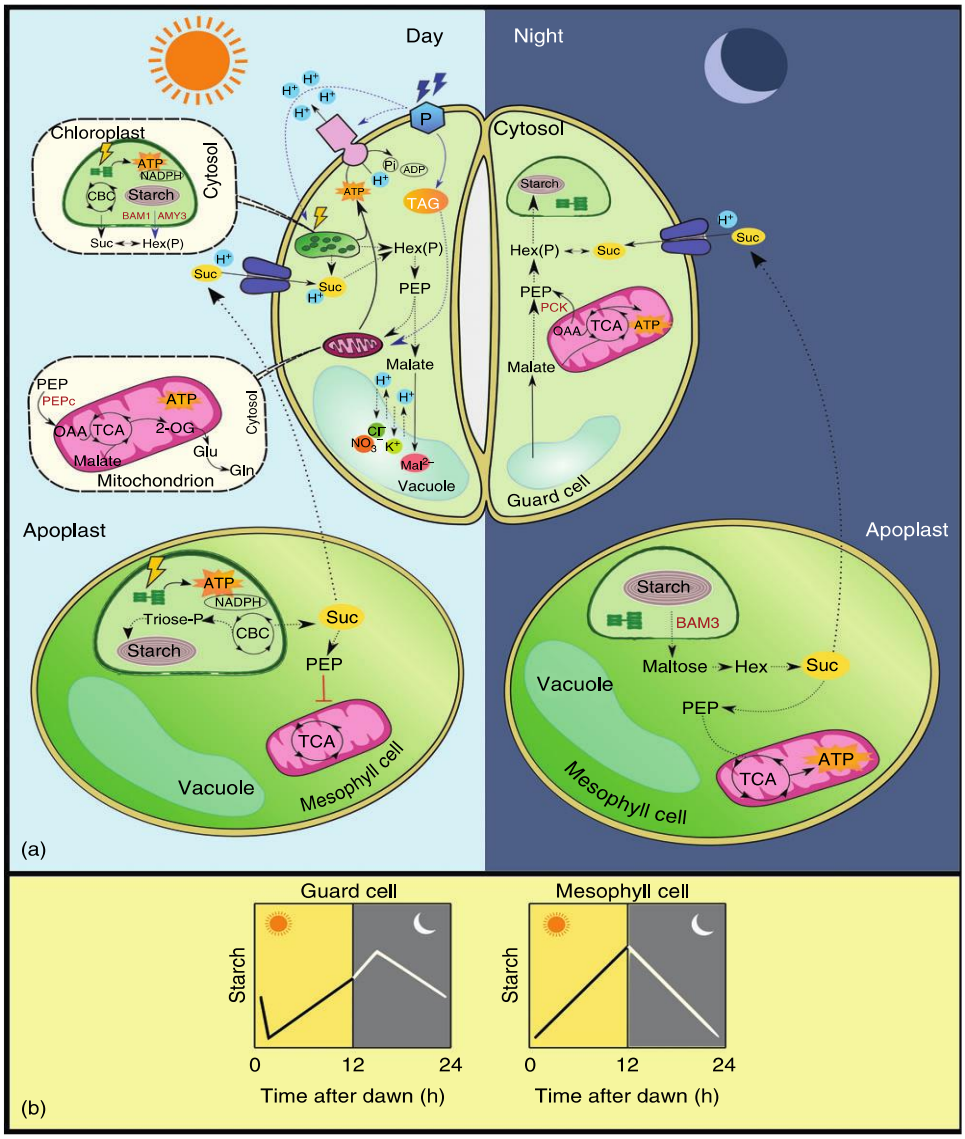

Fig. 1.2 Guard cell metabolism during day and night conditions (A) and diel course of starch synthesis and degradation in both mesophyll and guard cells (B) (Cândido-Sobrinho et al., 2019).

For example, when photosynthetic rate is high it is suggested that the overaccumulation of sucrose in apoplastic space of guard cells induce stomatal closure (Lu *et al.* 1997).

Malate is another important metabolite for guard cell that has important role in guard cell metabolism and stomatal aperture (Dong *et al.* 2018). Malate can be produced within guard cell through breakdown of starch or it can be imported from mesophyll cells. When malate accumulates in the vacuole it plays different roles (Lawson *et al.* 2014). It acts as a counter-ion of K^+ and acts as an activator of vacuolar Cl^- channels and S-type anion channels or as a respiratory substrate in the mitochondria in guard cell (Fig. 1.2A). During the night, malate is either degraded to produce starch (Fig. 1.2A) or released from guard cells through anion channels as mechanism to induce stomatal closure (Medeiros *et al.* 2018). Malate has important roles in guard cell metabolism including CO_2 fixation and starch degradation by induction of blue light sustaining the high rate of malate production (Fig. 1.2A) (Daloso *et al.* 2015; Horrer *et al.* 2016).

While starch metabolism is involved in regulation of stomata opening and closing there are also important differences between guard cells and mesophyll for regulation of starch turnover (Cândido-Sobrinho *et al.* 2019). As an example, while mesophyll cells have a linear pattern of starch synthesis during the day and starch degradation during the night (Dos Anjos *et al.* 2018) guard cells have shown a different circadian rhythm (Antunes *et al.* 2017). In the guard cells the dark-to-light transition stimulate degradation of starch that is mediated by phototropins as photoreceptors of blue-light (Fig. 1.2A) (Horrer *et al.* 2016). Furthermore, starch synthesis in the chloroplasts of guard cells has been proposed to act as a sink for carbon source during stomatal closure (Cândido-Sobrinho *et al.* 2019).

1.5 Extend of salinity stress and its effects on plants

Based on the current estimation the world population will increase in excess of 9.8 billion by 2050 (Liu et al. 2020). While world food production needs to be doubled by this year, several environmental stresses affect crop production (Zorb *et al.* 2019).

In respect to this fact, drought and salt stresses are two major abiotic stressors that reduce crop production globally (Golldack *et al.* 2011). Salinity stress impacts approximately one-fifth of arable land globally (Ruan *et al.* 2010). Thus,

deciphering primary salinity tolerance and adaptation mechanisms is a key step in engineering stress-tolerant plant species (Sanchez *et al.* 2011).

Salt stress can affect plant growth and productivity through three major ways including ion imbalance, hyperosmotic stress and oxidative damage (Flowers and Colmer 2008; Deinlein *et al.* 2014). Plants are able to deal with salt stress through various adaptation strategies such as salt sequestration, synthesis of compatible products, production of antioxidative enzymes and selective ion uptake or exclusion (Shabala 2013; Deinlein *et al.* 2014). Through physiology, genetics and functional genomics investigations some molecular and physiological information of plant tolerance to salt stress have been identified (Luo *et al.* 2018; Wang *et al.* 2018; Zhang *et al.* 2019a; Dugasa *et al.* 2020). These studies have determined some key genes encoding proteins for various physiological characteristics such as osmolyte synthesis, signalling factors, ion channels as well as genes related to stomatal function under saline conditions. This knowledge has provided the primary functions of the genes or proteins in response to salt stress in plants.

1.6 Stomatal performance in halophytes and glycophytes

Given the fact that stomata maintain water balance within the plant which in turn can influence the salt content of the shoot, stomatal function plays a key role in plant adaptation to saline environments. While there is advanced understanding of molecular mechanisms controlling stomatal function in glycophytes, there is scarce information about halophytic plants.

Halophytes have evolved numerous adaptation strategies including morphological, anatomical and physiological characteristics to deal with salt stress and even efficiently benefit from saline conditions (Flowers and Colmer 2008). It is suggested that halophytic plants are capable of better performance in more extreme environments through regulation of stomatal characteristics such as stomata number and degree of aperture (Kiani-Pouya *et al.* 2019a). Decreasing the number of stomata per unit of leaf area is a way to optimize the balance between photosynthesis and leaf water loss by which halophytes are able to decrease their stomatal density under salinity stress (Shabala 2013). This strategy also has been reported for ryegrass (Cen *et al.* 2016) and most tolerant barley varieties (Zhu *et al.* 2015) grown under saline conditions. In a large-scale screening of quinoa

accessions under saline conditions a negative correlation was found between salinity tolerance and stomata length in a salt-tolerant plants (Kiani-Pouya *et al.* 2019a). This study also indicated that salt-tolerant quinoa plants effectively coordinate stomata length and density and hence were able to efficiently regulate stomatal patterning to balance water loss and CO_2 assimilation under saline conditions.

In glycophytic plants, on the other hand, higher osmotic pressure imposed by salt stress results in a reduction in stomatal conductance (g_s) which in turn decrease both photosynthesis and transpiration rates (Chaves *et al.* 2016). However, due to the higher tolerance of halophytes to salinity stress, they show less g_s decline compared with glycophytes when exposed to the same salinity treatments.

1.6.1 The role of Na^+ in stomatal movements in halophytes

There have been some investigations demonstrating how halophytes are able to keep their stomata functional under salinity stress (Flowers et al., 1989; Hedrich and Shabala, 2018). Although this information is limited, two possible stomatal adaptation mechanisms to salt stress have been identified. In the first strategy it is suggested that halophytes are able to substitute Na^+ for K^+ in stomatal movement (Flowers et al., 1989; Robinson et al., 1997). The second adaptation mechanism suggests that halophytes are capable of restricting Na^+ entry into guard cells and thus K^+ ions play a primary role in stomata opening and closure (Robinson et al. 1997). In the latter mechanism, halophytic plants act similar to glycophytic plants and use K^+ as a major cation in stomatal movement.

As an example of the first strategy, the apparent ability of of Na^+ for K^+ substitution for opening and closing of stomata has been suggested by X-Ray microanalysis in *Suaeda maritima* (Flowers *et al.* 1989). This study demonstrated that under saline condition, Na^+ was determined as a primary cation in the guard cells of this plant while when the stomata was closed there was lower concentration of Na^+ in the guard cells (Flowers *et al.* 1989). (Raghavendra *et al.* 1976) also showed that Na^+ could replace K^+ in *Commelina communis* and revealed that it was even more effective than K^+ in stomatal function. It has also been argued that based on the selectivity of plant ion transport systems for K^+ over Na^+, there would be primary restriction on the degree of Na^+ substitution for K^+ in stomatal function (Flowers and Lauchli 1983).

Taking into account the differences between plant species in regard to their membrane permeability for cations such as K^+ and Na^+, it was supposed that in plant species with high permeability to Na^+, there might be a possibility that Na^+ could at least partially replace K^+ in stomatal movement (Robinson *et al.* 1997). Therefore, Na^+ may have an osmotic role in stomatal movement even as it functions in the vacuole (Humble and Hsiao 1970). In agreement with this result, it was shown that stomatal conductance was nearly normal when almost all (95%) of red beet K^+ was substituted by Na^+ (Subbarao *et al.* 2003).

1.6.2 The role of ABA and H_2O_2 in stomatal function in halophytes

Stomatal movement is regulated through several environmental and internal signals. When plants are grown under unfavourable conditions such as salinity stress, ABA and H_2O_2 are among the primary signals; and these are different between glycophytes and halophytes (Assmann 1993; Schroeder *et al.* 2001; Hedrich and Shabala 2018).

Salinity stress increases the ABA concentration that triggers stomatal closure (Pei *et al.* 1997; Park *et al.* 2009). This mechanism is described in detail previously section (1.3.2.2). However it is noteworthy that current knowledge regarding the role of ABA stimulation in stomatal closure has arisen from research using the model plant Arabidopsis, and the question of whether ABA signalling pathways are conserved between halophytic plant species and traditional plants remains to be elucidated (Hedrich and Shabala 2018).

Although all crop plants respond to salt stress through a rapid increase in the xylem sap ABA levels (Albacete *et al.* 2009), it has been shown that in some halophytes the ABA content is not increased under saline conditions (Clipson *et al.* 1988; Hedrich and Shabala 2018). Furthermore, it has also been shown that the ABA concentration of leaves in halophytes even under non-saline conditions is much lower than in traditional plants (Hedrich and Shabala 2018). Results have suggested that the ABA concentration of leaves is increased two to three fold under saline conditions compared to control grown plants, while it remained relatively stable in halophytes (Hedrich and Shabala 2018). These results suggest that the modulation of stomata movement in response to ABA concentration functions over a much higher concentration range in traditional plants than in halophytic plants.

Salt stress also triggers a rapid increase in H_2O_2 content in plant tissues (Niu *et al.* 2018). Under saline conditions, H_2O_2 which is produced in roots can travel to the shoot to adjust stomatal movement in response to altered soil conditions (Shabala *et al.* 2016). Halophytes produce higher levels of ROS under saline conditions compared to glycophytes (Ellouzi *et al.* 2011) suggesting that they are required to generate H_2O_2- based stress signals. As a result of this characteristic, there should be a difference between halophytes and glycophytes for ROS sensitivity of the guard cell channels (Hedrich and Shabala 2018).

1.7 Application of transcriptomics and proteomics technologies in biological science

Omics technologies embrace a comprehensive picture of the biological molecules that form an organism, tissue or cell (Horgan and Kenny 2011). Omics research can be at the level of genetic material and DNA variations (genome), messenger RNA (transcriptome), proteins and peptides (proteome) and products of metabolism (metabolome) in a specific biological sample under defined conditions (Wang *et al.* 2009a; Kumari *et al.* 2015).

The nuclear genome of organisms spans an enormous range, from 0.0023 GB to 148.8 GB (Hidalgo *et al.* 2017). In traditional methods, genes are analysed individually, and gene expression studies are limited to quantitative PCR analyses of a candidate gene. With the exponential development of next-generation sequencing (NGS) technologies in recent years, analysis of entire DNA and full range transcriptome are achievable (Wang *et al.* 2009a);(Urano *et al.* 2010).

Whole transcriptome shotgun sequencing, also called RNA-sequencing typically refers to sequencing all messenger RNA (mRNA) molecules expressed by particular cells or different type of cells of a tissue using high-throughput technologies (Kadakkuzha *et al.* 2016). Since RNA-seq analysis in response to environmental conditions identifies all mRNA transcripts (within detection limits) within the cell, the transcriptome reflects those genes that are expressed under those conditions (Rosenberg and Rosenberg 2012).

RNA-seq is a multiple step experimental procedure by which a complementary DNA (cDNA) is generated from mRNA by reverse transcriptase, cDNAs are fragmented and a library is prepared, followed by sequencing of cDNA using a sequencer (Han *et al.* 2015). To generate an expression profile, sequence

reads are annotated or mapped by aligning all the reads against a reference sequence which determines the correct position of the reads. In the process of alignment, the complete genomes, transcriptomes or *de novo* transcriptome assemblies use as a reference sequence (Li *et al.* 2018a).

RNA-seq is extensively used in biomedical research to provide overall prognosis and determine response to medicine. In plant research, discovery of new genes involved in various biological processes, has become increasingly available and cost-effective through transcriptome sequencing. Hence, this analysis is considered an ideal tool to discover mechanisms that controls biological process in molecular level (Wang *et al.* 2009b; Urano *et al.* 2010; Guo *et al.* 2019).

The proteome is defined as the entire complement of proteins in biological samples such as tissue or specific cell (Manzoni *et al.* 2018). Protein analysis can be categorized into three main groups 1) 'expression' proteomics, 2) structural proteomics and 3) protein-protein interactions. In contrast to the genome, the transcriptome and proteome profiles may be affected by external environmental factors which brings complexity in these studies. In addition, the protein biogenesis adds further levels of complexity compared to gene expression. Alternative splicing may result in multiple isoforms of the same protein from a specific gene and the final functional protein is often modified by the covalent addition of chemical groups known as post-translational modification. (Manzoni *et al.* 2018).

Due to these combined post-transcriptional and post-translational events, mRNA and protein levels often do not correlate well. As proteins are more directly associated with signalling and metabolic processes, it can be more informative to study biological responses at the protein level (Pennington and Dunn 2001). Thus, as an essential and complementary approach in the post-genomic era, proteomics studies has been applied to investigate global protein expression (Ning and Lo 2010; Pang *et al.* 2016).

1.8 Transcriptome analysis of plant response to salt stress

Plant adaptation to abiotic stresses such as salinity could be investigated at different levels of structural and functional organization, including molecular, cellular, biochemical and physiological levels (Sahu and Shaw 2009; Tang *et al.* 2015). Any salt-adaptive response includes dynamic transcriptome changes where the products of which are responsible for enabling plants to achieve cellular and

organismal homeostasis via coordination of different molecular events. Therefore, transcriptomic investigation of response to salinity by RNA-seq technology may identify genes related to this stress (De Vos *et al.* 2019).. Furthermore, with regard to current advancements in the area of NGS, whole-genome sequence data of many halophytic plants is now available (Yang *et al.* 2013; Khan *et al.* 2015; Jarvis *et al.* 2017; Zou *et al.* 2017) providing the possibility of identification of salt-responsive genes in halophytes and to conduct more detailed studies of the molecular mechanisms underlying salinity tolerance.

Whole-transcriptome sequencing under saline conditions provides a global view of salt-responsive genes in different plants and how interacting gene networks might confer salinity stress (Wang et al., 2009; Urano et al., 2010).

As an example of RNA-seq applied at a single-cell level, (Oh *et al.* 2015) conducted a transcriptome analysis of epidermal bladder cells (EBCs) isolated from intact plants of halophytic species *Mesembryanthemum crystallinum*, to investigate cell type-specific responses of these cells to salinity stress. The results indicated 7% of transcript-contigs differently expressed between salt-treated and control plants. This investigation also identified significant changes in biological process such as ion transport, metabolism related to energy generation and osmolyte accumulation, and stress signalling in response to salinity stress (Oh *et al.* 2015). This study exemplifies the potential for transcriptomics in specific cell-type subpopulations to understand salt-adaptive mechanisms in plants.

1.9 Proteome analysis of plant response to salt stress

Proteomic approaches have also been extensively applied to better understand the association between metabolic pathways in plants (Barkla *et al.* 2012; Kumari *et al.* 2015). With the ability to compare protein expression levels under e.g. saline and control conditions, proteomics investigation determine information on differential pathways regulation revealing primary players in salinity tolerance that can be then targeted in breeding program to enhance crop performance under saline conditions. Additionally, proteomics can help to elucidate the role of post-translational regulations in complex biological processes, such as the response to salinity stress in plants (Salekdeh *et al.* 2002). Unlike transcript-based analysis, MS-based proteomic studies, can identify specific protein isoforms (or proteoforms), that might play key roles, such as bioactive polypeptides with cryptic

activity that is unlocked after proteolytic processing. Such analysis can provide supplementary understanding to transcriptional studies and thus allow additional insights about environmental stress response pathways in plant species.

Recent studies of salt-responsive proteins in plants have provided more information for understanding the complex mechanisms of salt adaptation strategies (Zhu *et al.* 2012; Kumari *et al.* 2015). Those proteins that were identified proteins had roles in different plant physiological functions including ion homeostasis, osmotic adjustment, signal transduction, photosynthesis, ROS scavenging system and membrane transporter (Zhu *et al.* 2012; Kumari *et al.* 2015). Also, proteomics has been extensively used in many halophytic plants such as *Salicornia europaea* (Fan *et al.* 2011), *Suaeda aegyptiaca* (Askari *et al.* 2006), *Thellungiella halophila* (Wang *et al.* 2013). These studies have identified various salt-responsive proteins that contributed to salinity stress through different biochemical and physiological functions.

1.10 Application of omics technology in single-cell-type studies

Single-cell-type samples defined as population of the identical cells developing from common origin and functioning the same physiological role (Trapnell 2015). Single cell-type analysis has been highly focused by investigators in the field of medical (Navin and Hicks 2011), animal and plant science (Geng *et al.* 2017; Geilfus *et al.* 2018b) in recent years. In humans, understanding of many biological process such as developmental processes, aging and evaluation of diseases specially cancer have been improved by analysis of specific populations of single cell-types (reviewed by (Lafzi *et al.* 2018). Similarly, plants are made up of many types of highly specialised cells and tissues that differ physiologically and biochemically. With the exception of spores and pollen grains which are free moving single-cells, other types of specific cells such as root hair, trichome, epidermal bladder cells (EBCs) and guard cells are less readily available (Dai and Chen 2012). Thus, obtaining sufficient quantities of high-quality cells for many types of downstream analysis is challenging. To date, omics analyses of different identical cell population such as pollen (Honys and Twell 2003), EBC (Barkla and Vera-Estrella 2015), root hair (Li and Lan 2015) and stomata (Misra *et al.* 2014; Misra *et al.* 2015; Geilfus *et al.* 2018b; Misra *et al.* 2018) have been reported. For example, a transcriptome analysis of pollen in Arabidopsis detected 992 mRNAs,

approximately 40% of which were pollen-specific (Honys and Twell 2003). As an additional example, RNA-seq analysis of Arabidopsis root hair by (Li and Lan 2015)revealed differences in the most abundant genes between root hair and non-root hair tissues. In addition, 5409 genes were differently expressed between non-root hair and root hair cell populations and 61 genes were exclusively detected in root hair tissue (Li and Lan 2015). Single cells also have been the aim of metabolomics studies. In a metabolomics investigation (Misra *et al.* 2015) compared the responses of canola guard cell and mesophyll cell to increased CO_2. In this study, 268 metabolites were quantified that were expressed in guard and mesophyll cells.

Trichomes, the specialized epidermal cell that are responsible for defence against environmental stresses, are also an ideal model for single cell studies (Van Cutsem *et al.* 2011; Oh *et al.* 2015). Analysis of isolated trichome cells from *Nicotiana tabacum* identified 680 unique (trichome-specific) proteins (Van Cutsem *et al.* 2011). This study detected numerous enzymes that were associated with acyl sugar production and generation of terpenoid precursors in trichome cells. Identification oftrichome-specific stress-related proteins also supports the importance of trichome in plant defence (Van Cutsem *et al.* 2011). As another example, a proteomic study on EBC of the halophytic plant, *Mesembryanthemum crystallinum*, grown under saline condition indicated a significant change in protein profile compared to non-saline conditions (Barkla *et al.* 2012). The results of this study revealed a diverse biological function and cellular locations of identified proteins. This study also showed a high representation of proteins involved in ion and water homeostasis, carbohydrate metabolism, and photosynthesis (Barkla *et al.* 2012). Therefore proteomics has the potential to better understand the roles of single cells such as EBCs tand help elucidate proteins and pathways/networks involved in salinity tolerance and conseqently enhance salinity tolerance in plants.

1.10.1 Single cell isolation

Physiological, biochemical and molecular analyses of single cell types and single cells, have been applied initially in medical research, then extensively used in mammalian studies (Wilson and Nairn 2018b; Liu *et al.* 2019a) and then subsequently in plant science (Nelson *et al.* 2006; Galbraith 2012; Yuan *et al.* 2018; Kortz *et al.* 2019).

Several techniques have been utilised for single cell studies. One of these approaches which has been applied in medical and plant sciences for downstream analysis is fluorescent activated cell sorting (FACS). In this method, specific cell types are tagged with a reporter such as green fluorescent protein (GFP) and then the marked cells are separately collected. However, this method has not been sufficiently developed to be extensively used in plant research (Gautam and Sarkar 2015).

Another approach which has widely been used in gene expression profiling and RNA-sequencing studies on single cell type is laser assisted microdissection (LAM). In this technique, target cells are selected under an inverse microscope and then excised using a pulsed infrared laser (Gautam and Sarkar 2015). This microscope-based method can select cells of interest from a mixture of cell populations on a computer screen. The laser-capture approach has been developed in 1996 (Emmert-Buck *et al.* 1996) and has been a potent tool for diagnostic and pathological studies in medical science (Hirose *et al.* 2001). This method also has been used to explore cell or tissue specific transcriptomes in different plants (Brooks *et al.* 2009). This approach is still under development and there is no general protocol that suits all cell types and plant species (Gautam and Sarkar 2015). Moreover, this technique is more appropriate for RNA analyses, although obtaining sufficient amounts of high-quality RNA remains a challenge. Nevertheless, low amounts of extracted RNA using LAM can be amplified by a few rounds of cDNA amplification to get sufficient yields for analysis (Nelson *et al.* 2006). One of the disadvantages of this method is that there is no possibility for amplification of proteins and metabolites extracted by this method and thus would have limitation to be applied in these areas. It is noteworthy to mention that the current techniques used for detecting and quantifying of proteins remain insensitive to the low amounts of extracted protein from single-cell type samples (Wilson and Nairn 2018b).

Guard cells on leaf epidermis do not have plasmodesmata to connect to adjacent cells (Willmer and Sexton 1979), therefore they are attractive biological units for single cell or single cell-type investigations (Gardner *et al.* 2009). Successful omics experiments on guard cell samples requires isolation of a

sufficient number of guard cell (millions) with high purity and good RNA quality and integrity.

Isolating guard cell protoplasts in plants dates back more than four decades, when Zeiger and Hepler (1976) developed a protocol for protoplast isolation from onion and tobacco leaves. Guard cell protoplasts have been used both for proteomics (Zhao *et al.* 2008a) and microarray experiments (Pandey *et al.* 2010; Wang *et al.* 2011a).

Production of guard cell protoplasts is a multi-step process that requires prolonged enzymatic digestion for dissolving cell walls that might impose chemical and osmotic stresses to guard cells and hence changes in gene expression (Bates *et al.* 2012). Comparison of guard cell protoplasts with those obtained using dissection by microarray revealed that genes related to different kind of stresses were highly upregulated in protoplast samples compared with non-enzymatic method of isolation (Bates *et al.* 2012). Reduced digestion time, for example using cellulysin by cellulose "Onozuka" RS (Yao *et al.* 2018b) has been used to enhance the efficiency and viability of the guard cells obtained using the protoplast method. In addition, cell wall digestion in the presence of transcription inhibitors can also avoid expressions of stress-related genes (Obulareddy *et al.* 2013).. Despite these improvements, using protoplasts for downstream experiments still remains questionable because the enzymatic solutions used are derived from fungal cell-wall preparations and may cause contamination of guard cell samples with fungal elicitors (Fujikawa *et al.* 2012; Bauer *et al.* 2013).

Another technique that is infrequently used for isolation of guard cells is manual dissection from lyophilized leaf strips. In one microarray study (Bates *et al.* 2012) isolation of RNA from guard cells using this procedure, however, resulted in low RNA yield. Moreover, this method is not usable for other omics studies such as proteomics.

Reproducible results require some precautions. The time differences between harvesting epidermis and fixation should be minimum in order to maintain the biomolecule integrity, which is critical in achieving good results in downstream experiments such as proteomics and RNA-sequencing. Preparing epidermal peels or guard cell-enriched epidermal peel using a high-power blender (Jalakas *et al.* 2017b) could be a good option. Although guard cell enriched epidermis peels using

blender was proposed by (Raschke and Hedrich 1989) however, they used this method to prepare protoplast for electrophysiological analysis on guard cells.

1.10.2 Guard cell proteomics

To date, omics approaches have not been extensively applied to guard cell analysis. As shown in Table 1.1, relatively few investigations have applied proteomics approach to study the guard cell protein profile. Guard cell proteomics experiments began at the Pennsylvania State University by Assmann's laboratory. They isolated protoplast from epidermis through incubation of epidermal strips in cell-wall digestive enzymes and used proteomics methods including broad pH range and narrow pH range, two-dimensional gels as well as 2D LC-MALDI MudPIT method (Zhao *et al.* 2008a). In their analysis, using these three combined methods, they identified 1712 unique proteins in the guard cell of Arabidopsis. In their analysis, THIOGLUCOSIDE GLUCOHYDROLASE 1 (TGG1) was found as the most abundant protein in the guard cell. This protein, which is related to defence against pathogens was further analysed using genetic approaches which showed that this protein is required for responses of guard cells to ABA (Zhao *et al.* 2008a).

In another proteomics analysis of guard cells and mesophyll in *Brassica napus*, (Zhu *et al.* 2009) identified 1458 proteins where 74 proteins preferentially were found in the guard cells and these proteins were related to cell structure, signalling energy, transport, transcription (Zhu *et al.* 2009). This research showed that in contrast to guard cell, proteins involved in defence /disease/ stress, starch synthesis and photosynthesis were enriched in mesophyll cells.

A small number of proteomics studies have explored the responses of guard cell to various environmental cues such as CO_2, light and ABA (Zhao *et al.* 2010; Geng *et al.* 2017; Geilfus *et al.* 2018b). Various proteins, pathways and processes have been shown to be regulated in response to various signals. For instance, by proteomic and metabolomic analysis of guard cells a total of 1397 proteins and 411 metabolites were identified in *Brassica napus* in response to low CO_2 (Geng *et al.* 2017). Over-expressed proteins and metabolites were mainly involved in redox regulation, starch and sucrose metabolism, and fatty acid metabolism. In response to morning light (1h after dawn), (Geilfus *et al.* 2018b) found 84 upregulated proteins out of totally 994 identified proteins which were mainly enriched in glycolysis, oxidative phosphorylation and cation transport processes. In contrast, a

few proteins changed quantitatively in guard cell when exposed to ABA (Zhao *et al.* 2010). In another study and with the aim to get insights into the redox-regulation process in guard cells, labelling-based proteomics identified both redox-active molecules (thioredoxin) and thioredoxin target proteins (Zhang *et al.* 2016b).

1.10.3 Guard cell transcriptome

Although stomata are the main gaseous gates in plants, few transcriptome studies have been conducted on guard cells (Table 1.1). Microarray analyses of Arabidopsis identified 1309 and 1479 transcripts in guard cells and mesophyll, respectively (Leonhardt *et al.* 2004b). The functional classification of the transcripts showed that the majority of genes were involved in metabolic pathways in both guard cells and leaf mesophyll. However, 64 genes were preferentially expressed in guard cells in response to ABA (Leonhardt *et al.* 2004b).

A transcriptome study on leaf and guard cell of Arabidopsis (Wang *et al.* 2011b) revealed that ABREs and LTREs (as important promoter motifs which regulate the genes in response to ABA) were overexpressed in both leaf and guard cells. The result of this study showed that promotors in the guard cell were enriched in DRE/CRT and MYB elements (Wang *et al.* 2011b). This result indicates that specific transcription factor(s) may be differently utilized in leaves compared with guard cells. In this study, differentially expressed genes in both guard cell and leaf were enriched in GO terms such as response to abiotic stimulus and response to endogenous stimulus. But transcription factor activity was apparently enriched only in the guard cells. In contrast functional categories such as nucleobase metabolism and protein metabolism were overrepresented in leaf relative to guard cells.

There are also some evidence showing the interaction between heterotrimeric G-protein signalling and ABA signalling in response to stress. (Wang *et al.* 2011b) found that more G-protein genes are regulated in the leaf in response to ABA compare to that in the guard cell.

It is believed that sugars derived from photosynthesis have a role in regulation of stomata opening. Early studies showed that the accumulation of chloroplasts in guard cells was less than mesophyll cells and that guard cells rely more on imported CO_2 than photosynthesis to generate energy (Lu *et al.* 1997). In this context, (Bates *et al.* 2012) have provided trascriptome evidence to support this hypothesis. Their transcriptomics analysis revealed that the metabolism of sugar in

guard cells is different from that in mesophyll cells. Isolated guard cells from the sucrose treated Arabidopsis plants showed that 440 genes were differentially expressed in guard cell in response to sucrose (Bates *et al.* 2012). Sugars are synthesized in mesophyll cells through photosynthesis and are exported to apoplast and then phloem. Guard cells with low potentiall for carbon reduction, takes up sugars from the apoplast. Sugars can be stored as s starch or metabolized to generate energy in guard cells (Bates *et al.* 2012).

Guard cell responses to low levels of humidity have also been investigated by microarray analysis. (Bauer *et al.* 2013) identfied 1671 genes whose expression in guard cells were at least two times higher than in leaf. Moreover, this research determined 588 genes that were differentially regulated in response to low relative humidity, 20% of which were among guard cell enriched genes (Bauer *et al.* 2013). In response to drought hormone ABA, 470 genes were downregulated and 1080 were upregulated. Among these, ERD*14*, LEA; the dehydrins *ERD10*, *HVA22*, *RAB18*, *PP2CA*, *HAI1* and *HAI2* were significantly overrepresented. The authors also found that guard cells were able to synthesize ABA autonomously. This pathway, which tends to be upregulated when plants are exposed to ABA is essential and sufficient for stomata to close when plants are subsequently exposed to dry air.

In addition to these microarray experiments, RNA sequencing has also been used for transcriptome analysis of guard cells (Obulareddy *et al.* 2013; Adrian *et al.* 2015a; Yoo *et al.* 2016). (Obulareddy *et al.* 2013) modified the protoplast guard cell preparation method in order to reduce preparation time and limit RNA degradation. Consequently, these Improved isolation methods and new transcriptomics methods led to detection of 18,994 gene transcripts, 8,047 of which had not been previously reported in Arabidopsis.

Table 1.1 Omics studies on the guard cells of plants carried out using diffrent isolation methods.

Analysis	Species	Guard cell isolation approach	Treatment	Ref.
Proteomics	Arabidopsis	Protoplasts	None	(Zhao *et al.* 2008a)
Proteomics	*Brassica napus*	Protoplasts	None	(Zhu *et al.* 2009)
Proteomics	Arabidopsis	Protoplasts	ABA	(Zhao *et al.* 2010)
Proteomics	Arabidopsis	Protoplasts	-	(Zhang *et al.* 2016b)
Proteomics and Metabolomics	*Brassica napus*	Protoplasts	Reduced CO_2	(Geng *et al.* 2017)
Proteomics	Arabidopsis	Guard-cell-enriched epidermal fragment	Light	(Geilfus *et al.* 2018b)
Microarray	Arabidopsis	Protoplasts	ABA	(Leonhardt *et al.* 2004b)
Microarray	Arabidopsis		ABA	(Pandey *et al.* 2010)
Microarray	Arabidopsis		ABA	(Wang *et al.* 2011a)
Microarray	Arabidopsis	Manually dissected guard cells from lyophilized leaves	Sucrose	(Bates *et al.* 2012)
Microarray	Arabidopsis	Guard-cell-enriched epidermal fragment	Reduced humidity	(Bauer *et al.* 2013)
Re-analysed RNA-seq	*Brassica napus*	Protoplasts	ABA	(Yoo *et al.* 2016)
RNA-seq	Arabidopsis	Fluorescence-activated cell sorting (FACS)	Developmental stage	(Adrian *et al.* 2015a)
Metabolomics	*Brassica napus*	Protoplasts	Increased CO_2	(Misra *et al.* 2014)
Metabolomics	Arabidopsis	Epidermis	-	(Zhang *et al.* 2014)
Metabolomics	Arabidopsis	Protoplasts	-	(Jin *et al.* 2013)

1.11 Research aims

The ability of plants to grow under unfavourable conditions such as increased salinity depends on their ability to cope with a variety of resulting stresses that include osmotic, oxidative and ionic stresses. As mediators of gas exchange between plants and the atmosphere, stomata have important roles in plant performance under saline conditions. Hence, understanding stomata function under these conditions may help improve salinity tolerance in crop plants.

Although there have been significant advances in our understanding of stomatal function, particularly in glycophyte plants (Casson and Hetherington 2010), much less is known about stomatal function under saline conditions and specifically in halophytes (Hedrich and Shabala 2018). Therefore, a comparative analysis of effects of environmental stimuli (salt stress in particular) on stomatal operation in glycophytes and halophytes may be an important step in improving abiotic stress tolerance in traditional crops.

Secondly, given the importance of the guard cells system as a model system in plant cell biology and significance of guard cell functions to terrestrial vegetation and scarcity of investigation on GC and to fill some of above discussed gaps in our current information, this study aimed to:

- Investigate stomata patterning and operation in various plant species contrasting in their salinity stress tolerance.
- Investigate the difference in protein profile of stomata in related halophytic (quinoa) and glycophytic (spinach) plant species that might assist plant adaptation and stomata operation under hyperosmotic saline conditions.
- Conduct comparative RNA-sequencing analysis of guard cells of halophytic quinoa plants under control and saline conditions. By doing this we focused on understanding salt-induced transcriptome changes in GC and leaf lamina, as well as looking for proteins and ion transporters that likely are involved in salt stress responses and stomatal movement.

1.12 References

Adrian, J, Chang, J, Ballenger, CE, Bargmann, BO, Alassimone, J, Davies, KA, Lau, OS, Matos, JL, Hachez, C, Lanctot, A, Vaten, A, Birnbaum, KD, Bergmann, DC (2015) Transcriptome dynamics of the stomatal lineage: birth, amplification, and termination of a self-renewing population. *Developmental Cell* **33**, 107-18.

Ahmad, M, Cashmore, AR (1993) HY4 gene of *Arabidopsis thaliana* encodes a protein with characteristics of a blue-light photoreceptor. *Nature* **366**, 162-6.

Albacete, A, Martinez-Andujar, C, Ghanem, ME, Acosta, M, Sanchez-Bravo, J, Asins, MJ, Cuartero, J, Lutts, S, Dodd, IC, Perez-Alfocea, F (2009) Rootstock-mediated changes in xylem ionic and hormonal status are correlated with delayed leaf senescence, and increased leaf area and crop productivity in salinized tomato. *Plant, Cell and Environment* **32**, 928-38.

Antunes, WC, Daloso, DD, Pinheiro, DP, Williams, TCR, Loureiro, ME (2017) Guard cell-specific down-regulation of the sucrose transporter SUTI leads to improved water use efficiency and reveals the interplay between carbohydrate metabolism and K^+ accumulation in the regulation of stomatal opening. *Environmental and Experimental Botany* **135**, 73-85.

Askari, H, Edqvist, J, Hajheidari, M, Kafi, M, Salekdeh, GH (2006) Effects of salinity levels on proteome of *Suaeda aegyptiaca* leaves. *Proteomics* **6**, 2542-2554.

Assmann, SM (1993) Signal-transduction in guard-cells. *Annual Review of Cell Biology* **9**, 345-375.

Bai, JH, Qin, Y, Liu, JH, Wang, YQ, Sa, RL, Zhang, N, Jia, RZ (2017) Proteomic response of oat leaves to long-term salinity stress. *Environmental Science and Pollution Research* **24**, 3387-3399.

Barkla, BJ, Vera-Estrella, R (2015) Single cell-type comparative metabolomics of epidermal bladder cells from the halophyte *Mesembryanthemum crystallinum*. *Frontiers in Plant Science* **6**, 435.

Barkla, BJ, Vera-Estrella, R, Pantoja, O (2012) Protein profiling of epidermal bladder cells from the halophyte *Mesembryanthemum crystallinum*. *Proteomics* **12**, 2862-5.

Bates, GW, Rosenthal, DM, Sun, J, Chattopadhyay, M, Peffer, E, Yang, J, Ort, DR, Jones, AM (2012) A comparative study of the *Arabidopsis thaliana* guard-cell transcriptome and its modulation by sucrose. *PLoS One* **7**, e49641.

Bauer, H, Ache, P, Lautner, S, Fromm, J, Hartung, W, Al-Rasheid, KAS, Sonnewald, S, Sonnewald, U, Kneitz, S, Lachmann, N, Mendel, RR, Bittner, F, Hetherington, AM, Hedrich, R (2013) The stomatal response to reduced relative humidity requires guard cell-autonomous ABA synthesis. *Current Biology* **23**, 53-57.

Bertolino, LT, Caine, RS, Gray, JE (2019) Impact of stomatal density and morphology on water-use efficiency in a changing world. *Frontiers in Plant Science* **10**, 225.

Bose, J, Munns, R, Shabala, S, Gilliham, M, Pogson, B, Tyerman, SD (2017) Chloroplast function and ion regulation in plants growing on saline soils: lessons from halophytes. *Journal of Experimental Botany* **68**, 3129-3143.

Bose, J, Rodrigo-Moreno, A, Shabala, S (2014) ROS homeostasis in halophytes in the context of salinity stress tolerance. *Journal of Experimental Botany* **65**, 1241-57.

Brandt, B, Munemasa, S, Wang, C, Nguyen, D, Yong, TM, Yang, PG, Poretsky, E, Belknap, TF, Waadt, R, Aleman, F, Schroeder, JI (2015) Calcium specificity signaling mechanisms in abscisic acid signal transduction in Arabidopsis guard cells. *eLife* **4**, e03599.

Briggs, WR, Huala, E (1999) Blue-light photoreceptors in higher plants. *Annual Review of Cell and Developmental Biology* **15**, 33-62.

Brooks, L, III, Strable, J, Zhang, X, Ohtsu, K, Zhou, R, Sarkar, A, Hargreaves, S, Elshire, RJ, Eudy, D, Pawlowska, T, Ware, D, Janick-Buckner, D, Buckner, B, Timmermans, MCP, Schnable, PS, Nettleton, D, Scanlon, MJ (2009) Microdissection of shoot meristem functional domains. *PLOS Genetics* **5**, e1000476.

Cândido-Sobrinho, SA, Lima, VF, Daloso, DM (2019) Guard cell metabolism. In: eLS. John Wiley &Sons, Ltd: Chichester.

Case, AL, Curtis, PS, Snow, AA (1998) Heritable variation in stomatal responses to elevated CO_2 in wild radish, *Raphanus raphanistrum* (Brassicaceae). *American Journal of Botany* **85**, 253–258.

Casson, S, Gray, JE (2008) Influence of environmental factors on stomatal development. *New Phytologist* **178**, 9-23.

Casson, SA, Hetherington, AM (2010) Environmental regulation of stomatal development. *Current Opinion in Plant Biology* **13**, 90-5.

Cen, H, Ye, W, Liu, Y, Li, D, Wang, K, Zhang, W (2016) Overexpression of a chimeric gene, OsDST-SRDX, improved salt tolerance of perennial ryegrass. *Scientific Reports* **6**, 27320.

Chaves, MM, Costa, JM, Zarrouk, O, Pinheiro, C, Lopes, CM, Pereira, JS (2016) Controlling stomatal aperture in semi-arid regions-The dilemma of saving water or being cool? *Plant Science* **251**, 54-64.

Christie, JM (2007) Phototropin blue-light receptors. *Annual Review of Plant Biology* **58**, 21–45.

Clipson, NJW, Lachno, DR, Flowers, TJ (1988) Salt tolerance in the halophyte *Suaeda maritima* L.Dum.: abscisic acid contents in response to constant and altered salinity. *Journal of Experimental Botany* **39**, 1381-1388.

Dai, S, Chen, S (2012) Single-cell-type proteomics: toward a holistic understanding of plant function. *Molecular & Cellular Proteomics* **11**, 1622-30.

Daloso, DM, Antunes, WC, Pinheiro, DP, Waquim, JP, Araujo, WL, Loureiro, ME, Fernie, AR, Williams, TCR (2015) Tobacco guard cells fix CO_2 by both Rubisco and PEPcase while sucrose acts as a substrate during light-induced stomatal opening. *Plant, Cell and Environment* **38**, 2353-2371.

De Silva, DLR, Hetherington, AM, Mansfield, TA (1985) Synergism between calcium ions and abscisic acid in preventing stomatal opening. *New Phytologist* **100**, 473-482.

De Vos, S, Van Stappen, G, Sorgeloos, P, Vuylsteke, M, Rombauts, S, Bossier, P (2019) Identification of salt stress response genes using the Artemia transcriptome. *Aquaculture* **500**, 305-314.

Deinlein, U, Stephan, AB, Horie, T, Luo, W, Xu, G, Schroeder, JI (2014) Plant salt-tolerance mechanisms. *Trends in Plant Science* **19**, 371-379.

Dong, H, Bai, L, Zhang, Y, Zhang, GZ, Mao, YQ, Min, LL, Xiang, FY, Qian, DD, Zhu, XH, Song, CP (2018) Modulation of guard cell turgor and drought tolerance by a peroxisomal acetate-malate shunt. *Molecular Plant* **11**, 1278-1291.

Dos Anjos, L, Pandey, PK, Moraes, TA, Feil, R, Lunn, JE, Stitt, M (2018) Feedback regulation by trehalose 6-phosphate slows down starch mobilization below the rate that would exhaust starch reserves at dawn in Arabidopsis leaves. *Plant Direct* **2**, e00078.

Drake, PL, Froend, RH, Franks, PJ (2013) Smaller, faster stomata: scaling of stomatal size, rate of response, and stomatal conductance. *Journal of Experimental Botany* **64**, 495-505.

Driscoll, SP, Prins, A, Olmos, E, Kunert, KJ, Foyer, CH (2006) Specification of adaxial and abaxial stomata, epidermal structure and photosynthesis to CO_2 enrichment in maize leaves. *Journal of Experimental Botany* **57,** 381–390.

Dugasa, MT, Chala, IG, Wu, F (2020) Genotypic difference in secondary metabolism-related enzyme activities and their relative gene expression patterns, osmolyte and plant hormones in wheat. *Physiologia Plantarum* **168**, 921-933.

Ellouzi, H, Hamed, KB, Cela, J, Munne-Bosch, S, Abdelly, C (2011) Early effects of salt stress on the physiological and oxidative status of *Cakile maritima* (halophyte) and *Arabidopsis thaliana* (glycophyte). *Physiologia Plantarum* **142**, 128-43.

Emmert-Buck, MR, Bonner, RF, Smith, PD, Chuaqui, RF, Zhuang, Z, Goldstein, SR, Weiss, RA, Liotta, LA (1996) Laser capture microdissection. *Science* **274**, 998-1001.

Fan, PX, Feng, JJ, Jiang, P, Chen, XY, Bao, HXGDL, Nie, LL, Jiang, D, Lv, SL, Kuang, TY, Li, YX (2011) Coordination of carbon fixation and nitrogen metabolism in *Salicornia europaea* under salinity: comparative proteomic analysis on chloroplast proteins. *Proteomics* **11**, 4346-4367.

Fanourakis, D, Nikoloudakis, N, Pappi, P, Markakis, E, Doupis, G, Charova, SN, Delis, C, Tsaniklidis, G (2020) The role of proteases in determining stomatal development and tuning pore aperture: A review. *Plants* **9,** 340.

Flowers, TJ, Colmer, TD (2008) Salinity tolerance in halophytes. *New Phytologist* **179**, 945-63.

Flowers, TJ, Hajibagheri, MA, Leach, RP, Rogers, WJ, Yeo, AR (1989) Salt tolerance in the halophyte *Suaeda maritima.* In: Plant water relations and

growth under stress. *Proceedings of the Yamada conference XXII, Osaka, Japan*, 173–180

Flowers, TJ, Lauchli, A (1983) Sodium versus potassium: substitution and compartmentation. In: *Encyclopedia of plant physiology*, 651–681, Springer-Verlag, Berlin.

Franks, PJ, Farquhar, GD (2007) The mechanical diversity of stomata and its significance in gas-exchange control. *Plant Physiology* **143**, 78-87.

Fujikawa, T, Sakaguchi, A, Nishizawa, Y, Kouzai, Y, Minami, E, Yano, S, Koga, H, Meshi, T, Nishimura, M (2012) Surface α-1,3-glucan facilitates fungal stealth infection by interfering with innate immunity in plants. *PLOS Pathogens* **8**, e1002882.

Fujita, Y, Nakashima, K, Yoshida, T, Katagiri, T, Kidokoro, S, Kanamori, N, Umezawa, T, Fujita, M, Maruyama, K, Ishiyama, K, Kobayashi, M, Nakasone, S, Yamada, K, Ito, T, Shinozaki, K, Yamaguchi-Shinozaki, K (2009) Three SnRK2 protein kinases are the main positive regulators of abscisic acid signaling in response to water stress in Arabidopsis. *Plant and Cell Physiology* **50**, 2123-32.

Galbraith, DW (2012) Flow cytometry and fluorescence-activated cell sorting in plants: the past, present, and future. *Biomédica* **30**, 65-70

Garcia-Mata, C, Lamattina, L (2010) Hydrogen sulphide, a novel gasotransmitter involved in guard cell signalling. *New Phytologist* **188**, 977-984.

Gardner, MJ, Baker, AJ, Assie, JM, Poethig, RS, Haseloff, JP, Webb, AAR (2009) GAL4 GFP enhancer trap lines for analysis of stomatal guard cell development and gene expression. *Journal of Experimental Botany* **60**, 213-226.

Gautam, V, Sarkar, AK (2015) Laser assisted microdissection, an efficient technique to understand tissue specific gene expression patterns and functional genomics in plants. *Molecular Biotechnology* **57**, 299-308.

Geilfus, CM, Lan, J, Carpentier, S (2018) Dawn regulates guard cell proteins in *Arabidopsis thaliana* that function in ATP production from fatty acid beta-oxidation. *Plant Molecular Biology*, **98**, 525–543.

Geng, S, Yu, B, Zhu, N, Dufresne, C, Chen, S (2017) Metabolomics and proteomics of *Brassica napus* guard cells in response to low CO_2. *Frontiers in Molecular Biosciences* **4**, 51.

Golldack, D, Luking, I, Yang, O (2011) Plant tolerance to drought and salinity: stress regulating transcription factors and their functional significance in the cellular transcriptional network. *Plant Cell Reports* **30**, 1383-91.

Gotow, K, Taylor, S, Zeiger, E (1988) Photosynthetic carbon fixation in guard-cell protoplasts of *Vicia faba* L - Evidence from radiolabel experiments. *Plant Physiology* **86**, 700-705.

Guo, SM, Tan, Y, Chu, HJ, Sun, MX, Xing, JC (2019) Transcriptome sequencing revealed molecular mechanisms underlying tolerance of *Suaeda salsa* to saline stress. *PLoS One* **14**, e0219979.

Han, Y, Gao, S, Muegge, K, Zhang, W, Zhou, B (2015) Advanced applications of RNA sequencing and challenges. *Bioinformatics and Biology insights* **9**, 29-46.

Hanstein, S, de Beer, D, Felle, HH (2001) Miniaturised carbon dioxide sensor designed for measurements within plant leaves. *Sensors and Actuators B: Chemical* **81**, 107-114.

Hayashi, M, Inoue, S, Takahashi, K, Kinoshita, T (2011) Immunohistochemical detection of blue light-induced phosphorylation of the plasma membrane H^+-ATPase in stomatal guard cells. *Plant and Cell Physiology* **52**, 1238-1248.

Hedrich, R, Shabala, S (2018) Stomata in a saline world. *Current Opinion in Plant Biology* **46**, 87-95.

Hetherington, AM, Woodward, FI (2003) The role of stomata in sensing and driving environmental change. *Nature* **424**, 901-8.

Hidalgo, O, Pellicer, J, Christenhusz, M, Schneider, H, Leitch, AR, Leitch, IJ (2017) Is there an upper limit to genome size? *Trends in Plant Science* **22**, 567-573.

Hirose, Y, Aldape, K, Takahashi, M, Berger, MS, Feuerstein, BG (2001) Tissue microdissection and degenerate oligonucleotide primed-polymerase chain reaction (DOP-PCR) is an effective method to analyze genetic aberrations in invasive tumors. *The Journal of Molecular Diagnostics* **3**, 62-67.

Honys, D, Twell, D (2003) Comparative analysis of the Arabidopsis pollen transcriptome. *Plant Physiology* **132**, 640-52.

Horgan, R, Kenny, LC (2011) Omic technologies: genomics, transcriptomics, proteomics and metabolomics. *The Obstetrician & Gynaecologist* **13**, 189-195.

Horrer, D, Flutsch, S, Pazmino, D, Matthews, JS, Thalmann, M, Nigro, A, Leonhardt, N, Lawson, T, Santelia, D (2016) Blue light induces a distinct starch degradation pathway in guard cells for stomatal opening. *Current Biology* **26**, 362-70.

Horwitz, B, Gloria, M, Berrocal, T (1997) A spectroscopic view of some recent advances in the study of blue light photoreception. *Botanica Acta* **110**, 360-368.

Hossain, MA, Bhattacharjee, S, Armin, SM, Qian, P, Xin, W, Li, HY, Burritt, DJ, Fujita, M, Tran, LS (2015) Hydrogen peroxide priming modulates abiotic oxidative stress tolerance: insights from ROS detoxification and scavenging. *Frontiers in Plant Science* **6**, 420.

Hu, HH, Boisson-Dernier, A, Israelsson-Nordstrom, M, Bohmer, M, Xue, SW, Ries, A, Godoski, J, Kuhn, JM, Schroeder, JI (2010) Carbonic anhydrases are upstream regulators of CO_2-controlled stomatal movements in guard cells. *Nature Cell Biology* **12**, 87-93.

Hua, DP, Wang, C, He, JN, Liao, H, Duan, Y, Zhu, ZQ, Guo, Y, Chen, ZZ, Gong, ZZ (2012) A Plasma membrane receptor kinase, GHR1, mediates abscisic acid- and hydrogen peroxide-regulated stomatal movement in Arabidopsis. *Plant Cell* **24**, 2546-2561.

Huala, E, Oeller, PW, Liscum, E, Han, IS, Larsen, E, Briggs, WR (1997) Arabidopsis NPH1: a protein kinase with a putative redox-sensing domain. *Science* **278**, 2120-3.

Huang, D, Wu, W, Abrams, SR, Cutler, AJ (2008) The relationship of drought-related gene expression in *Arabidopsis thaliana* to hormonal and environmental factors. *Journal of Experimental Botany* **59**, 2991-3007.

Humble, GD, Hsiao, TC (1970) Light-dependent Influx and efflux of potassium of guard cells during stomatal opening and closing. *Plant Physiology* **46**, 483-7.

Humble, GD, Raschke, K (1971) Stomatal opening quantitatively related to potassium transport. *Plant Physiology* **48**, 447-453.

Iino, M, Ogawa, T, Zeiger, E (1985) Kinetic properties of the blue-light response of stomata. *Proceedings of the National Academy of Sciences of the United States of America* **82**, 8019-23.

Imes, D, Mumm, P, Bohm, J, Al-Rasheid, KA, Marten, I, Geiger, D, Hedrich, R (2013) Open stomata 1 (OST1) kinase controls R-type anion channel QUAC1 in Arabidopsis guard cells. *The Plant Journal* **74**, 372-82.

Inoue, SI, Kinoshita, T, Matsumoto, M, Nakayama, KI, Doi, M, Shimazaki, KI (2008) Blue light-induced autophosphorylation of phototropin is a primary step for signaling. *Proceedings of the National Academy of Sciences of the United States of America* **105**, 5626-5631.

Jalakas, P, Yarmolinsky, D, Kollist, H, Brosché, M (2017) Isolation of guard-cell enriched tissue for RNA extraction. *Bio-Protocol* **7**, e2447.

Jarvis, DE, Ho, YS, Lightfoot, DJ, Schmockel, SM, Li, B, Borm, TJ, Ohyanagi, H, Mineta, K, Michell, CT, Saber, N, Kharbatia, NM, Rupper, RR, Sharp, AR, Dally, N, Boughton, BA, Woo, YH, Gao, G, Schijlen, EG, Guo, X, Momin, AA, Negrao, S, Al-Babili, S, Gehring, C, Roessner, U, Jung, C, Murphy, K, Arold, ST, Gojobori, T, Linden, CG, van Loo, EN, Jellen, EN, Maughan, PJ, Tester, M (2017) The genome of *Chenopodium quinoa*. *Nature* **542**, 307-312.

Jin, X, Wang, RS, Zhu, M, Jeon, BW, Albert, R, Chen, S, Assmann, SM (2013) Abscisic acid-responsive guard cell metabolomes of Arabidopsis wild-type and gpa1 G-protein mutants. *Plant Cell* **25**, 4789-811.

Kadakkuzha, BM, Liu, X-a, Swarnkar, S, Chen, Y (2016) Genomic and proteomic mechanisms and models in toxicity and safety evaluation of nutraceuticals. In 'Nutraceuticals.' (Ed. RC Gupta.) pp. 227-237. (Academic Press: Boston)

Kagawa, T, Sakai, T, Suetsugu, N, Oikawa, K, Ishiguro, S, Kato, T, Tabata, S, Okada, K, Wada, M (2001) Arabidopsis NPL1: a phototropin homolog controlling the chloroplast high-light avoidance response. *Science* **291**, 2138-41.

Khan, A, Khan, H, Chung, EJ, Hossain, MT, Chung, YR (2015) Complete genome sequence of *Martelella endophytica* YC6887, which has antifungal activity associated with a halophyte. *Genome Announcements* **3**, 00366-15.

Kiani-Pouya, A, Rasouli, F, Bazihizina, N, Zhang, H, Hedrich, R, Shabala, S (2019) A large-scale screening of quinoa accessions reveals an important role of epidermal bladder cells and stomatal patterning in salinity tolerance. *Environmental and Experimental Botany* **168**, 103885.

Kim, TH, Bohmer, M, Hu, HH, Nishimura, N, Schroeder, JI (2010) Guard Cell signal transduction network: advances in understanding abscisic acid, CO_2, and Ca^{2+} signaling. *Annual Review of Plant Biology* **61**, 561-591.

Kinoshita, T, Doi, M, Suetsugu, N, Kagawa, T, Wada, M, Shimazaki, K (2001) Phot1 and phot2 mediate blue light regulation of stomatal opening. *Nature* **414**, 656-60.

Kinoshita, T, Shimazaki, K (1999) Blue light activates the plasma membrane H^+-ATPase by phosphorylation of the C-terminus in stomatal guard cells. *The EMBO Journal* **18**, 5548-58.

Kollist, H, Nuhkat, M, Roelfsema, MR (2014) Closing gaps: linking elements that control stomatal movement. *New Phytologist* **203**, 44-62.

Kollist, H, Zandalinas, SI, Sengupta, S, Nuhkat, M, Kangasjarvi, J, Mittler, R (2019) Rapid responses to abiotic stress: priming the landscape for the signal transduction network. *Trends in Plant Science* **24**, 25-37.

Kortz, A, Hochholdinger, F, Yu, P (2019) Cell type-specific transcriptomics of lateral root formation and plasticity. *Frontiers in Plant Science* **10**, 21.

Kumari, A, Das, P, Parida, AK, Agarwal, PK (2015) Proteomics, metabolomics, and ionomics perspectives of salinity tolerance in halophytes. *Frontiers in Plant Science* **6**, 537.

Lafzi, A, Moutinho, C, Picelli, S, Heyn, H (2018) Tutorial: guidelines for the experimental design of single-cell RNA sequencing studies. *Nature Protocols* **13**, 2742-2757.

Lakra, N, Kaur, C, Anwar, K, Singla-Pareek, SL, Pareek, A (2018) Proteomics of contrasting rice genotypes: identification of potential targets for raising crops for saline environment. *Plant, Cell and Environment* **41**, 947-969.

Lal, R (2010) Managing soils and ecosystems for mitigating anthropogenic carbon emissions and advancing global food security. *BioScience* **60**, 708-721.

Lau, OS, Bergmann, DC (2012) Stomatal development: a plant's perspective on cell polarity, cell fate transitions and intercellular communication. *Development* **139**, 3683.

Lawson, T (2009) Guard cell photosynthesis and stomatal function. *New Phytologist* **181**, 13-34.

Lawson, T, Oxborough, K, Morison, JI, Baker, NR (2003) The responses of guard and mesophyll cell photosynthesis to CO_2, O_2, light, and water stress in a range of species are similar. *Journal of Experimental Botany* **54**, 1743-52.

Lawson, T, Simkin, AJ, Kelly, G, Granot, D (2014) Mesophyll photosynthesis and guard cell metabolism impacts on stomatal behaviour. *New Phytologist* **203**, 1064-1081.

Lawson, T, Vialet-Chabrand, S (2019) Speedy stomata, photosynthesis and plant water use efficiency. *New Phytologist* **221**, 93-98.

Lee, SC, Lan, WZ, Buchanan, BB, Luan, S (2009) A protein kinase-phosphatase pair interacts with an ion channel to regulate ABA signaling in plant guard cells. *Proceedings of the National Academy of Sciences of the United States of America* **106**, 21419-21424.

Leonhardt, N, Kwak, JM, Robert, N, Waner, D, Leonhardt, G, Schroeder, JI (2004) Microarray expression analyses of Arabidopsis guard cells and isolation of a recessive abscisic acid hypersensitive protein phosphatase 2C mutant. *Plant Cell* **16**, 596-615.

Li, L, Li, M, Qi, X, Tang, X, Zhou, Y (2018) De novo transcriptome sequencing and analysis of genes related to salt stress response in *Glehnia littoralis*. *PeerJ* **6**, e5681.

Li, W, Lan, P (2015) Re-analysis of RNA-seq transcriptome data reveals new aspects of gene activity in Arabidopsis root hairs. *Frontiers in Plant Science* **6**, 421.

Liu, D, Horvath, D, Li, P, Liu, W (2019) RNA sequencing characterizes transcriptomes differences in cold response between northern and southern alternanthera philoxeroides and highlight adaptations associated with northward expansion. *Frontiers in Plant Science* **10**, 24.

Lu, P, Outlaw, WH, Smith, BG, Freed, GA (1997) A new mechanism for the regulation of stomatal aperture size in intact leaves - Accumulation of mesophyll-derived sucrose in the guard-cell wall of *Vicia faba*. *Plant Physiology* **114**, 109-118.

Lukowitz, W, Roeder, A, Parmenter, D, Somerville, C (2004) A MAPKK kinase gene regulates extra-embryonic cell fate in Arabidopsis. *Cell* **116**, 109-19.

Luo, MJ, Zhao, YX, Wang, YD, Shi, Z, Zhang, PP, Zhang, YX, Song, W, Zhao, JR (2018) Comparative Proteomics of contrasting maize, genotypes provides insights into salt-stress tolerance mechanisms. *Journal of Proteome Research* **17**, 141-153.

MacAlister, CA, Ohashi-Ito, K, Bergmann, DC (2007) Transcription factor control of asymmetric cell divisions that establish the stomatal lineage. *Nature* **445**, 537-540.

Manzoni, C, Kia, DA, Vandrovcova, J, Hardy, J, Wood, NW, Lewis, PA, Ferrari, R (2018) Genome, transcriptome and proteome: the rise of omics data and their integration in biomedical sciences. *Briefings in Bioinformatics* **19**, 286-302.

Marten, H, Hedrich, R, Roelfsema, MRG (2007) Blue light inhibits guard cell plasma membrane anion channels in a phototropin-dependent manner. *The Plant Journal* **50**, 29-39.

Marten, H, Hyun, T, Gomi, K, Seo, S, Hedrich, R, Roelfsema, MRG (2008) Silencing of NtMPK4 impairs CO_2-induced stomatal closure, activation of anion channels and cytosolic Ca^{2+} signals in *Nicotiana tabacum* guard cells. *The Plant Journal* **55**, 698-708.

Martin, C, Glover, BJ (2007) Functional aspects of cell patterning in aerial epidermis. *Current Opinion in Plant Biology* **10**, 70-82.

McAinsh, MR, Allen, GJ, Hetherington, AM, Sanders, D (1996) The role of cyclic-ADP-ribose in stomatal guard cells. *Plant Physiology* **111**, 692-692.

McKown, KH, Bergmann, DC (2018) Grass stomata. *Current Biology* **28**, 814-816.

Medeiros, DB, Souza, LP, Antunes, WC, Araujo, WL, Daloso, DM, Fernie, AR (2018) Sucrose breakdown within guard cells provides substrates for glycolysis and glutamine biosynthesis during light-induced stomatal opening. *The Plant Journal* **94**, 583-594.

Merilo, E, Jalakas, P, Laanemets, K, Mohammadi, O, Horak, H, Kollist, H, Brosche, M (2015) Abscisic acid transport and homeostasis in the context of stomatal regulation. *Molecular Plant* **8**, 1321-33.

Merilo, E, Laanemets, K, Hu, H, Xue, S, Jakobson, L, Tulva, I, Gonzalez-Guzman, M, Rodriguez, PL, Schroeder, JI, Brosche, M, Kollist, H (2013) PYR/RCAR receptors contribute to ozone-, reduced air humidity-, darkness-, and CO_2-induced stomatal regulation. *Plant Physiology* **162**, 1652-68.

Misra, BB, Assmann, SM, Chen, S (2014) Plant single-cell and single-cell-type metabolomics. *Trends in Plant Science* **19**, 637-46.

Misra, BB, de Armas, E, Tong, Z, Chen, S (2015) Metabolomic responses of guard cells and mesophyll cells to bicarbonate. *PLoS One* **10**, e0144206.

Misra, BB, Reichman, SM, Chen, S (2018) The guard cell ionome: understanding the role of ions in guard cell functions. *Progress in Biophysics & Molecular Biology*. ***146,*** 50-62.

Mott, KA, Sibbernsen, ED, Shope, JC (2008) The role of the mesophyll in stomatal responses to light and CO_2. *Plant, Cell and Environment* **31**, 1299-306.

Murata, Y, Pei, ZM, Mori, IC, Schroeder, J (2001) Abscisic acid activation of plasma membrane Ca^{2+} channels in guard cells requires cytosolic NAD(P)H and is differentially disrupted upstream and downstream of reactive oxygen species production in abi1-1 and abi2-1 protein phosphatase 2C mutants. *The Plant Cell* **13**, 2513-2523.

Mustilli, AC, Merlot, S, Vavasseur, A, Fenzi, F, Giraudat, J (2002) Arabidopsis OST1 protein kinase mediates the regulation of stomatal aperture by abscisic acid and acts upstream of reactive oxygen species production. *The Plant Cell* **14**, 3089-99.

Navin, N, Hicks, J (2011) Future medical applications of single-cell sequencing in cancer. *Genome Medicine* **3**, 31.

Nelson, T, Tausta, SL, Gandotra, N, Liu, T (2006) Laser microdissection of plant tissue: what you see is what you get. *Annual Review of Plant Biology* **57**, 181-201.

Nemhauser, JL, Hong, F, Chory, J (2006) Different plant hormones regulate similar processes through largely nonoverlapping transcriptional responses. *Cell* **126**, 467-75.

Ning, M, Lo, EH (2010) Opportunities and challenges in omics. *Translational Stroke Research* **1**, 233-7.

Niu, M, Huang, Y, Sun, S, Sun, J, Cao, H, Shabala, S, Bie, Z (2018) Root respiratory burst oxidase homologue-dependent H_2O_2 production confers salt tolerance on a grafted cucumber by controlling Na^+ exclusion and stomatal closure. *Journal of Experimental Botany* **69**, 3465-3476.

Nunes, TDG, Zhang, D, Raissig, MT (2020) Form, development and function of grass stomata. *The Plant Journal* **101,** 780-799.

Obulareddy, N, Panchal, S, Melotto, M (2013) Guard cell purification and RNA isolation suitable for high-throughput transcriptional analysis of cell-type responses to biotic stresses. *Molecular Plant-Microbe Interactions* **26**, 844-849.

Oh, DH, Barkla, BJ, Vera-Estrella, R, Pantoja, O, Lee, SY, Bohnert, HJ, Dassanayake, M (2015) Cell type-specific responses to salinity - the epidermal bladder cell transcriptome of *Mesembryanthemum crystallinum*. *New Phytologist* **207**, 627-44.

Ohashi-Ito, K, Bergmann, DC (2006) Arabidopsis FAMA controls the final proliferation/differentiation switch during stomatal development. *The Plant Cell* **18**, 2493–2505.

Pandey, S, Wang, RS, Wilson, L, Li, S, Zhao, Z, Gookin, TE, Assmann, SM, Albert, R (2010) Boolean modeling of transcriptome data reveals novel modes of heterotrimeric G-protein action. *Molecular Systems Biology* **6**, 372.

Pang, QY, Zhang, AQ, Zang, W, Wei, L, Yan, XF (2016) Integrated proteomics and metabolomics for dissecting the mechanism of global responses to salt and alkali stress in *Suaeda corniculata*. *Plant and Soil* **402**, 379-394.

Park, S-Y, Fung, P, Nishimura, N, Jensen, DR, Fujii, H, Zhao, Y, Lumba, S, Santiago, J, Rodrigues, A, Chow, T-fF, Alfred, SE, Bonetta, D, Finkelstein, R, Provart, NJ, Desveaux, D, Rodriguez, PL, McCourt, P, Zhu, J-K, Schroeder, JI, Volkman, BF, Cutler, SR (2009) Abscisic acid inhibits type

2C protein phosphatases via the PYR/PYL family of START proteins. *Science* **324**, 1068-1071.

Paulsen, CE, Carroll, KS (2013) Cysteine-mediated redox signaling: chemistry, biology, and tools for discovery. *Chemical Reviews* **113**, 4633-79.

Pei, ZM, Murata, Y, Benning, G, Thomine, S, Klusener, B, Allen, GJ, Grill, E, Schroeder, JI (2000) Calcium channels activated by hydrogen peroxide mediate abscisic acid signalling in guard cells. *Nature* **406**, 731-734.

Pei, ZM, Ward, JM, Harper, JF, Schroeder, JI (1997) Chloride and malate uptake channel in Vicia faba guard cell vacuoles activated by the serine/threonine kinase, CDPK. *Plant Physiology* **114**, 1405-1405.

Pennington, SR, Dunn, MJ (2001) *Proteomics: from protein sequence to function.* (CRC Press, Taylor & Francis)

Pillitteri, LJ, Sloan, DB, Bogenschutz, NL, Torii, KU (2007) Termination of asymmetric cell division and differentiation of stomata. *Nature* **445**, 501-505.

Raghavendra, AS, Rao, IM, Das, VSR (1976) Replacibility of potassium by sodium for stomatal opening in epidermal strips of *Commelina Benghalensis*. *Zeitschrift Fur Pflanzenphysiologie* **80**, 36-42.

Raschke, K, Hedrich, R (1989) Patch clamp measurements on isolated guard-cell protoplasts and vacuoles. *Methods in Enzymology* **174**, 312-330.

Raschke, K, Shabahang, M, Wolf, R (2003) The slow and the quick anion conductance in whole guard cells: their voltage-dependent alternation, and the modulation of their activities by abscisic acid and CO_2. *Planta* **217**, 639-650.

Ritte, G, Rosenfeld, J, Rohrig, K, Raschke, K (1999) Rates of sugar uptake by guard cell protoplasts of *Pisum Sativum* L. related to the solute requirement for stomatal opening. *Plant Physiology* **121**, 647-56.

Robinson, MF, Very, A-A, Sanders, D, Mansfield, TA (1997) How can stomata contribute to salt tolerance. *Annals of Botany* **80**, 387-393.

Rodrigues, O, Reshetnyak, G, Grondin, A, Saijo, Y, Leonhardt, N, Maurel, C, Verdoucq, L (2017) Aquaporins facilitate hydrogen peroxide entry into guard cells to mediate ABA- and pathogen-triggered stomatal closure.

Proceedings of the National Academy of Sciences of the United States of America **114**, 9200-9205.

Roelfsema, MR, Hedrich, R (2005) In the light of stomatal opening: new insights into the Watergate. *New Phytologist* **167**, 665-91.

Roelfsema, MR, Hedrich, R, Geiger, D (2012) Anion channels: master switches of stress responses. *Trends in Plant Science* **17**, 221-9.

Roelfsema, MRG, Hanstein, S, Felle, HH, Hedrich, R (2002) CO_2 provides an intermediate link in the red light response of guard cells. *The Plant Journal* **32**, 65-75.

Roelfsema, MRG, Konrad, KR, Marten, H, Psaras, GK, Hartung, W, Hedrich, R (2006) Guard cells in albino leaf patches do not respond to photosynthetically active radiation, but are sensitive to blue light, CO_2 and abscisic acid. *Plant, Cell and Environment* **29**, 1595-1605.

Rosenberg, LE, Rosenberg, DD (2012) Expression of genes and genomes. In *Human genes and genomes.* (Academic Press: San Diego)

Ruan, C-J, da Silva, JAT, Mopper, S, Qin, P, Lutts, S (2010) Halophyte improvement for a salinized world. *Critical Reviews in Plant Sciences* **29**, 329-359.

Sahu, BB, Shaw, BP (2009) Isolation, identification and expression analysis of salt-induced genes in *Suaeda maritima*, a natural halophyte, using PCR-based suppression subtractive hybridization. *BMC Plant Biology* **9**, 69.

Salekdeh, GH, Siopongco, J, Wade, LJ, Ghareyazie, B, Bennett, J (2002) Proteomic analysis of rice leaves during drought stress and recovery. *Proteomics* **2**, 1131-45.

Sanchez, DH, Pieckenstain, FL, Escaray, F, Erban, A, Kraemer, U, Udvardi, MK, Kopka, J (2011) Comparative ionomics and metabolomics in extremophile and glycophytic Lotus species under salt stress challenge the metabolic pre-adaptation hypothesis. *Plant, Cell and Environment* **34**, 605-17.

Scheres, B, Benfey, PN (1999) Asymmetric cell division in plants. *Annual Review of Plant Physiology and Plant Molecular Biology* **50**, 505-537.

Schoch, PG, Zinsou, C, Sibi, M (1980) Dependence of stomatal index on environmental factors during stomata differentiation in leaves of *Vigna signensis* L. *Journal of Experimental Botany* **31**, 1211–1216.

Schroeder, JI, Allen, GJ, Hugouvieux, V, Kwak, JM, Waner, D (2001) Guard cell signal transduction. *Annual Review of Plant Physiology and Plant Molecular Biology* **52**, 627-658.

Schroeder, JI, Hagiwara, S (1990) Repetitive increases in cytosolic Ca^{2+} of guard-cells by abscisic-acid activation of nonselective Ca^{2+} permeable channels. *Proceedings of the National Academy of Sciences of the United States of America* **87**, 9305-9309.

Schroeder, JI, Raschke, K, Neher, E (1987) Voltage dependence of K^+ channels in guard-cell protoplasts. *Proceedings of the National Academy of Sciences of the United States of America* **84**, 4108-12.

Serna, L (2013) Antagonistic regulation of the meristemoid to guard mother cell transition. *Frontiers in Plant Science* **4**, 401.

Serna, L, Torres-Contreras, J, Fenoll, C (2002) Clonal analysis of stomatal development and patterning in Arabidopsis leaves. *Developmental Biology* **241**, 24-33.

Shabala, S (2013) Learning from halophytes: physiological basis and strategies to improve abiotic stress tolerance in crops. *Annals of Botany* **112**, 1209-21.

Shabala, S, Bose, J, Fuglsang, AT, Pottosin, I (2016) On a quest for stress tolerance genes: membrane transporters in sensing and adapting to hostile soils. *Journal of Experimental Botany* **67**, 1015-31.

Shabala, S, Wu, H, Bose, J (2015) Salt stress sensing and early signalling events in plant roots: current knowledge and hypothesis. *Plant Science* **241**, 109-19.

Sharkey, TD, Raschke, K (1981) Effect of light quality on stomatal opening in leaves of *Xanthium strumarium* L. *Plant Physiology* **68**, 1170-4.

Shimazaki, K, Doi, M, Assmann, SM, Kinoshita, T (2007) Light regulation of stomatal movement. *Annual Review of Plant Biology* **58**, 219-247.

Shope, JC, DeWald, DB, Mott, KA (2003) Changes in surface area of intact guard cells are correlated with membrane internalization. *Plant Physiology* **133**, 1314-1321.

Sirichandra, C, Wasilewska, A, Vlad, F, Valon, C, Leung, J (2009) The guard cell as a single-cell model towards understanding drought tolerance and abscisic acid action. *Journal of Experimental Botany* **60**, 1439-1463.

Song, YW, Miao, YC, Song, CP (2014) Behind the scenes: the roles of reactive oxygen species in guard cells. *New Phytologist* **201**, 1121-1140.

Specht, H, Slavov, N (2018) Transformative opportunities for single-cell proteomics. *Journal of Proteome Research* **17**, 2565-2571.

Stange, A, Hedrich, R, Roelfsema, MRG (2010) Ca^{2+}-dependent activation of guard cell anion channels, triggered by hyperpolarization, is promoted by prolonged depolarization. *The Plant Journal* **62**, 265-276.

Subbarao, GV, Ito, O, Berry, WL, Wheeler, RM (2003) Sodium—A functional plant nutrient. *Critical Reviews in Plant Sciences* **22**, 391-416.

Tang, X, Mu, X, Shao, H, Wang, H, Brestic, M (2015) Global plant-responding mechanisms to salt stress: physiological and molecular levels and implications in biotechnology. *Critical Reviews in Biotechnology* **35**, 425-37.

Thomas, PW, Woodward, FI, Quick, PW (2003) Systemic irradiance signalling in tobacco. *New Phytologist* **161**, 193–198.

Trapnell, C (2015) Defining cell types and states with single-cell genomics. *Genome Research* **25**, 1491-1498.

Umezawa, T, Sugiyama, N, Mizoguchi, M, Hayashi, S, Myouga, F, Yamaguchi-Shinozaki, K, Ishihama, Y, Hirayama, T, Shinozaki, K (2009) Type 2C protein phosphatases directly regulate abscisic acid-activated protein kinases in Arabidopsis. *Proceedings of the National Academy of Sciences of the United States of America* **106**, 17588-93.

Urano, K, Kurihara, Y, Seki, M, Shinozaki, K (2010) Omics analyses of regulatory networks in plant abiotic stress responses. *Current Opinion in Plant Biology* **13**, 132-8.

Vahisalu, T, Puzorjova, I, Brosche, M, Valk, E, Lepiku, M, Moldau, H, Pechter, P, Wang, YS, Lindgren, O, Salojarvi, J, Loog, M, Kangasjarvi, J, Kollist, H (2010) Ozone-triggered rapid stomatal response involves the production of reactive oxygen species, and is controlled by SLAC1 and OST1. *The Plant Journal* **62**, 442-53.

Van Cutsem, E, Simonart, G, Degand, H, Faber, AM, Morsomme, P, Boutry, M (2011) Gel-based and gel-free proteomic analysis of *Nicotiana tabacum*

trichomes identifies proteins involved in secondary metabolism and in the (a)biotic stress response. *Proteomics* **11**, 440-54.

Wang, H, Ngwenyama, N, Liu, Y, Walker, JC, Zhang, S (2007) Stomatal development and patterning are regulated by environmentally responsive mitogen-activated protein kinases in Arabidopsis. *The Plant Cell* **19,** 63-73.

Wang, J, Zhu, J, Zhang, Y, Fan, F, Li, W, Wang, F, Zhong, W, Wang, C, Yang, J (2018) Comparative transcriptome analysis reveals molecular response to salinity stress of salt-tolerant and sensitive genotypes of indica rice at seedling stage. *Science Reports* **8**, 2085.

Wang, RS, Pandey, S, Li, S, Gookin, TE, Zhao, Z, Albert, R, Assmann, SM (2011a) Common and unique elements of the ABA-regulated transcriptome of Arabidopsis guard cells. *BMC Genomics* **12**, 216.

Wang, RS, Pandey, S, Li, S, Gookin, TE, Zhao, ZX, Albert, R, Assmann, SM (2011b) Common and unique elements of the ABA-regulated transcriptome of Arabidopsis guard cells. *BMC Genomics* **12**, 216.

Wang, X, Chang, L, Wang, B, Wang, D, Li, P, Wang, L, Yi, X, Huang, Q, Peng, M, Guo, A (2013) Comparative proteomics of *Thellungiella halophila* leaves from plants subjected to salinity reveals the importance of chloroplastic starch and soluble sugars in halophyte salt tolerance. *Molecular & Cellular Proteomics* **12**, 2174-95.

Wang, XC, Fan, PX, Song, HM, Chen, XY, Lil, XF, Li, YX (2009a) Comparative proteomic analysis of differentially expressed proteins in shoots of *Salicornia europaea* under different salinity. *Journal of Proteome Research* **8**, 3331-3345.

Wang, Z, Gerstein, M, Snyder, M (2009b) RNA-Seq: a revolutionary tool for transcriptomics. *Nature Reviews Genetics* **10**, 57-63.

Webb, AAR, McAinsh, MR, Mansfield, TA, Hetherington, AM (1996) Carbon dioxide induces increases in guard cell cytosolic free calcium. *The Plant Journal* **9**, 297-304.

Willmer, C, Fricker, MD (1996) *Stomata*. (Chapman and Hall, London)

Willmer, CM, Sexton, R (1979) Stomata and plasmodesmata. *Protoplasma* **100**, 113-124.

Wilson, RS, Nairn, AC (2018) Cell-type-specific proteomics: a neuroscience perspective. *Proteomes* **6**, 51.

Witzel, K, Weidner, A, Surabhi, GK, Borner, A, Mock, HP (2009) Salt stress-induced alterations in the root proteome of barley genotypes with contrasting response towards salinity. *Journal of Experimental Botany* **60**, 3545-57.

Woodward, FI (1987) Stomatal numbers are sensitive to increases in CO_2 from pre-industrial levels. *Nature Biotechnology* **327**, 617–618.

Woodward, FI, Kelly, CK (1995) The influences of CO_2 concentration on stomatal density. *New Phytologist* **131**, 311–327.

Wu, F, Chi, Y, Jiang, Z, Xu, Y, Xie, L, Huang, F, Wan, D, Ni, J, Yuan, F, Wu, X, Zhang, Y, Wang, L, Ye, R, Byeon, B, Wang, W, Zhang, S, Sima, M, Chen, S, Zhu, M, Pei, J, Johnson, DM, Zhu, S, Cao, X, Pei, C, Zai, Z, Liu, Y, Liu, T, Swift, GB, Zhang, W, Yu, M, Hu, Z, Siedow, JN, Chen, X, Pei, Z-M (2020) Hydrogen peroxide sensor HPCA1 is an LRR receptor kinase in Arabidopsis. *Nature* **578,** 577–581

Xue, S, Hu, H, Ries, A, Merilo, E, Kollist, H, Schroeder, JI (2011) Central functions of bicarbonate in S-type anion channel activation and OST1 protein kinase in CO_2 signal transduction in guard cell. *The EMBO Journal* **30**, 1645-58.

Yang, R, Jarvis, DE, Chen, H, Beilstein, MA, Grimwood, J, Jenkins, J, Shu, S, Prochnik, S, Xin, M, Ma, C, Schmutz, J, Wing, RA, Mitchell-Olds, T, Schumaker, KS, Wang, X (2013) The reference genome of the halophytic plant *Eutrema salsugineum*. *Frontiers in Plant Science* **4**, 46-46.

Yao, XH, Zhao, WC, Yang, R, Wang, JL, Zhao, FK, Wang, SH (2018) Preparation and applications of guard cell protoplasts from the leaf epidermis of *Solanum lycopersicum*. *Plant Methods* **14**, 26.

Yoo, MJ, Ma, TY, Zhu, N, Liu, LH, Harmon, AC, Wang, QM, Chen, SX (2016) Genome-wide identification and homeolog-specific expression analysis of the SnRK2 genes in *Brassica napus* guard cells. *Plant Molecular Biology* **91**, 211-227.

Yuan, Y, Lee, H, Hu, H, Scheben, A, Edwards, D (2018) Single-cell genomic analysis in plants. *Genes* **9**, 50.

Zeiger, E, Hepler, PK (1976) Production of guard cell protoplasts from onion and tobacco. *Plant Physiology* **58**, 492-498.

Zhang, L, Foreman, DP, Grant, PA, Shrestha, B, Moody, SA, Villiers, F, Kwak, JM, Vertes, A (2014) In situ metabolic analysis of single plant cells by capillary microsampling and electrospray ionization mass spectrometry with ion mobility separation. *Analyst* **139**, 5079-5085.

Zhang, T, Zhu, MM, Zhu, N, Strul, JM, Dufresne, CP, Schneider, JD, Harmon, AC, Chen, SX (2016) Identification of thioredoxin targets in guard cell enriched epidermal peels using cysTMT proteomics. *Journal of Proteomics* **133**, 48-53.

Zhang, X, Dong, FC, Gao, JF, Song, CP (2001) Hydrogen peroxide-induced changes in intracellular pH of guard cells precede stomatal closure. *Cell Research* **11**, 37-43.

Zhang, YJ, Li, DH, Zhou, R, Wang, X, Dossa, K, Wang, LH, Zhang, YX, Yu, JY, Gong, HH, Zhang, XR, You, J (2019) Transcriptome and metabolome analyses of two contrasting sesame genotypes reveal the crucial biological pathways involved in rapid adaptive response to salt stress. *BMC Plant Biology* **19**, 66.

Zhao, ZX, Stanley, BA, Zhang, W, Assmann, SM (2010) ABA-regulated G protein signaling in Arabidopsis guard cells: a proteomic perspective. *Journal of Proteome Research* **9**, 1637-1647.

Zhao, ZX, Zhang, W, Stanley, BA, Assmann, SM (2008) Functional proteomics of *Arabidopsis thaliana* guard cells uncovers new stomatal signaling pathways. *The Plant Cell* **20**, 3210-3226.

Zhao, C, Randall, D, Holford, P, Haigh, AM, Chen, ZH, (2019) Isolation of high purity guard cell protoplasts of *Arabidopsis thaliana* for omics research. *Plant Growth Regulation* **89,** 37–47.

Zhu, M, Dai, S, Chen, S (2012) The stomata frontline of plant interaction with the environment-perspectives from hormone regulation. *Frontiers in Biology* **7**, 96-112.

Zhu, M, Zhou, M, Shabala, L, Shabala, S (2015) Linking osmotic adjustment and stomatal characteristics with salinity stress tolerance in contrasting barley accessions. *Functional Plant Biology* **42**, 252-263.

Zhu, MM, Dai, SJ, McClung, S, Yan, XF, Chen, SX (2009) Functional differentiation of *Brassica napus* guard cells and mesophyll cells revealed by comparative proteomics. *Molecular & Cellular Proteomics* **8**, 752-766.

Zorb, C, Geilfus, CM, Dietz, KJ (2019) Salinity and crop yield. *Plant Biology* **21 Suppl 1**, 31-38.

Zou, C, Chen, A, Xiao, L, Muller, HM, Ache, P, Haberer, G, Zhang, M, Jia, W, Deng, P, Huang, R, Lang, D, Li, F, Zhan, D, Wu, X, Zhang, H, Bohm, J, Liu, R, Shabala, S, Hedrich, R, Zhu, JK, Zhang, H (2017) A high-quality genome assembly of quinoa provides insights into the molecular basis of salt bladder-based salinity tolerance and the exceptional nutritional value. *Cell Research* **27**, 1327-1340.

Chapter 2: Stomatal traits and photosynthetic responses in halophytes and glycophytes under saline conditions

Abstract

Understanding the adaptive strategies of halophytes to maintain their productivity under saline conditions is essential for plant breeding programs. Three halophytic species [quinoa (*Chenopodium quinoa* Wild.), sea barley (*Hordeum marinum*), and sea beet (*Beta maritima*)] and their glycophytic relatives [*Chenopodium album*, cultivated barley (*Hordeum vulgare*) and sugar beet (*Beta vulgaris*)] were grown under wide ranges of salt concentrations (0-500 mM NaCl). Plant agronomical (growth rate; biomass), ionic (Na^+, Cl^- and K^+ content in the leaves), and photosynthetic traits (stomatal conductance; CO_2 assimilation rate; the maximum velocity of carboxylation (V_{cmax}), rate of RuBP regeneration via electron transport (J), speed of stomatal opening and closing were then determined. Medium salinity levels stimulated growth in halophytic quinoa and sea beet species. Stomatal conductances decreased in a dose-dependent manner with increasing NaCl concentrations. However, CO_2 assimilation rates remained constant or displayed higher values at the medium level of salinity in quinoa, sugar beet and sea beet. High V_{cmax} and J were accountable for the high CO_2 assimilation rates and biomass productions under these conditions. Leaf K^+/Na^+ selectivity was found to be a good determinant of salt tolerance as higher values for K^+/Na^+ selectivity was observed in halophytes. Stomatal densities were lower in halophytic species; this trait is suggested to be a part of an adaptive mechanism to conserve the water and avoid desiccation. However, stomatal density increased with increasing salinity levels in the studied species except for *C. album* and quinoa in which stomata were less frequent under saline conditions. Stomatal size reduced with salinity in all studies species. Response of stomatal aperture to the light at the presence of different concentrations K^+ and Na^+ displayed that Na^+ can stimulates stomatal opening in quinoa even at low K^+/Na^+ ratio. The speed of stomatal response to light and dark was species-specific, with the highest values in the cultivated barley and sea barley and the lowest ones in sugar beet and sea beet. Halophytes exhibited a higher speed of stomatal opening and closure in response to light/dark fluctuations. Altogether,

halophytes were superior to glycophytes in terms of having higher maximum velocity of carboxylation, higher K^+/Na^+ selectivity, improved water status, and faster stomatal responses to environmental factors.

2.1 Introduction

The global population will grow from 7.7 billion in 2019 to nearly 10 billion in 2050 and 50% more food will be required to feed that ever-increasing population (FAO 2017). About 70% of global water is consumed in agriculture while competition between the agricultural sector other sectors for fresh water is increasing, making water a scarce resource globally. At the same time, the world is not short of saline water, with 97% of all water resources being in the oceans. Also, drylands cover 41% of the earth's land area (Prăvălie 2016) and can hypothetically be made productive provided that plants can handle irrigation with the seawater.

Plants vary notably in their tolerance to saline environments (Flowers *et al.* 2010). Most of them fall within the sensitive group, so their growth and productivity are adversely affected by salinity. There is a small group of terrestrial plants termed halophytes that are capable of growing and developing normally at high salinity levels and complete their life cycle at salt concentrations that would kill 99% of all plant species (Santos *et al.* 2016). Thus, they can be considered as a new source of crops (Lokhande and Suprasanna 2012) or be used as a source of tolerant genes for re-domestication of the existing crops (Tada *et al.* 2019). Understanding the mechanisms by which the halophytes are able to maintain productivity in saline environments is an essential step toward improving salt stress in glycophytic plants in the breeding program as well as generating salt resistance crop plants for the future (Rozema and Schat 2013).

As plant biomass is proportional to carbon gain, higher productivity of halophytes under high salinity levels originates from both efficient operation of photosynthetic machinery (non-stomatal limitation of PS) and the ability of plants to balance CO_2 assimilation and water loss via stomata (stomatal limitation). Even a minor increase in photosynthetic yields would be sufficient to create a major increase in biomass by the end of the growing season (Lawson and Blatt 2014). However, stomatal conductance has been shown to be hypersensitive to both osmotic and ionic components of salt stress (Yuan *et al.* 2014; Mohamed *et al.* 2020) impacting the productivity of the plants in saline conditions.

CO_2 assimilation through stomatal pores is accompanied by escaping water vapor via the transpiration process, suggesting the close dependence of carbon and water cycles (Hetherington and Woodward 2003b). Therefore, changes in stomatal response to environmental stimuli have a great impact on water fluxes (Lawson and Vialet-Chabrand 2019). Stomata and their behaviour in halophytes might possess some typical traits that improve their water status leading to reduced transpiration and enhanced CO_2 uptake. Upon exposure to short term salt stress, reduced transpiration is the earliest response of plants that can be achieved through controlling stomatal aperture by guard cell osmotic adjustment (Barbieri *et al.* 2012). Under prolonged stress, plants required a high level of adaptation such as modification in stomatal size and density as well as activation of some mechanisms to deal with toxic ions in guard cells. Reduction in stomatal density was found to operate as an adaptation mechanism for some halophytes such as quinoa upon exposure to salt stress (Shabala *et al.* 2013). Recent studies have shown that reduced stomatal density under stress can improve water use efficiency without adverse effects on crop yield (Hughes *et al.* 2017).

The speed of stomatal responses to changing environmental conditions can enhance the synchronization of CO_2 uptake with water loss (Lawson and Vialet-Chabrand 2019) and may help halophytes to maintain water status and CO_2 uptake under saline condition. Stomatal speed has been a target for improving water use efficiency and plant productivity in recent years (Vialet-Chabrand *et al.* 2016). Nonetheless, not much information is available concerning mechanisms governing the kinetics of stomatal movements in halophytes and its effect on plant performance. In this study, three halophytes (quinoa, sea barley and sea beet) and their relative glycophytes (*C. album*, cultivated barley, and sugar beet) were investigated. Two first pairs of species were chosen from the Amaranthaceae family (previously Chenopodiaceae) and the last pair from the Poaceae family (Gramineae). Amaranthaceae and Poaceae families include the largest number (3245 plants) of halophytic plants (353 and 120, respectively; (Santos *et al.* 2016). Biomass, photosynthesis parameters, stomatal density, size and index, stomatal response, and contribution of various ions in the stomatal movement were investigated. The results of this study revealed that halophytes had superior performance than their glycophyte counterparts under saline conditions through

higher photosynthetic capacity, higher selectivity of potassium over sodium, improve water content, reducing stomatal density and faster response of stomata to light and dark.

2.2 Materials and methods

2.2.1 Growth condition

Chenopodium quinoa (Wild.) (cultivar Q20), *Chenopodium album*, *Hordeum vulgare* (cultivated barley, cultivar Gairdner); *Hordeum marinum* (sea barley), *Beta vulgaris* (sugar beet, cultivar TAS004), *Beta maritima* (sea beet) were used as plant materials. The seeds obtained from the Leibniz Institute of Plant Genetics and Crop Plant Research (IPK) (gbis.ipk-gatersleben.de), Germany.

Seeds were sown in 8-inch diameter plastic pots filled with potting mix. The standard potting mix was made of 5% coco peat; 90% composted pine bark; 5% coarse sand; dolomite at 6 kg m^{-3}; gypsum at 1 kg m^{-3}; Osmoform Pre-mix at 1.25 kg m^{-3}, ferrous sulphate at 1.5 kg m^{-3} and Scotts Pro at 3 kg m^{-3}. Twelve seeds were sown in each pot and then watered regularly with a tap water for 2 weeks. The young seedlings were thinned to 4 uniform seedlings per pot three days before salinity treatments commenced. Salt treatments were commenced with increments of 50 mM NaCl, applied twice a day. When all treatments reach target concentrations of 100, 200, 300, 400 and 500 mM NaCl, salinity treatment lasted for three more weeks. The experiment was carried out in a glasshouse with a photoperiod of 12/12 h light/dark cycle and temperature regime of 24 °C and 16 °C during the day and the night, respectively. Five biological replicates for each species and each salinity level were measured.

2.2.2 Leaf ion content measurements

To determine Na^+, K^+, and Cl^- contents of leaves, the youngest fully expanded leaf of each plant species was harvested. For leaf sap extraction, samples were freeze-thawed and then squeezed by hand in 1.7 mL tubes. The sap then centrifuged at 4000 rpm for 5 min. For measurement of Na^+ and K^+, leaf saps were diluted 1:10 for 200 and 300 mM NaCl treatments and 1:50 for 400 and 500 mM NaCl treatments and ion quantifications were carried out using a flame photometer (Corning 410C, Essex, UK). Chloride concentration in the leaf sap was measured

using the non-invasive microelectrodes using MIFE measuring system as described elsewhere (Shabala and Newman 1999).

2.2.3. Photosynthetic traits and speed of stomatal opening and closure

Measurement of photosynthetic attributes such as CO_2 assimilation rate (*A*), stomatal conductance (*gs*), and leaf internal CO_2 concentration (C_i) were conducted using Li-Cor 6400 gas analyser system (Lincoln, NE, USA) under both saline and non-saline conditions. The measurements were carried out under 1500 µmol m^{-2} s^{-1} photon flux density and 400 µmol mol^{-1} CO_2 concentration background settings. The youngest fully expanded leaf in each plant species was used to determine photosynthetic parameters. All measurements were made between 11 am and 2 pm on five replications per plant species per treatment.

The *A:Ci* measurements began at a CO_2 concentration of 50 µmol mol^{-1} and progressed to 600-800 µmol mol^{-1} with 7 to 9 steps (50, 100, 200, 300, 400, 500, 600, 700 and 800 µmol mol^{-1}. Gas exchange parameters were recorded when steady-state conditions were achieved. The Farquhar et al. model (Farquhar *et al.* 1980) was used to establish the correlation curve of *A* against C_i. Version 2 of the spreadsheet was used (Sharkey 2016) for calculation of the maximum carboxylation rate of Rubisco (Vc_{max}) and rate of RuBP regeneration via electron transport (*J*).

For stomatal speed quantification, time-dependent changes in CO_2 assimilation and stomatal conductance in response to light or darkness were measured. For measurement of the speed of stomatal opening, plants were kept in the dark for 4 h and then exposed to the natural light at the greenhouse. The light intensity in the chamber of LICOR 6400 portable photosynthesis system was set to photon flux of 1500 µmol m^{-2} s^{-1} and gas exchange variables were recorded every 60 seconds until stomatal conductance met the steady-state conditions.

To measure the speed of stomatal closure, plants were moved from greenhouse to the shade house (Photosynthetically active radiation≈10 µmol m^{-2} s^{-1}) and photosynthesis system was set to zero photon flux and then changes in the gas exchange and the rate of CO_2 assimilation were recorded at intervals of 60 seconds. The following settings were performed for both opening and closure measurements: air flow rate: 500 µmol s^{-1}; reference CO_2 concentration: 400 ppm; leaf chamber temperature: 25 °C. To calculate stomatal half-response time, the

stomatal response to light or darkness was normalized on scale of 0 to 100%. Zero percent was set for the zero time point when light or darkness began and 100% was set for final time point when the response reached a steady state. The time at which 50% of stomatal opening or closure had occurred was reported as half-response times.

2.2.4 Stomatal density and area

Stomatal density was determined using the epidermal imprints method. Transparent nail polish was painted on the abaxial surface of the youngest fully expanded leaf of each species. Thin nail polish imprints were peeled off as soon as they had dried (10-15 min after application) and then were mounted on microscope slides. Imprints were then observed at 20X magnification using a light Olympus BX61 microscope and the number of stomata and epidermal cells in a field of view were counted. The stomatal area (μm^2) was reported as the product of guard cell length (μm) and guard cell pair width (μm) (Drake *et al.* 2013). The stomatal index was calculated as the ratio of the number of stomata for a given area divided by the total number of stomata and epidermal cells in that area. Measurements were made on two randomly selected positions on 10 leaves of each plant species per each treatment.

2.2.5 Stomatal response to Na^+ and K^+

Leaves from 4-week-old plants were excised after being in the darkness for 4 h. The epidermal strips from the abaxial side of leaves were peeled using fine forceps and floated in a Petri dish containing bathing solution (1 mM NaCl +1 mM KCl + 0.1 mM $CaCl_2$; pH = 5.6) for 2 h under dark conditions to cease wounding effects induced by peeling the epidermis. Epidermal strips were then transferred to the basic solution (25 mM KCl, 10 mM MES-KOH, pH 6.5, 10 μM $CaCl_2$ or 25 mM NaCl, 10 mM MES-NaOH, pH 6.5, 10 μM $CaCl_2$) and were kept in the darkness for 3 more hours. Then, the stomatal aperture was measured under green light (Eisinger *et al.* 2003) using an optical inverted microscope (Olympus BX61) linked to a camera (ALTRA20) that was connected to a personal computer. The epidermal strips were then transferred to the solutions containing targeted concentrations of Na^+ and K^+ (50 mM KCl, 100 mM KCl, 50 mM NaCl, 100 mM NaCl, 50 mM KCl + 50 mM NaCl, 25 mM KCl + 75 mM NaCl in basic solution) and illuminated by

the light with intensity of 300 µmol m^{-2} s^{-1} photon flux. Stomatal aperture was measured after 3 h.

2.2.6 Dehydration assay

Leaf dehydration assays were carried out according to (Hopper *et al.* 2014). Briefly, intact leaves were sprayed with 50 µM ABA. ABA applied one time in abaxial and adaxial sides of leaves until fully wet. After 30 min, a fully expanded leaf was detached from each species and weighed, then placed in solution containing 300 mM NaCl, and kept in an airtight glass box under light with intensity of 300 µmol m^{-2} s^{-1} photon flux. The leaf weighed every 30 min for 3 h. Water loss was calculated by differences between 2 subsequent weight measurements divided by leaf weight at the beginning of experiment.

2.2.7 Statistical analysis

Statistical analyses were performed with IBM SPSS Statistics software, version 26 (IBM Corp., Armonk, N.Y., USA). Statistical significance was determined by one-way ANOVA analysis based on Duncan's test. The differences between means were considered statistically significant as P-values were less than 0.05%. All graphs and charts were created using Microsoft Excel 10.0.

2.3 Results

2.3.1 Biomass

Dose-dependent effects of salinity on fresh weight (FW) of six studied species are shown in Figure 2.1. Impacts of NaCl on FW differed among species ranged between 2.9 and 1.0 g $plant^{-1}$ in *C. album*, 12.7 and 7.9 in quinoa, 29.2 and 15.7 in cultivated barley, 2.4 and 1.8 in sea barley, 11.6 and 5.5 in sugar beet and 9.7 and 5.6 g $plant^{-1}$ in sea beet over the range of salinity treatments (0 to 500 mM). Cultivated barley did not survive at 400 and 500 mM NaCl.

Stimulated growth has been observed for quinoa and sugar beet grown at 100 mM NaCl as compared to control conditions (18 and 14% increase in FW, respectively). Sea beet FW was also increased by 100 and 200 mM NaCl (14 and 19% over the control, respectively). Sea barley did not demonstrate an increased FW under salt stress. However, declines in FW, even under high salt levels, were not dramatic. Sea barley grown at 500 mM NaCl was able to produce 79% of FW

of the control, while cultivated barley showed most reductions in FW upon exposure to salt stress with an inability to survive at 400 mM and 500 mM NaCl.

Fresh weight in *C. album* gradually declined with increasing salinity levels showing a reduction by 64% at the highest level of salinity, while quinoa (as a halophytic relative of *C. album*) experienced only a 27 % reduction in FW. Sugar beet and its halophytic relative, sea beet, performed almost similar at 100 mM NaCl with 14% and 17% increase in FW. However, reduction in FW was less in sea beet than that in sugar beet at each level of salt concentration in excess of 100 mM NaCl.

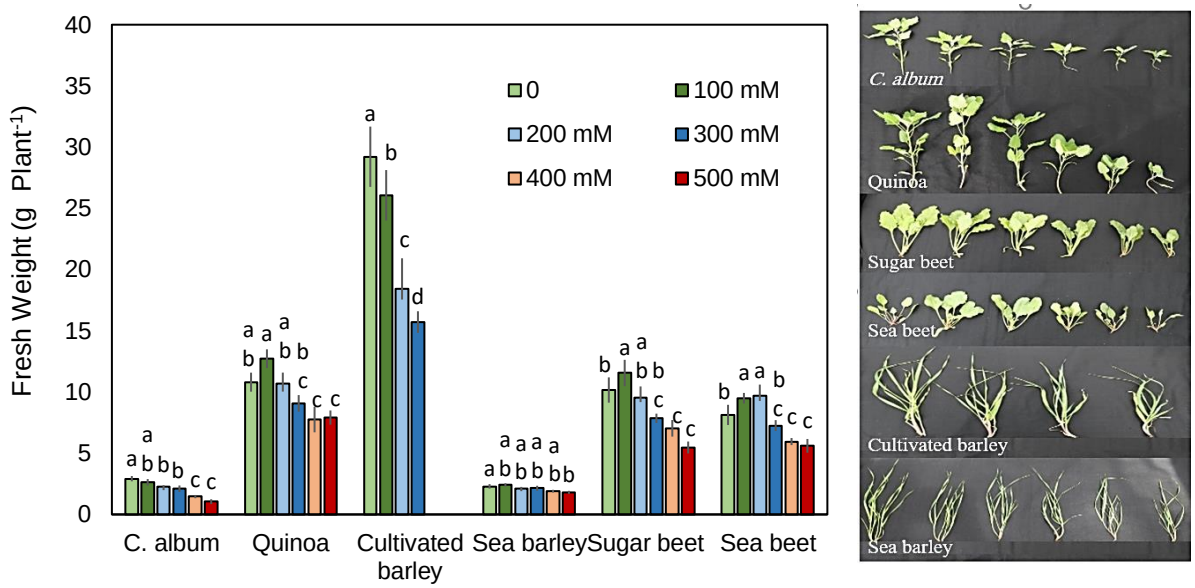

Fig. 2.1 The fresh weight (FW) of halophyte and glycophyte species grown at various concentration of NaCl (from zero to 500 mM). Mean ± SE (n = 5). Data labelled with different lower-case letters are significantly different at $P < 0.05$. Cultivated barley did not survive at 400 and 500 mM NaCl.

2.3.2 Photosynthetic traits

Dose-dependent reduction in stomatal conductance (g_s), internal CO_2 (C_i) and transpiration rate (T) was observed in all species in response to salt stress (Table 2.1). The rates of CO_2 assimilation (A) were inhibited by salinity proportionally to salinity levels in *C. album* and cultivated barley. However, it was not inhibited by salinity in quinoa, sugar beet and sea beet at lower levels of salinity (Table 1.2). In sugar beet grown at 100 mM NaCl, A was 11% higher than that under control

condition. Likewise, in sea beet, *A* was increased by 8% and 22 % at 100 mM and 200 mM NaCl treatments compared to non-stressed plants, respectively.

Table 2.1 Gas exchange parameters of three halophytes species and their glycophyte counterparts. Plants were grown under control and saline. Data labelled with different lower-case letters in each plant are significantly different at $p < 0.05$.

Species	0	100 mM	200 mM	300 mM	400 mM	500 mM
CO_2 assimilation rate (µmol CO_2 m^{-2} s^{-1})						
C. album	14.4a	11.7b	12.2b	9.6c	9.31c	6.0d
Quinoa	15.4a	16.4a	15.2a	13.1ab	11.5b	11.6b
Cultivated barley	15.4a	13.2b	10.8c	9.5c	*	*
Sea barley	21.3a	20.6a	18.6b	15.6c	12.2d	11.9d
Sugar beet	13.4ab	14.9a	11.9b	10.0c	8.31cd	6.5d
Sea beet	15.3bc	16.6ab	18.7a	15.4bc	13.7bc	13.1c
Stomatal conductance (mol H_2O m^{-2} s^{-1})						
C. album	0.29a	0.22b	0.16c	0.09d	0.06de	0.046e
Quinoa	0.35a	0.28b	0.14c	0.11cd	0.10d	0.091d
Cultivated barley	0.64a	0.45b	0.10c	0.07d	*	*
Sea barley	0.54a	0.33b	0.16c	0.13d	0.087e	0.087e
Sugar beet	0.33a	0.29b	0.12c	0.09d	0.087de	0.064e
Sea beet	0.49a	0.41b	0.30c	0.13d	0.09de	0.075e
Transpiration rate (mmol H_2O m^{-2} s^{-1})						
C. album	3.29a	2.36b	1.71c	1.06d	0.79de	0.54e
Quinoa	2.82a	2.63a	1.90b	1.23bc	1.04c	0.99c
Cultivated barley	4.33a	3.36b	1.16c	0.79d	*	*
Sea barley	5.52a	3.48b	2.00c	1.57d	1.13e	1.13e
Sugar beet	2.93a	2.67a	1.44b	0.99c	1.07c	0.85c
Sea beet	3.85a	3.16b	2.68b	1.40c	1.05cd	0.87d
Internal CO_2 (µmol CO_2 mol air^{-1})						
C. album	326a	287b	255c	208d	148e	158e
Quinoa	293a	285a	259b	228c	184d	178d
Sea barley	315a	278b	194c	186cd	161d	166d
Sugar beet	302a	288ab	222b	199c	196c	184d
Sugar beet	302a	288a	222b	199bc	196bc	184c
Sea beet	317a	298b	261c	216d	198e	189e

Quinoa also showed no reduction in CO_2 assimilation up to 200 mM NaCl. No significant differences for *A values* between plants grown under control and 100 mM NaCl conditions were also found in sea barley. These results showed that in salt-grown halophytes, the CO_2 assimilation rate is largely uncoupled from stomatal conductance. As a result, these plants were able to enhance their FW under saline conditions by maintaining a high level of carbon assimilation under low to medium salinity levels (Table 2.1).

Steady state g_s varied by two-fold among the studied species, with cultivated barley, sea barley and sea beet plants showing the highest levels of g_s and *C. album*, quinoa and sugar beet had the lowest values (Table 2.1).

Watering plants with saline solutions resulted in a noticeable reduction in the rate of transpiration in a dose-dependent manner irrespective of the plant species. Losing water through the transpiration process was higher in cultivated barley, sea barley and sea beet with respect to all other plants in both control and salt-treated plants. *C. album* and sugar beet had the lowest transpiration rates compared to other plant species.

A significant decrease in *Ci* values were also found under salt stress in all species (Table 2.1). At the highest level of salinity, *Ci* declined by 51% and 39%, in *C. album* and quinoa, 52% and 47%, in cultivated barley and sea barley and 39% and 41% in sugar beet and sea beet.

In addition to stomatal factors, biochemical processes which are performed in the cytosol, chloroplast and mitochondria determine the capacity of a plant for the net rate of CO_2 assimilation (known as non-stomatal factors) (Sharkey et al. 2007). The extent to which non-stomatal limitations impact the photosynthesis capacity is determined by analysing the response of the rate of CO_2 assimilation to changing internal CO_2 concentrations (*A*:*Ci* curve). Here, the initial slope of the *A*:*Ci* response curve is a function of the CO_2 concentration and Rubisco activity and defines as the maximum carboxylation rate of Rubisco (Vc_{max}). The response of CO_2 assimilation rate to a higher concentration of CO_2 is dependent on rate of electron transport through photosystem II (*J*) for regeneration of RuBP.

Two parameters derived from *A*:*Ci* response curves are shown in Figure 2.2 A-B. The maximum carboxylation rate of Rubisco in cultivated barley and sea barley were 82 and 113 μmol m^{-2} s^{-1} under non-stressed conditions respectively,

which remained unchanged in sea barley under 100 mM NaCl; Vc_{max} then progressively decreased with higher salinity levels (Fig. 2.2A) in cultivated barley and sea barley. Vc_{max} in quinoa and sea beet were not significantly altered by salt concentrations lower than 400 mM and 500 mM NaCl respectively, suggesting that Rubisco activity or its amount was not a limiting factor for CO_2 assimilation in some halophytes grown under high salinity levels (Fig. 2.2A).

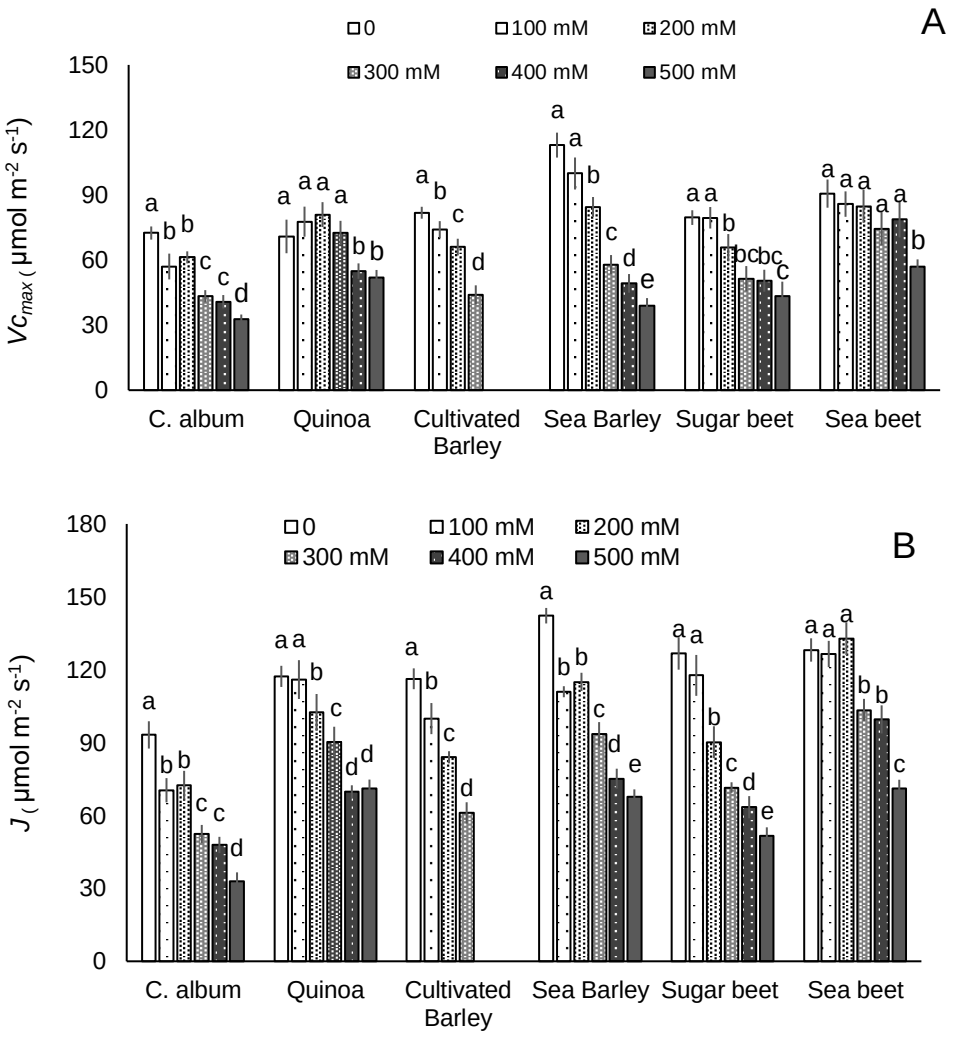

Fig. 2.2 Parameters derived from *A:Ci* response curves of halophytes and glycophytes under control and saline (100, 200, 300, 400, and 500 NaCl) conditions. (A) The maximum rate of Rubisco carboxylation (Vc_{max}). (B) rate of RuBP regeneration controlled by electron transport rate (*J*). Both Vc_{max} and *J* reported as µmol m^{-2} s^{-1}. Mean ± SE (n = 3). Data labelled with different lower-case letters are significantly different at $P < 0.05$. Cultivated barley did not survive at 400 and 500 mM NaCl.

Another biochemical process that can limit the rate of CO_2 assimilation under saline condition is a change in the rate of electron transport for the regeneration of substrate for the next cycle of carbon assimilation. This stage involves the situation in which enzymes of the Calvin cycle other than Rubisco restrict the rate of CO_2 assimilation. Results in Figure 2.2B show that rate of RuBP regeneration continuously decreased with increasing salinity level in cultivated barley amounting to 47% of that in the non-stressed plants. *C. album*, sea barley and sugar beet also displayed a marked (49-52%) decrease in *J* at the highest concentrations of NaCl. However, this parameter was least affected by salinity in quinoa and sea beet, suggesting that higher rate of RuBP synthesis and correspondingly higher carboxylation of CO_2 occurred in some halophytes at the same concentration of NaCl.

2.3.3 Ion content

Concentrations of Na^+, K^+, and Cl^- in leaf tissues are shown in Figure 2.3. The Na^+ and Cl^- concentrations gradually increased with the increasing salinity level in all species. *C. album* and quinoa accumulated less amount of Na^+ in their leaves compared to other species. The concentrations of Na^+ in quinoa were 5, 64, 143, 185, 235, 245 mM in control, 100, 200, 300, 400 and 500 mM NaCl respectively. corresponding values for *C. album* were 5, 41, 114, 171, 269 and 304 mM. The concentrations of Na^+ in sugar beet and sea beet were 19 and 20 mM at control conditions which reached 374 and 409 mM at 500 mM NaCl. A comparison of sea beet with its glycophytic relative showed that halophytic plant had higher Na^+ content in leaves in each level of salinity. Quinoa stored more Na^+ at low/medium salinity levels and less Na^+ at 400 and 500 mM NaCl compared to *C. album* (Fig. 2.3A). In grasses, sea barley showed less amount of Na^+ in its leaves compared with cultivated barley.

Potassium concentrations decreased in parallel with increasing salinity levels in cultivated barley and sugar beet and in their halophytic relatives. However, increased K^+ concentrations were found in *C. album* and quinoa leaves with increasing salinity levels. Under non-saline conditions, the K^+ concentrations were 235 and 302 mM in *C. album* and quinoa leaves respectively, and then increased to 461 and 541 mM, respectively, at 500 mM NaCl treatments (Fig. 2.3B).

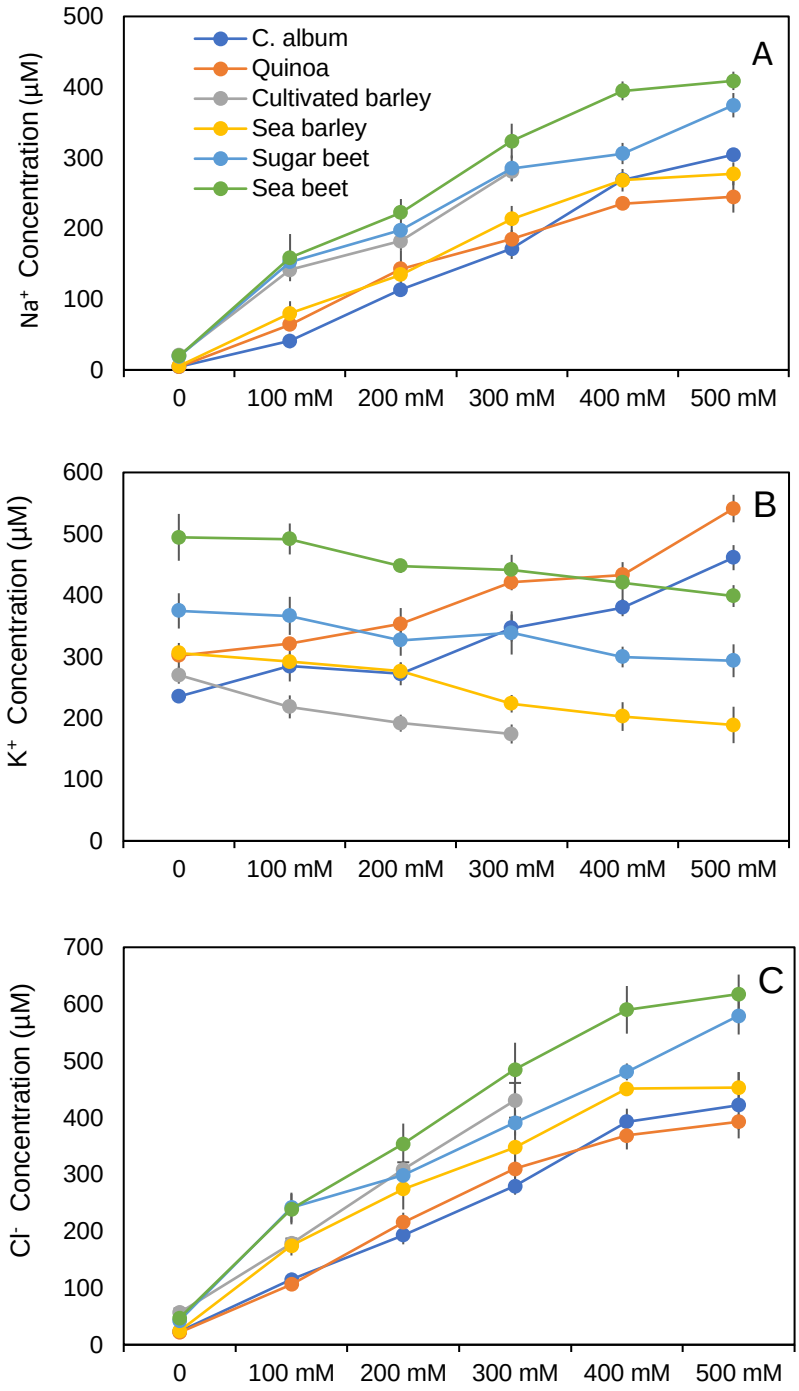

Fig. 2.3 Ion composition in leaf sap of the studied halophytes and their glycophyes counterparts in response to varying salinity level. (A) sodium, (B) potassium, and (C) chloride. Plants were grown under control and saline (100, 200, 300, 400, and 500 NaCl) conditions. Mean ± SE (n = 5). Cultivated barley did not survive at 400 and 500 mM NaCl.

Comparison of each glycophytic species with its halophytic relative revealed no significant differences in Cl^- concentration between these two groups for 100 mM NaCl treatment, while 11% and 20% lower Cl^- was observed in sea barley compared to cultivated barley at 200 mM and 300 mM salt concentrations. Cl^- concentrations in sugar beet and sea beet leaves displayed insignificant different at 100 mM salt concentrations. Sea beet contained 7-24% more Cl^- over its glycophytic counterpart at higher levels of NaCl. Comparable Cl^- concentrations were observed in each level of salinity in quinoa and *C. album* (Fig. 2.3C). These results show that halophytes may use different strategies for combating salt stress. Halophytic barley (sea barley) tends to accumulate less ions compared to its glycophytic relative, while halophyte sea beet showed higher leaf ion contents than glycophyte sugar beet.

2.3.4 Stomatal density and index

NaCl resulted in a significant decrease in stomatal density in *C. album* and quinoa (Fig. 2.4). The maximum number of stomata were 198 and 129 cells per mm^2 in *C. album* and quinoa respectively; these were observed under non-stressed conditions. While in plants grown at 500 mM NaCl, stomatal densities decreased to 123 and 65 cells per mm^2 in *C. album* and quinoa, respectively (Fig. 2.4A). For quinoa the biggest drop in stomatal density occurred at 100 mM NaCl, while the biggest drop for *C. album* happens at 300-400 mM NaCl. On the contrary, an increase in the number of stomata was observed in cultivated barley (23.8%), sea barley (51.2%) and sugar beet (27%). In the sea beet, stomatal densities remained unchanged with salinity (Fig. 2.4B-C).

Compared to glycophytic species, halophytic plants demonstrated a lower density of stomata for each level of salinity (Fig. 2.4). Cultivated barley had twice more stomata per leaf area than sea barley. *C. album* and sugar beet had 1.7 and 1.6-fold higher stomatal density than their halophytic relative counterparts, for same conditions (Fig. 2.4A-C).

The effect of salinity on stomatal development can be assessed by calculating the stomatal index, a ratio between the number of stomata to the epidermal cells per unit of leaf area. In this investigation, the stomatal index decreased under saline conditions in *C. album*, quinoa, and sea barley. Changes in

stomatal index in cultivated barley, sugar beet and sea beet were not statistically significant (Fig. 2.5).

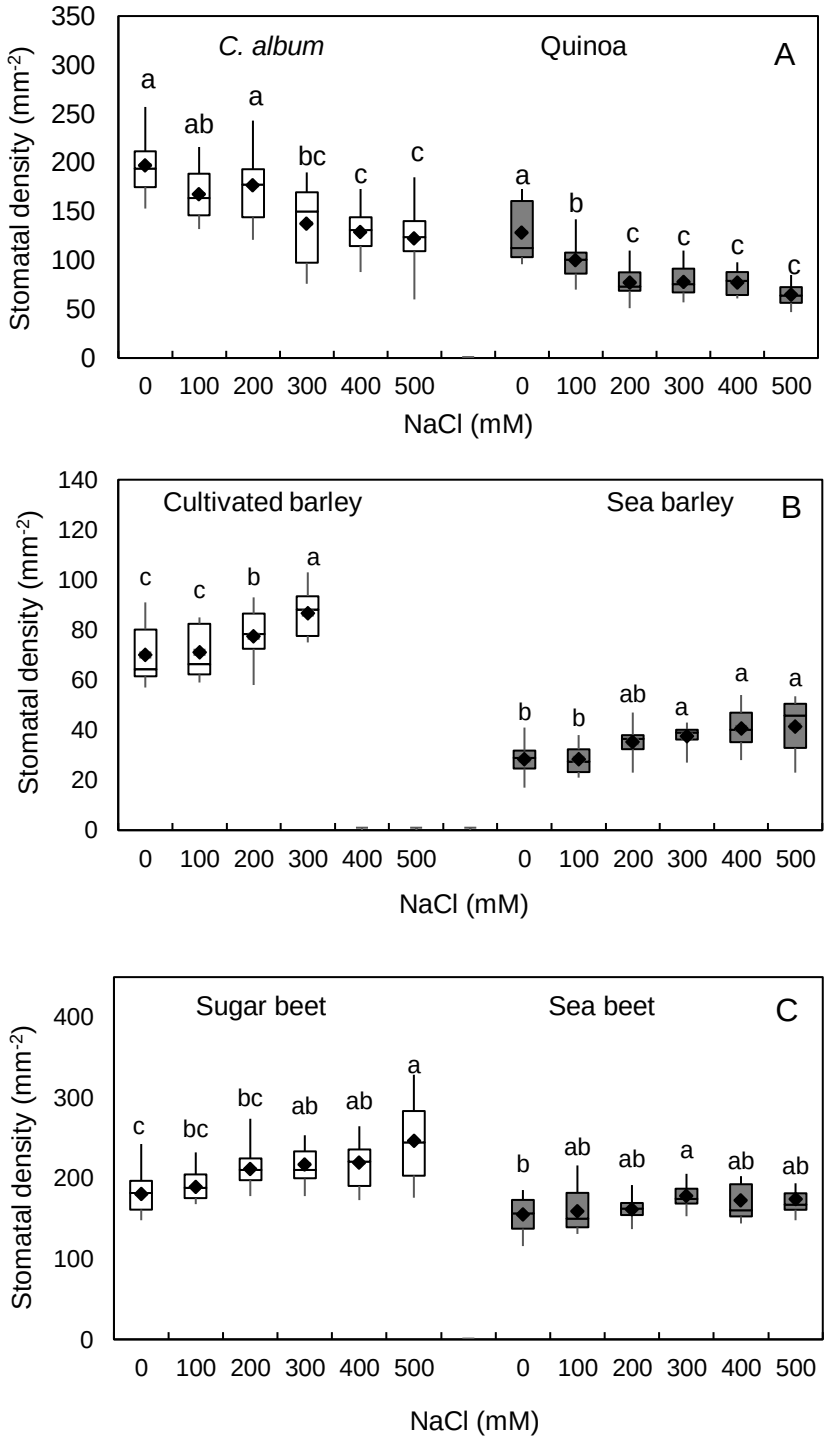

Fig. 2.4 Stomatal density of plants grown under control and saline (100, 200, 300, 400, and 500 NaCl) conditions. Mean ± SE (n = 10). Data labelled with different lower-case letters are significantly different at $P < 0.05$. Cultivated barley did not survive at 400 and 500 mM NaCl.

2.3.5 Stomatal pore area

Given that both stomatal length and width may affect by salinity stress, in our study we reported the product of length and width of the stomata as stomatal pore area (Drake *et al.* 2013). Our results revealed that stomatal size responses to salinity stress were different among studied plant species. The stomatal pore areas remained unchanged in quinoa at 100 mM NaCl while higher salt concentrations decreased stomatal size where it reduced by 38% at 200 mM NaCl and then remained constant in higher salinity levels (Fig. 2.6). In *C. album* and sugar beet, declining in stomatal pore area occurred when plants were grown at 300 and 400 mM NaCl, respectively. Reductions of 23% and 32% were observed in *C. album* and sugar beet respectively under above mentioned salinity levels. The high concentration of NaCl had a significant effect on stomatal pore size in sea barley where stomatal sizes were reduced by 22% and 23% at 400 and 500 mM NaCl, respectively. Stomatal size in sea beet was also affected at 200 mM NaCl, (27% reduction) and no dramatic change was observed by applying higher NaCl concentrations (Fig. 2.6).

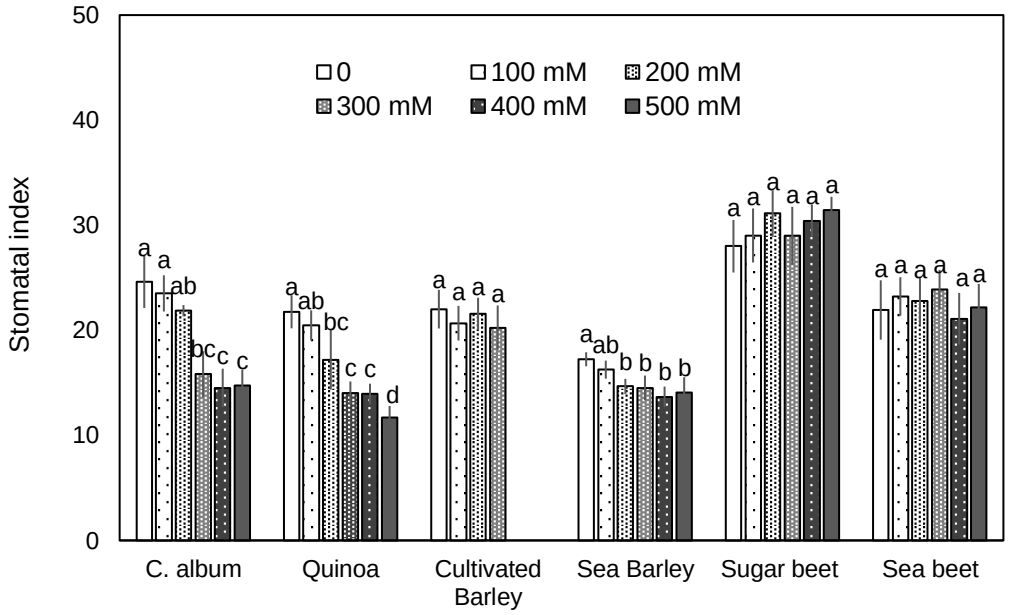

Fig. 2.5 Changes in stomatal index (% of pavement cells) of studied halophytes and glycophyes species. Plants were grown under control and saline (100, 200, 300, 400, and 500 mM NaCl) conditions. Mean ± SE (n = 15). Data labelled with different lower-case letters are significantly different at $P < 0.05$. Cultivated barley did not survive at 400 and 500 mM NaCl.

The stomatal pore sizes in quinoa, sea barley, and sea beet were smaller than their glycophyte relatives at each level of salinity suggesting that smaller size of stomata in halophytic species can support water conservation under hyperosmotic saline conditions.

2.3.6 The speed of stomatal opening and closure

The speed of stomatal movement is important as it determines to what extent the ratio of CO_2 assimilation rate to transpiration rate can be optimized (Lawson and Vialet-Chabrand 2019). Fast stomatal responses to environmental factors enable plants to cope with natural dynamic environments and provide superiority in regard to CO_2 up take and prevention of losing water (Kubarsepp *et al.* 2020).

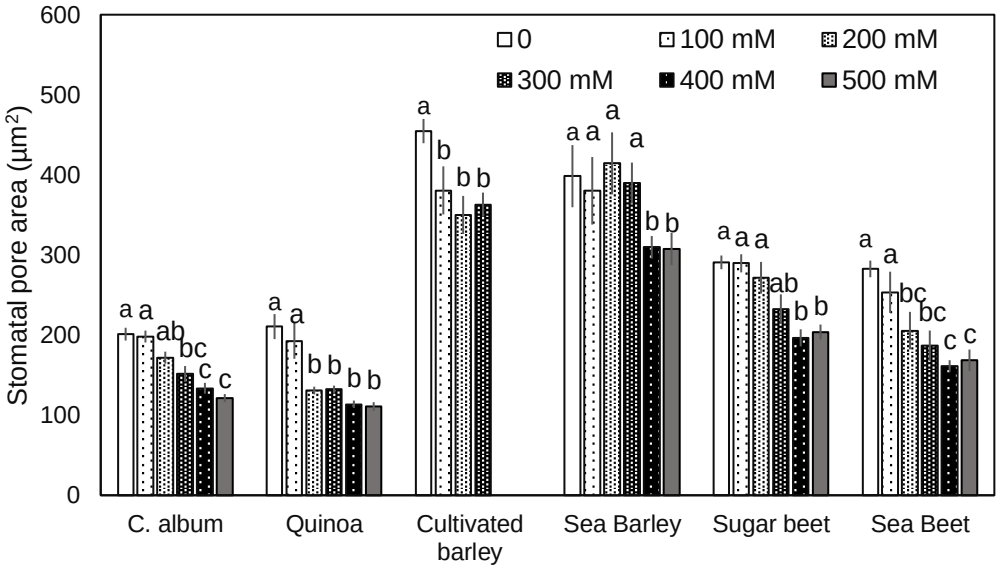

Fig. 2.6 Changes in stomatal size (area) of studied halophyte and glycophyte plants grown under control and saline (100, 200, 300, 400, and 500 NaCl) conditions. Mean ± SE (n = 15). Data labelled with different lower-case letters are significantly different at $P < 0.05$. Cultivated barley did not survive at 400 and 500 mM NaCl.

The time-series of CO_2 assimilation rate and stomatal opening and closure in both illumination and darkening phases are shown in Figure 2.7. Stomatal opening and closure in response to light and darkness followed similar pattern in all halophytes and glycophytes, increasing following the onset of illumination and reaching a maximum steady state value, and then started to decline with darkening of plants (reaching a minimum steady state value). Changes in CO_2 assimilation

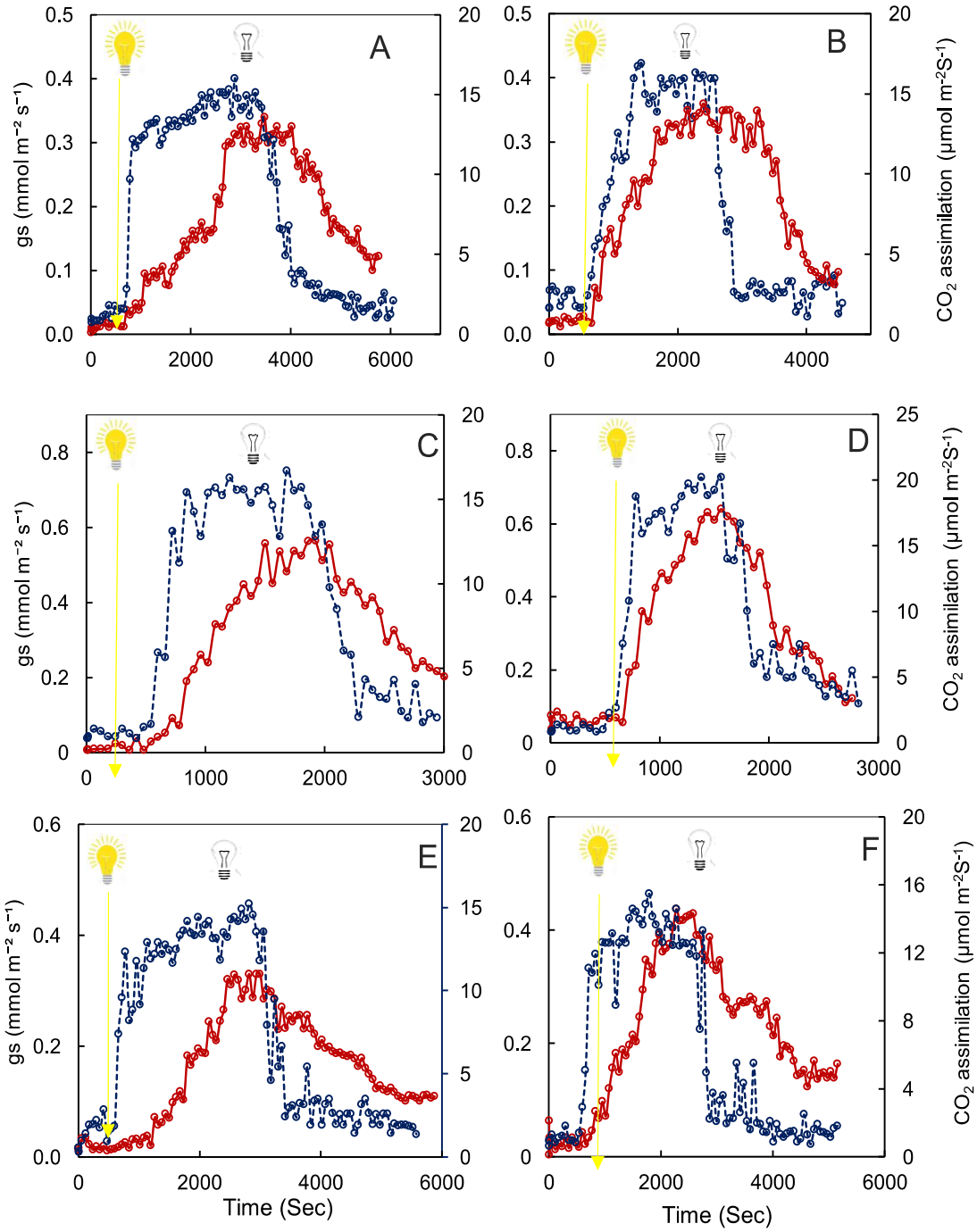

Fig. 2.7 Time-series of CO_2 assimilation rate (red line) and stomatal conductance (gs) as a measure of opening and closure of stomata in response to (blue line) illumination and darkening. The experiments for each species were conducted three times and typical data were exhibited. A: *C. album*, B: Quinoa, C: Cultivated barley, D: Sea barley, E: Sugar beet, F: Sea beet.

rate were accompanied by changes in stomatal conductance, increasing at the stomatal opening phase, and decreasing during stomatal closure. However, steady-state values for CO_2 assimilations were always achieved prior to those for stomatal conductance in both stage of illuminating and darkening (Fig. 2.7).

Given that the response of either stomatal kinetics or CO_2 assimilations in time are in a sigmoid pattern (Fg.2.7), half-response times are more appropriate for demonstrating the speed of stomatal reactions or CO_2 assimilations. The half-response times were derived from time-series responses curves and presented in Fig. 2.8A, B.

Calculated half-response opening time, which define as the required time for g_s to reach 50% of maximum level were 21.8, 10.9, 20.8 and 17.1 minutes in *C. album*, quinoa, sugar beet, and sea beet, respectively. Half-response times of opening for cultivated barley and sea barley as monocot species, were shorter than those in dicotyledonous species equaling to 9.2 and 6.4 minutes, respectively. Stomatal closing was relatively slower than opening as is evident from the data obtained from half time stomatal measurements in darkness. In all species, the half-time values for closure were significantly higher than those for opening (Fig. 2.8). Half-times for CO_2 assimilation rate in response to light /darkness were shorter than those for stomatal conductance (Fig. 2.7A-F). Half-time response of CO_2 assimilation in response to light was found to be between 3.2 and 5.9 minutes in different species with minimum values for cultivated barley and sea barley. All species had slow reactions to darkness. Similar to what was observed in stomatal conductance response, half-time responses of CO_2 assimilation increased by 57-114% in different species in response to darkness.

As illustrated in Figure 2.9, reduced responses to darkness were observed in plants grown at 300 mM salt stress. Therefore, it took more time for guard cells to mediate stomatal closure when plants were under stress.

2.3.7 The response of stomata to Na^+ and K^+

The ability of stomata to be open in the presence of Na^+ in leaf apoplast were studied in experiments on epidermal strips by substituting K^+ with Na^+ and measuring increases in stomatal aperture compared to aperture of stomata in dark-incubated strips in the basic solution (Fig. 2.10).

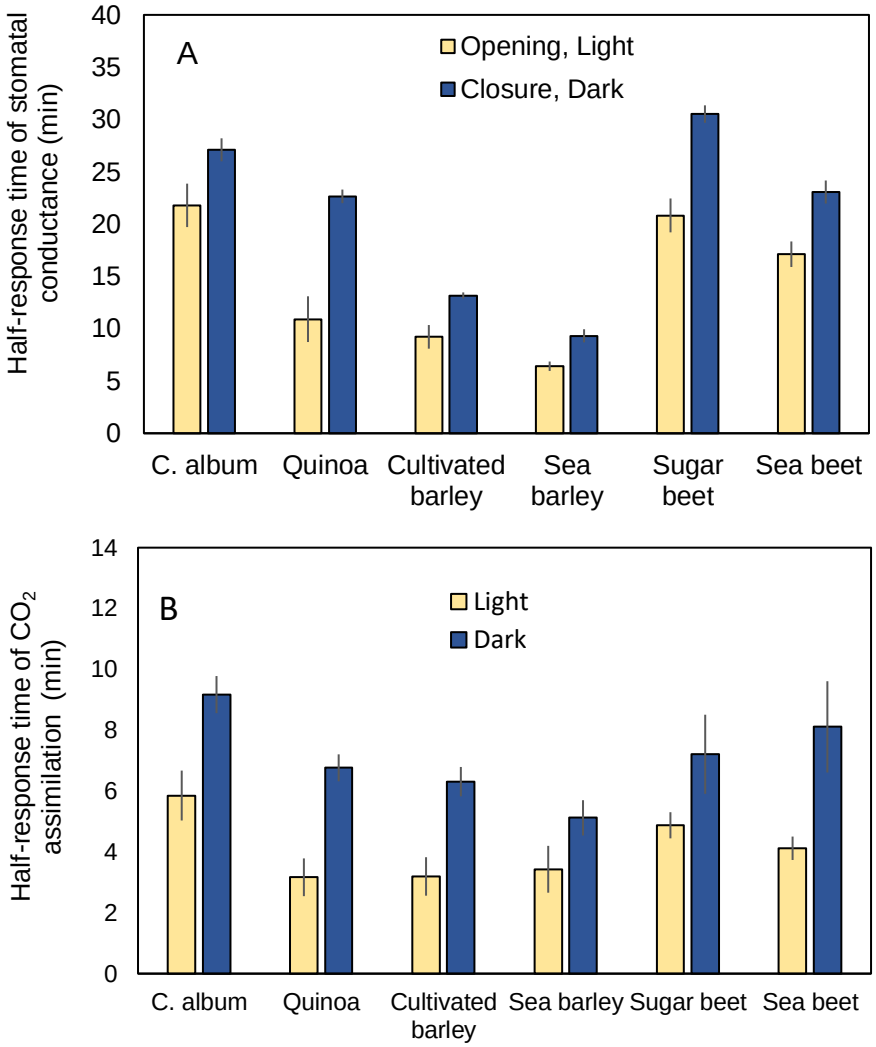

Fig. 2.8 Half-time stomatal opening and closing in response to light and darkness (A). Half-time of CO_2 assimilation response to light and darkness (B). Half-response times were calculated from the times at which light/darkness were commenced to the times at which 50% of the maximal responses were occurred.

We found that incubation of epidermal strips in the solution containing 100% K^+ (100 mM KCl) was the most optimal for stomatal opening in all species. A higher concentration of K^+ was associated with a wider aperture of stomata. In the presence of 100% Na^+ (50 and 100 mM NaCl), increased in the stomatal opening were still observed, however with smaller extend than 100% K^+. The combination of 50 mM K^+ and 50 mM Na^+ was equally as effective as 100% K^+ for stomatal opening in quinoa. In quinoa even lower ratios of K^+/Na^+ (25% K^+ and 75% Na^+) promoted as same degree of stomatal opening as 100% K^+. In sea barley K^+ stimulated stomatal

opening and Na^+ (without K^+) in apoplast resulted in smaller stomata apertures. As illustrated in Figure 2.10, a link between ratio of the appoplastic K^+/Na^+ and degree of stomatal opening was evident in cultivated barley and see barley. In the sugar beet and sea beet, replacing 50 or 75 % of K^+ with Na^+ reduced stomatal aperture compared to those in the 100% K^+.

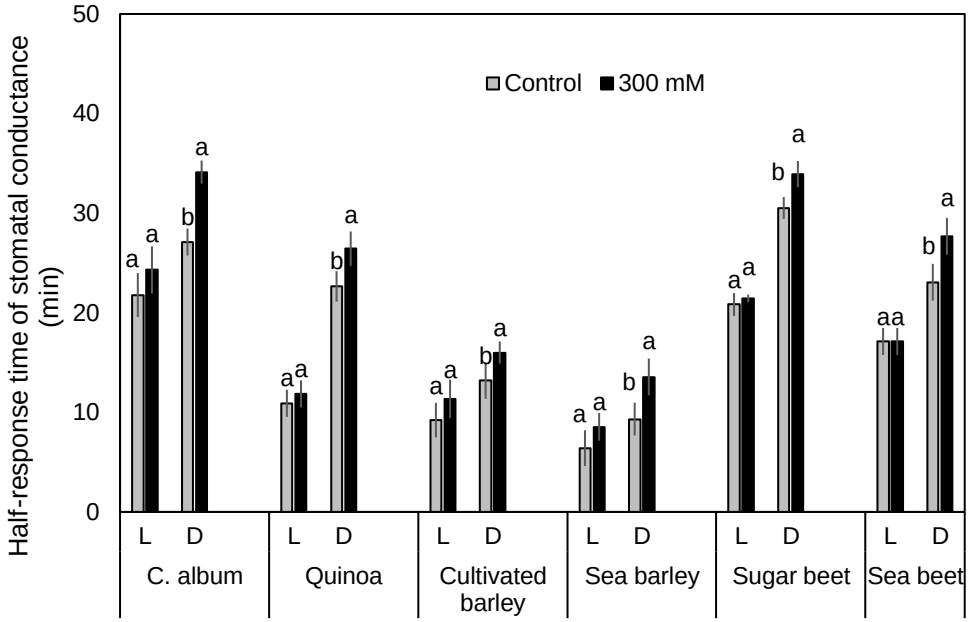

Fig. 2.9 A speed of stomatal opening (response to light: L) and stomatal closure (response to darkness: D) in halophyte and glycophyte plants grown under control and 300 mM NaCl conditions. Measurements were recorded at intervals of 60 seconds under the following conditions: leaf temperature:25°C, reference CO_2: 400 ppm, and leaf VPD: 1 kPa. Mean ± SE (n = 3). Data labelled with different lower-case letters are significantly different at $P < 0.05$.

A comparison of glycophyes with their relative halophytes showed that there are significantly lower stomatal apertures by 100 mM K^+ in quinoa, sea barley and sea beet compared to their glycophytes. The stomatal response of barley vs. sea barley and sugar beet vs. sea beet to different concentration of K^+ and Na^+ were similar. However, quinoa and *C. album* showed significant differences in stomatal aperture at solution containing different combination of K^+ and Na^+ (50 mM K^+ + 50 mM Na^+ and 25 mM K^+ + 75 mM Na^+) where larger stomatal apertures were observed in quinoa in solutions containing both K^+ and Na^+.

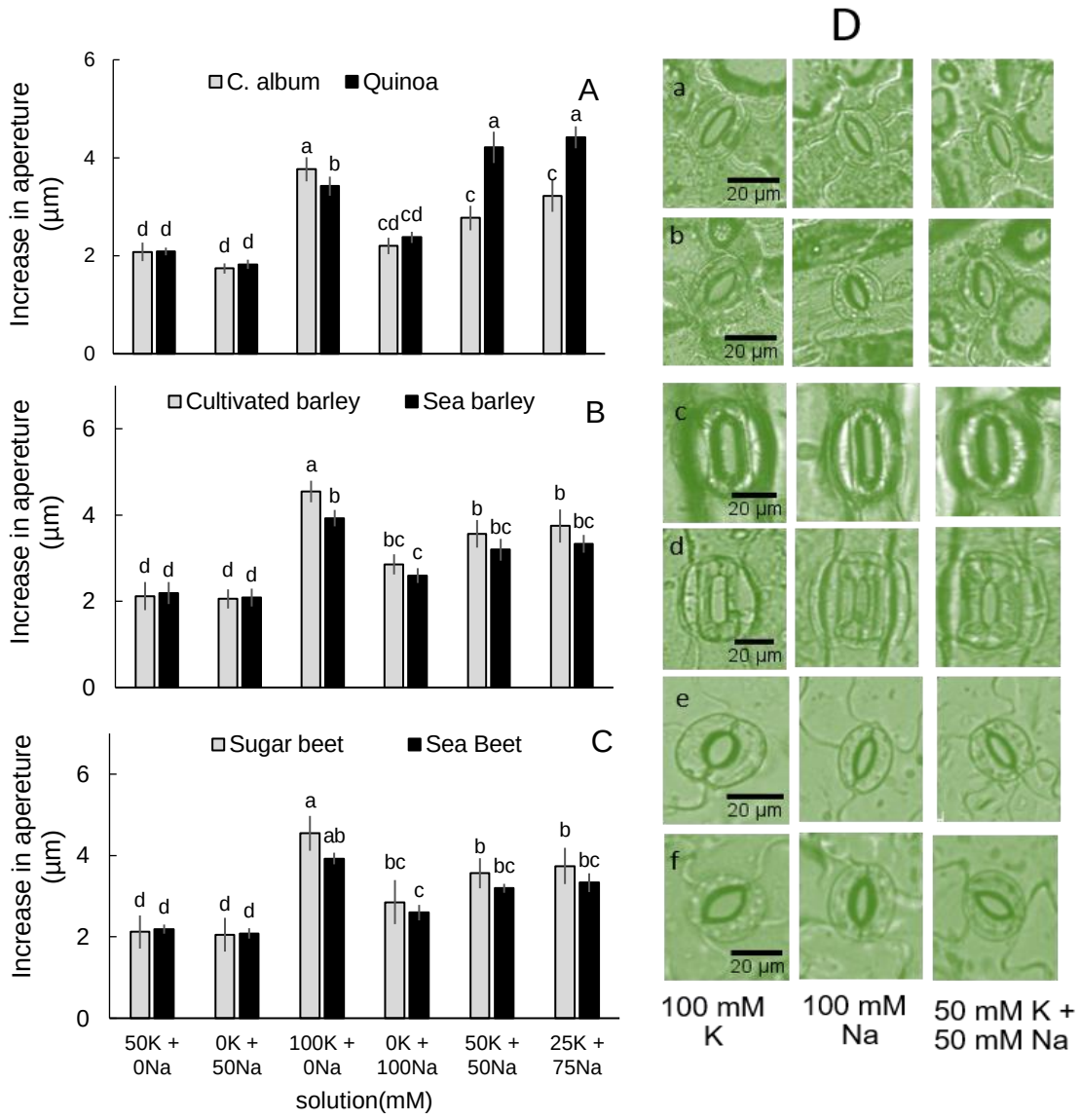

Fig. 2.10 Differences in stomatal aperture in epidermal strips incubated in various ion solutions. Epidermal strips were peeled off from fully expanded leaves of 4-week old plants grown under non-stress condition and were incubated in basic solution in darkness for 3 h. Stomatal apertures were then measured. Then epidermal strips were transfer into solutions containing different concentration of KCl and NaCl and exposed to light for 3 h. Then stomatal apertures were measured again. Differences between opening at dark and opening at light were reported as increase in stomatal aperture. (A): *C. album*, and Quinoa, (B): Cultivated barley and Sea barley, (C): Sugar beet and Sea beet. (D): Microscopic image of stomata aperture in epidermal strip (a - *C. album*; b - Quinoa; c - Cultivated barley; d - Sea barley; e - Sugar beet; f - Sea beet).

2.3.8. Leaf K^+/Na^+ selectivity and dehydration assay

K^+/Na^+ selectivity has been suggested to be a suitable proxy for plant salt tolerance (Ashraf *et al.* 2005; Rahman *et al.* 2017). In our report, studied species displayed a considerable variation in terms of K^+ versus Na^+ selectivity. Average of pooled K^+/Na^+ selectivity obtained from six levels of salinity for each plant are presented in Figure 2.11. This ratio was distinctively higher in halophytes compared to glycophyes suggesting that halophytes' leaves possess an ability to discriminate K^+ over Na^+ from a high-Na^+ content solution and maintain higher level of K^+ in their leaves through K^+ selective capacity.

Leaf water content is regarded as one of the physiological parameters that could limit photosynthesis efficiency and consequently biomass production. In the present study, quinoa, sea barley and sea beet leaves displayed significantly higher water content than their relative glycophytes upon exposure to 300 mM NaCl and ABA application (Fig. 2.12).

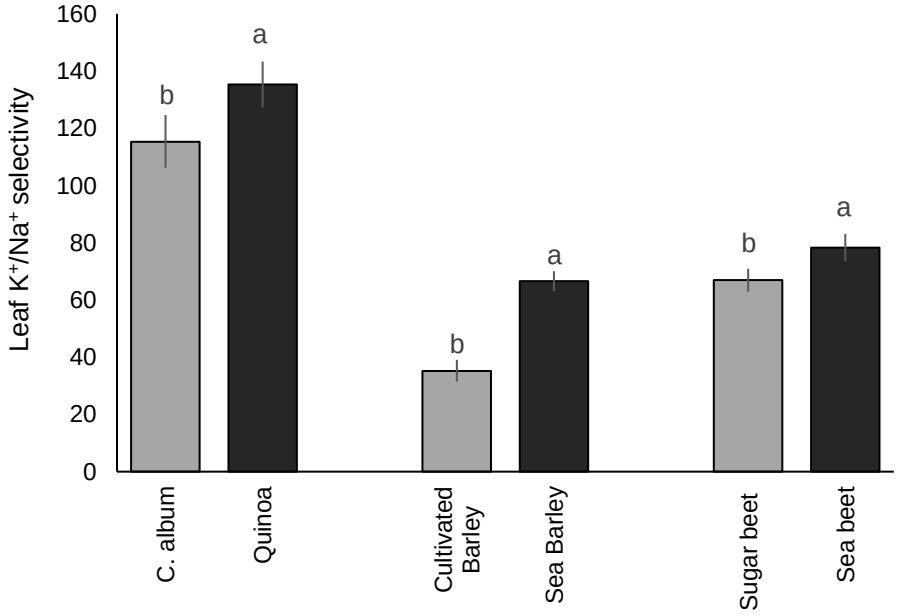

Fig. 2.11 Changes in K^+/Na^+ selectivity of studied halophyte and glycophyte plants. Values are means of 5 biological and 6 salinity levels. Asterisk (*) denotes a significant K^+/Na^+ selectivity difference between halophytes and glycophytes (Student's t test, $p < 0.05$).

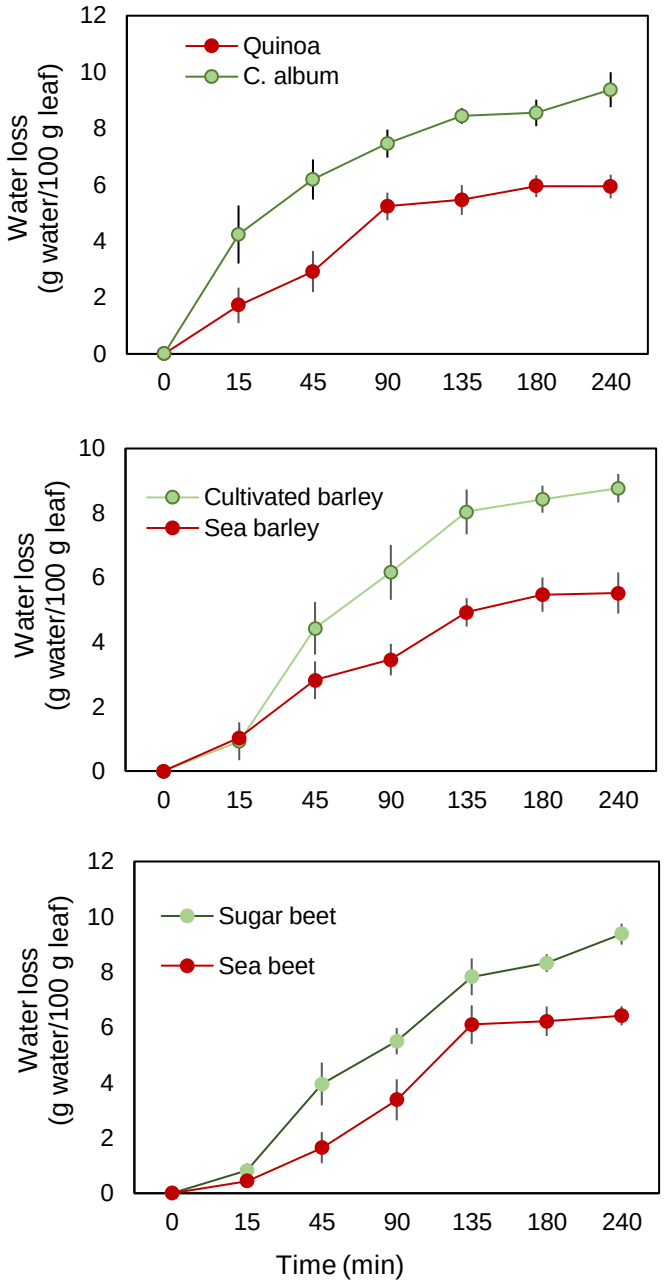

Fig. 2.12 Leaf dehydration assay of studied halophyte and glycophyte plants. Values are means of 5 biological replicates. Intact leaves were sprayed with 50 µM ABA. After 30 min, A leaf was detached from each species and weighed, then placed in solution containing 300 mM NaCl, and kept in an airtight glass box under light with intensity of 300 µmol m^{-2} s^{-1} photon flux. The leaf weighed every 30 min for 3 h. Water loss was calculated as a difference between 2 consequent weight measurements per leaf basis.

2.4 Discussion

2.4.1 Ionic regulation strategies were even diverse among halophytes

Four species in this work belong to Amaranthaceae family, with quinoa and *C. album* from the Chenopodium genus and sugar beet and sea beet from the Beta genus while two other species, cultivated barley and sea barley, belong to the grass family. Results obtained from this study revealed that ionic regulation strategies may differ among halophytes. In this context, our results showed that Na^+ concentration in sea beet (halophyte) leaves was 27% higher than that in sugar beet (glycophyte) (Fig. 2.3A). However, Na^+ content in sea barley was 31% lower than that in cultivated barley (Fig. 2.3A) suggesting that contrary to sea beet, sea barley can firmly restrict Na^+ uptake. In respect to this result, it has been reported that halophytic grasses use efficient Na^+ exclusion mechanisms rather than relying on Na^+ sequestration mechanisms that broadly employed by dicot halophytes (Rozema and Schat 2013).

Sugar beet is among recently domesticated crop adopted from its wild ancestors, *Beta maritima*, which is native to the coastal saline area (Skorupa *et al.* 2019). Sugar beet has not been adversely affected by domestication process and it has maintained salinity tolerance mechanisms (Rozema *et al.* 2014). Other studies, however, claimed that some tolerance mechanisms in sugar beet have been lost during domestication and they are manifested when sugar beet expose to salt stress for a long time (Skorupa *et al.* 2019). Thus, being technically classified as a glycophyte, this species displays relatively high salt-tolerance especially in vegetative stage and is often referred as *halophitic* in the literature. In our study, sugar beet demonstrated a stimulated growth under three-week-long exposition to the 100 mM NaCl. In sea beet, the optimal growth was achieved at 300 mM NaCl (Fig 2.1). Interestingly, at all external NaCl concentrations, the overall Na^+ content in plant shoots was significantly higher in sea beet, while K^+ levels remain largely unchanged (Fig 3B). This data is suggestive of an ability of species in genus Beta to use Na^+ for osmotic adjustment and turgor maintenance (Przemysław *et al.* 2018).

In a contrast, both species from Chenopodium genus showed a dose-depending increase in shoot K^+ content, while at higher salinity levels (above 300 mM) halophyte (*C. quinoa*) species had lesser Na^+ content compared with its

glycophytic relative *C. album*. While salinity stress can trigger the K^+ efflux from the cell membrane and reduce the K^+/Na^+ ratio (Percey *et al.* 2016; Gul *et al.* 2019) a recent study showed that of 114 quinoa accessions grown under 400 mM NaCl, 101 accessions had higher K^+ concentration compared to control conditions in quinoa (Kiani-Pouya *et al.* 2019a). Taken together, the data suggest that species in Chenopodium genus have a better ability to acquire K^+ and deliver it to the shoot, even under conditions of high salinity.

2.4.2 The CO_2 assimilation rate, maximum rate of Rubisco carboxylation (V_{cmax}) and a rate of electron transport through photosystem II for regeneration of RuBP (J) were higher in halophytic species.

The data presented here revealed that in glycophytes (except for sugar beet), a decline in CO_2 assimilation is directly associated with reduced stomatal conductance (Mohamed *et al.* 2020). Interestingly, NaCl-induced reductions in stomatal conductance and internal CO_2 were not quite coincident with changes in the rate of CO_2 assimilation for halophytic species and sugar beet where the rate of CO_2 assimilation remained unchanged or even increased at 100 and 200 mM NaCl, while stomatal conductance and internal CO_2 significantly decreased, suggesting that halophytic species were able to retain water through reduced stomatal conductance without penalty in the rate of CO_2 assimilation or fresh weight production at salinity levels under 300 mM NaCl.

At higher salinity levels, stomatal conductance and internal CO_2 and the rate of CO_2 assimilation were reduced simultaneously suggesting that biophysical processes such as CO_2 transport between leaves and atmosphere might be the main factors associated with lower photosynthesis capacity of halophytes under high saline conditions.

The extent of stomatal limitation on the rate of CO_2 assimilation depends on the magnitude of reduction in the internal CO_2 content (Sharkey *et al.* 2007). Declining in stomatal conductance is associated with minimizing water loss, however, it also decreases the diffusion of CO_2, leading to lowered carboxylation efficiency in plants. In the first stage of carbon assimilation, CO_2 is incorporated into RuBP (a five-carbon sugar) by the enzyme Rubisco, and at the final stage, RuBP is regenerated to continue the next cycle of CO_2 fixation (Sharkey 2016). While Rubisco activity is reduced by salt stress in sensitive plants (Aragão *et al.*

2005) an increase in Rubisco activity has been reported in *Halogeton glomeratus*, a succulent halophyte from the Chenopodiaceae family (Wang *et al.* 2015) and in wild halophytic rice (Sengupta and Majumder 2009). In this study, although Rubisco activity demonstrated high resistance to salinity in halophytes quinoa and sea beet, it showed moderate resistance to salt stress in sea barley (Fig. 2.2) suggesting that there was different capability for this trait among halophytes.

The results also revealed a reduction in *J* that occurred in lower concentrations of NaCl (Fig. 2.2). Unlike V_{cmax}, *J* is sensitive to environmental fluctuations and can have a wide variation across different plant species (Ge *et al.* 2014) because this process depends upon sufficient electron translocation from photosystem II which might be adversely impacted by salinity stress.

2.4.3 Halophytic species possess less stomatal density under control and saline conditions

Stomata and guard cells features exhibit a wide range of sizes, morphology and, numbers even within a species (Ge *et al.* 2014). Stomatal size and density of a specific species may also vary among various environments, suggesting that plants are able to adjust their stomatal size and abundance in response to stressful environments. In this context, the results of this investigation revealed a different mechanism between halophytic and glycophytic plants where the former demonstrated lower stomatal density at control as well as each level of salinity (Fig. 2.4), suggesting that stomatal densities were intrinsically lower in halophytic species. This feature may facilitate halophytes avoid dehydration and diminish the rate of salt load to the leaves driven by transpirational water fluxes (Morales-Navarro *et al.* 2018; Bertolino *et al.* 2019). Cuticular transpiration which mainly occurs through epidermal cells surrounding the stomatal pores is reduced with a low number of pores in the leaf epidermis (Shabala *et al.* 2012). In respect to this finding, transcription analysis of guard cells in quinoa has shown some negative regulators of stomatal development been highly upregulated in plants grown under salinity (Chapter 5).

It is noteworthy that decline in stomatal density in response to salinity occurred in quinoa and *C. album* suggesting that reducing the number of stomata is species-specific and may not be a general feature of halophytes. In some halophytes (*Prosopis strombulifera*) increased number of stomata has been reported when

plant exposed to salt stress (Reginato, et al. 2013) which is consistent with results obtained from sea barley in our study.

The results also demonstrated that the stomatal sizes in halophytic plants were smaller than their glycophyte relatives (Fig. 2.6) suggesting that a smaller size of stomata induced by salt stress might be an adaptive mechanism to avoid water loss in halophytes. As it is manifested in leaf dehydration assay (Fig. 2.12), less water loss occurred in halophytes after exogenous application on ABA. According to Frank and Beerling (2009) decreased pore depth which occurs in small stomata leads to reduced distance for gas diffusion through the stomatal pore and thus, may increase maximum stomatal conductance if total pore area remains unchanged.

Altogether, smaller and lower abundance of stomata under saline conditions in this study would be advantageous to osmotically stressed plants, offering an opportunity to the plants to optimize water use efficiency. As we can see from leaf dehydration assay, less amount water was lost in halophytic plants, the slops of first 60-min of water loss in halophytes are lower than glycophyes, suggesting that more saving water in halophytes depends on stomatal responses.

2.4.4 Stomatal movement is faster in halophytes than glycophytes

Stomatal pores on leaf epidermis allow CO_2 diffusion and carbon assimilation by leaves (Lawson and Blatt, 2014). Simultaneously, stomatal pores are the gates for escaping water vapor from the leaf. If CO_2 uptake and water loss were synchronized, carbon uptake would have been at a maximum level while water loss is minimum (Kubarsepp *et al.* 2020). However, as the results of this study demonstrated (Fig. 2.7), there was a lag phase for reaching a steady-state level between stomatal movement and the rate of CO_2 assimilation in response to changing environments. For this reason, plants that have faster stomatal responses to these changes are able to efficiently cope with environmental stresses (Kubarsepp *et al.* 2020).

Our stomatal movement data revealed that the stomatal opening/closure times in halophytic plants were shorter than their glycophyte counterparts (Figures 2.7 and 2.8) suggesting that halophytes had faster response to changing environmental conditions. This characteristic enables halophytes to have better gas exchange and photosynthesis capacity. Leaf CO_2 assimilation increases rapidly to a steady-state and further increase in the rate of CO_2 assimilation depends on the

rate of stomatal response (Lawson and Vialet-Chabrand 2019). Thus, adjustment of the rate of CO_2 assimilation occurs instantly in response to light while slow movements of stomata limit the rate of CO_2 assimilation. The slow stomatal opening rate in response to light limits the rate of CO_2 assimilation by 10%, which is substantial over the day (Vialet-Chabrand *et al.* 2016). Once light switches off, the rate of CO_2 assimilation drops in few minutes while stomata are still open. Therefore, unnecessary water loss will occur.

Stomatal responses were slower at saline condition, compared to control. Saving energy in the saline conditions might be the main reason for this response. It has been noted that frequent stomatal movement demands energy (Lawson and Vialet-Chabrand 2019), while under salt stress conditions the net energy that is saved by plants is reduced (Munns and Gilliham 2015). These facts show that the speed of stomatal response to internal and external factors is very critical especially under field conditions (Kubarsepp *et al.* 2020) where plants are grown under changing conditions that require adjusting stomatal movements many times a day. Given that the speed of stomatal response is an unexplored topic in halophytes, our results suggest that faster stomatal movements could be an adaptive mechanism to cope with salinity at least in some halophytic species.

2.4.5 While potassium is more effective than sodium to open stomata in studied plants, quinoa may use Na^+ for stomatal movement

Our results of the ability of stomatal opening in the presence of Na^+ has demonstrated that all the studies halophytes and their glycophyte counterparts strongly responded to K^+. Obtained results showed that in all the studied plants K^+ and Na^+ stimulated stomatal opening and K^+ was more effective than Na^+ in stomatal movement (Fig. 2.10). In quinoa the maximum aperture occurred when Na^+ and K^+ were both present in the incubation solution. This finding is similar to results obtained in *Commelina benghalensis*, where Na^+ and K^+ equally stimulated stomatal opening (Raghavendra et al. 1976). In quinoa, it is likely that maintaining higher K^+ contents under saline conditions was involved in faster stomatal movements in this species. In this context, K^+ selective transporters in guard cells have been highly upregulated at the transcriptome level in salt-stressed quinoa (Chapter 5).

Halophytic plants are known to utilise Na^+ to drive the guard cell osmotic motor (Hedrich and Shabala, 2018). The reliance of plants on K^+ for stomatal opening (Fig. 2.10) suggests that Na^+ may cause a disruption in the normal control of guard cell turgor (Robinson *et al.* 1997). However, this did not occur in quinoa, where stomatal opening was also efficient in the presence of Na^+ (Fig. 2.10). This suggests that quinoa may use Na^+ instead of K^+ for stomata operation under saline conditions where Na^+/K^+ ration in the apoplast is not optimal. This is consistent with a general view that, under conditions of reduced K^+ availability, Na^+ can replace K^+ in several physiological processes (Erel *et al.* 2014). Thus, we suggest that a facultative ability of quinoa to use either K^+ or Na^+ for stomatal opening or closure give this halophytic plant a competitive benefit under salinity stress. Under high Na^+/K^+ ration condition, it is suggested that guard cells in halophytes can overcome this condition of excessive Na^+ either by ability to replace Na^+ instead of K^+ as the main ion determining their alterations of turgor, or through Na^+ excluding strategy to enable K^+ to retain the primary role (Véry *et al.* 1998).

2.5 Conclusion

Altogether, the results of this work revealed that halophytes were superior to glycophytes in terms of having higher maximum velocity of carboxylation, higher K^+/Na^+ selectivity, improved water status, and faster stomatal responses to environmental factors (light and darkness).

It is suggested that the fast-stomatal responses to internal signals and environmental factors may be essential for the synchronization of photosynthetic and stomatal conductance responses, thus optimizing water use efficiency under changing conditions. Understanding the mechanistic basis of fast stomatal kinetics in halophytes represents an underutilized resource for improving adaptive responses to salinity in major staple crops.

2.6 References

Aragão, MEF, Guedes, MM, Otoch, MLO, Guedes, MIF, Melo, DF, Lima, MGS (2005) Differential responses of ribulose-1,5-bisphosphate carboxylase/oxygenase activities of two *Vigna unguiculata* cultivars to salt stress. *Brazilian Journal of Plant Physiology* **17**, 207-2012.

Ashraf, M, Shahbaz, M, McNeilly, T (2005) Phylogenetic relationship of salt tolerance in early Green Revolution CIMMYT wheats. *Environmental and Experimental Botany* **53**, 173-184.

Barbieri, G, Vallone, S, Orsini, F, Paradiso, R, De Pascale, S, Negre-Zakharov, F, Maggio, A (2012) Stomatal density and metabolic determinants mediate salt stress adaptation and water use efficiency in basil (*Ocimum basilicum* L.). *Journal of Plant Physiology* **169**, 1737-46.

Bazihizina, N, Colmer, TD, Cuin, TA, Mancuso, S, Shabala, S (2019) Friend or foe? chloride patterning in halophytes. *Trends Plant Sci* **24**, 142-151.

Bertolino, LT, Caine, RS, Gray, JE (2019) Impact of stomatal density and morphology on water-use efficiency in a changing world. *Frontiers in Plant Science* **10**, 225.

Bose, J, Munns, R, Shabala, S, Gilliham, M, Pogson, B, Tyerman, SD (2017) Chloroplast function and ion regulation in plants growing on saline soils: lessons from halophytes. *Journal of Experimental Botany* **68,** 3129-3143.

Drake, PL, Froend, RH, Franks, PJ (2013) Smaller, faster stomata: scaling of stomatal size, rate of response, and stomatal conductance. *Journal of Experimental Botany* **64**, 495-505.

Eisinger, WR, Bogomolni, RA, Taiz, L (2003) Interactions between a blue-green reversible photoreceptor and a separate UV-b receptor in stomatal guard cells. *American Journal of Botany* **90**, 1560–1566.

Erel, R, Ben-Gal, A, Dag, A, Schwartz, A, Yermiyahu, U (2014) Sodium replacement of potassium in physiological processes of olive trees (var. Barnea) as affected by drought. *Tree Physiology* **34**, 1102–1117.

FAO (2017) *The future of food and agriculture – Trends and challenges.* Food and Agriculture Organization of the United Nations, Rome, Italy.

Farquhar, GD, von Caemmerer, S, Berry, JA (1980) A biochemical model of photosynthetic CO_2 assimilation in leaves of C3 species. *Planta* **149**, 78–90.

Flowers, TJ, Galal, HK, Bromham, L (2010) Evolution of halophytes: multiple origins of salt tolerance in land plants. *Functional Plant Biology* **37**, 604-612.

Franks, PJ, Beerling, DJ (2009) Maximum leaf conductance driven by CO_2 effects on stomatal size and density over geologic time. *Proceedings of the National Academy of Sciences of the United States of America* **106**, 10343-7.

Ge, Z-M, Zhang, L-Q, Yuan, L, Zhang, C (2014) Effects of salinity on temperature-dependent photosynthetic parameters of a native C3 and a non-native C4 marsh grass in the Yangtze Estuary, China. *Photosynthetica* **52**, 484-492.

Hetherington, AM, Woodward, FI (2003) The role of stomata in sensing and driving environmental change. *Nature* **424**, 901-908.

Hopper, DW, Ghan, R, Cramer, GR (2014) A rapid dehydration leaf assay reveals stomatal response differences in grapevine genotypes. *Horticultural Research* **1**, 2.

Hughes, J, Hepworth, C, Dutton, C, Dunn, JA, Hunt, L, Stephens, J, Waugh, R, Cameron, DD, Gray, JE (2017) Reducing stomatal density in barley improves drought tolerance without impacting on yield. *Plant Physiology* **174**, 776-787.

Kubarsepp, L, Laanisto, L, Niinemets, U, Talts, E, Tosens, T (2020) Are stomata in ferns and allies sluggish? Stomatal responses to CO_2 , humidity and light and their scaling with size and density. *New Phytologist* **225**, 183-195.

Lawson, T, Blatt, MR (2014) Stomatal size, speed, and responsiveness impact on photosynthesis and water use efficiency. *Plant Physiology* **164**, 1556.

Lawson, T, Vialet-Chabrand, S (2019) Speedy stomata, photosynthesis and plant water use efficiency. *New Phytologist* **221**, 93-98.

Lokhande, VH, Suprasanna, P (2012) Prospects of halophytes in understanding and managing abiotic stress tolerance. In: *Environmental adaptations and stress tolerance of plants in the era of climate change.* (Springer, New York, NY)

Mohamed, IAA, Shalby, N, Bai, C, Qin, M, Agami, RA, Jie, K, Wang, B, Zhou, G (2020) Stomatal and photosynthetic traits are associated with investigating sodium chloride tolerance of *Brassica napus* L. cultivars. *Plants (Basel)* **9**, 62.

Morales-Navarro, S, Perez-Diaz, R, Ortega, A, de Marcos, A, Mena, M, Fenoll, C, Gonzalez-Villanueva, E, Ruiz-Lara, S (2018) Overexpression of a SDD1-like gene from wild tomato decreases stomatal density and enhances

dehydration avoidance in arabidopsis and cultivated tomato. *Frontiers in Plant Science* **9**, 940.

Munns, R, Gilliham, M (2015) Salinity tolerance of crops - what is the cost? *New Phytologist* **208**, 668-73.

Prăvălie, R (2016) Drylands extent and environmental issues. A global approach. *Earth-Science Reviews* **161**, 259-278.

Rahman, MM, Rahman, MA, Miah, MG, Saha, SR, Karim, MA, Mostofa, MG (2017) Mechanistic insight into salt tolerance of acacia auriculiformis: the importance of ion selectivity, osmoprotection, tissue tolerance, and Na^+ exclusion. *Frontier in Plant Science* **8**, 155.

Robinson, MF, Very, A-A, Sanders, D, Mansfield, TA (1997) How can stomata contribute to salt tolerance. *Annals of Botany* **80**, 387-393.

Rozema, J, Schat, H (2013) Salt tolerance of halophytes, research questions reviewed in the perspective of saline agriculture. *Environmental and Experimental Botany* **92**, 83-95.

Santos, J, Al-Azzawi, M, Aronson, J, Flowers, TJ (2016) eHALOPH a database of salt-tolerant plants: helping put halophytes to work. *Plant and Cell Physiology* **57**, e10.

Sengupta, S, Majumder, AL (2009) Insight into the salt tolerance factors of a wild halophytic rice, *Porteresia coarctata:* a physiological and proteomic approach. *Planta* **229**, 911-29.

Shabala, L, Mackay, A, Tian, Y, Jacobsen, SE, Zhou, D, Shabala, S (2012) Oxidative stress protection and stomatal patterning as components of salinity tolerance mechanism in quinoa (*Chenopodium quinoa*). *Physiologia Plantarum* **146**, 26-38.

Shabala, S, Hariadi, Y, Jacobsen, SE (2013) Genotypic difference in salinity tolerance in quinoa is determined by differential control of xylem Na^+ loading and stomatal density. *Journal of Plant Physiology* **170**, 906-14.

Shabala, S, Newman, I (1999) Light-induced changes in hydrogen, calcium, potassium, and chloride ion fluxes and concentrations from mesophyll and epidermal tissues of bean leaves. Understanding the ionic basis of light-induced bioelectrogenesis. *Plant Physiology* **119**, 1115–1124.

Sharkey, TD (2016) What gas exchange data can tell us about photosynthesis. *Plant, Cell and Environment* **39**, 1161-3.

Sharkey, TD, Bernacchi, CJ, Farquhar, GD, Singsaas, EL (2007) Fitting photosynthetic carbon dioxide response curves for C(3) leaves. *Plant, Cell and Environment* **30**, 1035-40.

Su, H, Balderas, E, Vera-Estrella, R, Golldack, D, Quigley, F, Zhao, C, Pantoja, O, Bohnert, HJ (2003) Expression of the cation transporter McHKT1 in a halophyte. *Plant Molecular Biology* **52**, 967-980.

Tada, Y, Kawano, R, Komatsubara, S, Nishimura, H, Katsuhara, M, Ozaki, S, Terashima, S, Yano, K, Endo, C, Sato, M, Okamoto, M, Sawada, Y, Hirai, MY, Kurusu, T (2019) Functional screening of salt tolerance genes from a halophyte Sporobolus virginicus and transcriptomic and metabolomic analysis of salt tolerant plants expressing glycine-rich RNA-binding protein. *Plant Science* **278**, 54-63.

Véry, A, Robinson, MF, Mansfield, TA, Sanders, D (1998) Guard cell cation channels are involved in Na^+–induced stomatal closure in a halophyte. *The Plant Journal* **14**, 509–521.

Vialet-Chabrand, S, Matthews, JSA, Brendel, O, Blatt, MR, Wang, Y, Hills, A, Griffiths, H, Rogers, S, Lawson, T (2016) Modelling water use efficiency in a dynamic environment: an example using Arabidopsis thaliana. *Plant Science* **251**, 65-74.

Wang, J, Meng, Y, Li, B, Ma, X, Lai, Y, Si, E, Yang, K, Xu, X, Shang, X, Wang, H, Wang, D (2015) Physiological and proteomic analyses of salt stress response in the halophyte *Halogeton glomeratus*. *Plant, Cell and Environment* **38**, 655-69.

Yuan, F, Yang, H, Xue, Y, Kong, D, Ye, R, Li, C, Zhang, J, Theprungsirikul, L, Shrift, T, Krichilsky, B, Johnson, DM, Swift, GB, He, Y, Siedow, JN, Pei, ZM (2014) OSCA1 mediates osmotic-stress-evoked Ca^{2+} increases vital for osmosensing in Arabidopsis. *Nature* **514**, 367-71.

Chapter 3: Developing and validating protocols for mechanical isolation of guard-cell enriched epidermal peels for omics studies[1]

Abstract

Stomata, which are microscopic valves on the leaf surface formed by two guard cells (GC), play a critical role in the regulation of leaf water and gas exchange and, hence, determine plant adaptive potential. However, little data is available on GC biochemistry, protein abundance, and gene expression, mainly due to technical difficulties and challenges in isolating sufficient amounts of high-quality pure GC. In this study, we applied some modifications to the mechanical isolation of guard-cell to generalize this method for diverse growth conditions as well as plant species. Epidermal peel fragments enriched in guard cells were mechanically isolated from quinoa, spinach and sugar beet leaves grown at two conditions (normal and salt stress). Multiple analysis was performed to confirm the suitability and superiority of the modified technique to the original method. At the first step, the viability and purity of GC-enriched epidermal fragments were assessed under the microscope. Then, the RNA integrity, gene expression, and 1D SDS-PAGE tests were performed to validate the suitability of this technique for omics studies. The data revealed a wide range of proteins as well as a high integrity of RNA extracted from guard cell samples. The expression level of several GC-specific genes and mesophyll- dominant genes were investigated using a comparative analysis of transcriptome datasets of GC and whole leaf samples. We found that Rubisco and photosynthesis-related proteins such as chlorophyll a/b binding protein were substantially higher in the whole leaf compared to the GCs. More importantly, GC-specific genes such as *OST1*, *SLAC1*, *MYB60*, *FAMA* and *HT1* were highly expressed in the GCs confirming that our guard cell preparation was highly

[1] This chapter has been published as: **Rasouli F.,** Kiani-Pouya A., Zhang H., Shabala S. 2020. Developing and validating protocols for mechanical isolation of guard-cell enriched epidermal peels for omics studies. Functional Plant Biology, 47, 803–814.

enriched in GC gene transcripts. Quantitative RT-PCR further confirm the efficacy of the GC isolation technique for exploring responses of GC to diverse types of stress at the molecular level.

3.1 Introduction

Multicellular organisms consist of various cell types; each of them was developed to fulfil some specific job and, thus, may respond to different signals in a highly specific manner that may be different from other cells. Thus, the holistic understanding of plant adaptive and developmental responses is critically dependent on our ability to understand a mechanistic basis of its operation at the single-cell level, to account for its heterogeneity (Altschuler and Wu 2010). Studies on different aspects of physiological and biochemical analysis of single-cell types were initially conducted in medical science and mammalian studies (Wilson and Nairn 2018a; Liu *et al.* 2019b). Several methods for single cell isolation have been also established for plant system, including a manual cell dissection (Bates *et al.* 2012), laser-assisted microdissection (LAM) (Day *et al.* 2005), digesting non-specific cells by protoplasting (Zhu *et al.* 2009), fluorescence-activated cell sorting (FACS), flow cytometry (Galbraith 2010) and mechanically cell isolation by blending and sonicating (Bauer *et al.* 2013; Geilfus *et al.* 2018a). However, there is no appropriate general protocol for all cell types and plant species using those methods (Gautam and Sarkar 2015). For example, LAM and FACS approaches are more suitable for RNA-sequencing and gene expression analyses, rather than proteomics and metabolomics studies as there is no chance to amplify the protein yield to get adequate material for omics studies. It noteworthy to mention that current approaches applied for detection and quantification of proteins are insensitive to the low amounts of extracted protein from single-cell type experiments (Wilson and Nairn 2018a).

Stomata, the microscopic valves on the leaf surface, play a critical role in the regulation of leaf water and gas exchange and, hence, determine plant adaptive potential. Stomata are formed by a pair of guard cells (GC) that do not have plasmodesmata connection and, thus, operate largely independently from the rest of the leaf (Voss *et al.* 2018). GCs have long been attractive targets for being studied at a single-cell level (Gardner *et al.* 2009). However, given the large number (millions) of cells required for omics studies, isolation of adequate cell numbers

with a sufficient purity is incredibly challenging. A few isolation techniques have been practiced to study GC; the isolation of protoplasts has been the most common approach for various purposes (Yao *et al.* 2018a). This method dates back to 1970s was first developed for protoplast isolation from onion and tobacco leaves (Zeiger and Hepler 1976). This approach has since been applied in different research such as proteomics (Zhao *et al.* 2008b) and microarray analysis (Leonhardt *et al.* 2004a; Wang *et al.* 2011a; Yao *et al.* 2018a). However, isolation of GC protoplasts requires multiple steps as well as extended enzymatic digestion to dissolve cell wall that might impose different stress to GCs (e.g. chemical and osmotic stresses) and hence, alters gene expression (Bates *et al.* 2012).

The required timespan for GC preparation is another disadvantage of this technique. Given that enzymatic digestion of a cell wall of GC requires long hours for the process to be completed, the time difference between harvesting leaf sample and protoplast fixation for omics application is rather high. This long processing time may cause disruption of biomolecule integrity that is a critical step in obtaining reliable results in proteomics and RNA-sequencing investigations.

GC-enriched epidermal fragments could be an alternative approach for the isolation of GCs. Leaf epidermal strips have been used to study ionic relation in GCs, gene expression through reverse transcription polymerase chain reaction (RT-PCR), western blotting and microarray analysis (Kopka *et al.* 1997; Bauer *et al.* 2013; Llanes *et al.* 2016). For omics studies the sufficient number of GCs needs to be isolated and using a high-speed blender could be one of the best options. This method of GC isolation is amazingly fast. Also, cells isolated by this method keeps the GC wall which plays a significant role in stomatal operation (Hunt *et al.* 2017).

Earlier Bauer *et al.* (2013) have successfully used a mechanical blending method to obtain guard cell-enriched epidermal peels for transcriptomic studies of humidity sensing in Arabidopsis stomata (Hunt *et al.* 2017). However, when we used the adopted protocol of this method (Jalakas *et al.* 2017a) for other species (such as quinoa, spinach, and sugar beet) we obtained GC samples with a high percentage of contamination with non-guard cell materials. This contamination was especially high in the salt-grown samples. It appears that growing conditions such as differences in the cultural media and different type of stresses could have an impact on the efficiency of the isolation method. Consistent with this finding, Yao *et al.* (2018a) found that substrate-cultured plants are not as effective as hydroponic

plants for isolation of GC. Similarly, salt stress increases leaf cuticle and parenchyma thickness as well as the increase of vascular bundle sheath thickness (Akcin *et al.* 2015) which can affect the capability of the method for GC isolation. Taking these facts into account, and given that to date, available studies conducted on mechanical GC isolation are limited even under non-saline conditions, modifications for development of efficient protocols for isolating purified GCs from salt-treated plants for various omics studies are needed. We emphasise that soil salinity is emerging as one of the major threats to agricultural sustainability and global food security, so an understanding of the molecular basis of stomata adaptation to salinity may be instrumental in the development of salt- and drought-tolerant cultivars.

In addition to the above, a lack of information about the GC-enriched epidermal fragments method means that it does not provide direct experimental evidence to test the quality and purity of GC epidermal fragments. Hence, the question as to whether this method is appropriate under diverse conditions remains to be answered.

In this study, we develop an optimised method for GC isolation from the leaf epidermis of spinach (glycophyte) sugar beet (salt-tolerant) and quinoa (halophyte) plant species under control and salt-stress conditions with high quality and purity. Some important modifications were devised based on the mechanically GC-enriched epidermal fragments method of Arabidopsis involving using basic solution instead of distilled water, mesh size, blending time, and number of runs. We successfully applied this method for proteomics and transcriptomics studies. Protein concentration and RNA quality and quantity were determined in GC samples. Additionally, transcriptome and 1D SDS-PAGE were performed and using determination of transcriptional levels of guard cell-specific genes in leaf and guard cell in quinoa, spinach, and sugar beet we provide direct evidence of the suitability of this GC isolation approach for these omics studies. The modified methods will facilitate the research of stomatal function and improves the experimental efficiency.

3.2 Materials and methods

3.2.1 Plant material and growth conditions

Three plant species, sugar beet (*Beta vulgaris*), spinach (*Spinach oleracea*) and

quinoa (*Chenopodium quinoa* Wild.) were used in this study. The seeds were obtained from the Leibniz Institute of Plant Genetics and Crop Plant Research (IPK) (gbis.ipk-gatersleben.de), Germany. Plants were grown under glasshouse conditions from August – October 2018 at the University of Tasmania, Hobart, Australia. The mean daily temperatures were 24°C (day) and 16°C (night) and relative humidity was 70%. Plants were grown in 20 cm diameter pots filled with the standard potting mixture. The potting mixture was consisted of 90% composted pine bark; 5% coco peat; 5% coarse sand; gypsum at 1 kg m^{-3}; dolomite at 6 kg m^{-3}; ferrous sulphate at 1.5 kg m^{-3}; Osmoform Pre-mix at 1.25 kg m^{-3} and controlled-release fertiliser, Scotts Pro at 3 kg m^{-3} (Kiani-Pouya *et al.* 2019b). Approximately 2 weeks after emergence, salt stress commenced by applying 50 mM NaCl increments daily until reaching a final concentration of 250 mM NaCl. Plants were kept under salt stress conditions for 3 more weeks.

3.2.2 Guard cell preparation

To prepare GC-enriched epidermal fragments, leaves of sugar beet, spinach and quinoa plants were cut, and all visible veins and edge of leaves were removed by a scissor. Approximately 60-70 leaf sections of 5 × 5 mm or smaller from each plant species were collected in distilled water or basic solution chilled with ice cubes. The leaves were ground in Grindomix blender (GRINDOMIX BLENDER GM 200, Retsch, Germany) with 300 mL double distilled water or basic solution and 100 mL crushed ice cubes by 3 pulses per minutes with the highest speed (10,000 rounds per minute). The mixtures were then passed through 250 µm nylon mesh (ELKO, Filtering co. USA) for all plants except for quinoa under salt stress which 190 µm nylon mesh was used (Table 3.1). The filtrates then rinsed a couple of times with ice-cold distilled water. The remaining small dark green tissue fragments were removed by a clean forceps and epidermal fragments were then returned to the blender by washing the mesh with ice-cold water above the blender chamber.

The above blending process was repeated three more times for spinach and sugar beet and four more times for quinoa. Double distilled water was used during the blending and washing process for all plants in the three first blender runs and basic solution containing (0.65 M sorbitol, 0.5 mM $CaCl_2$, $MgCl_2$, 10 µM KH_2, 0.5 mM PO_4 pH 5.5) was replaced with distilled water for remaining runs. Totally 4

runs were performed for sugar beet and spinach and quinoa in control conditions one more run was operated for quinoa grown under salt stress (Table 3.1).

Table 3.1 The comparison of GC isolation procedures for Arabidopsis, quinoa, sugar beet and spinach.

Species	Blending per run (Sec)		Number of Run		Mesh size (µm)		solution		Consideration
	C	S	C	S	C	S	C	S	
Quinoa	65	75	4	5	250	190	DW, BS	DW, BS	Removing main and secondary midrib and the leaf edge
Sugar beet and spinach	60	70	4	4	250	250	DW, BS	DW, BS	Removing main and secondary midrib and the leaf edge
Arabidopsis*	60	ND	3	ND	210	ND	DW	ND	Removing the main midrib

DW: distilled water; BS: basic solution; C: control condition; S: Saline conditions*: adapted from Arabidopsis protocol.

Epidermal fragments were collected and dried by tissue. The epidermal fragments were then transferred to an aluminium foil using a medical spatula and frozen by liquid nitrogen. Samples were kept in -80°C freezer until further usage. The required blending time in each run was 60 s for sugar beet and spinach and 65 s for quinoa under control conditions. In salt-treated plants, the blending time was extended for an additional 10 s.

3.2.3 Protein extraction

Proteins were extracted using trichloroacetic acid (TCA) method (Wang *et al.* 2006). Harvested GC samples and leaves from the saline and non-saline plants were ground to a fine powder in liquid nitrogen and total proteins were precipitated using 10% trichloroacetic acid (TCA) in a pre-chilled acetone containing 0.07% (v/v) 2-mercaptoethanol. After keeping the homogenate at -20°C overnight, the samples were then centrifuged at 20,000×g at 4°C for 30 min. The pellets were washed using 100% prechilled acetone containing 0.07% (v/v) 2-mercaptoethanol, and then centrifuged at 20,000×g at 4°C for 20 min. This process was repeated with 80% prechilled acetone. After air-drying the pellets, they were solubilized in 1m buffer containing 7 M urea, 2 M thiourea, and 40 mM Tris at 20°C for 1 h. The solution was then centrifuged at 20,000×g at 4°C for 30 min. To precipitate the protein from

extracts, 4 volumes of acetone were used, and the pellets were then resuspended in 50 µL of solubilization buffer containing 7 M urea, 2 M thiourea, 40 mM Tris. Protein concentrations were determined using Pierce 660nm Protein Assay Reagent.

3.2.4 RNA extraction and library preparation

The extraction of RNA was conducted by three biological replicates from GC-enriched samples for all three plant species. The total RNA was extracted from samples by grinding in liquid nitrogen using RNeasy Plant Mini Kit (Qiagen) following the manufacturer's instructions. RNA quality and quantity were then determined by Agilent Bioanalyser 2100 system (Agilent Technologies Co. Ltd). For library preparation, samples with RIN (RNA integrity number) values >7 were used for sequencing for all species. The NEBNext Ultra Directional RNA Library Prep Kit for Illumina (New England Biolabs) was used for mRNA-seq library following the manufacturer's protocol. To do this, 5 µg of total RNA of GC-enriched samples for all plant species were used to enrich the mRNA using polyT magnetic beads which was fragmented by divalent ions and then using random primers was subjected to first strand cDNA synthesis. The second strand cDNA was synthesised and PCR amplification was carried out as the subsequent step and to do this the second strand cDNA and part of the adaptor were removed using the USER enzyme, and adaptor-ligated first strand cDNA was prepared. The quality of libraries was determined using a Fragment Analyzer (Advanced Analytical Technologies, Inc) and the quantification was performed using Qubit (Thermo Fisher Scientific) and qPCR. The sequencing was performed on a HiSeq2500 using the SBS v4 reagent at the Core Facility for Genomics of the Shanghai Centre for Plant Stress Biology. Adaptor trimming and quality control was conducted using Trim Galore (http://www.bioinformatics.babraham.ac.uk/projects/trim_galore/). The cleaned high-quality reads were then mapped to the quinoa reference genome (Jarvis *et al.* 2017) using the RNA-seq aligner STAR (version 2.5.4b).

3.2.5 Quantitative Reverse Transcription PCR analysis

Five genes related to salt stress were selected from GCs and qRT-PCR analysis was performed for both control and salt stress. One mg of extracted RNA was reverse-transcribed with TransScript RT-PCR Kit and the cDNAs were used as templates

for amplifications. Primer3 program was used for designing the primer pairs (Supplemental Table S3.1). The PCR reaction conditions were as follows: heating at 94 ^{0}C for 3 min, then 35 cycles of heating at 94 ^{0}C for 30s and annealing at 55 ^{0}C for 30 s. Three biological replications and two technical measurements for each replicate were used.

3.3 Results

3.3.1 Assessment of epidermal fragments purity and GC viability

We used epidermal fragments containing intact GCs attached to the mechanically disrupted pavement cells as a molecular source of GC protein and omics analysis. Isolated GC-enriched fragments were inspected under the microscope to confirm that no mesophyll fragments or vascular particles (green tissue) were present (Fig. 3.1 and Supplemental Fig. S3.1). Unlike GCs, epidermal pavement cells are susceptible to mechanical manipulation and could be damaged even by manual peeling (Weyers and Travis 1981). Preparation of GCs by following the original protocol (Bauer *et al.* 2013) came up with a highly contaminated GC which was not acceptable for GC studies (Fig. 3.1A, B). Increasing the duration of time or number of runs made the samples more purified but reduced the viability of the guard cells. Using basic solution instead of distilled water maintained the viability of the cells. As one can see in Figure 3.1, the blended epidermal fragments represent highly enriched sources of purified GCs, with no contamination of pavement, mesophyll, or vascular cells. GC remained alive because they have thickened and structurally integrated cell walls to withstand the large increases in turgor pressure that have to be generated to open the pore that they surround.

3.3.2 Protein concentration and protein profiling

The proteins were extracted from combining 4 subsamples, each containing about 250 µg GC-enriched epidermal fragments. The results showed that there was consistency among harvested samples and protein concentrations for three species which ranged from 250 to 468 µgmL^{-1}. From the same amount of GC material, a greater amount of protein was extracted from quinoa samples (Table 3.2).

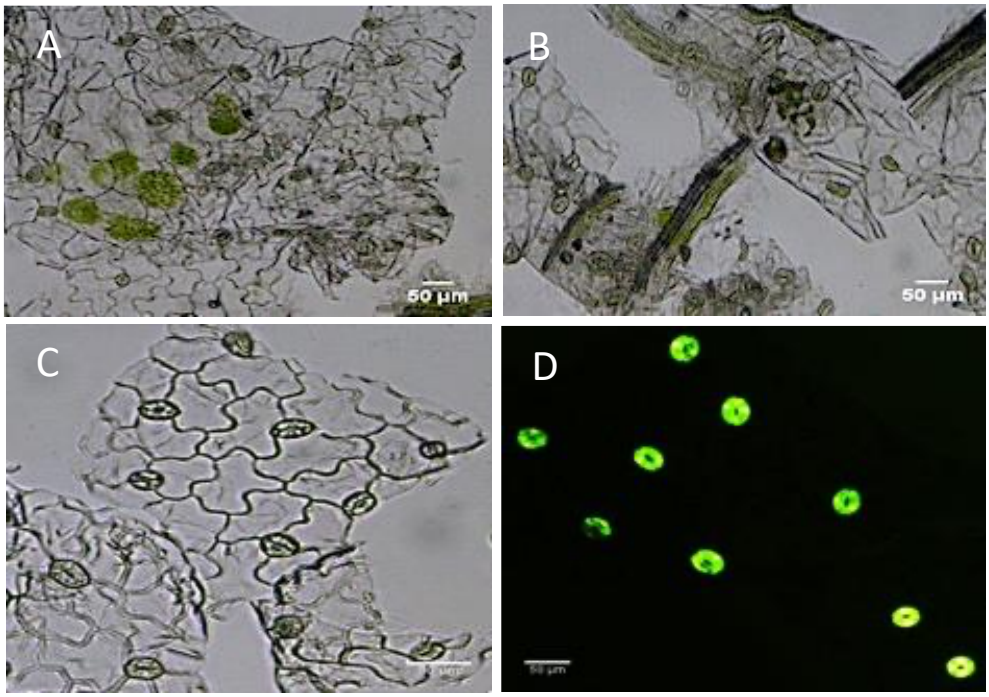

Fig. 3.1 Epidermal peels collected after blending process using original and modified protocol. One (of 6 to 10) typical examples is shown for each panel. Contamination of GC samples with mesophyll (A) and vascular tissue (B) in original protocol. Epidermal fragments in bright field microscopy (C) and fluorescein diacetate staining of GCs (D) in modified protocol. Epidermal peels collected after grinding process show the fluorescent signal only detectable in GCs, not in remaining pavement or mesophyll cells (Supplemental Fig. S3.1).

As a classical tool, one-dimensional SDS-Polyacrylamide Gel Electrophoresis (1D SDS-PAGE) is widely used for separating and visualizing the proteins in the mixture samples (Cai *et al.* 2017). This method has been also applied for comparative study of the efficacy of protein extraction methods (Fodor *et al.* 2017). Proteins extracted from sugar beet, quinoa and spinach GCs treated with 0 and 250 mM NaCl were analysed in SDS-PAGE- 1D (Fig. 3.2).

The pattern and relative intensity of proteins were different in GCs of all plant species. Proteins bands were distinct at lower and higher molecular weight regions of the gels where strong bands observed in the regions of 20 and 25 kDa and around 37 kDa protein markers in all the plants. The main difference between

Table 3.2 Protein concentration (µg mL^{-1}) of guard cell samples quantified by Pierce 660 nm Protein Assay Reagent. C and S denotes control and saline conditions.

Guard cell samples	Quinoa		Sugar beet		Spinach	
	C	S	C	S	C	S
R1	421	425	370	340	280	252
R2	424	381	342	364	268	260
R3	468	378	392	438	252	278
R4	332	349	368	358	256	250

the whole leaf samples and GC samples on the gel is a noticeably strong band in molecular mass of 50 kDa in the whole-leaf samples which is representative of ribulose-1, 5-bisphosphate carboxylase/oxygenase (Rubisco) protein. Rubisco accounts for higher than 50% of the total leaf protein and is a key enzyme for carbon fixation (Evans, 1989). Although GCs may also photosynthesise and thus contain some Rubisco, the volume of the GC is insignificant compared with the bulk of the leaf mesophyll. Because of this, the presence of the dominant band in the Rubisco region is considered as a contamination of the GC samples with the mesophyll tissue by some researchers (Zhao *et al.* 2008b).

3.3.3 RNA yield and quality in guard cell samples

Both quality and quantity of extracted RNA is critically important for omics studies such as transcriptomic analysis and hence, quality control assessment of total RNA is a crucial step for these analyses. We used an Agilent technologies bioanalyser (Agilent 2100 bioanalyser) for RNA assessment of GCs. In terms of quantity control, the RNA concentrations of GCs in both saline and non-saline conditions were ranged from 120 to 1220 ngμL^{-1} among plant species which was large enough for transcriptome analysis (Table 3.3).

In our study, RIN values varied from 7.3 to 9.5 in different plants and treatments in GC samples with RIN greater than 8 in 14 samples out of 18, showing the suitability of the GC preparation method for molecular and gene expression studies (Fig. 3.3).

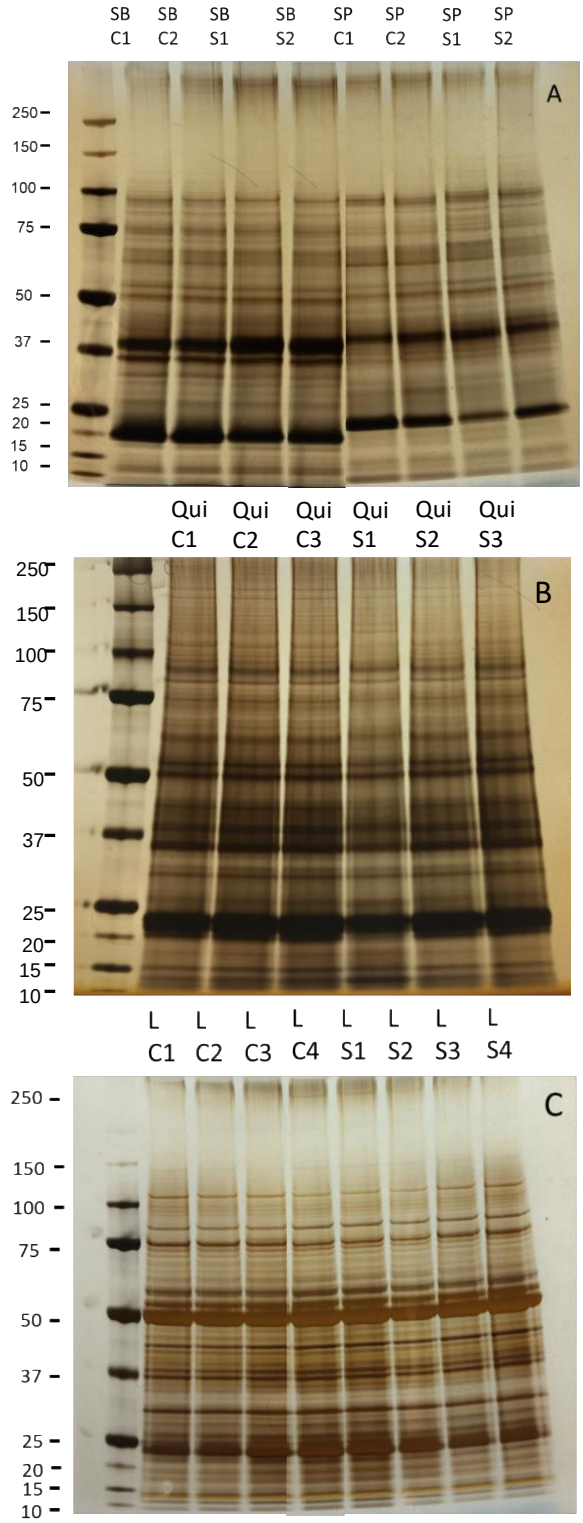

Fig. 3.2 Protein profiling using 1D-SDS-PAGE analysis of representative plants under control and salt stress conditions. GC-enriched fragments of sugar beet and spinach for control and salt conditions (A), GC-enriched fragments of quinoa under control and salt conditions (B), leaves of quinoa under control and salt conditions (C). SB: sugar beet, SP: spinach, Qui: quinoa, L: leaf, C: control, S: salt-treated sample. One (of 5-7) typical examples is shown for each panel.

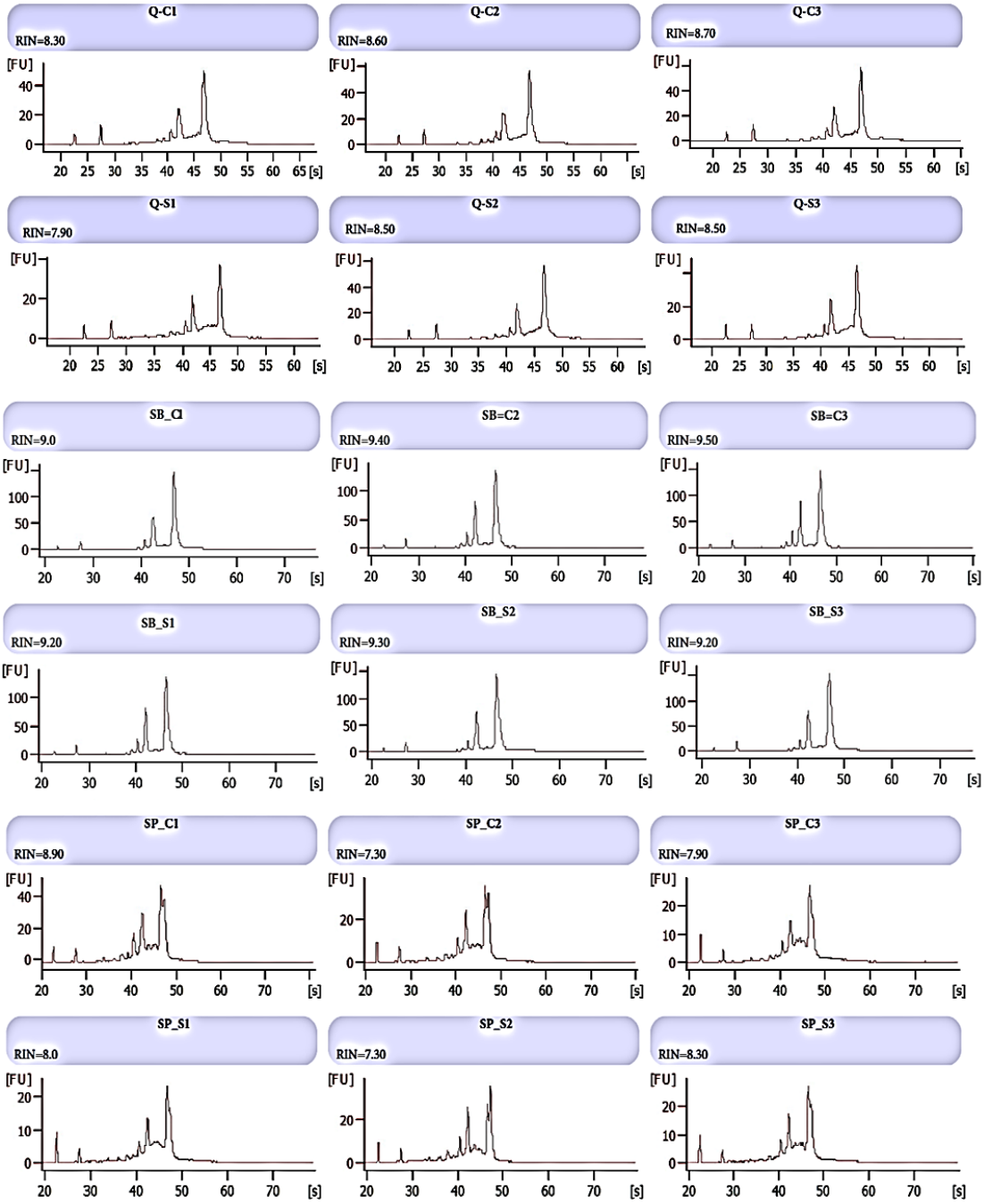

Fig. 3.3 RNA integrity of guard cell samples. The electropherograms were generated for guard cell RNA samples by Agilent 2100 Bioanalyzer and the RNA integrity were calculated using RIN algorithm. The peaks in the electropherograms show the size distribution of RNA fragments. Distinctive peaks at 18S and 28S and low abundance of short RNA fragments on the electropherogram are the hallmarks of RNA integration. Numbering system is used in RIN algorithm, RIN=10 in maximum RNA integrity and RIN=1 is maximum degradation in RNA profile.

Table 3.3 RNA concentration of guard cell samples quantified by Agilent 2100 bioanalyzer ($ng\mu L^{-1}$). C and S denotes control and saline conditions.

Guard cell samples	Quinoa		Sugar beet		Spinach	
	C	S	C	S	C	S
R1	275	192	749	1220	175	120
R2	257	254	780	853	169	220
R3	256	212	757	876	162	135

3.3.4 Transcriptional level of guard cell expressed genes

In order to validate the isolation method for gene expression, RNA sequencing was performed for both whole leaf and GC of quinoa. A total of eight genes that have been documented to be expressed preferentially in GC, were chosen to compare their expressions in leaves and GC samples (Fig. 3.4). The results of the present study indicated that these genes were significantly expressed in GC than leaves in all the plant species employed in this investigation.

Transcription factors *FAMA* which play critical roles in GC differentiation and transcription factor *MYB60* that is essential for stomatal movements (Galbiati *et al.* 2011; Shirakawa *et al.* 2014; Yamauchi *et al.* 2016) were highly expressed in GCs. Other transcription factors, such as (*stomatal carpenter 1*) that regulates differentiation of guard cell at the final stages (Negi et al. 2013) were significantly upregulated in GCs.

In addition to GC-specific transcription factors, some genes such as *OST1*, and *SLAC1* and transporter *ABCG31* that are involved in ABA stomatal responses (Francia *et al.* 2008; Deger *et al.* 2015; Wu *et al.* 2019) and play roles in controlling stomatal aperture in response to different stresses, especially water deficit conditions were significantly upregulated in GCs (Fig. 3.4).

HT1 another guard cell-specific gene is critical for regulation of stomatal movements especially in response to CO_2 (Hashimoto *et al.* 2006). This experimental evidence demonstrates that isolated GCs are enriched in GC specific genes suggesting the validation of this GC isolation approach for omics studies. This is further supported by the results of mesophyll-dominant genes in guard cells and leaf. GCs contain functional chloroplasts and active Calvin cycle, however

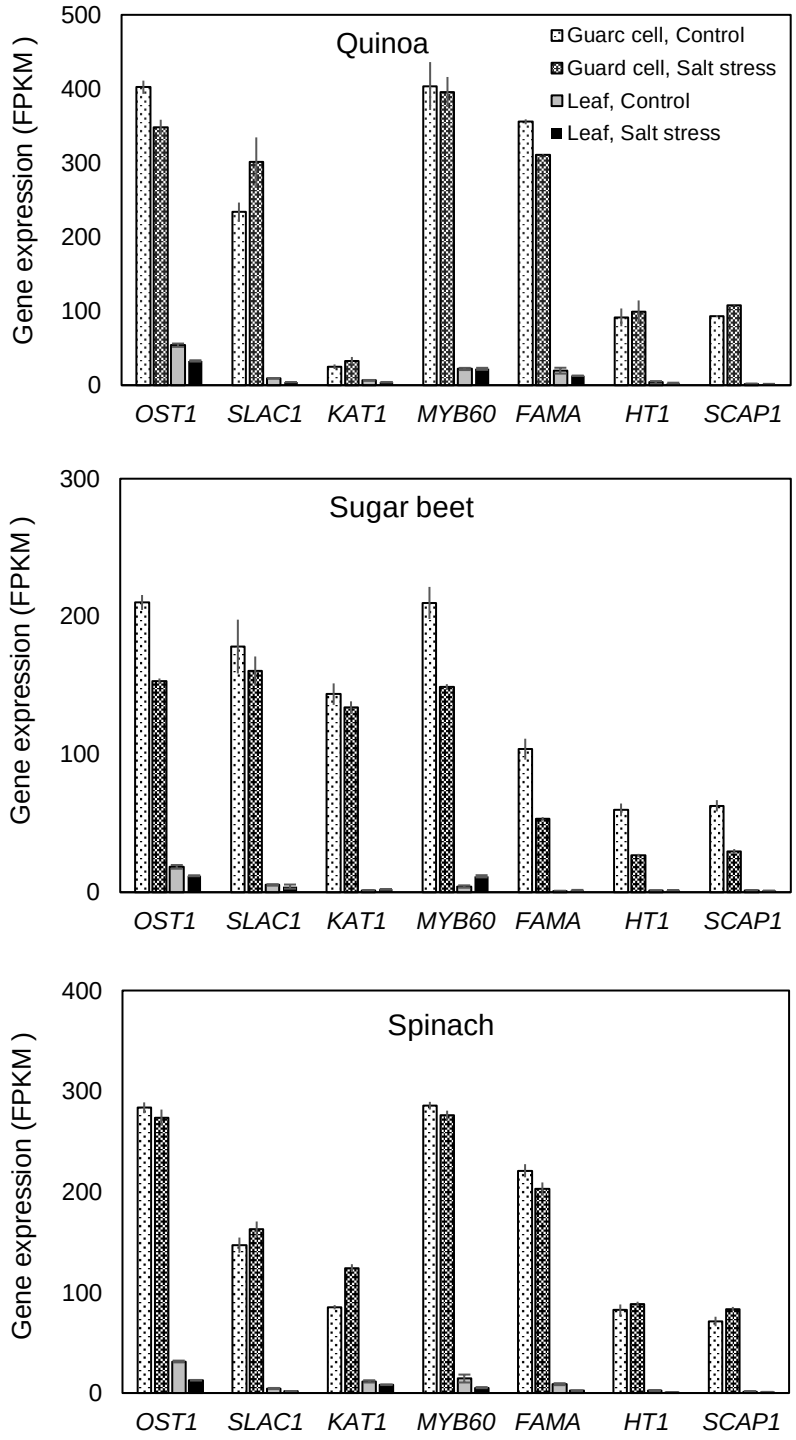

Fig. 3.4 Transcriptional levels of guard cell-specific genes in quinoa, sugar beet and spinach leaf and guard cell. Mean ± SE (n = 4 biological and 2 technical replicates). *OST1 -open stomata-1*; *SLAC1* - slow anion channel; *KAT1* - inward rectifier potassium channel; *MYB60* and *FAMA* - transcription factors; *HT1 - high leaf temperature 1*; *SCAP1-stomatal carpenter*.

lower activity of the Rubisco and other Calvin cycle enzymes and lower abundance of chloroplasts in guard cells results in a limited photosynthetic capacity in the GCs (Lawson *et al.* 2014). Therefore, we performed the comparative analysis for expression levels of mesophyll-dominant genes such as the ribulose-1,5-bisphosphate carboxylase (*Rubisco S*), chlorophyll a/b binding protein of photosystem II (*CAB*), rubisco activase, oxygen-evolving enhancer protein, photosynthesis-regulated genes (*PSI-D2*, *PSI subunit V*, *PsbY*). These genes could still be found in GCs, however, with much lower expression levels compared to whole leaf samples. As shown in Figure 3.5, the expression levels of those genes are substantially lower in guard cells compared to those in leaf samples suggesting the efficiency of the techinqe for GC isolation.

The efficiency of guard cell isolation method further confirmed using qRT–PCR, where we tested five genes that are normally induced in response to salt stress (Fig. 3.6). *NCED5* (nine-cis-epoxycarotenoid dioxygenase 5), and *ABI5* involve in ABA synthesis and ABA signalling during dehydration, respectively. *DREB2C* increases sensitivity of cells to ABA (Lee *et al.* 2010) and *inorganic pyrophosphatase 1* (*PS2*), contributes to the stomatal closure in response to ABA (Asaoka *et al.* 2019a). All the above genes were induced in response to salt stress, suggesting the suitability of the guard cell isolation for molecular experiments.

3.4 Discussion

In the present investigation, harvesting epidermal fragments by the blending method was effectively used to isolate GCs. The tissue prepared in this manner was the source of protein and RNA extractions for omics analysis of three plant species sugar beet, spinach and quinoa under control and salt-stress conditions. This provides direct experimental evidence for the suitability of mechanically isolated GC epidermal fragments method for omics studies.

3.4.1 GC-enriched epidermis is a faster and more reliable method

To achieve a good result in omics analysis such as transcriptome studies, maintaining the integrity of GC RNA is a critical step, and thus the time difference between harvesting the GCs and fixation of the samples in the liquid nitrogen should be minimised. In the commonly used protoplasting protocol, the GC sample is subjected to substantial manipulation before tissue fixation.

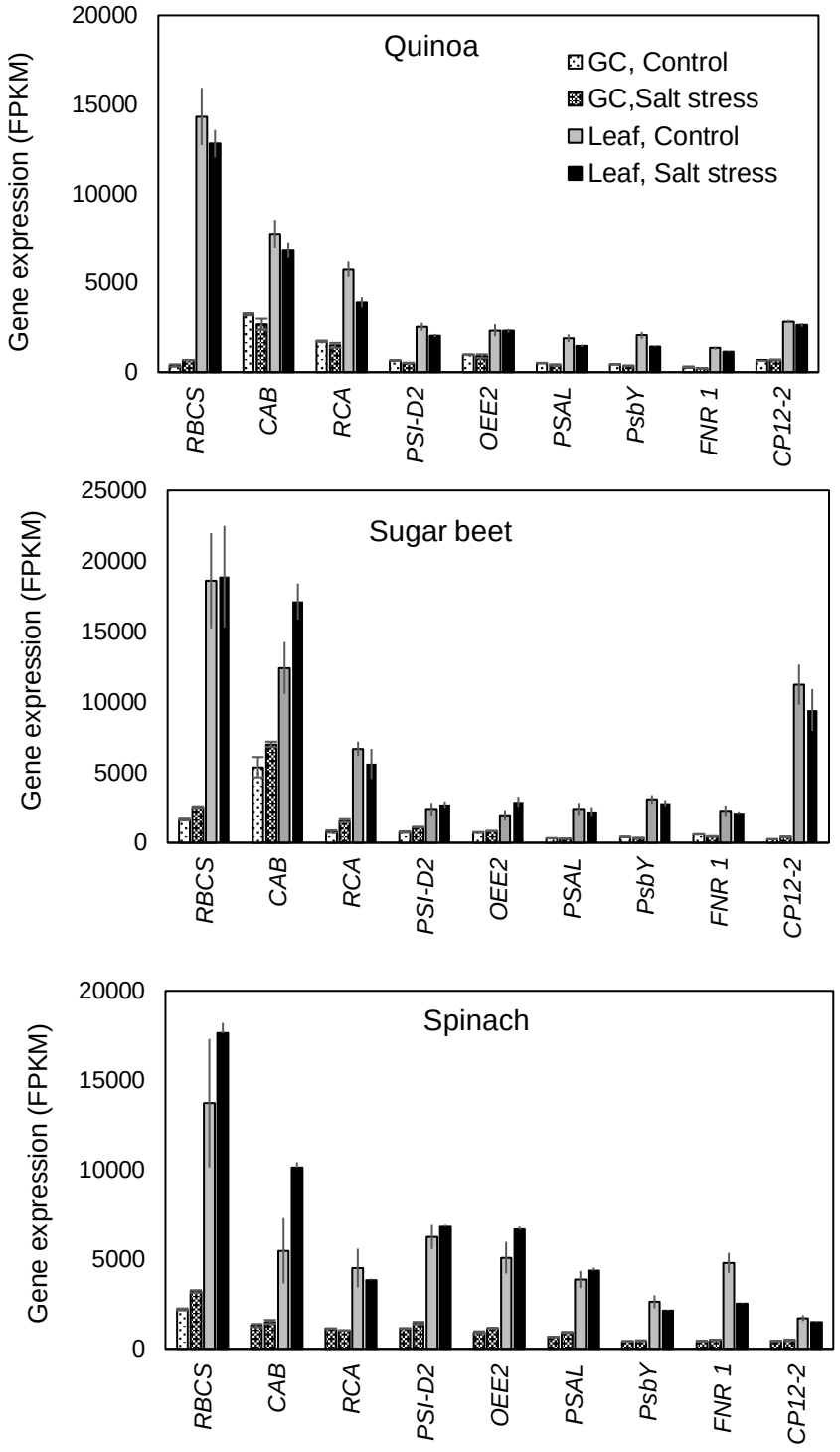

Fig. 3.5 Transcriptional levels of mesophyll-dominant genes in quinoa, sugar beet and spinach leaf and guard cell. Mean ± SE (n = 4 biological and 2 technical replicates). *RBCS-RuBisCO* small chain; *CAB*- Chlorophyll a-b binding protein; *RCA-RuBisCO activase*:; *PSI-D2*: Photosystem I reaction center subunit II; *OEE2*- Photosystem II oxygen-evolving enhancer protein 1; *PSAL*- Photosystem I reaction center subunit XI; *PsbY*- Photosystem II protein Y; *FNR 1*- Ferredoxin-NADP reductase, *CP12-2*- Calvin cycle protein CP12.

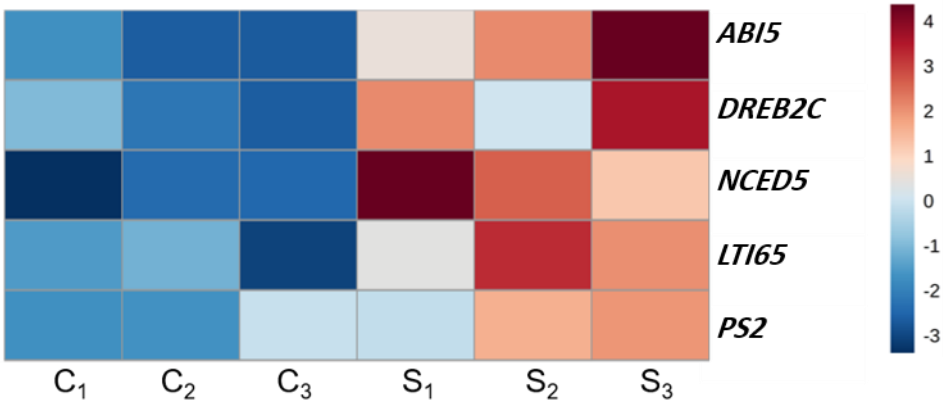

Fig. 3.6 Heat map for the quantitative RT-PCR expression analysis of selected genes in guard cells in control and salt conditions to confirm effectiveness of guard cell isolation method. *ABI5*- basic-leucine zipper (bZIP) transcription factor family; *DREB2C*- integrase-type DNA-binding superfamily protein; *NCED5*- nine-cis-epoxycarotenoid dioxygenase 5; *LTI65*- low-temperature-induced 65 kDa protein; *PS1*- inorganic pyrophosphatase 1. C-control; S - saline condition.

Hours of incubation in lytic enzymes with high osmotic strength to remove the cell walls imposes stress on GCs (Bates *et al.* 2012). As an example of this interference, a comparison of microarray analysis of GC protoplast with dissection method indicated that some genes related to stresses have been remarkably overexpressed in the protoplast method that could not be found in a non-enzymatic approach (Bates *et al.* 2012).

Additionally, prolonging the incubation time may lead to degradation of RNA over the course of GC preparation, and make RNA integrity a challenge. In a previous microarray study, the stability of mRNA in presence of inhibitors was determined over a 24-h period. The results revealed that half-lives of mRNAs varied from 0.2 to 24 h, with median of 3.8 h (Narsai *et al.* 2007). This finding revealed that decay rates of some transcripts are rapid and might affect the analysis abundance in RNA-seq experiments or gene expression studies.

3.4.2 GC-enriched technique includes cell wall in the omics studies

One of the most important advantages of the GC-enrich method over protoplast isolation is that the former keeps GC walls and hence, it could be incorporated to

the omics analyses. Some investigators have mentioned the importance of GC walls and its extracellular matrix in the stomatal movements (Jones *et al.* 2003).

Plant cell walls are complex mixture of various compounds including proteins, carbohydrates and lignin (Marom *et al.* 2017) and these vary among plant species and cell types. The structure and composition of cell walls further change at different developmental stages and exposure to abiotic stresses (Uddin *et al.* 2013; Cruz-Valderrama *et al.* 2019). Furthermore, the nature and functions of plant cell walls are fully dynamic and are affected by many factors such as, intercellular communications, environmental signalling and stimuli and plant defense (Karkonen and Kuchitsu 2015) which are incorporated in this technique of GC isolation.

Cell wall proteins play vital roles including modifications in cell wall components and structure, signalling and interactions with plasma membrane proteins (Jamet *et al.* 2006). For example, the data obtained from the analysis of the Arabidopsis genome (Jamet *et al.* 2006) has shown that the number of existing proteins in the cell wall is significant (17% of the whole genome)

Unlike the other types of cell wall, GC walls are exceptionally strong and tensile, so play an important role in stomatal development and function (Rui *et al.* 2018). Hence, proteins become even more important in the GC wall because the stomatal dynamics depend on structural and functional proteins embedded in the GC wall (Hunt *et al.* 2017). Thus, using the GC-enrich technique for isolation of GCs which incorporates the cell wall to analysis provides this opportunity to the function of these proteins in omics or other investigations.

3.4.3 Development of GC-enriched epidermis method for salt-grown plants

Our GC preparations obtained by following the original protocol by (Bauer *et al.* 2013) resulted in high levels of contamination, which was not acceptable for omics analysis (Fig. 3.1A, B). The highly contaminated samples produced especially under salt stress conditions, may be the result of an increase in vascular bundle sheath thickness or an increase in leaf cuticle and parenchyma thickness under these conditions (Akcin *et al.* 2015). However, through alterations such as the use of smaller leaf sections, removal of all visible veins, increased blending time and number of runs as well as using a basic solution instead of distilled water, we significantly increased purity of GCs and maintained their viability. These

modifications resulted in production of epidermal fragments that represented highly enriched sources of purified GCs that were not contaminated by any kind of pavement, mesophyll or vascular cells (Fig. 3.1). Quantitative RT-PCR analysis of genes under control and salt condition confirmed that the method would be reliable for exploring for response of GC to salt stress.

3.4.4 Validating GC-enriched epidermis method for omics studies

For proteomics analysis of GC-enriched fragments using 1D SDS-PAGE, our results showed a wide range of proteins between GC and leaf samples (Fig. 3.2). In respect to this result, the presence of the dominant band in the Rubisco region in leaf samples compared to GC samples suggesting that GC samples were not contaminated with the mesophyll tissue as it is proposed by some researchers as an indicator of sample contamination (Zhao *et al.* 2008b).

For transcriptomics analysis, the quality of the obtained RNA has primary importance. In this regard, the RIN value of 7 or greater is necessary for gene expression analysis (Jahn *et al.* 2008). In the present study, all GC samples had integrities >7.3, which would pass the quality control required or further experiments. Also, the preparation of GC-enriched epidermal fragments from harvesting the leaves to snap freezing into the liquid nitrogen was completed within 20 min, which was fast enough not to be disrupted by external factors.

3.4.5 Modified protocol was more efficient and more enriched in GC-specific genes

The enrichment of a total of 20 genes including GC- specific genes and some genes with major role in stomatal movement and development used to test the efficacy of a GC isolation method (Table 3.4). For this purpose, the abundance of genes in the GC samples were compared with those in the complete leaf samples for each species. Comparisons of some GC-specific genes enrichment in the GC obtained from our experiments and those from original protocol in Arabidopsis (Bauer *et al.* 2013) showed that our preparations were more enriched in GC-specific genes, suggesting that the alteration in the protocol resulted in a more purified GC sample. This will help to increase accuracy in further experiments with those samples.

Table 3.4 Fold change of selected GC-specific genes in guard cell samples compared to leaf in modified protocol (quinoa, sugar beet and spinach) and original protocol for Arabidopsis (Bauer *et al.* 2013).

Gene	Description	Quinoa	Sugar beet	Spinach	Arabidopsis*
OST1	*Open stomata 1*	8.2	11.6	9.1	4.3
SLAC1	*Slow anion channel*	38.9	35.6	31.3	7.8
KAT1	*Inward rectifier potassium channel;*	8.2	6.1	10.3	4.1
MYB60	*Transcription factors*	16.9	51.2	19.7	7.4
HT1	*High leaf temperature 1*	30.2	39.7	52.6	5.8
FAMA	*Transcription factors*	23.2	58.3	25.4	6.7
BLUS1	*Blue light signalling 1*	34.7	59.8	58.4	9.3
SCAP1	*Stomatal carpenter*	53.7	48.8	59.2	4.6
MAPK4	*Mitogen-activated protein kinase*	56.7	30.4	42.4	ND**
PP2C	*Protein phosphatase 2C*	9.0	3.8	2.9	4.2
CHX	*Cation/H antiporter*	4.1	51.8	GC**	7.2
ALMT12	*Quick-activating anion channel 1*	15.0	41.4	29.7	8.1
ATPase 4	*Plasma membrane H^+ATPase*	4.3	2.7	2.1	5.7
PYR1	*ABA receptor*	12.1	6.0	38.5	4.5
CRY2	*Cryptochrome-1*	4.7	2.2	8.2	ND
ICE1	*Inducer of CBF expression 1*	6.6	7.7	3.3	2.2
AREB3	*ABA-responsive element binding protein 3*	3.8	3.1	2.0	ND
CDPK1	*Calcium-dependent protein kinase 1*	3.7	2	3.1	2.1
ASPG	*Aspartic protease in guard cell*	2.9	7.9	24	2.3
NHX2	*Na^+/H^+ exchanger 2*	4.3	3.4	GC*	2.5

*:(Bauer *et al.* 2013); ** ND-not detected; GC- the gene was found only in guard cell.

3.5 Conclusions

Stomata play a critical role in the regulation of leaf water and gas exchange and, hence, determine plant adaptive potential. However, little data is available on GC biochemistry, protein abundance, and gene expression, mainly due to challenges in isolating sufficient amounts of purified GCs. In the present study, we developed mechanically GC-enriched epidermal fragments from quinoa (halophyte), sugar beet (salt-tolerant) and spinach (salt-sensitive) leaves grown under normal (control) or salt stress conditions. The efficacy of the method was proven by gene expression and SDS-PAGE analysis. Isolated GCs were enriched in GC-specific genes,

suggesting the suitability of this isolation approach for exploring responses of guard cells to stimuli and various types of stress at the molecular level.

3.6 References

Akcin, TA, Akcin, A, Yalcin, E (2015) Anatomical adaptations to salinity in *Spergularia marina* (Caryophyllaceae) from Turkey. *Proceedings of the National Academy of Sciences, India Section B: Biological Sciences* **85**, 625-634.

Altschuler, SJ, Wu, LF (2010) Cellular heterogeneity: do differences make a difference? *Cell* **141**, 559-63.

Asaoka, M, Inoue, SI, Gunji, S, Kinoshita, T, Maeshima, M, Tsukaya, H, Ferjani, A (2019) Excess pyrophosphate within guard cells delays stomatal closure. *Plant and Cell Physiology* **60**, 875-887.

Bates, GW, Rosenthal, DM, Sun, J, Chattopadhyay, M, Peffer, E, Yang, J, Ort, DR, Jones, AM (2012) A comparative study of the *Arabidopsis thaliana* guard-cell transcriptome and its modulation by sucrose. *PLoS One* **7**, e49641.

Bauer, H, Ache, P, Lautner, S, Fromm, J, Hartung, W, Al-Rasheid, KAS, Sonnewald, S, Sonnewald, U, Kneitz, S, Lachmann, N, Mendel, RR, Bittner, F, Hetherington, AM, Hedrich, R (2013) The stomatal response to reduced relative humidity requires guard cell-autonomous ABA synthesis. *Current Biology* **23**, 53-57.

Cai, F, Liu, S, Dijke, PT, Verbeek, FJ (2017) Image analysis and pattern extraction of proteins classes from one-dimensional gels electrophoresis. *International Journal of Bioscience, Biochemistry and Bioinformatics* **7**, 201-212.

Cruz-Valderrama, JE, Gómez-Maqueo, X, Salazar-Iribe, A, Zúñiga-Sánchez, E, Hernández-Barrera, A, Quezada-Rodríguez, E, Gamboa-deBuen, A (2019) Overview of the role of cell wall DUF642 proteins in plant development. *International Journal of Molecular Sciences* **20**, 3333.

Day, RC, Grossniklaus, U, Macknight, RC (2005) Be more specific! Laser-assisted microdissection of plant cells. *Trends in Plant Science* **10**, 397-406.

Deger, AG, Scherzer, S, Nuhkat, M, Kedzierska, J, Kollist, H, Brosche, M, Unyayar, S, Boudsocq, M, Hedrich, R, Roelfsema, MRG (2015) Guard cell SLAC1-type anion channels mediate flagellin-induced stomatal closure. *New Phytologist* **208**, 162-173.

Evans, JR (1989) Photosynthesis and nitrogen relationships in leaves of C3 plants. *Oecologia* **78,** 9-19.

Fodor, I, Valasek, A, Urbán, P, Kovács, M, Fekete, C, Kerepesi, I (2017) A comparative study on optimisation of protein extraction methods for *Saccharomonospora azurea*. *Acta Biologica Szegediensis* **61**, 45-50.

Francia, P, Simoni, L, Cominelli, E, Tonelli, C, Galbiati, M (2008) Gene trap-based identification of a guard cell promoter in Arabidopsis. *Plant Signaling & Behavior* **3**, 684-6.

Galbiati, M, Matus, JT, Francia, P, Rusconi, F, Canon, P, Medina, C, Conti, L, Cominelli, E, Tonelli, C, Arce-Johnson, P (2011) The grapevine guard cell-related VvMYB60 transcription factor is involved in the regulation of stomatal activity and is differentially expressed in response to ABA and osmotic stress. *BMC Plant Biology* **11**, 142.

Galbraith, DW (2010) Flow cytometry and fluorescence-activated cell sorting in plants: the past, present, and future. *Biomédica* **30**, 65-70.

Gardner, MJ, Baker, AJ, Assie, JM, Poethig, RS, Haseloff, JP, Webb, AAR (2009) GAL4 GFP enhancer trap lines for analysis of stomatal guard cell development and gene expression. *Journal of Experimental Botany* **60**, 213-226.

Gautam, V, Sarkar, AK (2015) Laser assisted microdissection, an efficient technique to understand tissue specific gene expression patterns and functional genomics in plants. *Molecular Biotechnology* **57**, 299-308.

Geilfus, CM, Lan, J, Carpentier, S (2018) Dawn regulates guard cell proteins in *Arabidopsis thaliana* that function in ATP production from fatty acid beta-oxidation. *Plant Molecular Biology* **98**, 525–543.

Hashimoto, M, Negi, J, Young, J, Israelsson, M, Schroeder, JI, Iba, K (2006) Arabidopsis HT1 kinase controls stomatal movements in response to CO_2. *Nature Cell Biology* **8**, 391-7.

Hunt, L, Amsbury, S, Baillie, A, Movahedi, M, Mitchell, A, Afsharinafar, M, Swarup, K, Denyer, T, Hobbs, JK, Swarup, R, Fleming, AJ, Gray, JE (2017) Formation of the stomatal outer cuticular ledge requires a guard cell wall proline-rich protein. *Plant Physiology* **174**, 689-699.

Jahn, CE, Charkowski, AO, Willis, DK (2008) Evaluation of isolation methods and RNA integrity for bacterial RNA quantitation. *Journal of Microbiological Methods* **75**, 318-24.

Jalakas, P, Yarmolinsky, D, Kollist, H, Brosché, M (2017) Isolation of guard-cell enriched tissue for RNA extraction. *Bio-Protocol* **7**, e2447.

Jamet, E, Canut, H, Boudart, G, Pont-Lezica, RF (2006) Cell wall proteins: a new insight through proteomics. *Trends in Plant Science* **11**, 33-9.

Jarvis, DE, Ho, YS, Lightfoot, DJ, Schmockel, SM, Li, B, Borm, TJ, Ohyanagi, H, Mineta, K, Michell, CT, Saber, N, Kharbatia, NM, Rupper, RR, Sharp, AR, Dally, N, Boughton, BA, Woo, YH, Gao, G, Schijlen, EG, Guo, X, Momin, AA, Negrao, S, Al-Babili, S, Gehring, C, Roessner, U, Jung, C, Murphy, K, Arold, ST, Gojobori, T, Linden, CG, van Loo, EN, Jellen, EN, Maughan, PJ, Tester, M (2017) The genome of *Chenopodium quinoa*. *Nature* **542**, 307-312.

Jones, L, Milne, JL, Ashford, D, McQueen-Mason, SJ (2003) Cell wall arabinan is essential for guard cell function. *Proceedings of the National Academy of Sciences of the United States of America* **100**, 11783-11788.

Karkonen, A, Kuchitsu, K (2015) Reactive oxygen species in cell wall metabolism and development in plants. *Phytochemistry* **112**, 22-32.

Kiani-Pouya, A, Rasouli, F, Bazihizina, N, Zhang, H, Hedrich, R, Shabala, S (2019) A large-scale screening of quinoa accessions reveals an important role of epidermal bladder cells and stomatal patterning in salinity tolerance. *Environmental and Experimental Botany* **168**, 103885.

Kopka, J, Provart, NJ, Muller-Rober, B (1997) Potato guard cells respond to drying soil by a complex change in the expression of genes related to carbon metabolism and turgor regulation. *The Plant Journal* **11**, 871-882.

Lawson, T, Simkin, AJ, Kelly, G, Granot, D (2014) Mesophyll photosynthesis and guard cell metabolism impacts on stomatal behaviour. *New Phytologist* **203**, 1064-1081.

Lee, SJ, Kang, JY, Park, HJ, Kim, MD, Bae, MS, Choi, HI, Kim, SY (2010) DREB2C interacts with ABF2, a bZIP protein regulating abscisic acid-responsive gene expression, and its overexpression affects abscisic acid sensitivity. *Plant Physiology* **153**, 716-27.

Leonhardt, N, Kwak, JM, Robert, N, Waner, D, Leonhardt, G, Schroeder, JI (2004) Microarray expression analyses of Arabidopsis guard cells and isolation of a recessive abscisic acid hypersensitive protein phosphatase 2C mutant. *The Plant Cell* **16**, 596-615.

Liu, Y, Chen, X, Zhang, Y, Liu, J (2019) Advancing single-cell proteomics and metabolomics with microfluidic technologies. *Analyst* **144**, 846-858.

Llanes, A, Arbona, V, Gomez-Cadenas, A, Luna, V (2016) Metabolomic profiling of the halophyte *Prosopis strombulifera* shows sodium salt-specific response. *Plant Physiology and Biochemistry* **108**, 145-157.

Marom, Z, Shtein, I, Bar-On, B (2017) Stomatal opening: the role of cell-wall mechanical anisotropy and its analytical relations to the bio-composite characteristics. *Frontiers in Plant Science* **8**, 2061.

Narsai, R, Howell, KA, Millar, AH, O'Toole, N, Small, I, Whelan, J (2007) Genome-wide analysis of mRNA decay rates and their determinants in *Arabidopsis thaliana*. *The Plant Cell* **19**, 3418-36.

Negi, J, Moriwaki, K, Konishi, M, Yokoyama, R, Nakano, T, Kusumi, K, Hashimoto-Sugimoto, M, Schroeder, JI, Nishitani, K, Yanagisawa, S, Iba, K (2013) A Dof transcription factor, SCAP1, is essential for the development of functional stomata in Arabidopsis. *Current Biology* **23**, 479-84.

Rui, Y, Chen, Y, Kandemir, B, Yi, H, Wang, JZ, Puri, VM, Anderson, CT (2018) Balancing strength and flexibility: how the synthesis, organization, and modification of guard cell walls govern stomatal development and dynamics. *Frontiers in Plant Science* **9**, 1202.

Shirakawa, M, Ueda, H, Nagano, AJ, Shimada, T, Kohchi, T, Hara-Nishimura, I (2014) FAMA is an essential component for the differentiation of two distinct cell types, myrosin cells and guard cells, in Arabidopsis. *The Plant Cell* **26**, 4039-52.

Uddin, MN, Hanstein, S, Leubner, R, Schubert, S (2013) Leaf cell-wall components as influenced in the first phase of salt stress in three maize (*Zea mays* L.) hybrids differing in salt resistance. *Journal of Agronomy and Crop Science* **199**, 405-415.

Voss, LJ, McAdam, SAM, Knoblauch, M, Rathje, JM, Brodribb, T, Hedrich, R, Roelfsema, MRG (2018) Guard cells in fern stomata are connected by

plasmodesmata, but control cytosolic Ca^{2+} levels autonomously. *New Phytologist* **219**, 206-215.

Wang, RS, Pandey, S, Li, S, Gookin, TE, Zhao, Z, Albert, R, Assmann, SM (2011) Common and unique elements of the ABA-regulated transcriptome of Arabidopsis guard cells. *BMC Genomics* **12**, 216.

Wang, W, Vignani, R, Scali, M, Cresti, M (2006) A universal and rapid protocol for protein extraction from recalcitrant plant tissues for proteomic analysis. *Electrophoresis* **27**, 2782-6.

Weyers, JDB, Travis, AJ (1981) Selection and preparation of leaf epidermis for experiments on stomatal physiology. *Journal of Experimental Botany* **32**, 837-850.

Wilson, RS, Nairn, AC (2018) Cell-type-specific proteomics: a neuroscience perspective. *Proteomes* **6**, 51.

Wu, Q, Wang, M, Shen, J, Chen, D, Zheng, Y, Zhang, W (2019) ZmOST1 mediates abscisic acid regulation of guard cell ion channels and drought stress responses. *Journal of Integrative Plant Biology* **61**, 478-491.

Yamauchi, S, Takemiya, A, Sakamoto, T, Kurata, T, Tsutsumi, T, Kinoshita, T, Shimazaki, K (2016) The plasma membrane H^+-ATPase AHA1 plays a major role in stomatal opening in response to blue light. *Plant Physiology* **171**, 2731-43.

Yao, XH, Zhao, WC, Yang, R, Wang, JL, Zhao, FK, Wang, SH (2018) Preparation and applications of guard cell protoplasts from the leaf epidermis of *Solanum lycopersicum*. *Plant Methods* **14**, 26.

Zeiger, E, Hepler, PK (1976) Production of guard cell protoplasts from onion and tobacco. *Plant Physiology* **58**, 492-498.

Zhao, ZX, Zhang, W, Stanley, BA, Assmann, SM (2008) Functional proteomics of *Arabidopsis thaliana* guard cells uncovers new stomatal signaling pathways. *The Plant Cell* **20**, 3210-3226.

Zhu, MM, Dai, SJ, McClung, S, Yan, XF, Chen, SX (2009) Functional differentiation of *Brassica napus* guard cells and mesophyll cells revealed by comparative proteomics. *Molecular & Cellular Proteomics* **8**, 752-766.

Chapter 4: Sugar beet (*Beta vulgaris*) guard cells responses to salinity stress: a proteomic analysis[2]

Abstract

Soil salinity is a major environmental constraint affecting crop growth and threatening global food security. Plants adapt to salinity by optimizing the performance of stomata. Stomata are formed by two guard cells (GCs) that are morphologically and functionally distinct from the other leaf cells. These microscopic sphincters inserted into the wax-covered epidermis of the shoot balance CO_2 intake for photosynthetic carbon gain and concomitant water loss. In order to better understand the molecular mechanisms underlying stomatal function under saline conditions, we used proteomics approach to study isolated GCs from the salt-tolerant sugar beet species. Of the 2088 proteins identified in sugar beet GCs, 82 were differentially regulated by salt treatment. According to bioinformatics analysis (GO enrichment analysis and protein classification), these proteins were involved in lipid metabolism, cell wall modification, ATP biosynthesis, and signaling. Among the significant differentially abundant proteins, several proteins classified as "stress proteins" were upregulated, including non-specific lipid transfer protein, chaperone proteins, heat shock proteins, inorganic pyrophosphatase 2, responsible for energized vacuole membrane for ion transportation. Moreover, several antioxidant enzymes (peroxide, superoxidase dismutase) were highly upregulated. Furthermore, cell wall proteins detected in GCs provided some evidence that GC walls were more flexible in response to salt stress. Proteins such as L-ascorbate oxidase that were constitutively high under both control and high salinity conditions may contribute to the ability of sugar beet GCs to adapt to salinity by mitigating salinity-induced oxidative stress.

[2] This chapter has been published as: **Rasouli F.,** Kiani-Pouya A., Li L., Zhang H., Chen Z., Hedrich R., Wilson R., Shabala S. 2020. Sugar beet (*Beta vulgaris*) guard cells responses to salinity stress: a proteomic analysis. International Journal of Molecular Sciences 21, 2331.

4.1 Introduction

Plant leaves are composed of diverse types of cells such as mesophyll, vascular tissues, epidermis, and guard cells (GCs), each of which play different roles in plant growth, development, and response to environmental stimuli. GCs are specialized paired cells in the leaf epidermis forming stomata for gas exchange between plant inside and surrounding atmosphere and are morphologically distinct from the other leaf cells. They adjust the stomatal aperture by changing turgor pressure in response to internal or environmental cues. When stomata are fully open, CO_2 passes through to be absorbed by mesophyll cells for photosynthesis and water transpires and escapes from the leaf surface. However, stomata pores can be closed or adjusted to only be partially open to save water in response to some stresses caused, for example, by reduced water availability. Among environmental factors, salinity can have a serious impact on plant yield. With the reported rate of soil salinization three ha/min (Shabala *et al.* 2014), salinity becomes a major challenge worldwide (Wu *et al.* 2018a). Moreover, the current trends in population dynamics, urbanization, and climate change will exacerbate the process of land salinization. Consequently, understanding stomatal control of plant water transport and CO_2 assimilation under saline conditions is becoming increasingly important (Lawson 2009). Currently, studies on stomatal operation under salt stress are mainly limited to physiological measurements such as stomatal conductance and stomatal apertures at the whole-plant level. Only a very limited number of studies have focused on transcriptional and metabolomic changes in GCs per se, largely because of challenges associated with obtaining a sufficient number of isolated and purified cells for the experiment (Zhao *et al.* 2008b).

Proteomic analysis has been applied in single cell-type studies as an effective method for detecting key proteins and pathways in biological systems (Dai and Chen 2012; Specht and Slavov 2018). While tissue-level studies can be informative, cell type-specific information is lost in tissues composed of multiple cell types such as whole leaf. In contrast, isolated populations of specific cell types have the potential to unravel novel biological processes underlying specific protein functions in the specialized differentiated cells. A good example is the study by Barkla *et al.* (Barkla *et al.* 2012), demonstrating differential abundance of proteins involved in ion and water homeostasis between leaf lamina and epidermal bladder cells (EBC) in *Mesembryanthemum crystallinum* (ice plant) under saline

conditions. In the current study, GC-enriched epidermal fragments were isolated from the leaves of sugar beet plants grown under control and saline conditions to study the proteome profile of GC-specific responses to salt stress. Few studies have used proteomics to investigate the protein profile of GCs and, to the best of our knowledge, there is no report of proteomic analysis of GCs under saline conditions. In the earliest proteomics study on GCs, Zhao *et al.* (Zhao *et al.* 2008b) used protoplasts isolated from Arabidopsis epidermis by enzymatic digestion of epidermal fragments, followed by a combination of 2-D gel and LC-MALDI MudPIT methods. Subsequently, Zhu *et al.* (Zhu *et al.* 2009) identified guard cell specific proteins in *Brassica napus* that were related to transcription, cell structure, signaling, and energy metabolism. In contrast to GCs, proteins involved in photosynthesis and starch synthesis were enriched in mesophyll cells. Proteomics has also been used to analyze the response of GCs to environmental cues, including light, CO_2, and ABA (Zhao *et al.* 2010; Geilfus *et al.* 2018b). For example, proteins and metabolites associated with fatty acid metabolism, redox regulation, and starch /sucrose metabolism were identified in *Brassica napus* GCs in response to low CO_2 (Geilfus *et al.* 2018b). This finding shows that the knowledge obtained from proteomic experiments on GCs can boost our understanding of specific cellular events and key proteins involved in stress conditions and provide information about molecular networks underlying the stomatal functions in different conditions.

For the current stomatal study, we chose sugar beet (*Beta vulgaris ssp. vulgaris*) because it is a species of the Amaranthaceae family with high-salinity stress tolerance. A wild ancestor of sugar beet is sea beet (*Beta vulgaris ssp. maritima*) which is well-adapted to high saline environments of coastal areas. Sugar beet has inherited salt-resistance characteristics and is classified as a salt-tolerant halophilic plant (Skorupa *et al.* 2019). Although this plant has been domesticated relatively recently, it has not been adversely affected by the domestication process as it has maintained its resistance to high salinity levels (Rozema *et al.* 2014). Therefore, this plant could be a good resource to explore salt tolerance mechanisms and to identify proteins and genes involved in salt tolerance (Zhang *et al.* 2016c). Currently, proteomic studies on salt tolerance in sugar beet have been limited to tissues such as shoot, root, and leaf (Cao *et al.* 2014; Yu *et al.* 2016; Wu *et al.* 2018a), with no studies on GCs reported to date. In this study, the GCs isolated for proteomic analysis were validated with microscopic observation, viability tests and

comparing guard cell-specific proteins in mesophyll and guard cell samples. We report the overall protein profile of the isolated GCs in addition to proteins differentially abundant under saline conditions. Functional classification and gene ontology (GO) enrichment analysis of the GC proteome and differentially abundant proteins were used to identify characteristic, dominant proteins, the most enriched biological processes in whole guard cell proteome and those proteins affected by salinity.

4.2 Materials and methods

4.2.1 Growth conditions and physiological parameters

Seeds of sugar beet (*Beta vulgaris ssp. vulgaris*) were obtained from Leibniz Institute of Plant Genetics and Crop Plant Research (IPK) (gbis.ipk-gatersleben.de), Germany. Plants were grown in 20 cm diameter pots (six plants per pot) filled with potting mix containing 90% composted pine bark; 5% coco peat; 5% coarse sand dolomite (6 kg m^{-3}); gypsum (1 kg m^{-3}); ferrous sulphate (1.5 kg m^{-3}); slow-released fertilizer and Osmoform Pre-mix (1.25 kg m^{-3}) Scotts Pro (3 kg m^{-3}) at the glasshouse facilities at the University of Tasmania in Hobart, Australia. The mean day/night temperatures were 24 °C/16 °C and relative humidity was 70%. Salt stress was imposed 3 weeks after planting by adding 300 mM NaCl to the irrigation water and lasted for another 3 weeks. For CO_2 assimilation rate and stomatal conductance (*gs*) measurement a Li-Cor 6400 gas analyzer system (Lincoln, NE, USA) was used (light intensity:1500 µmol m^{-2} S^{-1}, CO_2 concentration: 400 µmol mol^{-1}, atmospheric VDP : 75% RH and leaf temperature: 20 °C). A portable fluorometer (Heinz Walz GmbH, Effeltrich, Germany) was used for the maximal photochemical efficiency of PSII (Fv/Fm) measurements. Youngest fully expanded leaves were used for all measurements.

4.2.2 In situ detection of H_2O_2 in guard cells and ascorbic acid treatments

Hydrogen peroxide in guard cells was detected using 3,3'-Diaminobenzidine (DAB) staining. For this purpose, leaves from control and salt treated plants were incubated in DAB solution (1 mg mL^{-1}, DAB, and 10 mM Na_2HPO_4. Vacuum-infiltrating was applied for 5 min in the dark. Then samples, were kept on the shaker overnight at 80 rpm shaking speed (room temperature and darkness). For de-staining, the samples were washed with ethanol: glycerol: acetic acid (3:1:1)

solution two times before visualizing in light microscopy. DAB staining processes were repeated for the salt-grown leaves treated with different concentrations of ascorbic acid. For ascorbic acid experiment concentrations of 150, 300, and 450 mg L^{-1} ascorbic acid were sprayed on the leaf 3 times a day for three consecutive day, then the stomatal conductance were measured when plants were in the normal light in the glasshouse, then plants moved to a dark place and kept for 30 min then the stomatal conductance were measured again.

4.2.3 GC and mesophyll preparation

GC-enriched epidermal peels were prepared from fully expanded leaves of well-watered 3-4-week-old sugar beet. The leaves were ground in the Grindomix blender (GRINDOMIX LENDER GM 200, Retsch, Germany) with 200 mL water and 100 mL crushed ice by 3 pulses of 20 seconds at maximum speed. The leaf mixture was passed through a 210 µm Nylon mesh (ELKO, Filtering co. USA) and rinsed with ice-cold distilled water and small dark green tissue fragments were removed using clean forceps (three times). Samples were snap-frozen in liquid nitrogen and were kept in -80 °C freezer until used for protein extraction. Isolated GCs-enriched fragments were examined under the microscope to confirm that no contamination of mesophyll fragments or vascular particles (green tissue) were present. Separation of the mesophyll tissue was performed mechanically. Fully expanded leaves were excised and adaxial (upper) side of leaf was attached with double-sided tape strips that had been fixed on the laboratory bench. The epidermis of abaxial sides were peeled off using a forceps and mesophyll tissue were cut using a surgical scalper and collected in aluminum foil before snap freezing in liquid nitrogen.

4.2.4 Protein extraction

GC samples from the control and salt treatments were ground to a fine powder in liquid nitrogen (five biological replicates per treatment). Then, 10% trichloroacetic acid (TCA) in pre-chilled acetone containing 0.07% (*v*/*v*) 2-mercaptoethanol was used to precipitate total proteins. The homogenate was kept at -20 °C overnight. Then the samples were centrifuged at 20,000× *g* at 4 °C for 20 min and the pellets were washed in 100% pre-chilled acetone containing 0.07% (*v*/*v*) 2-mercaptoethanol. This wash step was repeated until all visible traces of chlorophyll were removed. After a final wash in 80% prechilled acetone containing 0.07% (*v*/*v*)

2-mercaptoethanol protein pellets were centrifuged then air-dried at room temperature. Proteins were then solubilized in 1 mL solubilization buffer (7 M urea, 2 M thiourea, and 40 mM Tris) at 20 °C for 1 h then clarified by centrifugation. Protein extracts were precipitated with 4 volumes of acetone and resuspended in 50 μL of solubilization buffer containing 7 M urea, 2 M thiourea, 40 mM Tris. Protein concentrations were measured using Pierce 660 nm Protein Assay Reagent. Protein concentrations were from 530 μg mL^{-1} to 750 μg mL^{-1} in different treatments and biological replications. Samples with higher concentrations of protein were diluted to obtain a constant amount of proteins in all samples. All centrifugation steps were at 20,000× *g* at 4 °C for 30 min.

4.2.5 Enzymatic digestion and off-line desalting

For each sample, 100 μg of precipitated proteins from GCs were reduced, alkylated, and digested with trypsin at a ratio of 1:50 and kept for 5 h at 37 °C. Digested samples were desalted using Millipore ZipTip C18 according to manufacturer's instructions and dried peptides were reconstituted in 12 μL HPLC loading buffer (2% acetonitrile and 0.05% TFA in water), then stored at −80 °C until LC–MS/MS analysis.

4.2.6 Protein identification by nanoLC–MS/MS

Peptides were first concentrated on a 20 mm × 75 μm PepMap 100 trapping column (3 μm C18) for 5 minutes then separated using a 250 mm × 75 μm PepMap 100 RSLC column (2 μm C18) at a flow rate of 300 nL min^{-1} and held at 45 °C. A 90-minute gradient from 98% mobile phase A (0.1% formic acid in water) to 50% mobile phase B (0.08% formic acid in 80% acetonitrile and 20% water) comprised the following steps: 2–10% B over 12 min, 10–25% B over 48 min, 25–45% B over 10 min, holding at 95% B for 5 min then re-equilibration in 2% B for 15 min. The nano HPLC system was coupled to a Q-Exactive HF mass spectrometer equipped with nanospray Flex ion source (Thermo Fisher Scientific, MA, USA) and controlled using Xcalibur 4.1 software. Spray voltage was set to 2.0 kV, S-lens RF level to 50 and heated capillary set at 250 °C. MS scans were acquired from 370–1500 m/z at 60,000 resolution, with an AGC target of 3 × 10e6 and a maximum fill time of 100 ms. Fragment ion scans were acquired at 15,000 resolution (scan range 200–2000 *m*/*z*), with an AGC target of 2 × 10e5 and a maximum fill time of 28 ms.

An isolation width of 1.4 *m/z* was used, and normalized collision energy for HCD set to 27eV. MS/MS spectra were acquired in data-dependent mode using a Top15 method with 30-second dynamic exclusion of fragmented peptides.

4.2.7 Database searching and protein quantitation

Raw data files were imported into MaxQuant version 1.6.5.0 (http://maxquant.org/) for label-free quantitative comparison between control and saline GC samples and mesophyll samples. GC samples were injected in duplicate and LFQ data combined at the sample level using the same Experiment identifiers in the MaxQuant experimental design table. Mesophyll samples were injected once only and defined as a separate parameter group, with the MaxLFQ algorithm applied separately to this sample group. MS/MS spectra were searched using the Andromeda search engine against protein databases downloaded from NCBI for *Beta vulgaris*. Default settings for protein identification by Orbitrap MS/MS were used, with the match-between-runs match time window set to 0.7 min, including a maximum of two missed cleavages, mass error tolerances of 20 ppm, then 4.5 ppm for initial and main peptide searches, respectively, 0.5 Da tolerance for fragment ions, carbamidomethyl modification of cysteine and variable methionine oxidation. A false discovery rate of 0.01 was used for both peptide-spectrum matches and protein identification. The MaxQuant peptides.txt and proteinGroups.txt output files are presented in Supplemental Tables S4.1 and S4.2. The mass spectrometry proteomics data have been deposited to the ProteomeXchange Consortium via the PRIDE partner repository with the dataset identifier PXD017583.

4.2.8 Determination of relative protein abundance and statistical analysis

We utilized MaxLFQ, the MaxQuant algorithm, for peptide intensity determination and normalization (Cox *et al.* 2014) using pair-wise comparison of unique and razor peptide intensities and a minimum ratio count of 2. The proteinGroups output files generated by MaxQuant analysis were processed as follows: The normalized label-free quantification (LFQ) intensity values, MS/MS counts, and the numbers of razor and unique peptides for each of the identified proteins were imported into Perseus software version 1.5.031 (http://perseus-framework.org/). Protein groups identified either as potential contaminants (prefixed with CON), identified by modified site only, by reverse database matching or on the basis of a single

matching peptide, were removed. LFQ intensity values were then log2−transformed and then a filter applied to include only proteins detected in a minimum of 70% of the samples. Missing values were replaced with random intensity values for low-abundance proteins based on a normal distribution of protein abundances using default MaxQuant parameters. A Student's T-test was run on log2− transformed values to identify the differentially abundant proteins between non stressed and salt-stressed samples. Proteins with an FDR < 0.05 were considered to have statistically significant changes in abundance.

4.2.9 Real-time quantitative reverse transcription PCR analysis

To validate the abundance of some proteins at the transcription level, mRNA levels of seven differentially abundant proteins were carried out. The primers were designed for amplification of differentially expressed genes using primer-blast software (https://www.ncbi.nlm.nih.gov/tools/primer-blast/). Actin was used as a reference gene (Hossain *et al.* 2017). The list of gene-specific primer sequences is provided in the Supplemental Table S4.3. Total RNAs were extracted from GC samples taken from control and salt-treated plants using QIAGEN Kit and TransScript RT-PCR Kit was used for reverse transcription for cDNA synthesis. The reaction conditions for RT- PCR were as follows: 94 °C for 3 min for initial denaturation, followed by 35 cycles of 94 °C (30 s), 55 °C (30 s) and 72 °C (30 s) with final extension of 5 min at 72 °C. Quantifications for each gene was normalized to actin DNA.

4.2.10 Annotation and gene ontology (GO) enrichment analysis

The Basic Local Alignment Search Tool (BLAST) was used for obtaining the protein sequences of each accession number in GCs proteome. Amino acid sequences of all GCs proteins used as input in most recent version of MapMan4 tool, using Mercator4 software (https://plabipd.de/portal/mercator4) (Schwacke *et al.* 2019a) to obtain functional classification of GCs proteins. MapMan framework like The Kyoto Encyclopedia of Genes and Genomes (KEGG) ontology covers various aspects of biology based on massive databases. Both frameworks use the same structure of protein function terms (Schwacke *et al.* 2019a).

Gene ontology (GO) term annotation and GO enrichment analysis for GC proteins and differentially abundant proteins were determined using agriGO ver.2

(Tian *et al.* 2017). Heatmap and PCA plots were drawn using MetaboAnalyst software (https://www.metaboanalyst.ca) and volcano plots were obtained from Origin software (https://www.originlab.com).

4.2.11 Statistical analyses

Statistical analyses on physiological data were performed with IBM SPSS Statistics software, version 26 (IBM Corp., Armonk, NY, USA). Statistical significance was determined by one-way ANOVA analysis based on Duncan's test. The differences between means were considered statistically significant as *p*-values were less than 5%.

4.3 Results

4.3.1 Stomatal traits and conductance in sugar beet

We recognized sugar beet growth was stimulated at 100 mM NaCl with a small reduction in fresh weight at 200 mM NaCl (Supplemental Fig. S4.1). In the present study, treatment with 300 mM NaCl for three weeks resulted in 21% and 11% decline in fresh weight and net CO_2 assimilation, respectively (Figures 4.1 and 4.2), which can be attributed to the limited stomatal conductance and consequently lower concentration of CO_2 in the intercellular spaces of the leaf. We observed that stomatal length was reduced by salinity in sugar beet, while at the same time stomata density was increased (Figures 4.1 and 4.3).

More importantly, the stomatal index (the ratio between the number of stomata and epidermal cells per unit area) remained unchanged, suggesting that stomatal development and differentiation was not influenced by salinity in sugar beet and suggests that the increased number of stomata is more likely to be attributed to decline in total leaf area due to osmotic stress. The maximal photochemical efficiency of PSII (Fv/Fm) was 0.87 in control treatment and did not change significantly at 300 mM NaCl treatment suggesting that PSII reaction centers may not be the main target of salinity stress.

Given that reduced transpiration increases leaf temperature, infrared thermal imaging was used to compare the temperature of sugar beet leaves under control and salinity stress (Fig. 4.2). The temperature of the salt-treated leaves was higher than those of the control leaves, suggesting a reduced rate of transpiration in salt-treated plants.

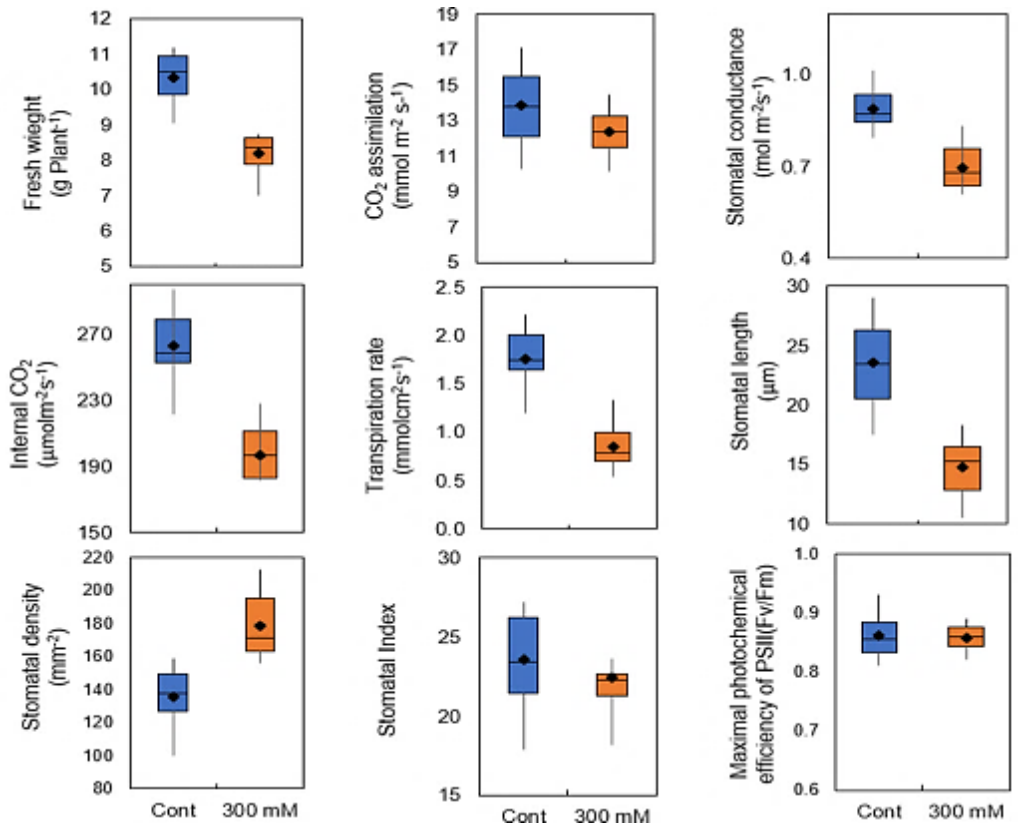

Fig. 4.1 Fresh weight, CO_2 assimilation, stomatal conductance, and stomatal length, density in the sugar beet exposed to 300 mM NaCl for three weeks. Error bars correspond to the SE of at least 5-15 biologically independent measurements.

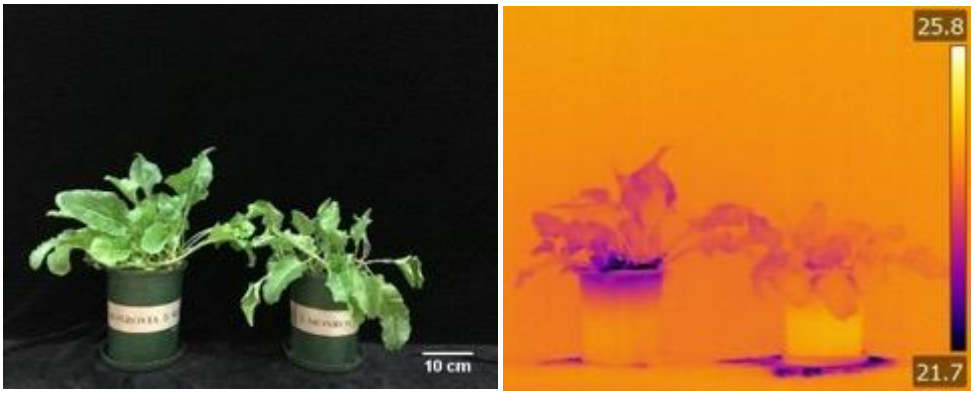

Fig. 4.2 Sugar beet grown for three weeks under control and 300 mM NaCl, normal imaging shows the effect of salinity stress on sugar beet growth (**A**) and thermal imaging indicates higher rates of transpirational cooling in plants under control conditions (B). One (of 5) typical images are shown for each panel.

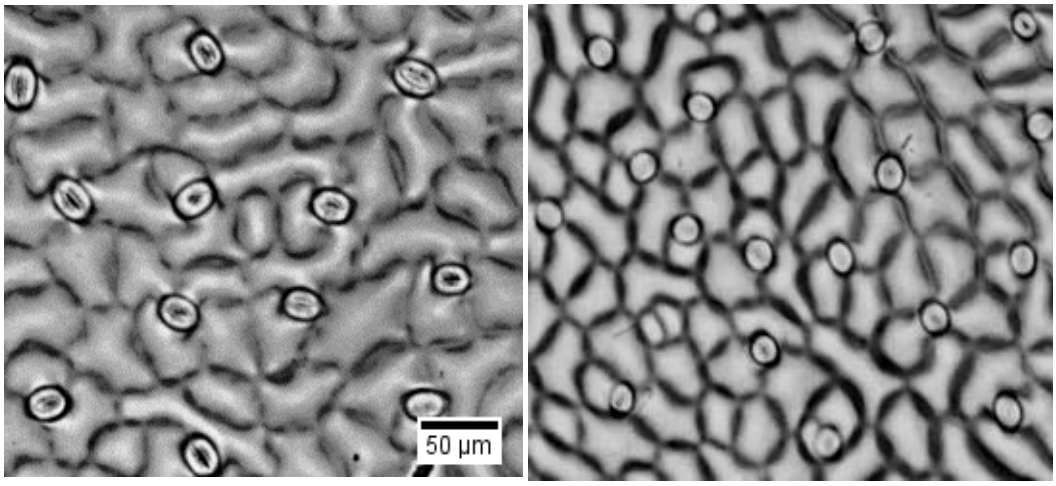

F**ig. 4.3** Stomatal density and size in the abaxial leaf surface of sugar beet plants grown under control (A) and saline (300 mM NaCl for 3 weeks) conditions. One (of 8-12) typical images is shown for each panel.

4.3.2 Comparison of ground state mesophyll and GCs proteome

To investigate responses of stomata to salt stress, we used proteomics to analyse mechanically prepared guard-cell enriched epidermal peels. Isolated GCs-enriched fragments were first examined under the microscope to confirm that no contamination of mesophyll fragments or vascular particles were present. Unlike GCs, epidermal pavement cells are vulnerable and could be destroyed even by manual peeling (Weyers and Travis 1981). Viability test showed that 90% of GCs on epidermis were alive. Typical examples of contaminated GC and purified GC samples have been provided in Supplemental Figures S4.2 and S4.3, respectively. To demonstrate the effectiveness of our technique for GC isolation, we first compared proteomic datasets for GC-enriched samples with whole mesophyll samples. At the level of individual proteins, we found that Rubisco (XP_010669829.1) and chlorophyll-related proteins such as chlorophyll a-b binding protein (XP_010666865.1) and photosynthetic NDH (XP_010672059.1) were substantially higher in the mesophyll compared to the GCs (data points indicated in green in Fig. 4.4). These findings are fully consistent with the fact that GCs have functional chloroplasts just as mesophyll cells. However, GCs contain much lower number of chloroplasts per cell and lower amount of Rubisco (Rother *et al.* 1988).

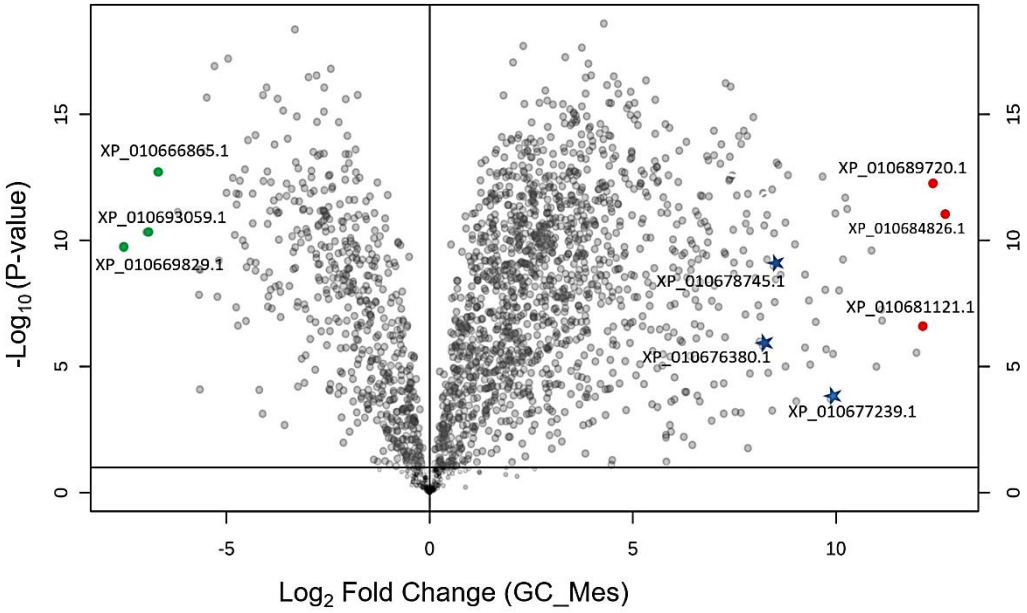

Fig. 4.4 Comparison of differently abundant proteins in mesophyll and guard cells (GCs). Volcano plots displaying differentially abundant proteins in mesophyll and guard cell (FDR < 0.05). Three proteins with highest abundance and three proteins with lowest abundance in GCs relative to mesophyll are marked in red and green, respectively. GC: guard cell; Mes: mesophyll, C: control conditions, S: saline conditions (300 mM NaCl).

Interestingly, stress related proteins such as GDSL esterases/lipases (XP_010684826.1), peroxidase P7-like (XP_010689720.1), and hothead-like protein (XP_010681121.1) were more abundant in GC's (data points indicated in red). Among the stress related proteins, the abundance of abscisic acid receptor PYL2 (XP_010667133.1) and transporter cation/H antiporter 18 (XP_010676380.1) in GCs were 81 and 54 times higher than those expressed in the mesophyll. More importantly, GC-specific proteins such as open stomata1 (OST1), aspartic protease in guard cell 1 (ASPG1), phototropin-1, transcription factor FMA, and serine/threonine-protein kinase BLUS1, high leaf temperature 1 (HT1) were highly accumulated in the GCs (Fig. 4.5), confirming that our guard cell preparation was highly enriched in guard cell proteins. It should be commented that the current procedures for protein extraction or detection are not sufficient for identifying all membrane-bound proteins (Nguyen *et al.* 2019). Thus, some GCs specific channel proteins such as SLAC1 and KAT1 were not observed in our study. This is in an

agreement with previous proteomics reports conducted in Arabidopsis (Zhao *et al.* 2008b; Geilfus *et al.* 2018b).

In addition, to identify any major functional differences between the two cell types, enriched GO terms were identified using the web-based AgriGO tool (Tian *et al.* 2017). The complete list of GO categories in mesophyll and GCs are listed in Supplemental Table S4.4. Generation of precursor metabolites and energy were the most enriched GO categories in GCs, whereas the most significantly-enriched GO categories in the mesophyll were translation and photosynthesis process, suggesting carbon fixation is a major activity in the mesophyll which is consistent with previous findings that the mesophyll proteome was enriched in photosynthesis-related proteins (Zhu *et al.* 2009).

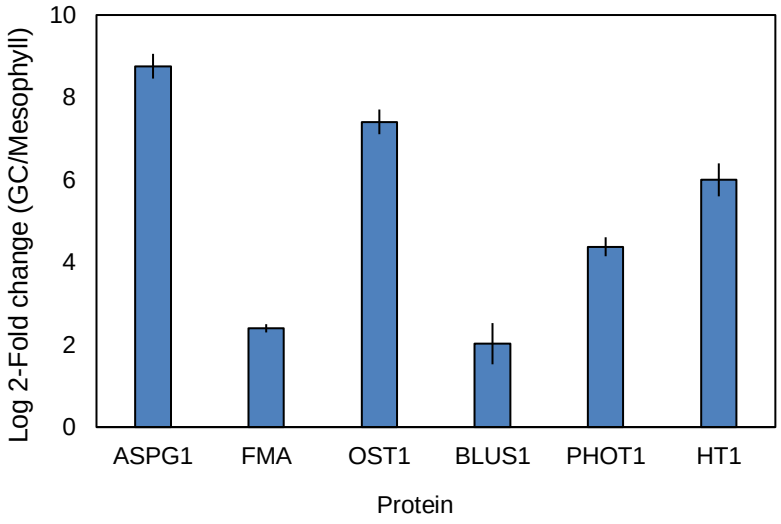

Fig. 4.5 Fold-change of selected guard cell-specific proteins in guard cell samples compared to mesophyll. Values are means of 5 replicates for GCs and 4 replicates for mesophyll ± SE. ASPG1: aspartic protease in guard cell 1; FMA: transcription factor; OST1: open stomata-1; BLUS1: blue light signaling 1; PHOT1: Phototropin-1; HT1: high leaf temperature 1.

To further characterize the GC proteome, we used Mercator4 software in conjunction with MapMan pathway analysis for protein functional classification. Based on the 2,079 GC proteins identified by mass spectrometry, we obtained protein classification for 35 ‘binned’ biological processes (Fig. 4.6).

Protein assignment to the major processes revealed that the largest single group of proteins (~20%) included those involved in protein biogenesis and disposal (e.g. ribosomal subunits, molecular chaperones, and proteasomal subunits). The next most abundant protein categories were identified as "stress" (4.8%), "signaling" (3.7%), "cell wall" (3.6%), "amino acid metabolism" (3.5%), and "photosynthesis" (3.4%). Stress-associated proteins were mainly related to oxidative stress, while signaling proteins and included proteins such as G-proteins, 14-3-3 proteins, MAP kinases, calcium signaling, phosphoinositides, light signaling, signaling in sugar and nutrient physiology, and receptor kinases leucine rich proteins. The complete list of functionally classified GC proteins is provided in the Supplemental Table S4.5.

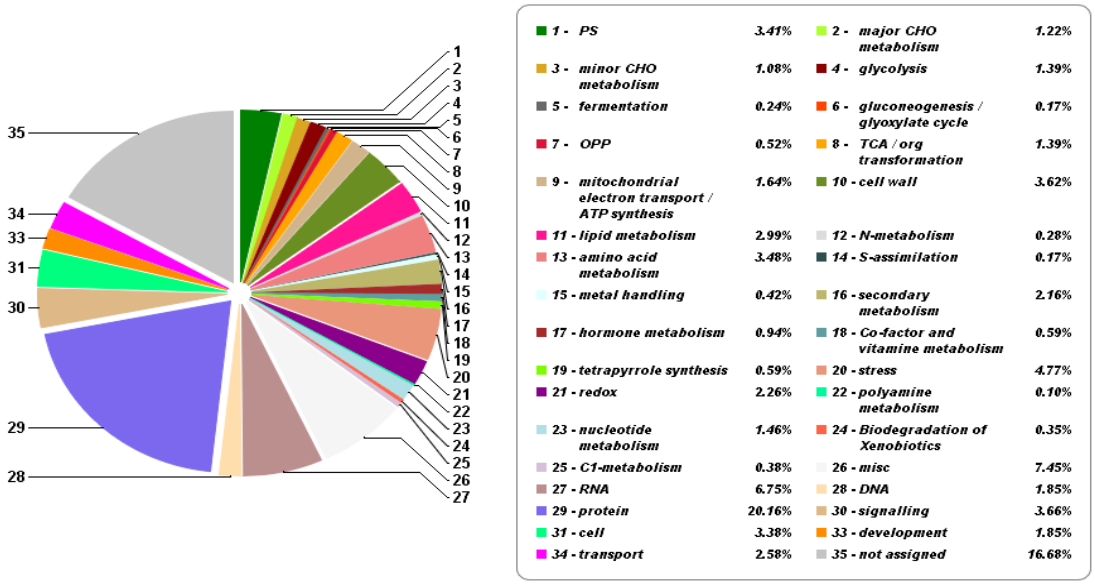

Fig. 4.6 Protein classification of the sugar beet proteome GCs using Mercator 3.6.

4.3.3 Differentially abundant proteins in response to salt treatment in GCs

To identify proteins significantly affected by salt stress we applied a t-test using an FDR-adjusted *p*-value threshold of 0.05 and fold-change cut-off of two. Based on these stringent criteria, changes in abundance of 82 proteins were statistically significant, of which 54 were upregulated and 28 were downregulated by the salt treatment. The 15 most highly modulated proteins by fold-change (10 upregulated and 5 downregulated proteins) are numbered in the volcano plot (Fig. 4.7) and listed

in Table 4.1. The complete list of differentially abundant proteins is provided in Supplemental Table S4.6.

We then used MapMan4 to classify the groups of up- and down-regulated proteins according to their major biological functions. These functions, together with the proteins and their associated Z-scored LFQ expression data, are represented as heatmaps in Figure 4.8. Of the 82 significantly affected proteins, the largest group were assigned to the category "stress", of which eight were downregulated, and 19 were upregulated under salinity conditions. Several of these proteins are known to be involved in salt and drought stresses (non-specific lipid-transfer protein, inorganic pyrophosphatase 2, 60 kDa jasmonate-induced protein) (Szypulska *et al.* 2017; Asaoka *et al.* 2019b; Odintsova *et al.* 2019) and pathogenic stress and other biotic stresses (proteins germin-like) (Ji *et al.* 2018).

In the cell wall category, we also observed a mixed pattern of up- and down-regulated proteins. Two isoforms of the expansin family of cell wall proteins were modulated, of which expansin A10 was upregulated, while expansin A4 was downregulated.

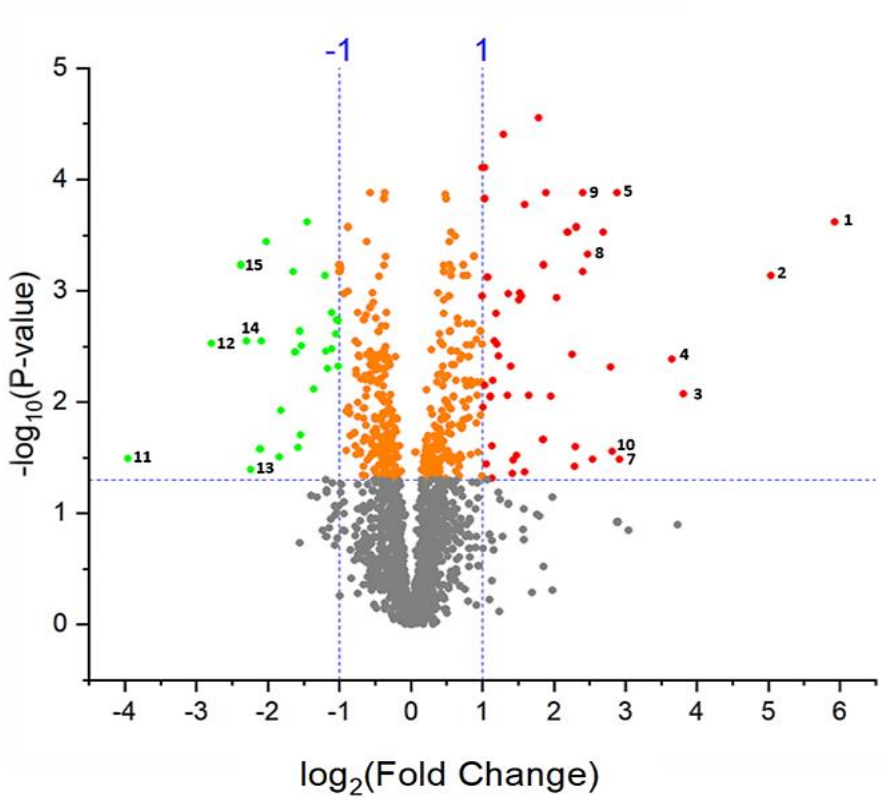

Fig. 4.7 Volcano plot of differentially abundant proteins in the guard cells in response to salt stress.

Table 4.1 The 15 most highly modulated proteins (10 upregulated and 5 downregulated proteins).

No.	Accession Number	Log2 LFQ Intensity (Control)	Log2 LFQ Intensity (Salt Stress)	Unique Peptides	Fold Change	t-Test q Value	Annotation
1	XP_010683515.1	23.1	29.0	4	60.9	2.4×10^{-4}	non-specific lipid-transfer protein
2	XP_010690044.1	23.1	28.6	8	45.0	7.3×10^{-4}	inorganic pyrophosphatase 2
3	XP_010680759.1	23.9	27.3	7	10.3	8.5×10^{-3}	chitotriosidase-1
4	XP_010679746.1	25.2	28.5	14	10.2	4.2×10^{-3}	peroxidase 27
5	XP_010679767.1	26.0	28.9	14	7.5	1.3×10^{-4}	mannan endo-1,4-beta-mannosidase 7
6	XP_010686587.1	28.0	30.7	24	6.6	3.0×10^{-4}	phosphoethanolamine N-methyltransferase
7	XP_010676511.1	22.6	25.1	4	5.7	3.3×10^{-2}	thaumatin-like protein 1
8	XP_010679501.1	26.9	29.4	2	5.3	4.7×10^{-4}	glycine-rich cell wall structural protein
9	KMT11925.1	27.0	29.4	16	5.3	1.3×10^{-4}	endoglucanase 6
10	XP_010687451.1	23.0	25.4	2	5.2	2.8×10^{-2}	endochitinase EP3
11	XP_010678753.1	26.5	23.1	3	−10.25	3.2×10^{-2}	heat shock 70 kDa protein 18-like
12	XP_010677928.1	26.5	23.8	8	−6.51	3.0×10^{-3}	malate synthase, glyoxysomal
13	XP_010686038.1	27.1	24.6	2	-5.72	3.1×10^{-2}	protein suppressor of K^+ transport growth defect1
14	KMT14555.1	30.2	27.8	6	-5.39	2.8×10^{-3}	glucan endo-1,3-beta-glucosidase, acidic-like
15	XP_010676519.1	30.3	27.8	8	-5.32	5.9×10^{-4}	alpha-amylase/trypsin inhibitor

Previously it was reported (Pitann *et al.* 2009) that expansin 2 proteins, which contribute to cell wall extensibility, were upregulated by salt in salt-tolerant genotype but downregulated in salt sensitive one. In addition, enhanced abundance of three members of the family of glycine-rich proteins was also observed.

In the category of protein and RNA biosynthesis, some important proteins with roles in stomatal movement were differentially abundant in response to salt stress. Abundance of aspartic protease in guard cell 1 and transcription factor bHLH130 and heat shock cognate 70 kDa protein increased by 2.5, 2.1, and 2.9-fold, respectively by the salt treatment, whereas other proteins in this category, such as suppressor of K^+ transport growth defect 1 and protein sieve element occlusion B were markedly decreased by salinity stress. Protein sieve elements have been also found in previous proteomics studies on GC, however, its function in GC is unknown (Zhao *et al.* 2008b).

In plants, reactive oxygen species (ROS) are generated in response to biotic and environmental factors. In guard cells, in addition to external stimuli, endogenous signals such as abscisic acid induce H_2O_2 generation and it has been shown that ROS at low levels act as messengers in stomatal movement (Medeiros *et al.* 2020). In the redox group, we observed that the abundance of peroxiredoxin Q and super oxide dismutase (SOD) enhanced 3.6 and 2.1-fold by salinity while catalase, an antioxidant enzyme with a significant role in protection against oxidative stress, declined 2-fold compared to control.

Another central process in stomatal guard cells is transmembrane ion exchange. This process requires energy provided by photosynthesis and ATP production in mitochondria (Santelia and Lawson 2016). In stress condition, more energy is needed to maintain metabolic adjustment (Gharat *et al.* 2016). In our study, the abundance of two proteins involved in mitochondrial ATP synthesis was enhanced (3.2 and 2.1-fold) by salinity; no downregulated proteins were found in this group.

Non-specific lipid-transfer proteins are involved in key processes in the plant cell, such as signal transduction, cell wall modification, membrane stabilization, and conferring resistance to salt stress (Liu *et al.* 2015). In this study, two proteins in this group were more abundant in salt-stressed GCs compare to control, including one non-specific lipid-transfer protein that was the most highly increased (61-fold) overall.

4.3.4 Transcription-level analysis of genes corresponding to proteins modulated in salt-stressed guard cells

Salt stress altered the abundance of 82 proteins in sugar beet GCs according to our proteomic analysis. To verify whether alterations in protein abundance are controlled by changes in gene transcription, qRT-PCR was performed for seven genes (Fig. 4.9) known to play an important role in stomatal movement and salt stress responses including transcription factor bHLH130 (XP_010673593.1), sucrose synthase 7 (XP_010675238.1), spiral1-like 1 (XP_010680669.1), choline monooxygenase (XP_010682183.1), cell wall/vacuolar inhibitor of fructosidase 1 (XP_010685378.1), sugar carrier protein C (XP_010686277.1), and inorganic pyrophosphatase 2 (XP_010690044.1).

The mRNA abundance of four genes including transcription factor bHLH130, choline monooxygenase, cell wall/vacuolar inhibitor of fructosidase 1, and inorganic pyrophosphatase 2 in the GCs were all increased by salt stress, while transcript levels of sucrose synthase 7 and sugar carrier protein C were suppressed (Fig. 4.9); these results are fully consistent with the proteomics data. In contrast, expression of spiral1-like 1 at the gene transcript level, which was 2-fold decreased in GCs at the protein level, did not change significantly.

4.3.5 Differentially abundant proteins in mesophyll under salinity treatment

Our initial comparison of the mesophyll and GC proteins highlighted differences in composition at level of the functional (GO term) classification and enriched proteins, as would be expected from their fundamentally different roles. This is further supported by results of PCA (plot shown in Fig. 4.10) that illustrates the clear separation between mesophyll and guard cell in PC1, which accounts for ~90% of the variation between samples. To identify whether salinity-induced changes in the GC proteome were also manifest in mesophyll tissue, we compared the two sets of differentially abundant proteins. While fewer proteins were found to be affected in mesophyll tissue based on the same criteria (FDR < 0.05 and FC > 2; Supplemental Table S4.7), four of the 12 upregulated proteins were also upregulated in GCs. These included non-specific lipid-transfer protein, heat shock cognate 70 kDa protein 2, choline monooxygenase, and phosphoethanolamine N-methyltransferase.

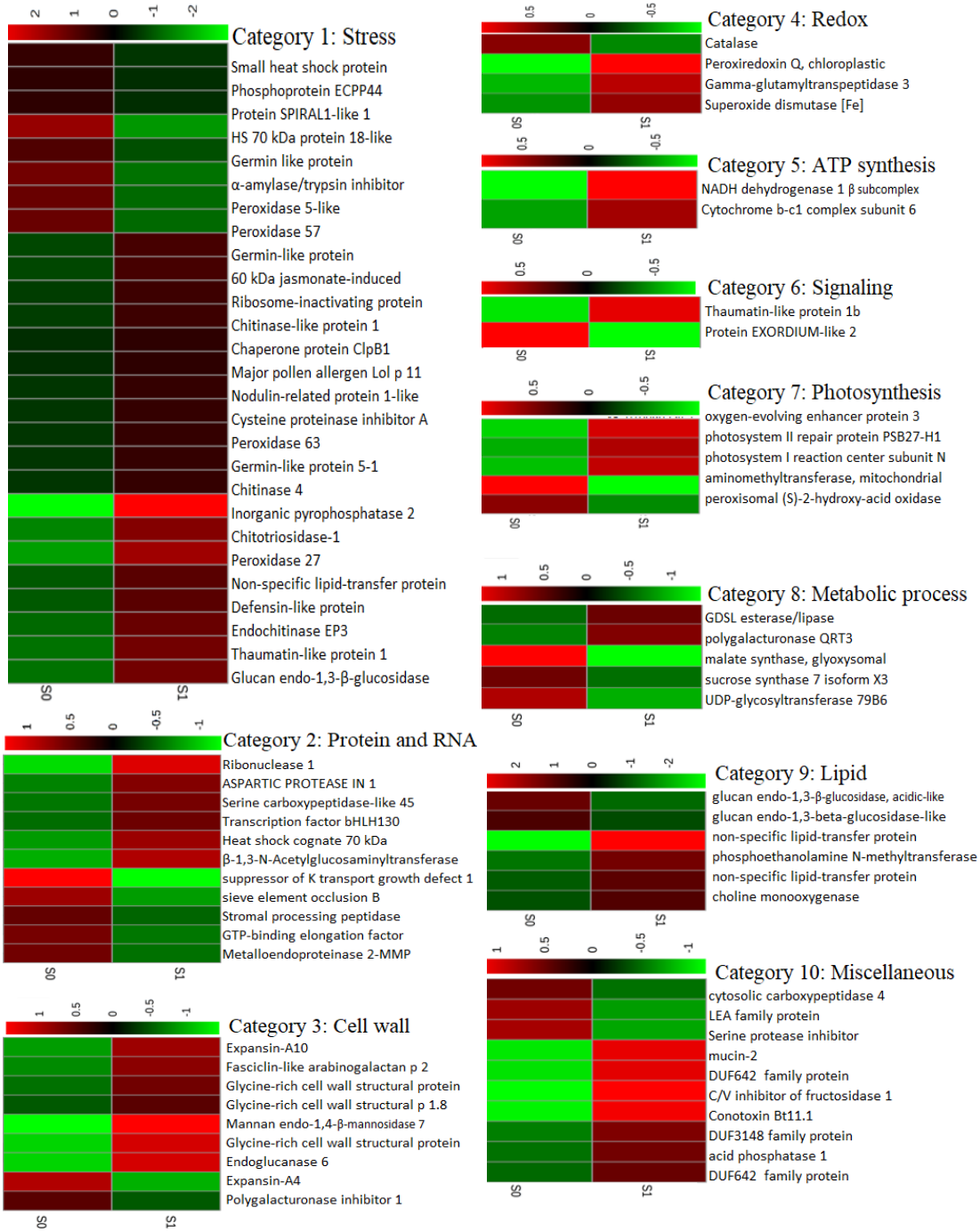

Fig. 4.8 Heat maps (based on Z-scores of the protein abundance measurements) demonstrating abundance patterns of individual proteins within each functional category in sugar beet guard cells. The color intensities shown correspond to the Z-scored LFQ intensities, according to the key shown at the top of each heat map. S0 and S1 denote control and saline treatments, respectively.

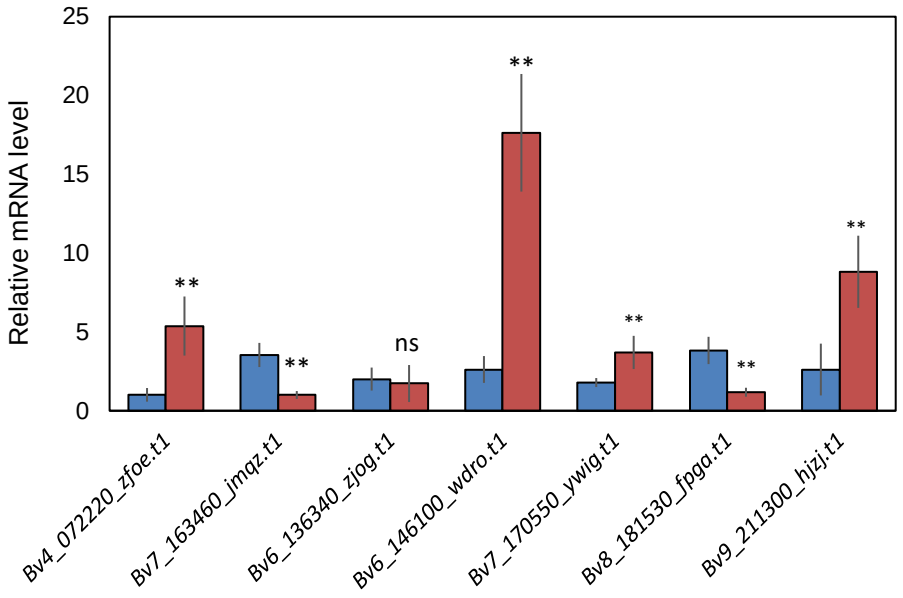

Fig. 4.9 Transcript levels of genes encoding seven altered abundance proteins. *Bv4_072220_zfoe.t1*- Transcription Factor bHLH130; *Bv7_163460_jmqz.t1*- Sucrose synthase 7; *Bv6_136340_zjog.t1*- Spiral1-like 1; *Bv6_146100_wdro.t1*- Choline monooxygenase; *Bv7_170550_ywig.t1*- Cell wall / vacuolar inhibitor of fructosidase 1; *Bv8_181530_fpga.t1*- Sugar carrier protein C; *Bv9_211300_hjzj.t1*- Inorganic pyrophosphatase 2. Values are means of 3 biological and 3 technical measurements ± SE. Asterisk (*) denotes a significant mRNA difference between control and salt stress.

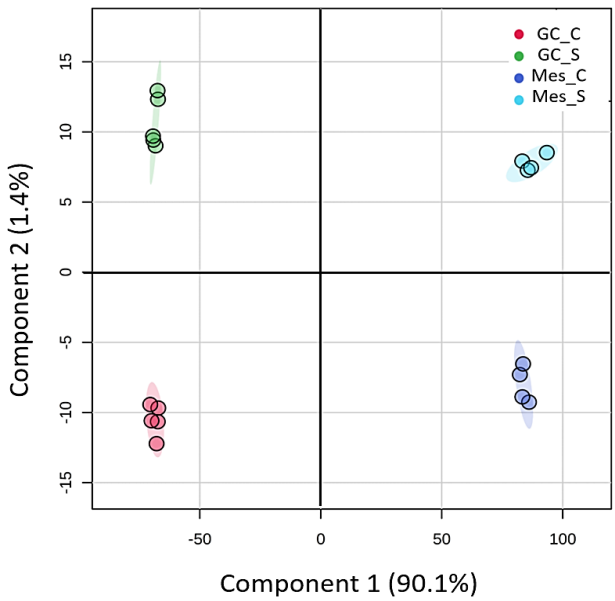

Fig. 4.10 PCA clustering based on mesophyll and guard cell proteome data under control and salt conditions. Proteomics analyses were performed with 4 and 5 biological replicates for mesophyll and guard cells respectively. GC: guard cell; Mes: mesophyll, C: control conditions, S: saline conditions (300 mM NaCl).

4.3.6 H_2O_2 accumulation in guard cell in response to salt stress and ascorbic acid

When plants are exposed to environmental stresses, the level of ROS such as H_2O_2 increases and results in oxidative stress and reduction in growth. Consequently, we used DAB (3,3'-Diaminobenzidine) staining to detect H_2O_2 in GCs, where formation of brown stain in tissue shows DAB oxidation by H_2O_2 (Figures 4.11 and 4.12). Our results clearly show elevated H_2O_2 levels in salt-stressed GCs compared with controls (Fig. 4.11A, B), which was alleviated by foliar spray of ascorbic acid in a dose-dependent manner (Fig. 4.11C–E). A higher concentration of ascorbic acid was associated with less oxidative status in guard cells. Application of 450 mg L^{-1} ascorbic acid on leaf dramatically reduced the accumulation of H_2O_2 in GCs (Figures 4.11 and 4.12A). Stomatal conductance measured at natural light conditions in the glasshouse showed that salt-induced reduction in stomatal conductance can be mitigated by application of ascorbic acid. Stomatal conductance measurements in plants after kept under dark conditions for 30 min showed that higher concentrations of ascorbic acid had detrimental effects on stomatal closure. As it can be seen in Figure 4.12B, stomatal conductance under control conditions was 458 µmol m^{-2} s^{-1} in the light and then reduced to 36 µmol m^{-2} s^{-1} when plants were kept in darkness for 30 min, implying a 92% reduction in stomatal conductance. At the same time, the corresponding values for plants treated with 450 mgL^{-1} of ascorbic acid were 413 and 92 µmol m^{-2} s^{-1} in light and dark, respectively (a 77% reduction).

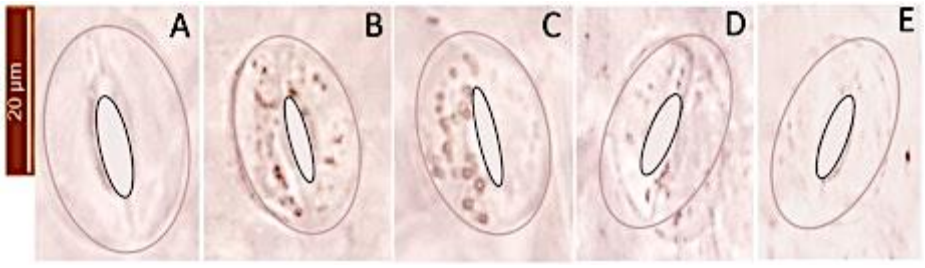

Fig. 4.11 DAB (3,3'-Diaminobenzidine) staining for detection of H_2O_2 in guard cell under control (**A**) and 300 mM NaCl (**B–E**). (**B**) control (no ascorbic acid, AsA); (**C**) 150 mg L^{-1} AsA; (**D**) 300 mg L^{-1} AsA; **E**: 450 mg L^{-1} AsA. Formation of brown precipitates showed the generation of H_2O_2 by guard cells. The borders of guard cells and stomatal pores were lined to make it more contrasting with the background. Raw images (without GC outlines) are provided in the Supplemental Fig. S4.4 One (of 15) typical images is shown.

These results indicate that H_2O_2 is needed for optimal operation of the stomata, suggesting that tempering with H_2O_2 concentration in GCs may result in a lower speed of stomatal closure in response to dark, with the consequences of reducing water use efficiency.

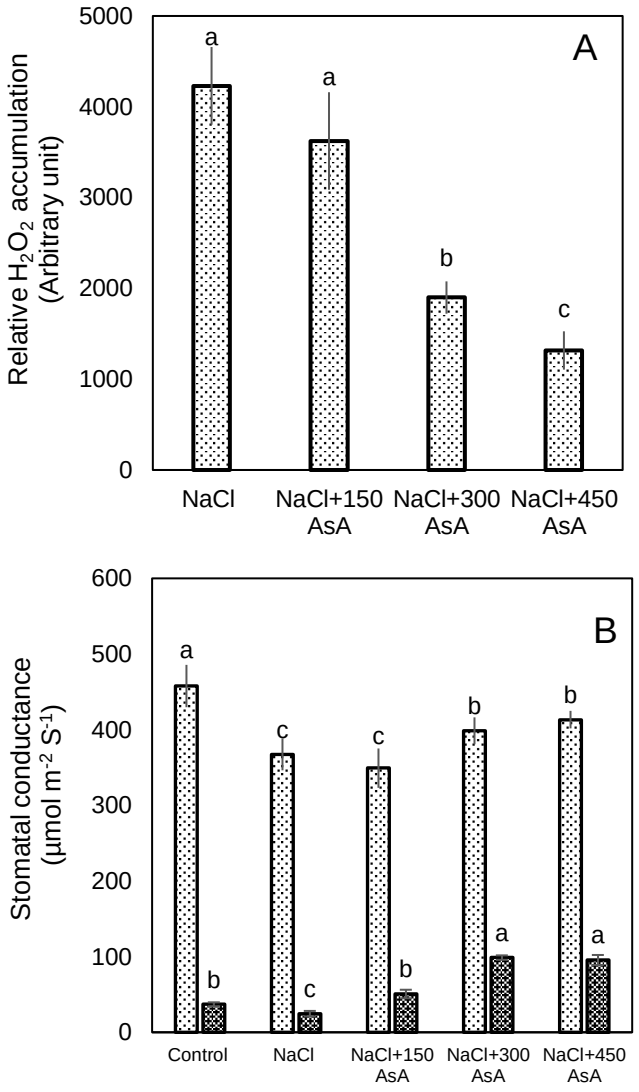

Fig. 4.12 (**A**) Effect of different concentrations of ascorbic acid on H_2O_2 of levels in the GCs of sugar beet plants grown under saline conditions, relative to non-stressed controls. Relative signal intensities of DAB staining were quantified using ImageJ software. (**B**) Stomata conductance in non- stressed sugar beet leaves and salt- stressed leaves with or without ascorbic acid treatment. The light bar and dark bar are stomata conductance measurements under natural light conditions and under 30 min-dark conditions, respectively. Values are means of 5 replicates ± SE. Data labeled with different lower-case letters are significantly different at $p < 0.05$.

4.4 Discussion

In most proteomics studies, GCs are not analyzed separately but included in the bulk of the leaf samples, thus masking GC-specific mechanisms underlying stomatal operation under stress conditions. To date, a very limited number of studies have used proteomics to analyze GCs specifically (Zhao *et al.* 2008b; Zhu *et al.* 2009; Zhao *et al.* 2010; Geng *et al.* 2017; Geilfus *et al.* 2018b) and none have investigated the specific response of GCs to salt stress. In this study, the efficiency of the GC isolation method was validated with a combination of techniques, including microscopic observation, viability tests, and at the proteome level. Several proteins encoded by GC-specific genes such as ASPG1, OST1, PHOT1, and BLUS1 were markedly higher in GC-enriched samples compared to mesophyll, suggesting that our approach for GC isolation was appropriate for proteomics studies.

4.4.1 Most abundant proteins in GCs

The top protein according to overall abundance (LFQ value) in both control and salt-treated sugar beet GCs was a protein with as-yet uncharacterized function in sugar beet and most plants. However, it is known to be an orthologue of DUF642 protein, encoded by AT5G11420 gene in Arabidopsis. There is evidence that this member of the DUF642 family regulates the activity of pectin methyl esterase (Zúñiga-Sánchez *et al.* 2014) which plays a significant role in GCs wall flexibility (Amsbury *et al.* 2016). DUF642 overexpression increased plant tolerance to pathogenic infection and accelerated plant growth in tomato.

GDSL esterase/lipase a lipolytic enzyme GDSL esterase/lipase along with auxin binding proteins (ABP19) were also among the most highly abundant proteins in sugar beet GCs. The higher abundance of GDSL protein has been reported in response to biotic and abiotic environmental factors (Lee *et al.* 2009a). Increased in GDSL esterase/lipases proteins and stomatal apertures were observed in response to low CO_2 in Arabidopsis (Geng *et al.* 2017).

The plant hormone auxin is required for stomatal patterning and development (Le *et al.* 2014) and auxin signaling is dependent on auxin binding proteins. Accumulation of ABP1 protein resulted in higher sensitivity to potassium current in tobacco GCs (Bauly *et al.* 2000), showing the importance of this protein in GCs performance. Another highly abundant protein in sugar beet GCs was DNA

damage-responsive protein (DDR48). This protein is reported to be involved in mitigating oxidative stress and resistance against fungal attack (Dib *et al.* 2008), suggesting the constitutive accumulation of those proteins can confer augmented tolerance to GCs when exposed to salt stress.

4.4.2 Stress related proteins differentially abundant proteins in GCs under salinity treatment

A high proportion of differentially abundant proteins in the GCs of salt-treated plants were related to various types of stresses including salinity, drought, oxidative, cold, and biotic stresses. Three enzymes that were among the most highly up-regulated proteins under salinity stress, namely pyrophosphatase (PPase), chitotriosidase-1, and peroxidase, are well documented for their roles in conferring salt tolerance in multiple species, especially halophytes (Gao *et al.* 2006; Sun *et al.* 2010). Pyrophosphatase, which was upregulated 45-fold by salt stress, is a proton pump capable of energizing the vacuolar membrane for generating electric potential and transporting H^+ across the membrane (Maeshima 2000) and thus is crucial for ion transport in the GCs. Overexpression of halophytic PPase genes in glycophytes resulted in a higher accumulation of Na^+ by plants (Gao *et al.* 2006), while PPase loss-of-function mutants showed high susceptibility to water deficiency. Stomata malfunction is the main interpretation for the drought sensitivity of mutant plants with a low abundance of this enzyme, where stomatal closure is delayed after ABA treatments in H^+-PPase mutants.

Nodulin-related protein 1 was 2-fold higher in GCs of salt-treated plants compared with controls. Previously, it was shown that this gene was induced by the cold stress and suppressed by the heat stress in Arabidopsis, and changes in this protein are associated with increased tolerance to various types of biotic and abiotic stress (Fu *et al.* 2010).

Multiple non-specific lipid-transfer proteins (LTPs) were highly induced by salt in the GCs. LTPs (Arondel *et al.* 2000) mediate cell signaling in response to environmental factors and have been associated with adaptation of plants to stresses and stimuli (Liu *et al.* 2015). XP_010683515.1 and XP_010690794.1 (upregulated by 61- and 4-fold, respectively) are homologous of LTP4 in Arabidopsis which is involved in response to salt and dehydration (Pan *et al.* 2016; Hairat *et al.* 2018; Odintsova *et al.* 2019). Induction of this gene has been reported in foxtail millet in

response to salt stress and ABA treatment. Furthermore, overexpression of LTPs using gene editing increased plant tolerance to desiccation and osmotic stress, by the accumulation of soluble sugars and proline. Analysis of a specific LTP gene promotor region (isolated from *Setaria italica*) identified two dehydration-responsive elements (DRE) proteins that could bind to abscisic acid–responsive transcription factor. Thus, LTP is likely a downstream gene of this ABA-responsive transcription factor (Pan *et al.* 2016).

A wide variety of chitinases have been identified in plants (class I-class V). While plants do not contain chitin compounds, chitinase enzymes are either expressed constitutively or induced in response to biotic and abiotic stresses (Ohnuma *et al.* 2011). In our study, four chitinase isoforms were found among upregulated proteins. Levels of chitotriosidase-1 increased 10.3-fold in salt-stressed GCs compared to the control. This protein is homologous of chitinase V in Arabidopsis which has a significant role in salt stress in addition to defense against pathogenic attack (Ohnuma *et al.* 2011), and loss of function of the gene encoding chitinase-like protein results in overaccumulation of Na^+ in the cytosol (Kwon *et al.* 2007). In stomata, it has been reported that chitosan, which can be produced by chitinase, mediates stomatal narrowing and it may be advantageous for both the salt stress responses and plant defense (Lee *et al.* 1999; Hidangmayum *et al.* 2019).

Several proteins involved in biotic stress (such as the disease-related protein 60 kDa jasmonate-induced protein) and defense response to fungus (such as defensin-like protein) were also upregulated in response to salt stress. In addition, other proteins related to biotic and abiotic stress, such as stress protein DDR48, various isoform of peroxidase and L-ascorbate oxidase were constitutively accumulated in the sugar beet GCs. This data supports a role for these proteins in the inherent tolerance of sugar beet GCs to tolerate multiple stresses, which can then be further enhanced by upregulation of other proteins in response to salinity.

4.4.3 Redox-related proteins

Salt stress causes an overproduction of ROS, which can damage DNA, proteins, and carbohydrates. In order to prevent accumulation of ROS to toxic levels, enzymatic and non-enzymatic antioxidants are usually generated to scavenge the surplus of ROS. In the current study, we found an increase in two peroxidase isoforms (POD27 and POD63) and enhanced levels of superoxide dismutase

(SOD), while catalase and two other POD isoforms showed lower abundances in GCs of salt-treated plants. Additionally, L-ascorbate oxidase was among the most highly abundant proteins in sugar beet GCs, under both control and salt treatment. This protein is plant specific and involved in cellular redox regulation through decreasing oxygen content (thus limiting ROS generation) and oxidizing AsA which is a crucial antioxidant (De Tullio *et al.* 2013). The essentiality of stress-induced increase in AsA was tested in direct experiments by studying effects of exogenous supplied ascorbic acid onto redox status of guard cells. A high concentration of H_2O_2 was detected in GCs due to salt stress (Figures 4.11 and 4.12); this stress-induced elevation was mitigated by the application of ascorbic acid. Concurrently, AsA-treated plants had a higher degree of stomatal aperture opening, and consequently higher stomatal conductance, under salt stress. Interestingly, when salt-grown plants that had been sprayed with ascorbic acid were exposed to the darkness, they showed a delay in the stomatal closure. These findings are consistent with the role of H_2O_2 as a modulator of stomata functioning (Wu *et al.* 2020).

4.4.4 Photosynthesis and ATP synthesis

It has been documented that GC photosynthesis is necessary for stomatal opening (Santelia and Lawson 2016) and closure (Iwai *et al.* 2019). We found that three proteins related to photosynthesis and two related to ATP synthesis were upregulated by salt in sugar beet GCs, including oxygen-evolving enhancer protein 3 and photosystem I reaction center subunit N. Another photosynthesis-related protein highly upregulated under saline conditions was photosystem II repair protein PSB27-H1, which is involved in the stability of photosynthesis systems and repairing PSII after damage. Moreover, peroxiredoxin Q, which is involved in redox homeostasis in the chloroplast, was also induced by salt showing the ability of sugar beet GCs in maintaining photosynthesis under saline conditions. Stomata rely on the production of ATP in the GCs for their movements. Under salinity stress, more energy is required for osmotic adjustment and dealing with toxin ions (Tyerman *et al.* 2019). Therefore, it is not surprising that proteins associated with ATP synthesis were upregulated in the GCs by salinity treatment.

4.4.5 Protein and RNA biosynthesis

Transcription factor bHLH130, a member of the basic helix-loop-helix (bHLH) family and homologous with the Arabidopsis ABA-responsive kinase substrate 1 gene, was upregulated by salt treatment. Under non-stress conditions this gene promotes stomatal opening by the transcription of genes encoding potassium channels (Takahashi *et al.* 2013). However, in the presence of ABA, its activity is suppressed through phosphorylation of bHLH, causing a reduction in light-induced stomatal opening (Takahashi *et al.* 2013).

The GC-specific protein aspartic protease in guard cell 1 was also upregulated in response to salinity. Following previous results, this protein was among the most highly differentially abundant compared with mesophyll tissue (Leonhardt *et al.* 2004a). Overexpression of this protein was previously found to be accompanied by drought avoidance by higher sensitivity to ABA in the stomatal closure and lower the rate of transpirational water loss (Yao *et al.* 2012).

4.4.6 Cell wall

The function of the GC cell walls is crucial in stomatal dynamics and differentiation (Rui *et al.* 2018). The cell wall of GCs is required to be stiff and sufficiently strong to withstand high turgor pressure when stomata are opening and be flexible to reverse this when stomata are closing. Cell wall modifications, such as loosening, is important in plants under drought and salt stress conditions (Tenhaken 2014) and may affect stomatal movements. As such, mannan endo-1,4-beta-mannosidase 7, which is known for loosening the cell wall, was strongly upregulated (7.5-fold) in sugar beet GCs. Some structural proteins which allow flexibility of cell wall such as glycine-rich proteins (GRP) were also highly abundant in the GCs. It has been reported that some isoforms of this family (GRP1.8) have been digested by collagenase, suggesting that they are structurally similar to collagen in animals and allow cell extensibility (Ringli *et al.* 2001).

4.4.7 Lipid metabolism

In the category of lipid metabolism, two key enzymes phosphoethanolamine N-methyltransferase and choline monooxygenase, which are involved in choline and glycine betaine biosynthesis, were highly upregulated (6.6- and 3.7-fold). Glycine betaine is a water-soluble molecule involved in abiotic stresses by mitigating ROS

impacts (Shabala *et al.* 2012) and contributing to osmotic adjustment as a compatible solute (Lambou *et al.* 2013). Successful germination of sugar beet seeds under high salt levels was attributed to the high accumulation of glycine betaine in the seed (Catusse *et al.* 2008).

4.4.8 Proteins downregulated in sugar beet GCs in response to salinity

About one-third of total differentially abundant proteins in response to salt stress were downregulated in sugar beet GCs. Previous studies have documented the down-regulation of specific proteins in adaptation to salinity, including the microtubule organizer spiral1 protein which is degraded in order to dissemble microtubules and to accelerate the plant response to salinity (Wang *et al.* 2011c). In our study, this protein was down-regulated 2-fold in GCs under salinity stress. Generally, salt stress causes spiral1 proteolysis and lower abundance of this protein is required for managing salt stress.

The abundance of protein suppressor of K^+ transport growth defect 1 declined by salinity in our study. It has been reported that decreased expression of this gene in Arabidopsis resulted in reduced salinity tolerance through an imbalanced Na^+/K^+ ratio (Ho *et al.* 2010).

Sugar carrier protein C was suppressed by salinity in the GCs in this study. In *Pisum sativum,* it has been reported that sugars act as the osmoticum and support the stomatal opening (Ritte *et al.* 1999). Downregulation of this protein may associate with less turgor pressure in the GCs and less stomatal aperture, which is advantageous for plants under salt stress.

4.5 Conclusions

In this study, we have used proteomics to investigate the effects of salinity on guard cells for the first time, using a halophilic plant species with potential to be cultivated under saline conditions. The abundances of proteins related to lipid metabolism, cell wall modification, ATP biosynthesis, and signaling were modified in the GCs of sugar beet plants in response to salt stress. A high proportion of differentially abundant proteins were involved in various types of stresses including salt, drought, oxidative, cold, and biotic stresses. Moreover, some proteins involved in mitigation of oxidative stress were presented at elevated levels under non-stress conditions suggesting the constitutive accumulation of those proteins in sugar beet GCs that

can confer augmented tolerance to GCs when exposed to salt stress. Among those proteins that were most highly abundant and/or accumulated by salinity treatment were several proteins currently of unknown function. These proteins represent good candidates for further research into their functions in GCs using molecular and genetic approaches.

4.6 References

Amsbury, S, Hunt, L, Elhaddad, N, Baillie, A, Lundgren, M, Verhertbruggen, Y, Scheller, HV, Knox, JP, Fleming, AJ, Gray, JE (2016) Stomatal function requires pectin de-methyl-esterification of the guard cell wall. *Current Biology* **26**, 2899-2906.

Arondel, VV, Vergnolle, C, Cantrel, C, Kader, J (2000) Lipid transfer proteins are encoded by a small multigene family in *Arabidopsis thaliana*. *Plant Science* **157**, 1-12.

Asaoka, M, Inoue, SI, Gunji, S, Kinoshita, T, Maeshima, M, Tsukaya, H, Ferjani, A (2019) Excess pyrophosphate within guard cells delays stomatal closure. *Plant & Cell Physiology* **60**, 875-887.

Barkla, BJ, Vera-Estrella, R, Pantoja, O (2012) Protein profiling of epidermal bladder cells from the halophyte *Mesembryanthemum crystallinum*. *Proteomics* **12**, 2862-5.

Bauly, JM, Sealy, IM, Macdonald, H, Brearley, J, Droge, S, Hillmer, S, Robinson, DG, Venis, MA, Blatt, MR, Lazarus, CM, Napier, RM (2000) Overexpression of auxin-binding protein enhances the sensitivity of guard cells to auxin. *Plant Physiology* **124**, 1229-1238.

Cao, D, Baskin, CC, Baskin, JM, Yang, F, Huang, Z (2014) Dormancy cycling and persistence of seeds in soil of a cold desert halophyte shrub. *Annals of Botany* **113**, 171-9.

Catusse, J, Strub, JM, Job, C, Van Dorsselaer, A, Job, D (2008) Proteome-wide characterization of sugarbeet seed vigor and its tissue specific expression. *Proceedings of the National Academy of Sciences of the United States of America* **105**, 10262-7.

Cox, J, Hein, MY, Luber, CA, Paron, I, Nagaraj, N, Mann, M (2014) Accurate proteome-wide label-free quantification by delayed normalization and

maximal peptide ratio extraction, termed MaxLFQ. *Molecular & Cellular Proteomics* **13**, 2513-26.

Dai, S, Chen, S (2012) Single-cell-type proteomics: toward a holistic understanding of plant function. *Molecular & Cellular Proteomics* **11**, 1622-30.

De Tullio, MC, Guether, M, Balestrini, R (2013) Ascorbate oxidase is the potential conductor of a symphony of signaling pathways. *Plant Signaling & Behavior* **8**, e23213.

Dib, L, Hayek, P, Sadek, H, Beyrouthy, B, Khalaf, RA (2008) The *Candida albicans* Ddr48 protein is essential for filamentation, stress response, and confers partial antifungal drug resistance. *Medical Science Monitor* **14**,113-121.

Fu, Q, Li, S, Yu, D (2010) Identification of an Arabidopsis Nodulin-related protein in heat stress. *Molecules and Cells* **29**, 77-84.

Gao, F, Gao, Q, Duan, X, Yue, G, Yang, A, Zhang, J (2006) Cloning of an H^+-PPase gene from *Thellungiella halophila* and its heterologous expression to improve tobacco salt tolerance. *Journal of Experimental Botany* **57**, 3259-70.

Geilfus, CM, Lan, J, Carpentier, S (2018) Dawn regulates guard cell proteins in *Arabidopsis thaliana* that function in ATP production from fatty acid beta-oxidation. *Plant Molecular Biology* **98,** 525-543.

Geng, S, Yu, B, Zhu, N, Dufresne, C, Chen, S (2017) Metabolomics and proteomics of *Brassica napus* guard cells in response to low CO_2. *Frontiers in Molecular Biosciences* **4**, 51.

Gharat, SA, Parmar, S, Tambat, S, Vasudevan, M, Shaw, BP (2016) Transcriptome analysis of the response to NaCl in *Suaeda maritima* provides an insight into salt tolerance mechanisms in halophytes. *PLoS One* **11**, e0163485.

Hairat, S, Baranwal, VK, Khurana, P (2018) Identification of *Triticum aestivum* nsLTPs and functional validation of two members in development and stress mitigation roles. *Plant Physiology and Biochemistry* **130**, 418-430.

Hidangmayum, A, Dwivedi, P, Katiyar, D, Hemantaranjan, A (2019) Application of chitosan on plant responses with special reference to abiotic stress. *Physiology and Molecular Biology of Plants* **25**, 313-326.

Ho, LW, Yang, TT, Shieh, S-S, Edwards, GE, Yen, HE (2010) Reduced expression of a vesicle trafficking-related ATPase SKD1 decreases salt tolerance in Arabidopsis. *Functional Plant Biology* **37**, 962-973.

Hossain, MS, ElSayed, AI, Moore, M, Dietz, KJ (2017) Redox and reactive oxygen species network in acclimation for salinity tolerance in sugar beet. *Journal of Experimental Botany* **68**, 1283-1298.

Iwai, S, Ogata, S, Yamada, N, Onjo, M, Sonoike, K, Shimazaki, KI (2019) Guard cell photosynthesis is crucial in abscisic acid-induced stomatal closure. *Plant Direct* **3**, e00137.

Ji, FS, Tang, L, Li, YY, Wang, WC, Yang, Z, Li, XG, Zeng, C (2018) Differential proteomic analysis reveals the mechanism of *Musa paradisiaca* responding to salt stress. *Molecular Biology Reports* **46**, 1057-1068.

Kwon, Y, Kim, SH, Jung, MS, Kim, MS, Oh, JE, Ju, HW, Kim, KI, Vierling, E, Lee, H, Hong, SW (2007) Arabidopsis hot2 encodes an endochitinase-like protein that is essential for tolerance to heat, salt and drought stresses. *The Plant Journal* **49**, 184-93.

Lambou, K, Pennati, A, Valsecchi, I, Tada, R, Sherman, S, Sato, H, Beau, R, Gadda, G, Latge, JP (2013) Pathway of glycine betaine biosynthesis in *Aspergillus fumigatus*. *Eukaryotic Cell* **12**, 853-63.

Lawson, T (2009) Guard cell photosynthesis and stomatal function. *New Phytologist* **181**, 13-34.

Le, J, Liu, XG, Yang, KZ, Chen, XL, Zou, JJ, Wang, HZ, Wang, M, Vanneste, S, Morita, M, Tasaka, M, Ding, ZJ, Friml, J, Beeckman, T, Sack, F (2014) Auxin transport and activity regulate stomatal patterning and development. *Nature Communications* **5**, 3090.

Lee, DS, Kim, BK, Kwon, SJ, Jin, HC, Park, OK (2009) Arabidopsis GDSL lipase 2 plays a role in pathogen defense via negative regulation of auxin signaling. *Biochemical and Biophysical Research Communications* **379**, 1038-42.

Lee, S, Choi, H, Suh, S, Doo, IS, Oh, KY, Choi, EJ, Schroeder Taylor, AT, Low, PS, Lee, Y (1999) Oligogalacturonic acid and chitosan reduce stomatal aperture by inducing the evolution of reactive oxygen species from guard cells of tomato and *Commelina communis*. *plant physiology* **121**, 147-52.

Leonhardt, N, Kwak, JM, Robert, N, Waner, D, Leonhardt, G, Schroeder, JI (2004) Microarray expression analyses of Arabidopsis guard cells and isolation of a recessive abscisic acid hypersensitive protein phosphatase 2C mutant. *The Plant Cell* **16**, 596-615.

Liu, F, Zhang, X, Lu, C, Zeng, X, Li, Y, Fu, D, Wu, G (2015) Non-specific lipid transfer proteins in plants: presenting new advances and an integrated functional analysis. *Journal of Experimental Botany* **66**, 5663-81.

Maeshima, M (2000) Vacuolar H^+-pyrophosphatase. *Biochimica et Biophysica Acta (BBA) - Biomembranes* **1465**, 37-51.

Medeiros, DB, Barros, JAS, Fernie, AR, Araujo, WL (2020) Eating away at ROS to regulate stomatal opening. *Trends in Plant Science **25,*** 220-223.

Nguyen, CDL, Malchow, S, Reich, S, Steltgens, S, Shuvaev, KV, Loroch, S, Lorenz, C, Sickmann, A, Knobbe-Thomsen, CB, Tews, B, Medenbach, J, Ahrends, R (2019) A sensitive and simple targeted proteomics approach to quantify transcription factor and membrane proteins of the unfolded protein response pathway in glioblastoma cells. *Scientific Reports* **9**, 8836.

Odintsova, TI, Slezina, MP, Istomina, EA, Korostyleva, TV, Kovtun, AS, Kasianov, AS, Shcherbakova, LA, Kudryavtsev, AM (2019) Non-specific lipid transfer proteins in *Triticum kiharae* Dorof. et Migush.: identification, characterization and expression profiling in response to pathogens and resistance inducers. *Pathogens* **8**, 221.

Ohnuma, T, Numata, T, Osawa, T, Mizuhara, M, Lampela, O, Juffer, AH, Skriver, K, Fukamizo, T (2011) A class V chitinase from *Arabidopsis thaliana*: gene responses, enzymatic properties, and crystallographic analysis. *Planta* **234**, 123-37.

Pan, Y, Li, J, Jiao, L, Li, C, Zhu, D, Yu, J (2016) A non-specific *Setaria italica* lipid transfer protein gene plays a critical role under abiotic stress. *Frontiers in Plant Science* 7, 1752.

Pitann, B, Zorb, C, Muhling, KH (2009) Comparative proteome analysis of maize (*Zea mays* L.) expansins under salinity. *Journal of Plant Nutrition and Soil Science* **172**, 75-77.

Ringli, C, Keller, B, Ryser, U (2001) Glycine-rich proteins as structural components of plant cell walls. *Cellular and Molecular Life Sciences* **58**, 1430-1441.

Ritte, G, Rosenfeld, J, Rohrig, K, Raschke, K (1999) Rates of sugar uptake by guard cell protoplasts of *Pisum sativum* L. related to the solute requirement for stomatal opening. *Plant Physiology* **121**, 647-56.

Rother, T, Acker, G, Scheibe, R (1988) Immunogold localization of chloroplast protein in spinach leaf mesophyll, epidermis, and guard-cells. *Botanica Acta* **101**, 311-320.

Rozema, J, Cornelisse, D, Zhang, Y, Li, H, Bruning, B, Katschnig, D, Broekman, R, Ji, B, van Bodegom, P (2014) Comparing salt tolerance of beet cultivars and their halophytic ancestor: consequences of domestication and breeding programmes. *AoB Plants* **7**, plu083.

Rui, Y, Chen, Y, Kandemir, B, Yi, H, Wang, JZ, Puri, VM, Anderson, CT (2018) Balancing strength and flexibility: how the synthesis, organization, and modification of guard cell walls govern stomatal development and dynamics. *Frontiers in Plant Science* **9**, 1202.

Santelia, D, Lawson, T (2016) Rethinking guard cell metabolism. *Plant Physiology* **172**, 1371-1392.

Schwacke, R, Ponce-Soto, GY, Krause, K, Bolger, AM, Arsova, B, Hallab, A, Gruden, K, Stitt, M, Bolger, ME, Usadel, B (2019) MapMan4: a refined protein classification and annotation framework applicable to multi-omics data analysis. *Molecular Plant* **12**, 879-892.

Shabala, L, Mackay, A, Tian, Y, Jacobsen, SE, Zhou, D, Shabala, S (2012) Oxidative stress protection and stomatal patterning as components of salinity tolerance mechanism in quinoa (*Chenopodium quinoa*). *Physiologia Plantarum* **146**, 26-38.

Shabala, S, Bose, J, Hedrich, R (2014) Salt bladders: do they matter? *Trends in Plant Science* **19**, 687-91.

Skorupa, M, Golebiewski, M, Kurnik, K, Niedojadlo, J, Kesy, J, Klamkowski, K, Wojcik, K, Treder, W, Tretyn, A, Tyburski, J (2019) Salt stress vs. salt shock - the case of sugar beet and its halophytic ancestor. *BMC Plant Biology* **19**, 57.

Specht, H, Slavov, N (2018) Transformative opportunities for single-cell proteomics. *Journal of Proteome Research* **17**, 2565-2571.

Sun, Q, Gao, F, Zhao, L, Li, K, Zhang, J (2010) Identification of a new 130 bp cis-acting element in the TsVP1 promoter involved in the salt stress response from *Thellungiella halophila*. *BMC Plant Biology* **10**, 90.

Szypulska, E, Jankowski, K, Weidner, S (2017) ABA pretreatment can limit salinity-induced proteome changes in growing barley sprouts. *Acta Physiologiae Plantarum* **39**, 190.

Takahashi, Y, Ebisu, Y, Kinoshita, T, Doi, M, Okuma, E, Murata, Y, Shimazaki, K-i (2013) bHLH transcription factors that facilitate K^+ uptake during stomatal opening are repressed by abscisic acid through phosphorylation. *Science Signaling* **6**, ra48.

Tenhaken, R (2014) Cell wall remodeling under abiotic stress. *Frontiers in Plant Science* **5**, 771.

Tian, T, Liu, Y, Yan, H, You, Q, Yi, X, Du, Z, Xu, W, Su, Z (2017) agriGO v2.0: a GO analysis toolkit for the agricultural community, 2017 update. *Nucleic Acids Research* **45**, 122-129.

Tyerman, SD, Munns, R, Fricke, W, Arsova, B, Barkla, BJ, Bose, J, Bramley, H, Byrt, C, Chen, Z, Colmer, TD, Cuin, T, Day, DA, Foster, KJ, Gilliham, M, Henderson, SW, Horie, T, Jenkins, CLD, Kaiser, BN, Katsuhara, M, Plett, D, Miklavcic, SJ, Roy, SJ, Rubio, F, Shabala, S, Shelden, M, Soole, K, Taylor, NL, Tester, M, Watt, M, Wege, S, Wegner, LH, Wen, Z (2019) Energy costs of salinity tolerance in crop plants. *New Phytologist* **221**, 25-29.

Wang, S, Kurepa, J, Hashimoto, T, Smalle, JA (2011) Salt stress-induced disassembly of Arabidopsis cortical microtubule arrays involves 26S proteasome-dependent degradation of SPIRAL1. *The Plant Cell* **23**, 3412-27.

Weyers, JDB, Travis, AJ (1981) Selection and preparation of leaf epidermis for experiments on stomatal physiology. *Journal of Experimental Botany* **32**, 837-850.

Wu, F, Chi, Y, Jiang, Z, Xu, Y, Xie, L, Huang, F, Wan, D, Ni, J, Yuan, F, Wu, X, Zhang, Y, Wang, L, Ye, R, Byeon, B, Wang, W, Zhang, S, Sima, M, Chen, S, Zhu, M, Pei, J, Johnson, DM, Zhu, S, Cao, X, Pei, C, Zai, Z, Liu, Y, Liu, T, Swift, GB, Zhang, W, Yu, M, Hu, Z, Siedow, JN, Chen, X, Pei, Z-M

(2020) Hydrogen peroxide sensor HPCA1 is an LRR receptor kinase in Arabidopsis. *Nature* **578**, 577–581

Wu, GQ, Wang, JL, Feng, RJ, Li, SJ, Wang, CM (2018) iTRAQ-based comparative proteomic analysis provides insights into molecular mechanisms of salt tolerance in sugar beet (*Beta vulgaris* L.). *International Journal of Molecular Sciences* **19**, 3866.

Yao, X, Xiong, W, Ye, TT, Wu, Y (2012) Overexpression of the aspartic protease ASPG1 gene confers drought avoidance in Arabidopsis. *Journal of Experimental Botany* **63**, 2579-2593.

Yu, B, Li, JN, Koh, J, Dufresne, C, Yang, N, Qi, SS, Zhang, YX, Ma, CQ, Duong, BV, Chen, SX, Li, HY (2016) Quantitative proteomics and phosphoproteomics of sugar beet monosomic addition line M14 in response to salt stress. *Journal of Proteomics* **143**, 286-297.

Zhang, Y, Nan, J, Yu, B (2016) Omics technologies and applications in sugar beet. *Frontiers in Plant Science* **7**, 900.

Zhao, ZX, Stanley, BA, Zhang, W, Assmann, SM (2010) ABA-regulated G protein signaling in Arabidopsis guard cells: a proteomic perspective. *Journal of Proteome Research* **9**, 1637-1647.

Zhao, ZX, Zhang, W, Stanley, BA, Assmann, SM (2008) Functional proteomics of *Arabidopsis thaliana* guard cells uncovers new stomatal signaling pathways. *The Plant Cell* **20**, 3210-3226.

Zhu, MM, Dai, SJ, McClung, S, Yan, XF, Chen, SX (2009) Functional differentiation of *Brassica napus* guard cells and mesophyll cells revealed by comparative proteomics. *Molecular & Cellular Proteomics* **8**, 752-766.

Zúñiga-Sánchez, E, Soriano, D, Martínez-Barajas, E, Orozco-Segovia, A, Gamboa-deBuen, A (2014) BIIDXI, the At4g32460 DUF642 gene, is involved in pectin methyl esterase regulation during *Arabidopsis thaliana* seed germination and plant development. *BMC Plant Biology* **14,** 338.

Chapter 5: A comparative study of the guard cell proteomics in halophyte *Chenopodium quinoa* (Wild.) and its modulation by salt stress

Abstract

Epidermal fragments enriched in guard cells (GCs) were isolated from the halophyte quinoa *(Chenopodium quinoa* Wild.*)* species, and the response at the proteome level was studied after salinity treatment of 300 mM NaCl for 3 weeks. In total, 2147 proteins were identified, of which 36% were differentially expressed in response to salinity stress in GCs. Up and downregulated proteins included signaling molecules, enzyme modulators, transcription factors and oxidoreductases. Several proteins involved in stress in general and osmotic/salt stresses in particular, were found to be highly abundant in GCs following salinity treatment, including desiccation-responsive protein 29B (50-fold), osmotin-like protein OSML13 (13-fold), PLAT domain-containing protein 3-like (8-fold), and dehydrin ERD14 (8-fold). Ten proteins related to the gene ontology term "response to ABA" were upregulated in quinoa GC such as aspartic protease in guard cell-1, phospholipase D and plastid-lipid-associated protein. In addition, seven proteins in the sucrose-starch pathway were upregulated in the GC in response to salinity stress. Furthermore, the accumulation of two enzymes involved in the amino acid biosynthesis (tryptophan synthase and L-methionine synthase) was observed in the GC under salt stress. Exogenous application of sucrose and amino acids on stomatal conductance showed that tryptophan, L-methionine and sucrose were associated with less stomatal aperture and conductance, which could be advantageous for plants under salt stress.

5.1 Introduction

Photosynthesis, the most important biochemical reaction in the world, will not occur unless carbon dioxide is allowed to enter the leaves through stomatal pores, the apertures of which are controlled by guard cell (GC) movements. At the same time, stomata serve as major getaways for water loss through transpiration. The stomatal pore area may be only as much as 1% of total leaf surface, but diffusion

rates from the leaf could be 95% as much evaporation as from the stomata (Ache *et al.* 2010). It has been estimated that a tremendous amount of water (32×10^{15} kg yr^{-1}) and CO_2 (440×10^{15} g CO_2) is passing through stomata of plants leaves each year (Hetherington and Woodward 2003a). Thus, changes in stomatal action in response to environmental factors impact on the flux of both carbon dioxide and water at a global level (Lawson and Blatt 2014).

Salinity stress is one of the most detrimental environmental stresses that affects water balance through stomatal conductance. Salinity as a major abiotic stress affects 20% of arable land globally (Mickelbart *et al.* 2015). Understanding responsive adaptation strategies has a primary role in enhancing salt tolerance of crop plants and water use efficiency (Chaves *et al.* 2016). The plant response to salt stress is a complex trait, regulated by many genes and different pathways (Zhang *et al.* 2019b) that help a plant restore cellular homeostasis, repair the stress damage and ultimately determine growth rate under salt stress. Salt stress activates signaling pathways related to osmotic and ionic stress, detoxification and growth regulation (Zhu 2002), and is augmented by the transport of water and other small molecules that can diffuse across membranes.

As highly salt tolerant plant species, halophytes have evolved mechanisms to efficiently benefit from adverse saline conditions (Flowers and Colmer 2015). In glycophytes, salinity stress reduces stomatal conductance causing decline in photosynthesis and transpiration rates (Chaves *et al.* 2016); this reduction is much smaller in halophytes. Also, halophytes have superior abilities to regulate stomata number and length. For example, it has been demonstrated that salt-tolerant quinoa plants were able to efficiently regulate water loss and CO_2 assimilation under saline condition through stomata length and density (Kiani-Pouya *et al.* 2019a).

Studies on stomatal physiology and anatomy have provided insights into understanding of stomatal differentiation and function. However, most studies on the effects of environmental stimuli on stomata at the cellular level have used whole leaf samples which consist of diverse cell types. In such heterogenous samples, it is likely that important mechanisms in response to stimuli related specifically to stomata GCs have been at least partially masked by other more abundant cell types. In recent years, single cell-type analysis has become focus for number of investigators in the field of biology and plant science. For instance, studies on

isolated trichome (Takemori *et al.* 2019) and epidermal bladder cells (Barkla *et al.* 2016) and guard cell (Zhu *et al.* 2009; Geilfus *et al.* 2018b) have been undertaken. However, obtaining purified specialized cells in quantities sufficient for biochemical and standard molecular approaches remains challenging.

Quinoa as a halophytic plant is a cultivated species that has a high tolerance to abiotic stresses such as salinity and drought (Shabala 2013; Kiani-Pouya *et al.* 2019a). Studies investigating the GC response to salt stress in halophytes have to date focused on physiological or anatomical aspects. Given that the stomatal response of halophytes to salt stress is not well understood at the molecular level. quinoa represents an interesting model plant. However, no studies to date have used global "omics" based techniques such as proteomics for the discovery of novel adaptive mechanisms in the GCs of halophytes under saline conditions.

A previous study on functional proteomics of Arabidopsis GCs (Zhao *et al.* 2008b) resulted in identification of 1734 unique proteins in the Arabidopsis GC. Another study compared the proteome of *Brassica napus* GCs with mesophyll cells (Zhu *et al.* 2009) leading to the discovery of 74 proteins preferentially expressed in the GCs and 143 proteins with higher abundance in the mesophyll. Specific GC proteins related to thioredoxin signaling (Zhang *et al.* 2016b) or ATP production (Geilfus *et al.* 2018b) were also identified. The response of the GC proteome to CO_2 levels (Geng *et al.* 2017) and ABA (Zhao *et al.* 2010) are to date the only published research papers using proteomics to address the GC response to environmental factors.

Our study applying proteomics to investigate the effects of salt stress on the GCs of sugar beet revealed a significant proportion of differentially expressed proteins related to different abiotic stress e.g. salinity, drought and oxidative stresses, as well as some proteins related to biotic stress (Chapter 4). Salt stress also altered the abundances of some proteins related to signalling, cell wall modification and ATP biosynthesis indicating the high impact of salt on GCs in sugar beet. Furthermore, high levels of some proteins related to adaptation to oxidative stress under non-saline conditions suggested some constitutively active proteins may play a role in tolerance of GCs to salt stress in the latter species (Chapter 4). Here, we sought to identify whether similar mechanisms exist in the GCs of halophytic quinoa species, and to what extent they differed from those reported for sugar beet.

It should be commented that most studies using proteomics methods to

investigate the response of GCs to environmental factors have employed the model plant Arabidopsis. To the best of our knowledge, it is the first time that experimental study on proteomics of GCs under salinity stress is reported in halophytes. Investigation of the salt-induced proteins in quinoa GCs as a halophyte species will direct us towards identification of salt responsive proteins in GC involved in salt tolerance and adaptation mechanisms of halophytes at the GC level.

5.2 Materials and methods

5.2.1 Growth conditions and guard cell preparation

Six seeds of quinoa were planted in temperature-controlled glasshouse at (22 °C, 70% relative humidity, and 12/12 h day/night) at the University of Tasmania. Plants were grown in 8-inch diameter pots filled with potting mix containing 90% composted pine bark; 5% coarse sand; 5% coco peat; gypsum (1 kg m^{-3}); dolomite (6 kg/m3); ferrous sulphate (1.5 kg m^{-3}); Osmoform Pre-mix (1.25 kg m^{-3}) and slow-released fertiliser, Scotts Pro (3 kg m^{-3}). Salt stress was imposed 3 weeks after planting by adding 250 mM NaCl to irrigation water over a period of 3 weeks. GC-enriched epidermal peels were prepared as it is described in Chapter 3. Briefly fully expanded leaves of well-watered 3-4-week-old quinoa were grinded in Grindomix blender with a basic solution and crushed ice, then it was passed through a Nylon mesh and rinsed with ice-cold distilled. Entire process was repeated four times. The sample were snap-froze in liquid nitrogen and were kept at -80 °C until used for protein extraction.

5.2.2 Protein extraction

Five biological replicates per treatment of guard cell were ground to a fine powder in liquid nitrogen. Then, 10% trichloroacetic acid (TCA) in pre-chilled acetone containing 0.07% (v/v) 2-mercaptoethanol was used to precipitate total proteins. The homogenate was kept at -20 °C overnight. Then the samples were centrifuged at 20,000× g at 4 °C for 20 min and the pellets were washed in 100% pre-chilled acetone containing 0.07% (v/v) 2-mercaptoethanol. After a final wash (80% prechilled acetone containing 0.07% (v/v) 2-mercaptoethanol) pellets were centrifuged then air-dried at room temperature. Proteins were then solubilized in 1 mL buffer containing 7 M urea, 2 M thiourea, and 40 mM Tris (pH=7.5) at 20 °C for 1 h then clarified by centrifugation. Protein extracts were precipitated with 4

volumes of acetone and resuspended in 50 µL of solubilization buffer. Protein concentrations were measured using Pierce 660 nm Protein Assay Reagent.

5.2.3 Protein identification by nanoLC–MS/MS

Peptides were first concentrated on a 20 mm x 75 µm PepMap 100 trapping column (3 µm C18) for 5 minutes then separated using a 250 mm x 75 µm PepMap 100 RSLC column (2µm C18) at a flow rate of 300 nL min^{-1} and held at 45 °C. A 90 min gradient from 98% mobile phase A (0.1% formic acid in water) to 50% mobile phase B (0.08% formic acid in 80% acetonitrile and 20 % water) comprised the following steps: 2-10% B over 12 min, 10-25% B over 48 min, 25-45% B over 10 min, holding at 95% B for 5 min then re-equilibration in 2% B for 15 min. The nanoHPLC system was coupled to a Q-Exactive HF mass spectrometer equipped with nanospray Flex ion source (Thermo Fisher Scientific, MA, USA) and controlled using Xcalibur 4.1 software. Spray voltage was set to 2.0 kV, S-lens RF level to 50 and heated capillary set at 250 °C. MS scans were acquired from 370-1500 m/z at 60,000 resolution, with an AGC target of 3×10^6 and a maximum fill time of 100 ms. Fragment ion scans were acquired at 15,000 resolution (scan range 200-2000 m/z), with an AGC target of 2×10^5 and a maximum fill time of 28 ms. An isolation width of 1.4 m/z was used, and normalized collision energy for HCD set to 27eV. MS/MS spectra were acquired in data-dependent mode using a Top15 method with 30-second dynamic exclusion of fragmented peptides.

5.2.4 Database searching and protein quantitation

Raw data files were imported into MaxQuant version 1.6.5.0 (http://maxquant.org/) and MS/MS spectra were searched using the Andromeda search engine against protein databases downloaded from NCBI for *Chenopodium quinoa* (Wild) (63,475 entries on 20/10/2017). Extracts collected at different times were defined as fractions 1 and 2 in the MaxQuant experimental design table to achieve sample-level data. Default settings for protein identification by Orbitrap MS/MS were used, with the match-between-runs function enabled, including a maximum of two missed cleavages, mass error tolerances of 20 ppm then 4.5 ppm for initial and main peptide searches, respectively, 0.5Da tolerance for fragment ions, carbamidomethyl modification of cysteine and variable methionine oxidation. A false discovery rate of 0.01 was used for both peptide-spectrum matches and protein identification.

5.2.5 Determination of relative protein abundance and statistical analysis

We utilized MaxLFQ, the MaxQuant algorithm for peptide intensity determination and normalization using pair-wise comparison of unique and razor peptide intensities and a minimum ratio count of 2. The protein groups output files generated by MaxQuant analysis were processed as follows: the normalised label-free quantification (LFQ) intensity values, MS/MS counts and the numbers of razor and unique peptides for each of the identified proteins were imported into Perseus software version 1.5.031 (http://perseus-framework.org/). Protein groups identified either as potential contaminants (prefixed with CON_), identified by modified site only, by reverse database matching or on the basis of a single matching peptide were removed. LFQ intensity values were then log2–transformed and then a filter applied to include only proteins detected in a minimum of 70% of the samples. Missing values were replaced with random intensity values for low-abundance proteins based on a normal distribution of protein abundances using default MaxQuant parameters.

5.2.6 Stomatal conductance in plant treated by sucrose, tryptophan, L-methionine

To investigate the effect of sucrose, tryptophan, L-methionine concentrations of 10, and 30 mM of sucrose, tryptophan, L-methionine were sprayed on the leaf. Then the stomatal conductance was measured after two hours in plants under normal light in the glasshouse using a Li-Cor 6400 gas analyzer system (Lincoln, NE, USA).

5.3 Results

In the present study, quinoa plants were treatment with 300 mM NaCl for three weeks. A proteomics approach was then applied to analyse mechanically prepared guard-cell enriched epidermal peels. Isolated GCs-enriched fragments were first examined under the microscope to confirm that no contamination of mesophyll fragments or vascular particles were present as it is described in Chapter 4. In total, searching the acquired MS/MS data against the *Chenopodium quinoa* (Wild.) protein database identified 2,147 proteins, based on two or more matching peptides (Supplemental Table S5.1).

Rubisco activase (XP_021757275.1), a lipolytic enzyme GDSL esterase/lipase (XP_021763378.1) and auxin binding protein; ABP19 (XP_021750120.1) were found to be three most abundant proteins in quinoa guard

cells. Rubisco activase is a chloroplastic enzyme that is required for the activation of rubisco; this enzyme is also a responder to various abiotic stresses such as heat, cold, drought and salt stresses and contribute to plant acclimation to a variety of environmental stress (Chen *et al.* 2015). GDSL esterases/lipases are subfamily of lipolytic enzymes with a wide range of substrates that confer pathogenic resistance to plants (Lee *et al.* 2009a); it was the second most abundant protein in quinoa GC.

It is noteworthy that multiple isoforms of peroxidase enzymes, including peroxidase 4 (XP_021732931.1), peroxidase 12 (XP_021771547.1) catalase (XP_021754464.1) and L-ascorbate peroxidase (XP_021745974.1) and aspartic protease were also among the top 10% most abundant proteins in the quinoa GC.

5.3.1 Protein classification in the guard cell

In this study we used protein classification and gene ontology (GO) analysis as complementary tools for bioinformatic analysis of the global quinoa proteomics dataset and the differentially abundant proteins under salinity stress. The Basic Local Alignment Search Tool (BLAST) was first used to obtain the protein sequences of each accession number in GCs proteome. Amino acid sequences of all GCs proteins used as input in the most recent version of MapMan framework, using Mercator4 software (https://plabipd.de/portal/mercator4) (Schwacke *et al.* 2019a) to obtain the functional classification of GCs proteins based on homologues of well-annotated proteins such as Arabidopsis.

The Mercator pipeline was used for protein functional classification analysis based on the 2,147 quinoa GC proteins identified (Fig. 5.1). This software aligns each set of protein sequence against various databases including the Conserved Domain Database (CDD), SwissProt/Uniprot plant proteins, TAIR10 proteins, Clusters of Orthologous Groups (COG) and then generates MapMan bin codes. Similar to KEGG, the MapMan framework uses massive databases spaning many pathways and functional terms but has been specifically developed for plant cell biology (Schwacke *et al.* 2019b). The key functions identified in our dataset included protein synthesis, degradation and folding, signal transduction, post-translational modifications, biotic and abiotic stresses, development, photosynthesis, ion transporter lipid metabolism oxido-reductase and miscellaneous. The eight most significantly enriched GO categories in the GC proteome are presented in Table 5.1. Translation, metabolic process, generation of

precursor metabolites and energy were also most significantly enriched GOs, while in most proteomic studies on whole leaf or mesophyll tissue, photosynthesis has been presented among the top GOs.

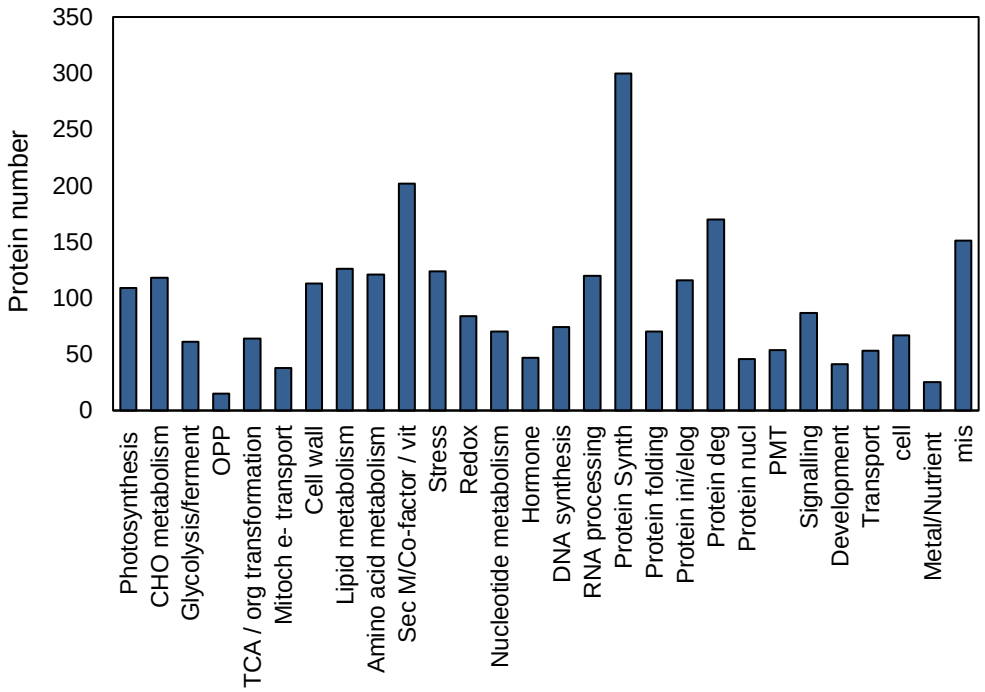

Fig. 5.1 Protein functional classification of quinoa guard cell proteome based on the identified 2147 proteins. Amino acid sequences of all GCs proteins used as input in the most recent version of MapMan framework to obtain the functional classification of GCs proteins based on homologues of well-annotated proteins such as Arabidopsis.

5.3.2 Identified signalling proteins in quinoa GC proteome

The 78 signalling proteins including 14-3-3 proteins, GTP-binding proteins, mitogen-activated protein kinases, calcium-binding protein and proteins involved in light signalling were found in the GC proteome. The 14-3-3 proteins are small acidic proteins that form homodimers and heterodimers that bind to phosphorylated target proteins and play a role in stomatal movement through the regulation of blue light responses and plasma membrane and tonoplast channels (Cotelle and Leonhardt 2015). G proteins participate in several signal transduction pathways. Mutants lacking the G subunit, presented hypo-sensitivity to ABA activation of anion channels and hyposensitivity to ABA inhibition of potassium channels and stomatal opening (Zhao *et al.* 2010).

Table 5.1 Top eight GO terms of quinoa GC proteome.

GO Term	Term	Query item	FDR
GO:0006412	translation	122	2.4×10^{-22}
GO:0008152	metabolic process	854	3.1×10^{-18}
GO:0006091	generation of precursor metabolites and energy	46	4.5×10^{-15}
GO:0015979	photosynthesis	39	3.9×10^{-12}
GO:0005975	carbohydrate metabolic process	115	4.4×10^{-12}
GO:0009056	catabolic process	59	4.4×10^{-10}
GO:0009058	biosynthetic process	253	9.6×10^{-7}
GO:0006950	response to stress	76	1.8×10^{-4}

5.3.3 Identified transporters proteins in quinoa GC proteome

Various ABC transporters from C, F, G and I subfamilies were detected in quinoa GCs. ABC transporters (ATP-binding cassette) contribute to multiple physiological processes that lead to plant adaptation to changing environments for example they enhance ABA signalling which results in reduced-transpiration phenotype in plant under salt stress conditions (Kretzschmar *et al.* 2011).

V-ATPases are vacuolar H^+ pumps that increase sequestration of Na^+ into vacuoles, enhancing vacuolar capacity for osmoregulation and maintaining Na^+ and K^+ homeostasis (Hubbard and Webb 2015). The rate of vacuole-type ATPase activity is constitutively high in GCs compared to other cell-type to meet the requirement of rapid and large ion fluxes across tonoplast for stomatal movements (Willmer *et al.* 1995). In our study, different subunits of V-type ATPase including sub-A, A3, B2, C, D, E and G were identified in quinoa GC (Table 5.2).

5.3.4 Differentially abundant proteins in response to salt stress

The GC proteome data was subjected to Principal Component Analysis, (PCA), as presented in the two-dimensional biplot to find out whether the GC proteome profiles of control and salt-treated plants differ from each other. In PCA plot, PC1 accounts for the difference between the salt-treated and control treatments and PC2 shows differences between biological replicates. As it can be observed in Figure 5.2, PC1 explained 55.3 % of the variance in data, while PC2 captured small variance in protein expression profiles of GC. Hence, separation of unstressed control and salt treatments into non-overlapping clusters suggests major differences between experimental treatments.

Table 5.2 A representative selection of the signalling proteins were identified in quinoa GC proteome- the complete list of signalling proteins is provided in Supplemental Table S5.1.

Protein code	Name	Signal type
XP_021772273	mitochondrial proton/calcium exchanger protein-like	calcium
XP_021720398	Calcium-binding EF-hand family protein	calcium
XP_021730224	probable calcium-binding protein CML13	calcium
XP_021743759	calcium-binding allergen Ole e 8-like	calcium
XP_021724195	calcium-binding protein CML49	calcium
XP_021740220	cryptochrome-1-like isoform X3	calcium
XP_021761282	calnexin homolog	calcium
XP_021742145	serine/threonine protein phosphatase 2A	calcium
XP_021751211	14-3-3-like protein	14.3.3
XP_021775698	14-3-3-like protein D	14.3.3
XP_021772761	GTP-binding protein SAR1A	G-proteins
XP_021772956	mitochondrial Rho GTPase 1	G-proteins
XP_021760299	dynamin-related protein 5A	G-proteins
XP_021768021	ras-related protein RABD2c-like	G-proteins
XP_021763216	guanylate-binding protein 2-like	G-proteins
XP_021738598	ras-related protein Rab7-like	G-proteins
XP_021731959	nuclear pore complex protein NUP50A-like	G-proteins
XP_021765995	guanylate-binding protein 3-like	G-proteins
XP_021736812	nuclear pore complex protein NUP50A-like	G-proteins
XP_021735409	nucleolin 1-like	G-proteins
XP_021748152	RAN GTPase-activating protein 2	G-proteins
XP_021736812	nuclear pore complex protein NUP50A	G-proteins
XP_021735409	nucleolin 1-like	G-proteins
XP_021748152	RAN GTPase-activating protein 2	G-proteins
XP_021751681	G- nucleotide diphosphate dissociation inhibitor	G-proteins
XP_021716254	phototropin-1-like isoform X1	light
XP_021740244	protein EXORDIUM-like	light
XP_021774295	phytochrome B-like	light
XP_021750479	NAD(P)-binding Rossmann-fold superfamily	light
XP_021738894	COP9 signalosome complex subunit 5a-like	light
XP_021714332	PLC-like phosphodiesterases superfamily	MAP kinases
XP_021774801	mitogen-activated protein kinase MMK1	MAP kinases
XP_021754221	mitogen-activated protein kinase MMK2	MAP kinases
XP_021723308	Leucine-rich repeat protein kinase family protein	RK. LRR III
XP_021746237	LRR receptor-like ser/thre-protein kinase	RK. LRR VI
XP_021749023	inactive LLR receptor-like protein kinase	RK. LRR VII
XP_021775620	leucine-rich repeat receptor-like protein kinase	RK. LRR VII
XP_021718843	leucine-rich repeat receptor-like protein kinase	RK. LRR VII
XP_021772032	DNA damage-repair/toleration protein DRT100	RK. LRR XI

Table 5.3 A representative selection of the transporter proteins were identified in quinoa GC proteome. The full list of transporter proteins is given in Supplemental Table S5.1.

Accession no.	Name	Transporter
XP_021715294	plasma membrane-associated cation-binding protein	cation
XP_021762724	ABC transporter F family member 4-like	ABC
XP_021743351	ABC transporter C family member 2-like	ABC
XP_021776035	ABC transporter G family member 22-like	ABC
XP_021766195	ABC transporter I family member 19-like	ABC
XP_021720939	calcium-transporting ATPase 4	calcium
XP_021751211	calcium-transporting ATPase 10	calcium
XP_021744756	bifunctional monothiol glutaredoxin-S16	calcium
XP_021760697	pyrophosphate-energized vacuolar membrane H^+ pump	H^+ pump
XP_021769151	probable aquaporin PIP1-4	PIP
XP_021765658	mitochondrial carnitine/acylcarnitine carrier-like protein	metabolite
XP_021738293	mitochondrial dicarboxylate/tricarboxylate transporter DTC	metabolite
XP_021756032	mitochondrial phosphate carrier protein 3, mitochondrial	metabolite
XP_021757591	cation/H^+ antiporter 18-like	cation
XP_021736780	plastidic ATP/ADP-transporter-like	Misc
XP_021738681	V-type proton ATPase subunit a3-like	ATPases
XP_021730105	V-type proton ATPase subunit C-like	ATPases
XP_021761683	ATPase 11, plasma membrane-type-like	ATPases
XP_021765334	V-type proton ATPase subunit G 1-like	ATPases
XP_021739675	V-type proton ATPase catalytic subunit A	ATPases
XP_021732700	V-type proton ATPase catalytic subunit A-like	ATPases
XP_021738896	plasma membrane ATPase 4-like	ATPases
XP_021762284	V-type proton ATPase subunit d2	ATPases
XP_021765533	V-type proton ATPase subunit B 2	ATPases
XP_021754298	V-type proton ATPase subunit E-like	ATPases
XP_021772280	V-type proton ATPase subunit H-like isoform X2	ATPases
XP_021714458	mitochondrial outer membrane protein porin 2-like	Porin
XP_021761841	mitochondrial import receptor subunit TOM40-1-like	Porin
XP_021758463	mitochondrial outer membrane protein porin of 34 kDa	Porin
XP_021717525	K^+ efflux antiporter 2, chloroplastic-like	Potassium
XP_021762166	probable voltage-gated potassium channel subunit beta	Potassium
XP_021753247	monosaccharide-sensing protein 2-like	Sugar
XP_021726328	sugar carrier protein C-like	Sugar
XP_021757156	plastidic glucose transporter 4-like	Sugar
XP_021760460	sucrose transport protein-like isoform X1	Sucrose
XP_021752898	chloride channel protein CLC-b-like	anions
XP_021739774	ATPase ASNA1 homolog	anions
XP_021772050	ADP, ATP carrier protein 1, mitochondrial-like	cation

To identify the differentially expressed proteins under saline conditions, t-test using an FDR adjusted p-value < 0.05 was performed and the data were analysed in terms of fold-change relative to unstressed control (ratio values of treated/control). Proteins were considered differentially expressed between control and salt stress conditions if they met two criteria: the statistical criterion (FDR < 0.05) and the biological measure (fold-change >2). Statistical significance of changes and deviations from control could be observed in a volcano plot (Fig. 5.3). Based on these two measures, 387 proteins were differentially abundant under salt stress (185 upregulated and 202 downregulated).

Heat maps were then used to provide an overview of abundance patterns of individual proteins in the whole proteome data (Fig. 5.4). These heatmaps displayed similarities between biological samples in each treatment.

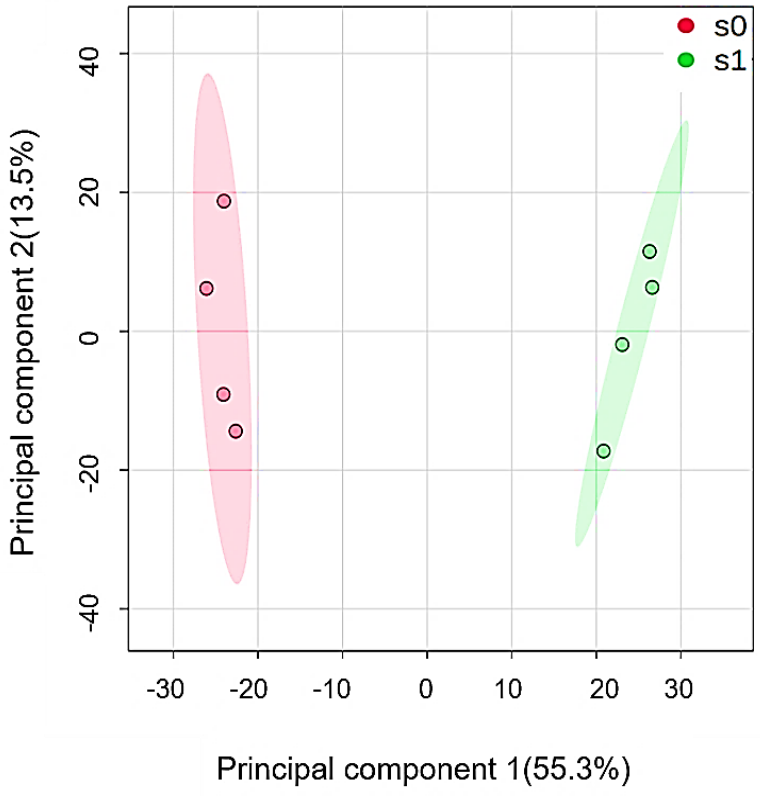

Fig. 5.2 PCA clustering based on guard cell proteome data under control and salt conditions. Proteomics analyses were performed with 4 replicates. S0 and S1 denote control and saline treatments, respectively.

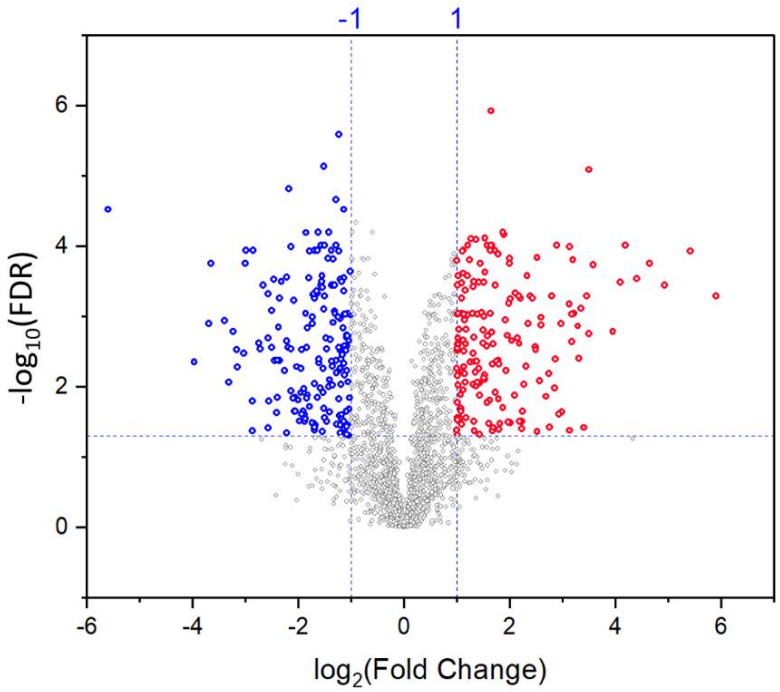

Fig. 5.3 Volcano plot of differentially abundant proteins in the quinoa guard cells in response to salt stress. Proteins with decreased and increased abundances (fold change >2, FDR < 0.05) are illustrated as blue and red dots respectively. Proteins with non-significant expressions and/or fold change of less than 2 are shown as grey dots.

Sequence-based functional annotations of 185 upregulated and 202 down regulated proteins was then performed using Mercator (Fig. 5.5) to identify possible functions of the differentially abundant proteins. The distribution of protein functions demonstrated that around 20% of proteins did not classify to any functional group. A large number of known functional proteins were classified as the following categories: protein synthesis, protein degradations, post-translational modification, RNA binding, regulation of transcription, DNA (DNA-binding, synthesis and repair), signalling, transport, biotic and abiotic stresses, development, lipid metabolism, cell wall and photosynthesis.

Several proteins involved in general stress responses (including those for osmotic and salt stresses), were found to be upregulated in GC of quinoa following salinity treatment (Supplemental Table S5.1), including protein DR29B (50-fold), osmotin-like protein OSML13 (13-fold), PLAT domain-containing protein 3-like (8-fold), dehydrin ERD14 (8-fold), cationic peroxidase 1 (18-fold). Moreover, antioxidant

molecules responsible for cell redox homeostasis such as glutaredoxin-C2-, thioredoxin H-type 1 (TRX) accumulated in salt-treated quinoa GC. However, downregulation in expression of the enzymatic antioxidant catalase (CAT) and L-ascorbate peroxidase 5 (APX) were observed in GC. In our study, PER2, PER5, and PER50 were decreased, while PER1 and PER4, PER12 and PER29 were highly increased in quinoa GC in response to salt stress suggesting that various member of a protein family might be expressed differently, suggesting potentially different functional roles.

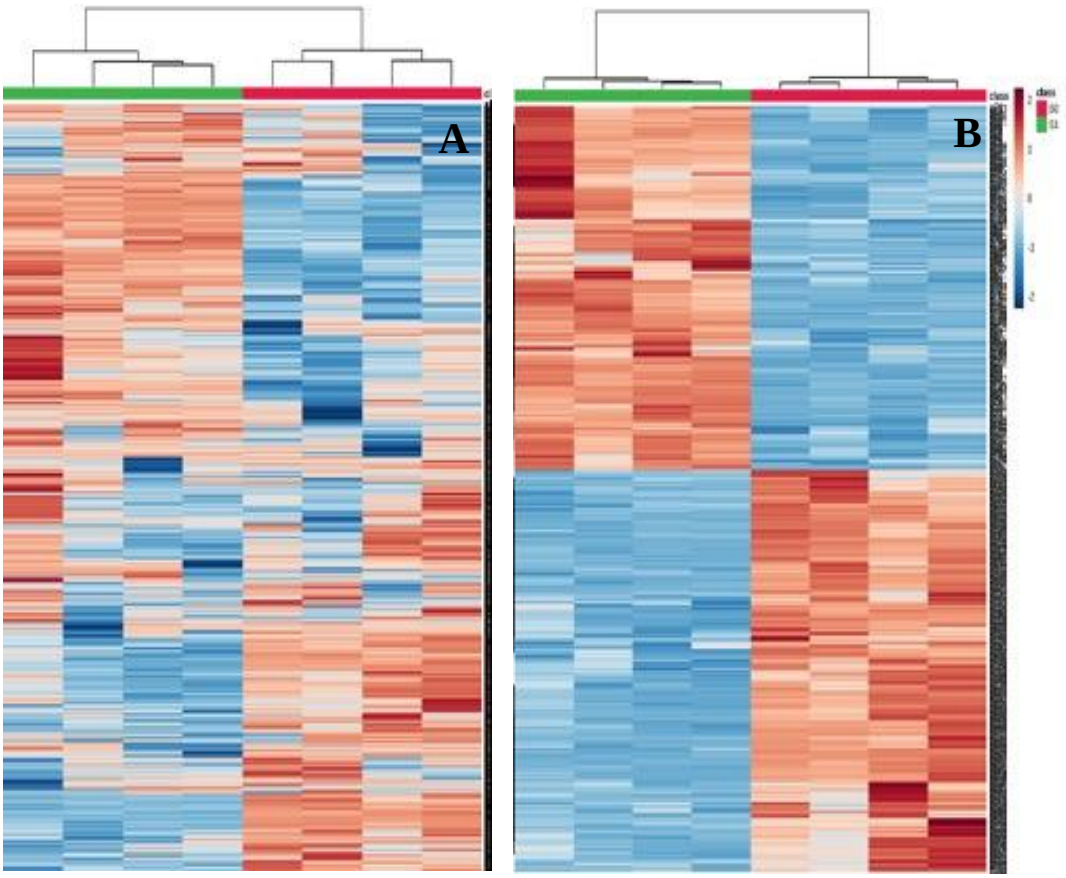

Fig. 5.4 Heat maps based on Z-scores of protein abundance measurements demonstrating abundance patterns of individual proteins in the whole proteome (A) and differentially accumulated proteins (B). S0 and S1 denote control and saline treatments, respectively.

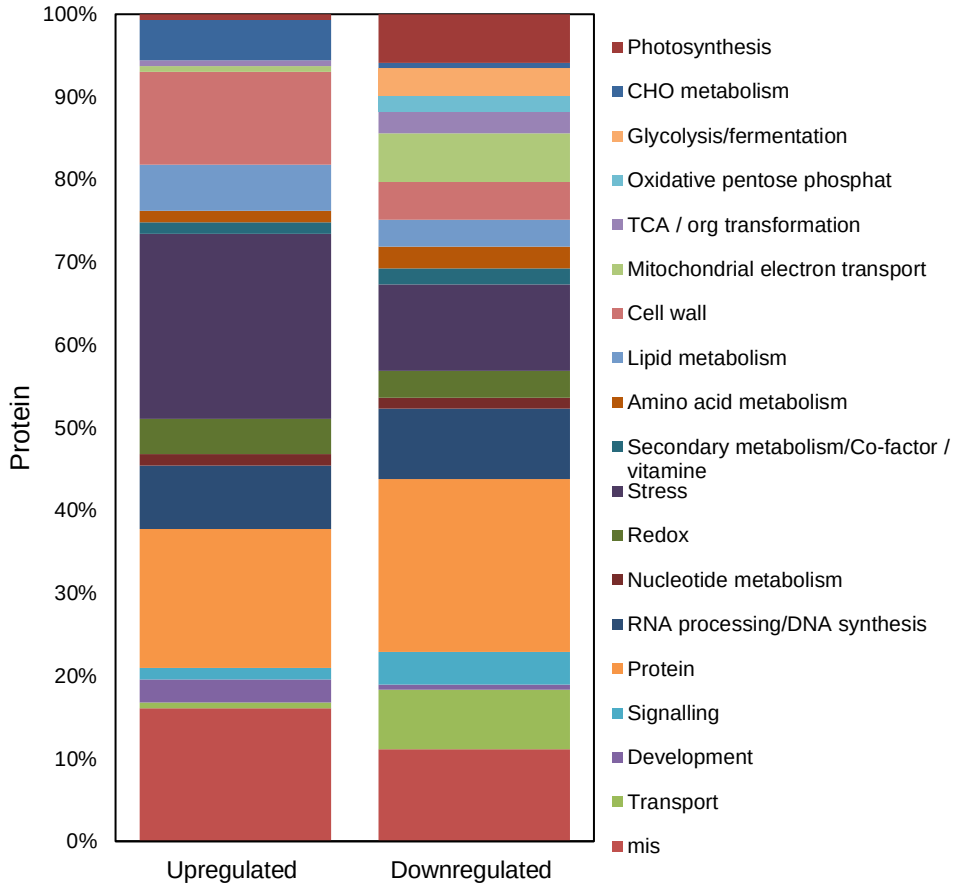

Fig. 5.5 Comparison of differentially accumulated proteins in salt-responsive proteomes of quinoa guard cell. Up-regulated (185 proteins) and down-regulated (202 proteins) proteins identified from quinoa guard cells have been classified into different categories based on their biological function according to MapMan terms. The Y axes indicate the % of proteins differentially accumulated in the quinoa guard cell under 250 mM NaCl.

Metabolism of carbohydrates is rapidly modulated in response to environmental stresses. Glucan endo-1,3-beta-D-glucosidase and chitinase are hydrolases, which have been recognized as antifungal proteins, were highly overexpressed in quinoa GCs under salt conditions (Supplemental Table S5.1). Glucan endo-1,3-beta-D-glucosidase (increased 27-fold in saline conditions) is a pathogenesis-related (PR) protein, also reported to be associated with salt tolerance and ROS-scavenging in stressed plants (Taji *et al.* 2004). High expression of this protein in GC especially in quinoa may imply the importance of this protein in conferring salt tolerance in halophytes.

Salt stress has been shown to alter patterns of gene expression, potentially via modulation of transcription factors and other proteins, including those involved

in alternative splicing. Alternative splicing is a process through which several transcripts and multiple forms of protein are produced from the same gene leading to an increase in proteome diversity. This post translational modification process is induced in plant under various stresses resulted in quick adjustment of the function and abundance of key components of stress responses (Laloum *et al.* 2018). In our study, splicing factor U2af small subunit B-like which is upregulated 6-fold in quinoa GsC belongs to a Zinc finger CCCH domain-containing protein which may be important in salt tolerance of plants (Sun *et al.* 2007). NAP1-related protein X2, belongs to a family of chaperones and involved in DNA repair is also critical under stress conditions (Zhang *et al.* 2016a). This protein was also upregulated under salt stress (2-fold).

Salinity altered the physical properties of the GC wall. Cell wall-modifying enzymes such as acetyl- and methyl-esterifications of pectin (PME and PAE) were upregulated in GCs in our study. The acetyl- and methyl-esterifications of pectin are critical for the regulating mechanical properties of cell wall (Wu *et al.* 2018b). Pectin methylesterification is essential for plant responses to environment stresses (Huang *et al.* 2017). For example, PME34 regulate GC flexibility in response to heat stress. Glycine-rich cell wall proteins (GRPs) were upregulated in GC of quinoa (18-fold). GRPs in the cell wall have 60-70% glycine amino acid residues. GRPs generally are involved in the strengthening of biological structural system or can support the development of expandable organs (Ringli *et al.* 2001). Our results are therefore consistent with increased mechanical strength in GCs exposed to salt stress.

5.3.5 Proteins with a role in stomatal movement

Thirty-five proteins were found in this GC proteome study that have a role in stomatal movement (Table 5.4) For instance, accumulation of ABA receptors, PP2Cs protein in the ABA signalling pathway can be found in the GC proteome. However, ABA receptor (PYL) showed no differential abundance in GC of quinoa in response to salt stress while OST1 in GC was only marginally upregulated by salt stress (1.4-fold increase).

5.3.6 Protein involved in response to ABA in guard cell proteome

The ABA levels in a plant tissue tend to elevate with exposure to salt or osmotic

stress, indicating contribution of ABA in stress signal transduction. In this study, ten proteins involved in response to ABA were found to be upregulated in quinoa GC (Fig. 5.6) including LTI65 (50-fold), ASPG1(4.1 fold), PLD (3.3 fold), α enzyme (21 fold), EDR14 (7.8 fold), LTP3 (8.1 fold), Chitinase 1(10.4 fold), Chit1(5.8 fold), BFRUC4 (3 fold), PAP (22.2 fold).

5.3.7 Sucrose and starch metabolism in the guard cell

A pathway found to be upregulated in the GC in response to salt stress in quinoa was sucrose/starch metabolism pathway (Fig. 5.7). The abundance of alpha-amylase1 that is involved in starch breakdown, increased by 21-fold under salt stress. Isoform 3 of sucrose synthase was also more abundant under salt conditions in this study.

5.3.8 The effect of sucrose, tryptophan and L- methionine on stomatal conductance

In our study, sucrose synthase and two proteins related to biosynthesis of tryptophan and 5-methyltetrahydropteroyltriglutamate (involved in L-methionine biosynthesis) were accumulated in the GCs in response to salinity. We further explored the effect of exogenous sucrose, tryptophan and methionine on stomatal conductance (Fig. 5.8). The results showed that application of sucrose, tryptophan and L- methionine was associated with lesser stomatal conductance. Stomatal conductance values were 1.10, 1.39 and 1.02 mol m^{-2} s^{-1} at the control conditions which decreased to 0.62, 0.93 and 0.77 mol m^{-2} s^{-1} by the application of 30 mM sucrose, tryptophan and methionine respectively.

5.4 Discussion

5.4.1 Most abundant proteins in the guard cells isolated from quinoa

Rubisco activase was the most abundant protein in quinoa GCs. This is not surprising as Rubisco activase in some halophytes such as *Suaeda salsa* and *Eutrema halophila* is present at higher amounts compared to glycophytes (Bose *et al.* 2017). Furthermore, it has been reported that the promotor region of Rubisco activase gene is enriched in stress responsive elements including two for temperature, three for dehydration and five for light responses which means Rubisco activase is a light- and stress-regulated gene (Chen *et al.* 2015).

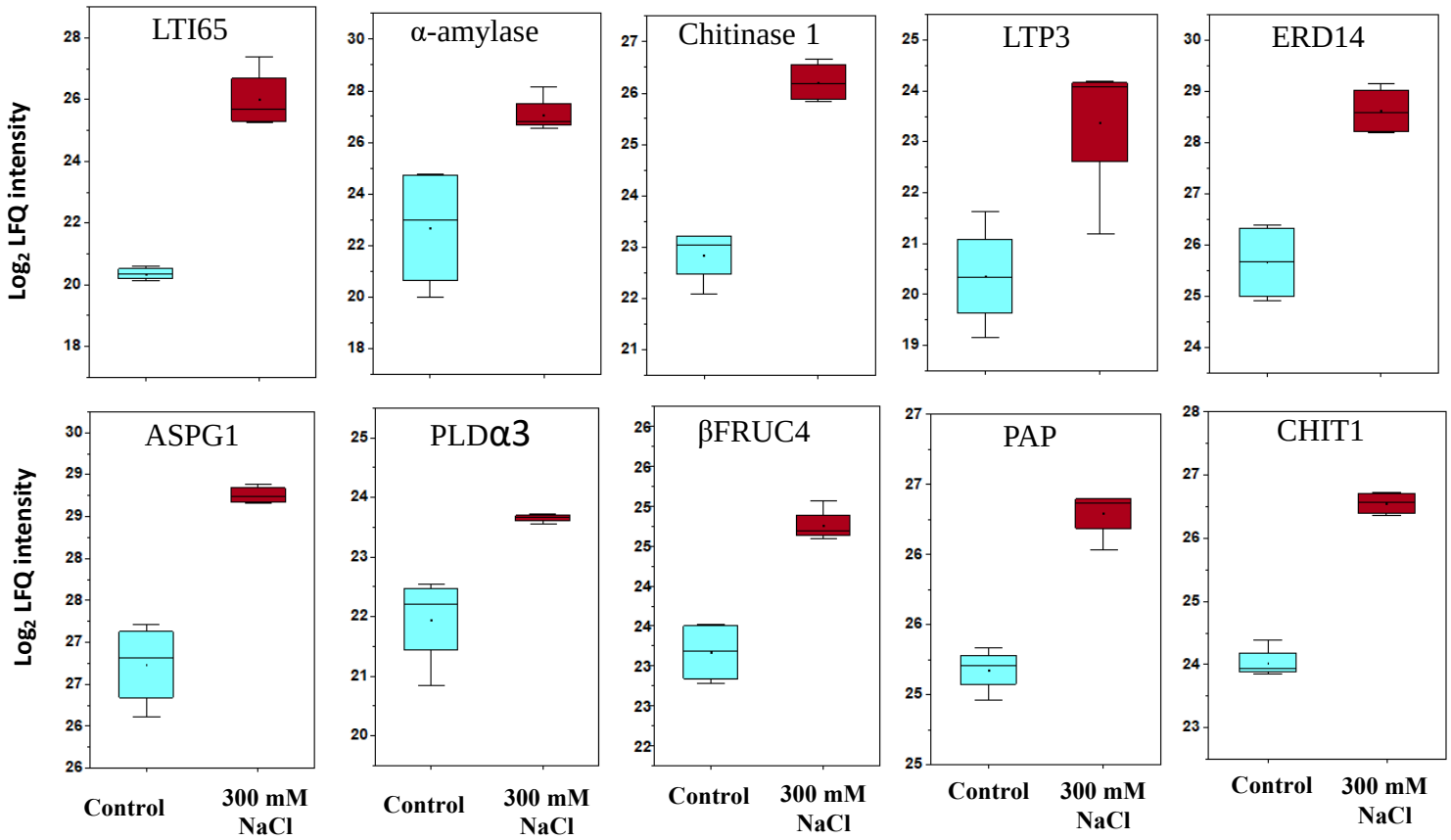

Fig. 5.6 proteins involved in ABA response, LTI65-Low-temperature-induced 65 kDa protein, α-amylase -Alpha-amylase, Chitinase 1- Chitinase 1, LTP3: Non-specific lipid-transfer protein 3, EDR14- Dehydrin, ASPG1- protein aspartic protease in guard cell 1-like, PLD α 3-Phospholipase D,Bfruc4- acid beta-fructofuranosidase-like,PAP- Plastid-lipid-associated protein, CHIT1-Chitinase 1.

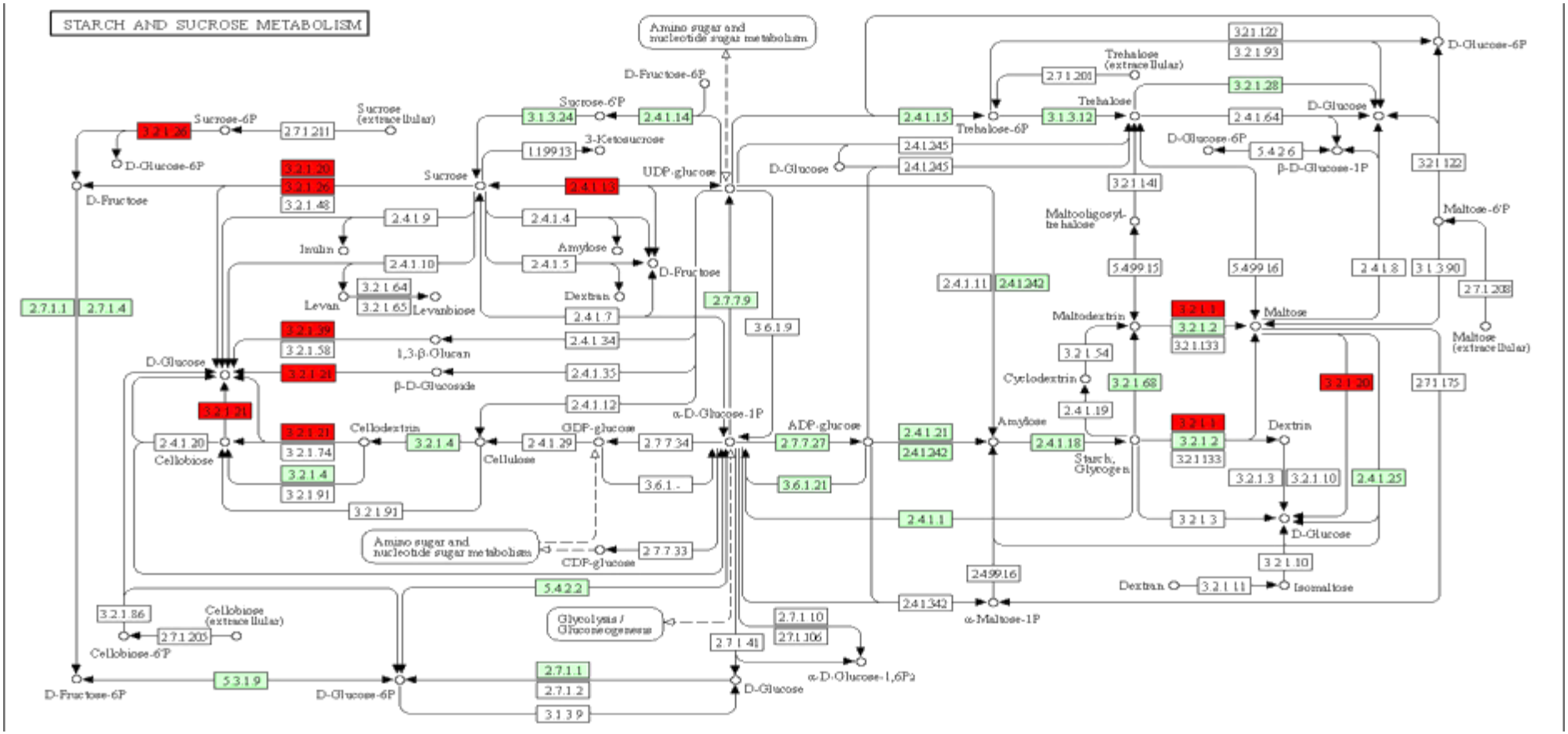

Fig. 5.7 Sucrose and starch metabolism KEGG pathway. The red proteins are up-regulated by NaCl in the quinoa guard cells. Salinity seems to activate genes related to degradation of both starch and sucrose pathways.

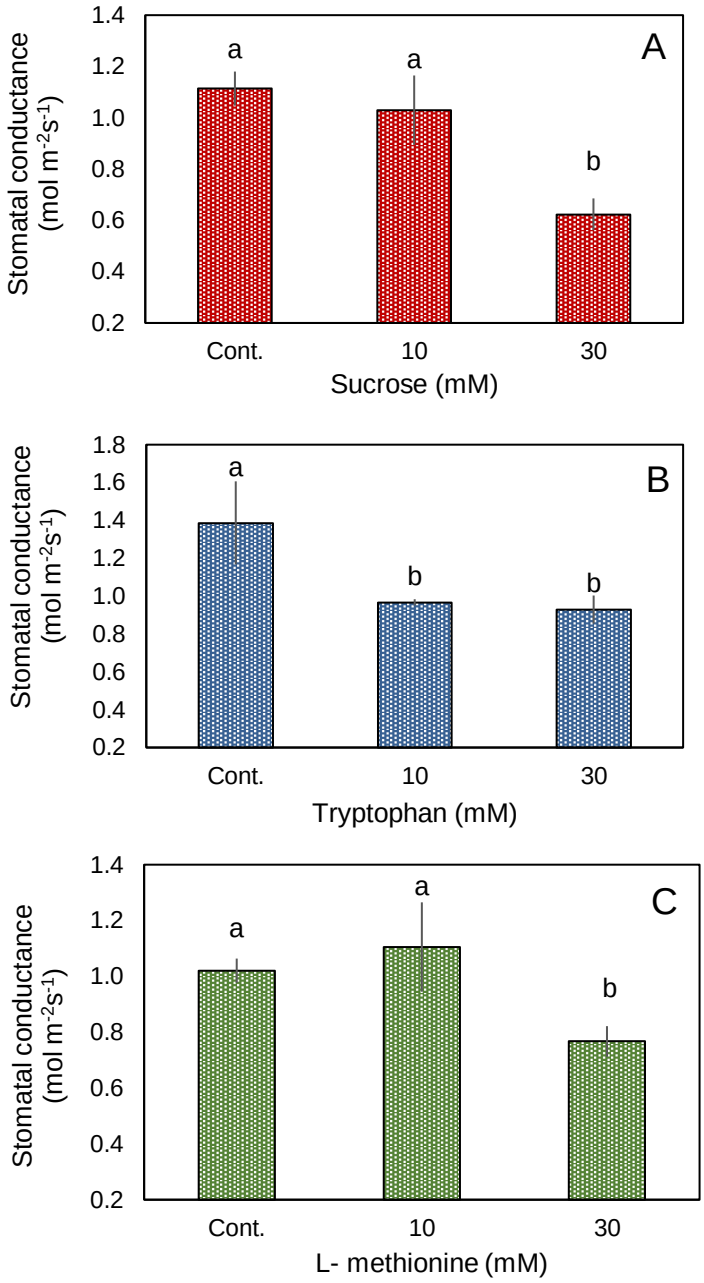

Fig. 5.8 The effect of sucrose (A), tryptophan (B) and L-methionine (C) on stomatal conductance.

In addition to Rubisco activase, GDSL motif containing esterases/lipases was found to be among the most highly abundant proteins in quinoa GCs. Previous studies found that the degree of stomatal aperture in response to low CO_2 corresponds to increased levels of GDSL esterase/lipases (Geng *et al.* 2017). Furthermore, there is some evidence to suggest involvement of this protein in salt tolerance mechanism, as a gene belonging to the GDSL-motif lipase family was

found to confer enhanced salt and pathogen resistance in Arabidopsis (Naranjo *et al.* 2006).

ABP19 was also an abundant protein in quinoa GCs. ABP19 is a receptor for a hormone auxin that is involved in stomatal development and patterning pathways (Le *et al.* 2014).

Auxin is also involved in modulation of K^+ channel in the GC (Thiel *et al.* 1993). In *Paphiopedilum tonsum*, ABP decreased GC cytoplasmic pH and induced stomatal opening (Gehring *et al.* 1998).

5.4.2 Photosynthesis in the guard cells

Analysis of GC proteins demonstrated that photosynthesis was among top 10 GO terms in the GC proteome (Supplemental Table S5.1). Photosynthesis in GCs has been a controversial topic for many years. Rubisco and other enzymes for carbon reduction are both present and active in GCs, and while the emerging consensus is that photosynthesis does takes place in GCs, the role of GC photosynthesis in relation to stomatal behaviour is still unclear. Recent experiments on transgenic Arabidopsis (Azoulay-Shemer et al. 2015) with targeted chlorophyll deficiency in GCs) found that GCs are thin and flaccid suggesting that photosynthesis in is essential for GC turgor. Another recent study (Iwai *et al.* 2019) demonstrated that photosynthesis in GC is necessary for ABA signaling. Photosynthetic electron transport in GCs generates ROS, which act as signaling molecules in stomatal closure induced by ABA.

5.4.3 Stress and defence-related proteins

The high upregulation of dehydrins (LTI65 and ERD14) salt-treated quinoa GC implies dehydrin proteins play a role in stomata of halophytes such as quinoa under saline conditions. Early responsive to dehydration (ERD14) belongs to the dehydrins family of proteins containing highly hydrophilic and charged residues that allows a highly flexible structure. They contribute to multiple functions as protecting macromolecular and stabilizing proteins and are the best representative of late embryogenesis abundant (LEA) proteins (Lüttge *et al.* 2011). In addition to functioning as a chaperone protein, they also act as osmoticum being able to attract water towards the cell to adjust osmotic potential and maintain water status (Nylander *et al.* 2001).

Table 5.4 Proteins with a direct role in guard cell function.

Accession No	Name	**Fold change NaCl/Control**
XP_02174988	abscisic acid receptor PYL2	**1.1**
XP_021736717	phospholipase D alpha 1-like	**3.3***
XP_021739586	GDPDL3-like	**2.1***
XP_021760770	ricin B-like lectin EULS3	**2.0***
XP_021754221	MMK2-like	**1.6***
XP_021759066	GDPDL3-like	**1.5***
XP_021738483	OST1	**1.3***
XP_021723531	hexokinase-1-like	**0.9***
XP_021715572	clathrin heavy chain 1-like	**0.8***
XP_021723433	plasma membrane ATPase 4-like	**0.5***
XP_021761237	calcium sensing receptor, chloroplastic-like	**0.5***
XP_021734330	protein flowering locus t-like	**0.3***
XP_021776446	protein thylakoid formation1	**0.3***
XP_021775775	uncharacterized protein LOC110739633	**0.2***
XP_021776385	protein phosphatase 2C	**0.4**
XP_021714641	DNA-directed RNA polymerases II, IV and V	**2.5**
XP_021721800	BLUS1-like	**2.2**
XP_021757551	MMK2-like	**1.9**
XP_021723484	serine/threonine-protein kinase STY8-like	**1.8**
XP_021760806	carbonic anhydrase, chloroplastic	**1.7**
XP_021740220	cryptochrome-1-like isoform X3	**1.4**
XP_021753299	phototropin-2-like	**1.3**
XP_021731588	glycine-rich RNA-binding, ABA-inducible protein	**1.1**
XP_021774295	phytochrome B-like	**1.1**
XP_021742577	translationally-controlled tumor protein homolog	**1.1**
XP_021716254	phototropin-1-like isoform X1	**1.0**
XP_021741723	carbonic anhydrase, chloroplastic-like	**1.0**
XP_021774801	MMK1-like	**0.9**
XP_021760799	phospholipase D alpha 1-like	**0.9**
XP_021758723	chlorophyll a-b binding protein 3, chloroplastic	**0.7**
XP_021745518	plasma membrane-associated cation-binding protein 1	**0.7**
XP_021731589	glycine-rich RNA-binding protein-like	**0.7**
XP_021723344	phosphoglycerate mutase-like	**0.6**
XP_021760744	vesicle-associated membrane protein 711	**0.6**
XP_021769207	clathrin heavy chain 1-like	**0.5**

* denotes a significant protein difference between control and salt stress (Student's t-test, $p < 0.05$; FC >2.0).

PLAT domain-containing protein (Polycystin-1, Lipoxygenase, Alpha-toxin and Triacylglycerol lipase), is generally expressed in water regulation structures such as vascular tissue and GCs. Levels of this protein increases under salt and ABA stresses and it confers tolerance to stress (Hyun *et al.* 2014). This protein binds to ABF/AREB (bZIP) transcription factors which mediates the ABA signalling pathway (Hyun *et al.* 2014). Protein aspartic protease in guard cell 1 was found to increase 4-fold in response to salinity. This protein is highly expressed in tolerant genotypes but highly repressed in sensitive ones, indicating a potential role in osmotic stress regulation by osmotic adjustment (Kaashyap *et al.* 2018).

In this study, ten proteins involved in response to ABA were found to be upregulated in quinoa GC (Fig. 5.6). Among them, LTI65 is involved in abscisic acid-activated signalling pathway, as the promoter region of this gene contains two ABREs (ABA-responsive elements).

PLD α enzyme is activated by ABA and produce phosphatidic acid (a signaling molecule) that induce stomatal closure (Saucedo-Garcia *et al.* 2015). Plastid-lipid-associated proteins are lipid-binding physically bind to ABI2 as a key regulator of ABA-mediated response. Overexpression of protein aspartic protease in GCs has been associated with an increase in ABA sensitivity in the stomatal closure (Yao *et al.* 2012).

5.4.4 Sucrose, tryptophan and L- methionine induced stomatal closure

Sucrose/starch metabolism pathway was found to be upregulated in the GC in response to salt stress in quinoa (Fig. 5.7). The abundance of alpha-amylase1 that is involved in starch breakdown, increased by 21-fold under salt stress. This enzyme in GC takes part in degradation of starch to release sugars and organic acids to promote stomatal opening (Thalmann and Santelia 2017). Under stresses such as high salinity, starch could be a key molecule to manage stress where starch remobilization to meet the enhanced energy demand (Krasensky and Jonak 2012). Isoform 3 of sucrose synthase (SUS3) which is preferentially expressed in the GCs was also more abundant under salt conditions in this study. This enzyme can catalyze the reversible conversion of sucrose into UDP-glucose and fructose and increases sucrose degradation (Lawson and Matthews 2020) to provides fructose and UDP-glucose for metabolic pathways or is account for the generation of ADP-glucose for starch synthesis in GCs (Bates *et al.* 2012). The sucrose breakdown is

proposed to provide carbon for organic acid production which could be accumulated in the GCs vacuole to act as counter ions for K^+. Considering the high respiration rate in GCs, sucrose breakdown may provide substrates for GCs respiration.

In our study, two proteins related to biosynthesis of tryptophan and 5-methyltetrahydropteroyltriglutamate (involved in L-methionine biosynthesis) were increased by salinity. In GCs, while some amino acids (phenylalanine, glycine, threonine, lysine, arginine, proline, alanine, leucine, tryptophan) induce stomatal closure, others (asparagine, methionine, glutamic acid, histidine, aspartic acid, and glutamine) promote opening through changes in membrane potential and regulating K^+ flux into the GC (Sharma and Rai 1989).

These interactions can be balanced to a stage which results in optimum gaseous exchange and water conservations at the same time. Therefore, in our study we further explored the role of these two amino acids that may be affected by salt stress in quinoa.

The results showed that application of tryptophan and L- methionine and sucrose was associated with lesser stomatal aperture and conductance, which could be advantageous for plants under salt stress. It was shown that hexokinase, the product of sucrose breakdown, can initiates an abscisic acid stomatal closure pathway by production of NO and H_2O_2 (Granot and Kelly 2019). Both earlier and recent work on the effect of amino acids on stomata operation supported a role for amino acids in changing permeability of membranes to ions including potassium, and regulate the flux of K^+ and other ions and thus change the stomatal conductance (Sharma and Rai 1989; Kong *et al.* 2016).

5.5 Conclusion

This study demonstrated that salinity stress significantly altered protein profile of quinoa GCs where abundance of many proteins including signalling molecules, enzyme modulators, transcription factors and oxidoreductases were changed. Furthermore, many proteins involved in osmotic or salinity stress as well as in response to ABA were found to be highly abundant or upregulated in quinoa GC following salinity treatment. Also, exogenous application of sucrose and amino acids (tryptophan and L-methionine) resulted in less stomatal aperture and

conductance suggesting that it could be advantageous for plant adaptation to salt stress.

5.6 References

Ache, P, Bauer, H, Kollist, H, Al-Rasheid, KA, Lautner, S, Hartung, W, Hedrich, R (2010) Stomatal action directly feeds back on leaf turgor: new insights into the regulation of the plant water status from non-invasive pressure probe measurements. *The Plant Journal* **62**, 1072-82.

Azoulay-Shemer, T, Palomares, A, Bagheri, A, Israelsson-Nordstrom, M, Engineer, CB, Bargmann, BO, Stephan, AB, Schroeder, JI (2015) Guard cell photosynthesis is critical for stomatal turgor production, yet does not directly mediate CO_2 - and ABA-induced stomatal closing. *The Plant Journal* **83**, 567-81.

Barkla, BJ, Vera-Estrella, R, Raymond, C (2016) Single-cell-type quantitative proteomic and ionomic analysis of epidermal bladder cells from the halophyte model plant Mesembryanthemum crystallinum to identify salt-responsive proteins. *BMC Plant Biology* **16**, 110.

Bates, GW, Rosenthal, DM, Sun, J, Chattopadhyay, M, Peffer, E, Yang, J, Ort, DR, Jones, AM (2012) A comparative study of the *Arabidopsis thaliana* guard-cell transcriptome and its modulation by sucrose. *PLoS One* **7**, e49641.

Bose, J, Munns, R, Shabala, S, Gilliham, M, Pogson, B, Tyerman, SD (2017) Chloroplast function and ion regulation in plants growing on saline soils: lessons from halophytes. *Journal of Experimental Botany* **68**, 3129-3143.

Chaves, MM, Costa, JM, Zarrouk, O, Pinheiro, C, Lopes, CM, Pereira, JS (2016) Controlling stomatal aperture in semi-arid regions-The dilemma of saving water or being cool? *Plant Science* **251**, 54-64.

Chen, Y, Wang, XM, Zhou, L, He, Y, Wang, D, Qi, YH, Jiang, DA (2015) Rubisco activase is also a multiple responder to abiotic stresses in rice. *PLoS One* **10**, e0140934.

Cotelle, V, Leonhardt, N (2015) 14-3-3 proteins in guard cell signaling. *Frontiers in Plant Science* **6**, 1210.

Flowers, TJ, Colmer, TD (2015) Plant salt tolerance: adaptations in halophytes. *Annals of Botany* **115**, 327-331.

Gehring, CA, McConchie, RM, Venis, MA, Parish, RW (1998) Auxin-binding-protein antibodies and peptides influence stomatal opening and alter cytoplasmic pH. *Planta* **205**, 581-6.

Geilfus, CM, Lan, J, Carpentier, S (2018) Dawn regulates guard cell proteins in *Arabidopsis thaliana* that function in ATP production from fatty acid beta-oxidation. *Plant Molecular Biology* **98,** 525-543.

Geng, S, Yu, B, Zhu, N, Dufresne, C, Chen, S (2017) Metabolomics and proteomics of *Brassica napus* guard cells in response to low CO_2. *Frontiers in Molecular Biosciences* **4**, 51.

Granot, D, Kelly, G (2019) Evolution of guard-cell theories: the story of sugars. *Trends in Plant Science* **24**, 507-518.

Hetherington, AM, Woodward, FI (2003) The role of stomata in sensing and driving environmental change. *Nature* **424**, 901-8.

Huang, YC, Wu, HC, Wang, YD, Liu, CH, Lin, CC, Luo, DL, Jinn, TL (2017) Pectin methylesterase 34 Contributes to heat tolerance through its role in promoting stomatal movement. *Plant Physiology* **174**, 748-763.

Hubbard, K, Webb, A (2015) Circadian rhythms in stomata: physiological and molecular aspects. *Rhythms in Plants: Dynamic Responses in a Dynamic Environment* (Springer international publishing switzerland).

Husaini, AM, Zainul Abdin, M (2008) Overexpression of tobacco osmotin gene leads to salt stress tolerance in strawberry (*Fragaria* × *ananassa* Duch.) plants. *Indian Journal of Biotechnology* **7**, 465-471.

Hyun, TK, van der Graaff, E, Albacete, A, Eom, SH, Grosskinsky, DK, Bohm, H, Janschek, U, Rim, Y, Ali, WW, Kim, SY, Roitsch, T (2014) The Arabidopsis PLAT domain protein1 is critically involved in abiotic stress tolerance. *PLoS One* **9**, e112946.

Iwai, S, Ogata, S, Yamada, N, Onjo, M, Sonoike, K, Shimazaki, KI (2019) Guard cell photosynthesis is crucial in abscisic acid-induced stomatal closure. *Plant Direct* **3**, e00137.

Kaashyap, M, Ford, R, Kudapa, H, Jain, M, Edwards, D, Varshney, R, Mantri, N (2018) Differential regulation of genes involved in root morphogenesis and cell wall modification is associated with salinity tolerance in chickpea. *Science Reports* **8**, 4855.

Kiani-Pouya, A, Rasouli, F, Bazihizina, N, Zhang, H, Hedrich, R, Shabala, S (2019) A large-scale screening of quinoa accessions reveals an important role of epidermal bladder cells and stomatal patterning in salinity tolerance. *Environmental and Experimental Botany* **168**, 103885.

Kong, D, Hu, HC, Okuma, E, Lee, Y, Lee, HS, Munemasa, S, Cho, D, Ju, C, Pedoeim, L, Rodriguez, B, Wang, J, Im, W, Murata, Y, Pei, ZM, Kwak, JM (2016) L-Met activates Arabidopsis GLR Ca^{2+} channels upstream of ROS production and regulates stomatal movement. *Cell Reports* **17**, 2553-2561.

Krasensky, J, Jonak, C (2012) Drought, salt, and temperature stress-induced metabolic rearrangements and regulatory networks. *Journal of Experimental Botany* **63**, 1593-608.

Kretzschmar, T, Burla, B, Lee, Y, Martinoia, E, Nagy, R (2011) Functions of ABC transporters in plants. *Essays in Biochemistry* **50**, 145-60.

Laloum, T, Martín, G, Duque, P (2018) Alternative splicing control of abiotic stress responses. *Trends in Plant Science* **23**, 140-150.

Lawson, T, Blatt, MR (2014) Stomatal size, speed, and responsiveness impact on photosynthesis and water use efficiency. *Plant Physiology* **164**, 1556-1570.

Lawson, T, Matthews, J (2020) Guard cell metabolism and stomatal function. *Annual Review of Plant Biology* .10.1146/annurev-arplant-050718-100251

Le, J, Liu, XG, Yang, KZ, Chen, XL, Zou, JJ, Wang, HZ, Wang, M, Vanneste, S, Morita, M, Tasaka, M, Ding, ZJ, Friml, J, Beeckman, T, Sack, F (2014) Auxin transport and activity regulate stomatal patterning and development. *Nature Communications* **5**, 3090.

Lee, DS, Kim, BK, Kwon, SJ, Jin, HC, Park, OK (2009) Arabidopsis GDSL lipase 2 plays a role in pathogen defense via negative regulation of auxin signaling. *Biochemical and Biophysical Research Communications* **379**, 1038-42.

Lüttge, U, Beck, E, Bartels, D (2011) *Plant dessication tolerance.* Ecological Studies Book 215, (Springer, Heidelberg)

Mickelbart, MV, Hasegawa, PM, Bailey-Serres, J (2015) Genetic mechanisms of abiotic stress tolerance that translate to crop yield stability. *Nature Reviews Genetics* **16**, 237-51.

Naranjo, MA, Forment, J, Roldan, M, Serrano, R, Vicente, O (2006) Overexpression of *Arabidopsis thaliana* LTL1, a salt-induced gene

encoding a GDSL-motif lipase, increases salt tolerance in yeast and transgenic plants. *Plant, Cell and Environment* **29**, 1890-900.

Nylander, M, Svensson, J, Tapio Palva, E, Welin, BV (2001) Stress-induced accumulation and tissue-specific localization of dehydrins in *Arabidopsis thaliana*. *Plant Molecular Biology* **45**, 263–279.

Ringli, C, Keller, B, Ryser, U (2001) Glycine-rich proteins as structural components of plant cell walls. *Cellular and Molecular Life Sciences* **58**, 1430-1441.

Saucedo-Garcia, M, Gavilanes-Ruiz, M, Arce-Cervantes, O (2015) Long-chain bases, phosphatidic acid, MAPKs, and reactive oxygen species as nodal signal transducers in stress responses in Arabidopsis. *Frontiers in Plant Science* **6**, 55.

Schwacke, R, Ponce-Soto, GY, Krause, K, Bolger, AM, Arsova, B, Hallab, A, Gruden, K, Stitt, M, Bolger, ME, Usadel, B (2019a) MapMan4: a refined protein classification and annotation framework applicable to multi-omics data analysis. *Molecular Plant* **12**, 879-892.

Shabala, S (2013) Learning from halophytes: physiological basis and strategies to improve abiotic stress tolerance in crops. *Annals of Botany* **112**, 1209-21.

Sharma, UD, Rai, VK (1989) Modulation of osmotic closure of stomata, stomatal resistance and K^+ fluxes by exogenous amino acids in *Vicia faba* L. Leaves. *Biochemie Und Physiologie Der Pflanzen* **185**, 369-376.

Sun, J, Jiang, H, Xu, Y, Li, H, Wu, X, Xie, Q, Li, C (2007) The CCCH-type zinc finger proteins AtSZF1 and AtSZF2 regulate salt stress responses in Arabidopsis. *Plant and Cell Physiology* **48**, 1148-1158.

Taji, T, Seki, M, Satou, M, Sakurai, T, Kobayashi, M, Ishiyama, K, Narusaka, Y, Narusaka, M, Zhu, JK, Shinozaki, K (2004) Comparative genomics in salt tolerance between Arabidopsis and Arabidopsis-related halophyte salt cress using Arabidopsis microarray. *Plant Physiology* **135**, 1697-709.

Takemori, A, Nakashima, T, Omura, H, Tanaka, Y, Nakata, K, Nonami, H, Takemori, N (2019) Quantitative assay of targeted proteome in tomato trichome glandular cells using a large-scale selected reaction monitoring strategy. *Plant Methods* **15**, 40.

Thalmann, M, Santelia, D (2017) Starch as a determinant of plant fitness under abiotic stress. *New Phytologist* **214**, 943-951.

Thiel, G, Blatt, MR, Fricker, MD, White, IR, Millner, P (1993) Modulation of K^+ channels in vicia stomatal guard-cells by peptide homologs to the auxin-binding protein-C terminus. *Proceedings of the National Academy of Sciences of the United States of America* **90**, 11493-11497.

Willmer, CM, Grammatikopoulos, G, LascÈve, G, Vavasseur, A (1995) Characterization of the vacuolar-type H^+-ATPase from guard cell protoplasts of Commelina. *Journal of Experimental Botany* **46**, 383-389.

Wu, HC, Bulgakov, VP, Jinn, TL (2018) Pectin Methylesterases: cell wall remodeling proteins are required for plant response to heat stress. *Frontiers in Plant Science* **9**, 1612.

Yao, X, Xiong, W, Ye, TT, Wu, Y (2012) Overexpression of the aspartic protease ASPG1 gene confers drought avoidance in Arabidopsis. *Journal of Experimental Botany* **63**, 2579-2593.

Zhang, T, Zhu, M, Zhu, N, Strul, JM, Dufresne, CP, Schneider, JD, Harmon, AC, Chen, S (2016a) Identification of thioredoxin targets in guard cell enriched epidermal peels using cysTMT proteomics. *Journal of Proteomics* **133**, 48-53.

Zhang, T, Zhu, MM, Zhu, N, Strul, JM, Dufresne, CP, Schneider, JD, Harmon, AC, Chen, SX (2016b) Identification of thioredoxin targets in guard cell enriched epidermal peels using cysTMT proteomics. *Journal of Proteomics* **133**, 48-53.

Zhang, YJ, Li, DH, Zhou, R, Wang, X, Dossa, K, Wang, LH, Zhang, YX, Yu, JY, Gong, HH, Zhang, XR, You, J (2019) Transcriptome and metabolome analyses of two contrasting sesame genotypes reveal the crucial biological pathways involved in rapid adaptive response to salt stress. *BMC Plant Biology* **19**, 66.

Zhao, ZX, Stanley, BA, Zhang, W, Assmann, SM (2010) ABA-regulated G protein signaling in Arabidopsis guard cells: a proteomic perspective. *Journal of Proteome Research* **9**, 1637-1647.

Zhao, ZX, Zhang, W, Stanley, BA, Assmann, SM (2008) Functional proteomics of *Arabidopsis thaliana* guard cells uncovers new stomatal signaling pathways. *The Plant Cell* **20**, 3210-3226.

Zhu, JK (2002) Salt and drought stress signal transduction in plants. *Annual Review of Plant Biology* **53**, 247-73.

Zhu, MM, Dai, SJ, McClung, S, Yan, XF, Chen, SX (2009) Functional differentiation of *Brassica napus* guard cells and mesophyll cells revealed by comparative proteomics. *Molecular & Cellular Proteomics* **8**, 752-766.

Chapter 6: Comparative transcriptome analysis of halophyte (*Chenopodium quinoa* Wild.) and glycophyte (*Spinacia oleracea*) guard cells in response to salt stress

Abstract

Salinity stress is a critical environmental limiting factor for crop growth and productivity. Early response of plants to limited water availability is stomatal closure which imposes yield penalty due to reducing CO_2 uptake for photosynthesis. However, responses of halophytes' and glycophytes' stomata might be different when plants are exposed to salinity for longer times. In the present study, the guard cells (GCs) response of quinoa (halophyte) and spinach (glycophyte) were evaluated after three weeks of salt treatment (250 mM NaCl) to identify the transcriptional changes caused by salinity stress. For this purpose, mechanically prepared guard cell-enriched epidermal fragments were used for RNAseq transcriptome analysis. In both species salt-responsive genes were mainly related to biological processes such as protein metabolism, secondary metabolites, signal transduction, and transport systems. Genes related to ABA signaling and ABA biosynthesis were strongly induced in quinoa GCs. Also, expression of the amino acids, proline, sugars, sucrose and potassium transporters increased in quinoa GCs under salt stress conditions. Analysis of cell-wall-related genes revealed that spinach developed a more rigid guard cell wall while quinoa had a flexible cell wall upon exposure to salt stress which resulted in higher speed of stomatal reactions to light and dark. Furthermore, genes involving in inhibition of stomata development and differentiation highly expressed by salt in quinoa, but not in spinach. The phenotype of this alteration was manifested in reduced stomatal density and index in quinoa leaf while salinity did not alter stomatal formation in the epidermal tissue of spinach. Altogether, comparative RNA-sequencing analysis of quinoa and spinach GCs revealed that GCs had higher salt-adaptability in quinoa than spinach. This GCs superiority in quinoa was achieved through fine modulation of transporters, cell wall modification and controlling stomatal development which were resulted in a high K^+/Na^+ balance, less stomatal conductance and more resilience of stomata in response to environmental stimuli.

6.1 Introduction

Due to the heterogeneity observed in cell populations of organisms, analysing a single cell makes it possible to explore mechanisms which are masked when a mixed population of cells is studied (Libault and Chen 2016; Wilson and Nairn 2018b). This is very critical while working with highly specialised cells such as stomata guard cells (GCs). Stomata play a key role in leaf gas exchange and plant water use (Hetherington and Woodward 2003a). During the establishment of plants in the land, stomata were developed as a survival tool to overcome the challenges for maintaining water status while allowing gas exchange (Richardson and Torii 2013). GCs as two specialized cells that form a stoma pore, regulating stomatal opening and closure process by changes in turgor pressure in response to environmental and internal signals (Hedrich and Shabala 2018).

Salinity stress is a critical environmental limiting factor for crop growth and productivity. It is estimated that 50% of arable land will be affected by salinity by 2050 (Butcher *et al.* 2016) and as the majority of staple crops are sensitive to salt stress, this problem could be a serious threat for food security. Response to salt stress on the other hand is a complex phenomenon that is regulated by many genetic factors and involved multiple functional genes. Many studies have been carried out on the molecular mechanisms associated with plant salt tolerance. Most of these investigations in the last decades have focused on using new technologies such as transcriptomic analysis to isolate genes for salinity tolerance and many genes have been identified in different plants that function as salt-responsive genes. These gens have been involved with various biological processes such as signal transduction, accumulation of osmoregulation substances, ion transport and transcriptional regulation (Zhang *et al.* 2013; Jin *et al.* 2016; Atzori *et al.* 2017).

A small group of plants called halophytes which are very tolerant to salt are still capable of developing and reproducibility under high saline environments (Shabala 2013). Thus, halophytic species could be perfect model plants for studying genetics of salt tolerance using transcriptome analyses. Various tissues and cell types have been analysed in comparative transcriptomic experiments in response to salt stress. Transcriptome analysis of leaf and root of mangrove, a coastal halophytic plant, showed that 19 pathways appeared in leaf and root tissues and were associated with energy metabolism, amino acids and lipid metabolism, and

environmental adaptation indicating high cost (energy and more biological substances) of salt tolerance (Huang *et al.* 2012) *Mesembryanthemum crystallinum* (ice plant) is a halophyte capable of switching from C3 to CAM type of photosynthesis under drought and salt stress (Diray-Arce *et al.* 2016). Leaf transcriptomic analysis of this plant after exposing it to 500 mM NaCl for 48 hours resulted in 9733 expressed sequence tags. Upregulated genes were mostly categorized in pathogenesis, cell death, senescence-associated genes, and heat shock proteins and CAM-related enzymes, while genes encoding light-harvesting and photosystem complexes and were down regulated in salt stress treatment. In another transcriptome study (Gharat *et al.* 2016), responses of a succulent halophyte *Suaeda maritima* to the application of salt (2% NaCl for 9 h) resulted in differential modulation of genes related to carbohydrate metabolism, cell wall, redox responses, hormones and G proteins. Sodium exclusion and sequestration have been shown to be important salt tolerance mechanisms in this halophyte.

Recently, attention has been drawn to the single-cell type to understand the molecular basis underlying the salt tolerance in halophytes. For example, transcriptome analysis of epidermal bladder cells (EBC) in ice plant showed that some genes related to ion transport including *NHX2* and *SOS1* were constitutively high in the bladder cells (Oh *et al.* 2015). As for the GCs, only a very few transcriptome studies have been conducted focusing on a model plant Arabidopsis using microarray-based assay as an earlier transcriptome analysis technique (Leonhardt *et al.* 2004b; Wang *et al.* 2011a; Bates *et al.* 2012; Bauer *et al.* 2013; Obulareddy *et al.* 2013; Adrian *et al.* 2015b). None of them dealt with salt stress.

In the case of GCs studies on halophytes, there is a lack of detailed information on stomata operation. Also, there is scarce knowledge on the molecular basis of adaptation of GCs to salinity, and no comprehensive comparisons between halophytic and glycophytic plants on this matter.

Quinoa is a promising halophytic species that has been a focus of numerous salinity tolerance investigations in the last decade (Hariadi *et al.* 2011; Adolf *et al.* 2013; Kiani-Pouya *et al.* 2019a; Manaa *et al.* 2019; Angeli *et al.* 2020). This halophyte could be used as an alternative crop instead of traditional (sensitive) staple crops or as a source for salt-resistant genes for enhancing tolerance of current staple crops via breeding programs and genome editing. The ability of plants to

control the number of stomata under saline conditions is an adaptive mechanism to reduce transpirational water loss and optimize water use efficiency in salt-affected environments. Hence, a comparative transcriptomics investigation of GCs between a halophytic plant and a glycophytic counterpart may reveal efficient salt adaptation mechanism(s) that benefits halophytes over glycophytes under saline conditions. In light of this fact, in the current investigation we performed transcriptome analysis using next generation sequencing (RNA-Seq) technology for GCs of quinoa (a halophyte) and spinach (a glycophytic) plants that also belongs to the Amaranthaceae family, under control and salt-treated conditions. It was assumed that a transcriptomics analysis of these plant species with contrasting salinity tolerance ability from the same family might shed a light on physiological mechanisms and genes conferring superior performance of GCs in halophytes.

6.2 Materials and methods

6.2.1 Plant growth conditions

Two plant species, spinach (*Spinacia oleracea*) and quinoa (*Chenopodium quinoa* Wild.) were used in this investigation. The spinach seeds were obtained from the local seed stores (cv Winter Giant) and quinoa seeds (cv Q20) were a gift from Prof S.E. Jacobsen (University of Copenhagen, Denmark). Seeds were sown in 15 cm diameter pots filled with standard potting mix (details have been provided in Chapter 3). Plants were grown under glasshouse conditions with the following conditions: mean day/night temperatures were 25/16 °C; humidity 65% to 70%; day length 16 h. The experiment was conducted at the University of Tasmania in Hobart, Australia, in October-November 2018. Plants were grown for 3 weeks under non-saline conditions and salinity stress was commenced by adding 50 mM NaCl to the irrigation water on a daily bases until reached the final concentration of 250 mM salt after 3 days. Plants were grown for another 3 weeks under salt stress.

6.2.2 Stomata density and index

Stomata density was measured on both abaxial and adaxial leaf surfaces of the youngest fully expanded leaf. Measurements were made on two randomly selected positions on 10 leaves per each treatment for each plant species. Leaf surfaces were coated with clear nail varnish and left for about 20 min to be dried out. The dried

nail varnish layer was peeled off using tweezers and then stuck onto a glass slide. The number of stomata was counted in three different fields of view of each slide (as described in detail in section 2.2.4). The stomata index was calculated as the ratio of the number of stomata in a unit area divided by the total number of stomata and epidermal cells in that area. Presented data are the mean ± SE of measurements of 20 counts per leaf of each treatment for each plant species.

6.2.3 Kinetics of stomatal conductance

Stomatal conductance was measured using a Li-Cor 6400 gas analyser system (Lincoln, NE, USA) on the youngest fully expanded leaves. For opening measurements, plants were kept in the dark for 16 h and then exposed to light and the light chamber of gas analyser was set to 1500 μmol m^{-2} s^{-1} and gas exchange parameters were recorded every 30 s until the stomatal conductance reached the steady state value. For measuring kinetics of stomatal closing in response to darkness plants transferred to the darkness and chambers set to zero light. Stomatal conductance was measured using a Li-Cor 6400 gas analyser system (Lincoln, NE, USA) on youngest fully expanded leaves with the following settings: leaf chamber temperature, 25 °C; CO_2 reference, 400 ppm; flow rate, 500 μmol s^{-1}; atmospheric VDP: 75% RH.

6.2.4 Cell wall digestion

In order to compare the stiffness of guard cell wall in quinoa and spinach under saline conditions, we dissolved the cell walls in enzymatic solution and recorded the required time for digestion of guard cell walls for both species. Digestion of the cell walls in the epidermal strip was carried out according to a protocol developed by (Zhu *et al.* 2016) for both spinach and quinoa. First, the epidermises was peeled off from quinoa and spinach leaves in both control and salt-treated plants. Experiments were performed with five replicates, each replication included 10 epidermal fragments) and then digested in a basic solution containing 1 % Cellulase R-10, 0.04 % Macerozyme R-10, 1.1 % (w/v) Onozuka RS cellulase, and 0.03 % (w/v) Pectolyase Y-23.The osmolality of the solution adjusted to 600 mOsm mM. the epidermises were randomly inspected under microscope every 10 min after one hr incubation. Then the required time for at least 90% of cell wall digestion for each of plant species under both control and salt stressed conditions were determined.

6.2.5 GC preparation

Details of GC-enriched epidermal peels preparation have provided in Chapter 3. Briefly, leaves of spinach and quinoa were ground in the Grindomix blender (GRINDOMIX LENDER GM 200, Retsch, Germany) with 200 mL water and 100 mL crushed ice and the mixture was passed through an appropriate Nylon mesh (ELKO, Filtering co. USA). The previous step was repeated 3 and 4 more times for spinach and quinoa. The purity of isolated GCs-enriched fragments samples was examined under the microscope to confirm that no contamination of mesophyll fragments or vascular particles were present. Collected samples were kept in aluminium foil and stored at -80 °C until conducting RNA extraction.

6.2.6 RNA extraction and cDNA library preparation

Total RNA of spinach and quinoa GC-enriched epidermal peels were extracted from 3 biological samples using RNeasy Plant Mini Kit (Qiagen) following the manufacturer's instructions. The quality and quantity of RNA were then measured using an Agilent 2100 Bioanalyzer system (Agilent Technologies, Inc., Santa Clara, CA, USA). Only high-quality RNA samples with RIN (RNA integrity number) values higher than 7 were used for the sequencing libraries construct. Library construction conducted using the NEBNext Ultra Directional RNA Library Prep Kit for Illumina (New England Biolabs) following the manufacturer's protocol. For each sample, 5 μg of total RNA was used to enrich the mRNA using polyT magnetic beads which was fragmented by divalent ions and then using random primers was subjected to first-strand cDNA synthesis. Taking these short fragments as templates, double-stranded cDNA was synthesized and PCR amplification was carried using the second strand cDNA and part of the adaptor was removed using the USER enzyme, and adaptor-ligated first-strand cDNA was prepared. The quality of libraries was determined using a Fragment Analyzer (Advanced Analytical Technologies, Inc) and the quantification was performed using Qubit (Thermo Fisher Scientific) and qPCR. RNA-seq libraries were sequenced HiSeq2500 using the SBS v4 reagent at the Core Facility for Genomics of the Shanghai Centre for Plant Stress Biology.

6.2.7 Transcriptome functional annotation

Raw reads were filtered to remove low-quality reads and cleaned by removing adapters. The quality control of raw sequencing was conducted using Trim Galore (http://www.bioinformatics.babraham.ac.uk/projects/trim_galore/). Low-quality bases (quality value < 20) were cut and if the quality value of the residual sequence was still less than 10, the entire sequence was removed, otherwise the read was retained. The cleaned high-quality reads of quinoa and spinach were then mapped to the quinoa reference genome (Jarvis et al. 2017) and (Xu *et al.* 2017) using the RNA-seq aligner STAR (version 2.5.4b).

6.2.8 Analysis of differentially expressed genes (DEGs)

Differential expression analysis and identification of DEGs were performed using DESeq2 (version 1.22.2) (Love *et al.* 2014) in the R platform (version 5.1). Read counts were input to the R platform and the screening criteria for significant DEGs was set to a false discovery rate (FDR) <0.05 and fold-change ≥ 2. Gene expression levels were reported in Fragments Per Kilobase of transcript per Million mapped reads (FPKM) values. Gene ontology (GO) term annotation was performed to identify significant enriched DEGs using AHRD (https://github.com/groupschoof/AHRD) and GO enrichment analysis was performed using agriGO (Tian *et al.* 2017).

6.2.9 Quantitative Reverse Transcription PCR analysis of selected DEGs

Total RNA of quinoa GC-enriched epidermal peels was extracted as described above. In quinoa, 20 up- or down-regulated DEGs, which were related to salinity response were selected for quantitative real-time PCR (qRT-PCR) assays. One mg of extracted RNA was used for reverse transcription with TransScript RT-PCR Kit (TransGen, Beijing, China) according to the manufacturer's instructions and cDNAs were used as templates for amplification. The expression of *EF1-a* gene was used as the internal reference gene. The PCR reaction conditions were as follows: heating at 94 °C for 3 min, then 35 cycles of heating at 94 °C for 30s and annealing at 55 °C for 30 s. Three biological replications and two technical measurements for each replicate were used. Relative gene expression was analysed using the $2^{-\Delta\Delta Ct}$ method (Livak and Schmittgen 2001). List of all qRT-PCR primers used for both quinoa and spinach are provided in Supplemental Table S6.1.

6.3 Results

6.3.1 Overview of sequencing and transcriptome assembly

To obtain a global overview of the quinoa and spinach transcriptomes under salinity stress, 12 cDNA libraries were constructed and then RNA-seq was performed, which yielded 356.98 million reads in total with 125 bp for both paired ends. After adapter removal and refining, we obtained 89.74 Gb of clean data, and quality scores were higher than 88%. The ratio of reads mapping to BGI quinoa and spinach genomes were high, with a mapping rate falling into a range between 81% and 83% (Table 6.1). To assemble the total transcriptomes, the high-quality filtered reads were used for reference guided transcriptome assembly using BGI genomic sequences as the references. For each sample, the mapped reads were assembled according to the updated reference gene models, and the expression values were calculated for each gene and each isoform separately.

Table 6.1 Sequencing statistics for 11 RNA-seq libraries.

Sample	Raw _read _pairs	Raw_bases	Clean_ read _pairs	%	Clean_bases	%	Uniquely mapped reads	%	Assigned reads	%
QC1	14388886	4316665800	14356495	100	4219903606	98	11822935	82	9799089	83
QC2	12815163	3844548900	12776061	100	3766195456	98	10631009	83	8855458	83
QS1	11619760	3485928000	11588116	100	3414481158	98	9859134	85	7936332	81
QS2	13348167	4004450100	13288217	100	3852367042	96	11015165	83	8909994	81
QS3	14493655	4348096500	14442955	100	4248903572	98	12458729	86	10000000	81
SC1	23188805	6956641500	23142823	100	6699027431	99	20637321	91	17211984	83
SC2	21421399	6426419700	21378258	100	6855685108	99	20968488	91	16990615	81
SC3	23617726	7085317800	23569283	100	6326025601	98	19338779	90	15875820	82
SS1	20521803	6156540900	20482421	100	6983183492	99	21321019	90	17336845	81
SS2	24445151	7333545300	24398545	100	6067526607	99	18513917	90	15123044	82
SS3	24165727	7249718100	24118848	100	7231116112	99	22130512	91	18312677	83
SS4	23137338	6941201400	23089447	100	7147743282	99	22030635	91	18164191	82

Q-quinoa; S-spinach; C-Control; S-Salt-stressed

6.3.2 Top genes and GO in quinoa and spinach GC

The top 20 genes based on average FPKM in the control and salt treated GC samples are presented in Table 6.2. The most abundant gene in quinoa GCs was *AUR62010822* which was homologue of ubiquitin-protein ligase 2 in Arabidopsis

and similar to salt-induced hydrophilic protein in *Suaeda glauca* and *Atriplex nummularia* and thus presumably involved in salt resistance. The most expressed gene in the spinach GCs was homologe of *Jacalin-related lectin* in Arabidopsis whose function is not well- characterised.

Several genes including *DNA cross-link repair protein SNM1*, *cysteine proteinase inhibitor* and *chlorophyll A/B binding proteins* homologes were highly expressed in both quinoa and spinach guard cells. *AUR62011314* which is homologues of *AtGRP7* (which encodes cold, circadian rhythm, and RNA binding 2 protein) in Arabidopsis shows a high abundance in quinoa GCs (Table 6.2). This gene is known for involving in the regulation of stomatal aperture and conferring tolerance to plant under stress. Another high abundance gene in quinoa GCs was *AUR62009317* which is similar to *MLP-like protein 31* that contributes to stress tolerance in Arabidopsis. Similarly, in spinach some stress-related genes such as *non-specific lipid-transfer protein* (*Spo06845*) and stress response protein *NST1* (*Spo09045*) were abundant (Table 6.2). The majority of the genes in quinoa GCs were not changed with salt stress except for *Nodulin-related protein 1* (*AUR62003131)* which was down-regulated.

Topmost expressed genes (20 genes) in GCs were compared with corresponding genes in quinoa leaf (Fig. 6.1A) and spinach (Fig. 6.1B). This analysis demonstrated that with an exception of two gens in spinach – namely, *Spo06839* (*Antimicrobial peptide 2*) and *Spo12437* (*Rubisco small chain*), all the top 20 genes were highly expressed in GCs than leaves in both quinoa and spinach.

6.3.3 GO analysis in genes of quinoa and spinach guard cells

To obtain overrepresented GO categories, GO enrichment analysis was performed on total expressed genes in the guard cells for each species. This analysis revealed that 485 and 408 GO were significantly abundant in GCs of quinoa and spinach, respectively. The top two GO in both quinoa and spinach GCs were single-organism processes and cellular processes and responses to the abiotic stimulus; responses to stimulus and transport were also among the top 40 GO in both species. A detailed GO analysis was conducted to identify main cellular processes in GCs regardless of salt treatment. The results revealed that around 43% of the genes in both species were localized to the nucleus and were involved in the regulation of transcription in different biological processes such as circadian rhythm, cell

Table 6.2 Top 20 most abundant genes in quinoa and spinach guard cells.

Gene ID	FPKM control	FPKM salt	TAIR*	Description
AUR62010822	36579	53236	AT1G70320	Ubiquitin-protein ligase
AUR62026058	34324	23172	AT1G73040	Mannose/glucose-specific lectin
AUR62023435	24179	19198	AT4G16500	cysteine proteinase inhibitor
AUR62015894	17101	11852	AT2G43730	Horcolin
AUR62023434	10650	10823	AT3G12490	Multicystatin
AUR62031520	10570	6818	AT3G26680	Jasmonate-induced protein
AUR62027587	9984	7137	AT1G29930	Chlorophyll a-b binding protein
AUR62019822	6611	8591	AT2G16595	Queuine tRNA-ribosyltransferase
AUR62016835	6285	6504	AT2G25320	Cyclin-F
AUR62009317	4622	2522	AT1G70840	Kirola
AUR62019082	3424	2324	AT3G09390	Metallothionein-like protein
AUR62016836	3198	4990	AT4G10930	Testis-expressed protein 13C-1
AUR62013085	2651	1383	AT2G16600	Peptidyl-prolyl cis-trans isomerase
AUR62003131	2494	1169	AT1G13930	Nodulin-related protein 1
AUR62011314	2360	1638	AT2G21660	Glycine-rich RNA-binding protein
AUR62010383	2263	4423	AT2G25320	Electrogenic Na bicarbonate cotransporter 1
AUR62040599	2237	1257	AT4G15030	Abscisic stress-ripening protein 2
AUR62020548	2195	1751	AT4G05320	Polyubiquitin
AUR62023496	2125	1477	AT5G41761	Uncharacterized protein C18orf25
AUR62010089	1964	1277	AT2G16600	Peptidyl-prolyl cis-trans isomerase
Spo21973	86704	56286	AT1G19715	Mannose/glucose-specific lectin
Spo10943	24033	23621	AT4G04980	Jasmonate-induced protein
Spo02904	32398	21647	AT5G02380	Metallothionein-like protein
Spo02304	21887	17534	AT2G38870	Wound-induced proteinase inhibitor 1
Spo25931	5207	13584	AT1G01320	Protein lifeguard 1
Spo23862	12362	10080	AT3G19190	Protein TIC 214
Spo06839	5290	8778	AT2G43620	Antimicrobial peptide 2
Spo02301	16439	6776	AT2G38870	Chymotrypsin inhibitor I, A, B, C
Spo08228	2912	5960	AT3G22170	Biorientation of chromosomes in cell division
Spo06845	1459	5518	AT2G38530	Non-specific lipid-transfer protein
Spo16408	12835	4805	AT2G40880	Multicystatin
Spo03266	2470	3827	AT3G22440	FRIGIDA-like protein 4a
Spo15438	3294	3664	AT2G16600	Peptidyl-prolyl cis-trans isomerase
Spo12437	2202	3211	AT1G67090	Rubisco small chain 2
Spo24687	2603	3001	AT1G13440	Glyceraldehyde-3-phosphate dehydrogenase
Spo20055	2926	2902	AT1G10390	Ice nucleation protein
Spo23861	3579	2822	AT1G68020	Inversin-B
Spo10529	2179	2708	AT1G29930	Chlorophyll a-b binding protein,
Spo10691	2759	2464	AT1G78680	Jasmonate-induced protein
Spo09045	3038	2434	AT4G32840	Stress response protein NST1

*TAIR- The Arabidopsis Information Resource

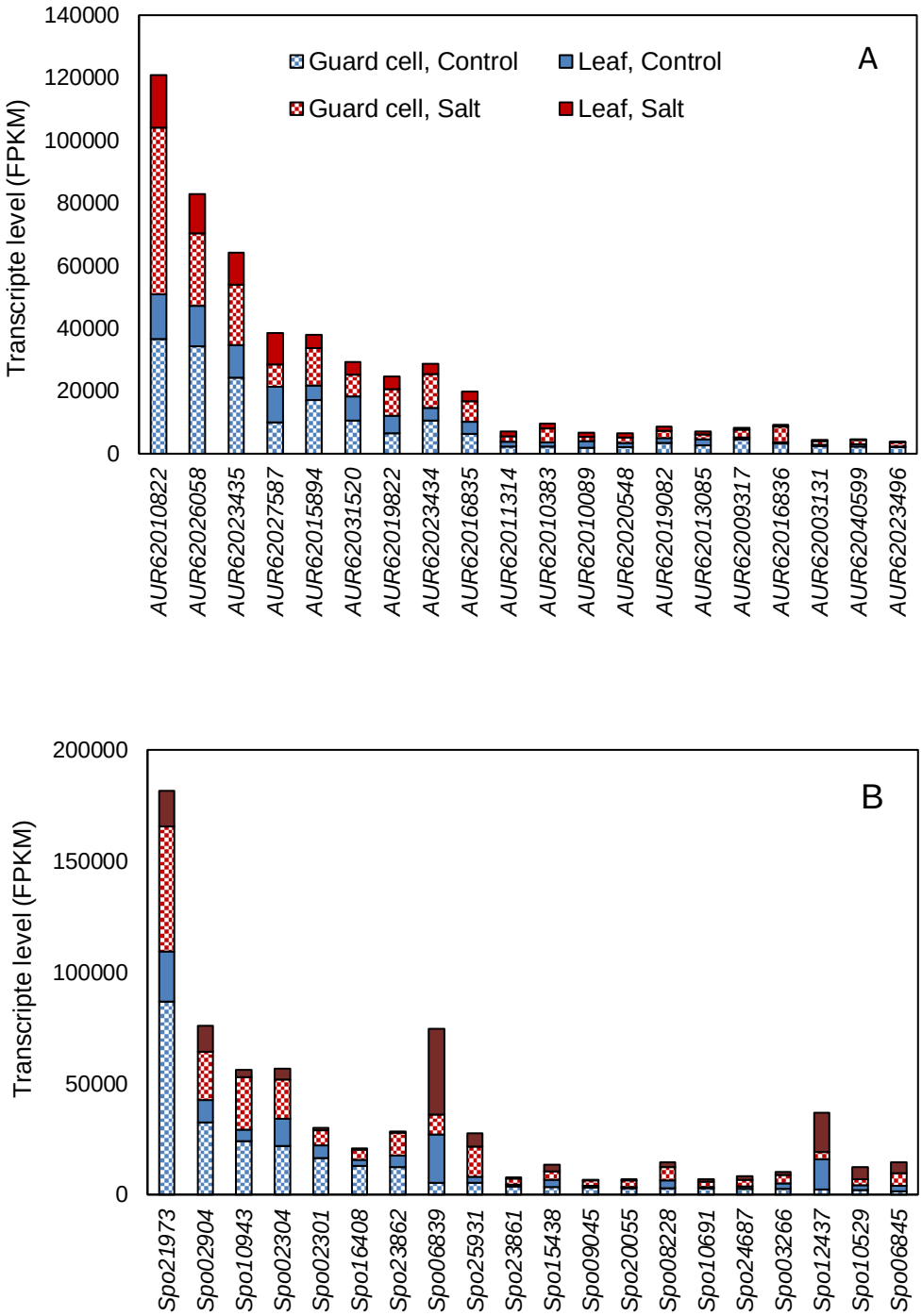

Fig. 6.1 Transcript level of topmost 20 expressed genes in quinoa (A) and spinach (B) guard cells and comparisons with gene transcripts in their leaves under control and salt stress conditions.

differentiation and response to various hormones including abscisic acid, gibberellin and auxin (Supplemental Table S6.2). A detailed analysis of GO single-organism process showed that many genes in this GO were involved in response to

salt stress, response to abscisic acid, signal transduction, defense response to bacterium, response to light stimulus and response to cold. Moreover, GOs genes associated with modulating stomatal movement and development including stomatal complex patterning (GO:0010375), stomatal complex morphogenesis (GO:0010103), regulation of stomatal opening (GO:1902456), regulation of stomatal closure (GO:0090333) and guard cell differentiation (GO:0010052) were observed in our dataset for both quinoa and spinach (Table 6.3).

Table 6.3 GO terms related to stomata found in quinoa and spinach guard cells transcriptome.

GO accession	Term	Number of gene in		
		Quinoa GC	Spinach GC	Ref*
GO:0010118	Stomatal movement	80	84	109
GO:0010119	Regulation of stomatal movement	50	51	67
GO:0010374	Stomatal complex development	33	37	54
GO:0010103	Stomatal complex morphogenesis	15	19	26
GO:0010375	Stomatal complex patterning	15	12	16
GO:0010440	Stomatal lineage progression	11	9	17
GO:0090332	Stomatal closure	18	20	26
GO:0090333	Regulation of stomatal closure	8	9	12
GO:1902456	Regulation of stomatal opening	8	9	10
GO:1990069	Stomatal opening	11	12	13
GO:2000037	Regulation of stomatal complex patterning	8	6	9
GO:2000038	Regulation of stomatal complex development	9	10	13
GO:2000122	Negative regulation of stomatal complex development	5	5	6
GO:0010052	Guard cell differentiation	10	11	15
GO:0010444	Guard mother cell differentiation	6	6	11

Ref: reference (*Arabidopsis thaliana*)

6.3.4 Differently expressed genes in GCs of quinoa and spinach

After three weeks of exposure of quinoa and spinach plants to 250 mM NaCl, quinoa had more DEGs than spinach under saline conditions. While 1005 genes were found to be differentially expressed in quinoa (558 upregulated and 447 down-

regulated), spinach on the other hand had lower DEGs where 459 and 177 genes were differently expressed in GCs of this plant.

6.3.4.1 MapMan classification of DEGs

To identify the function of DEGs in GC transcriptome in response to salt stress, protein classification and annotation were performed using Mercator4-Mapman software (Schwacke *et al.* 2019a). In quinoa, 558 up- and 447 down-regulated genes were assigned to 456 and 371 homologs in the model plant *Arabidopsis thaliana*, respectively. Similarly, in spinach 459 and 177 genes were assigned to 356 and 107 Arabidopsis homologs. As it has been shown in Figure 6.2, the expression of genes related to the cell wall, secondary metabolism, stress, signaling and transporters differentially modulated by salt stress in quinoa and spinach guard cells.

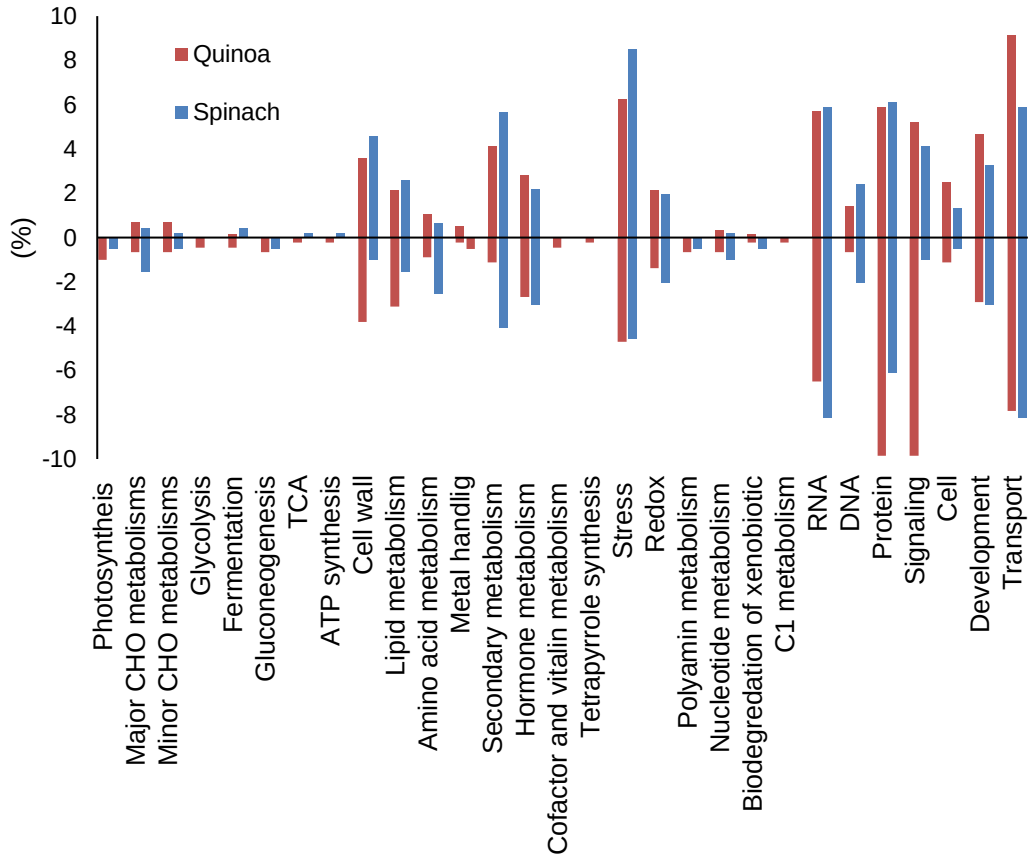

Fig. 6.2 Protein classification of *differently expressed genes in GCs* in quinoa and spinach. Protein classification and annotation were performed using Mercator4-Mapman software.

6.3.4.2 Common genes shared between quinoa and spinach

For quinoa and spinach comparison, reciprocal BLAST analysis was performed using the top hit (e-value < 10^{-5}) from species against the Arabidopsis. Arabidopsis is the most well-annotated plant genome and could be used as reference for obtaining insight into function of gene in other plant species as well as interspecies comparisons in gene regulation. The analysis revealed that a total of 11163 genes were commonly expressed between quinoa and spinach, with mainly not differentially expressed by salt stress.

As mention before, 456 genes were upregulated in quinoa, of which 322 genes were shared with spinach and 134 genes were uniquely up regulated in quinoa (Fig. 6.3). In addition, 371 genes were down regulated in quinoa of which 200 genes were shared with spinach GCs (Fig. 6.3).

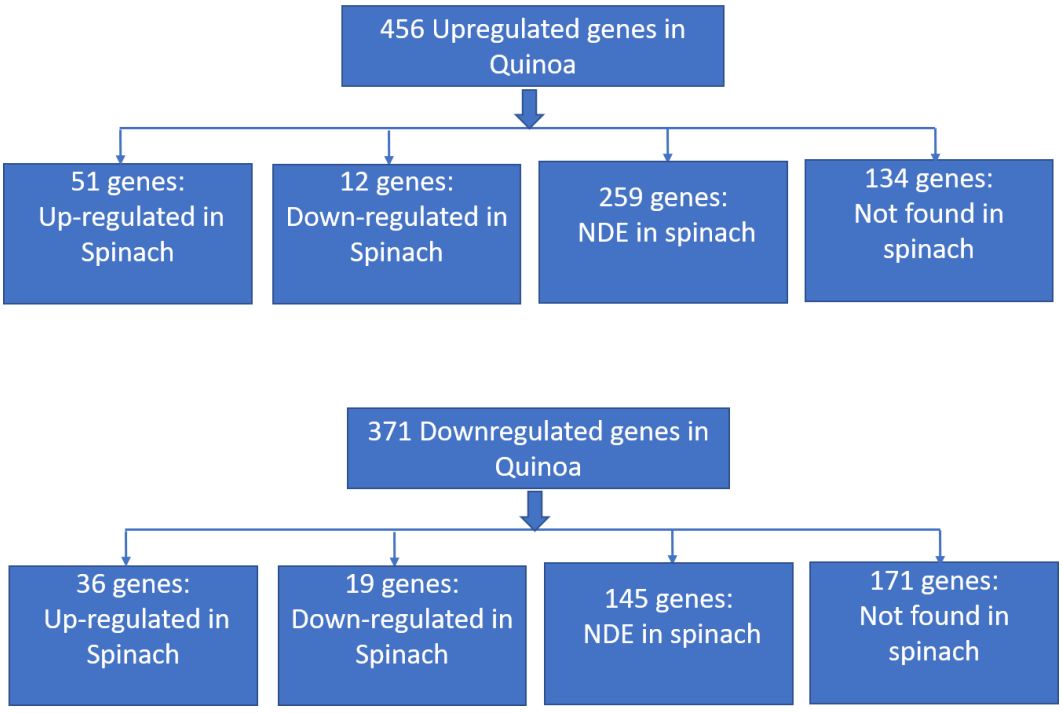

Fig. 6.3 Differently expressed genes in response to salinity in quinoa and spinach. A diagram showing the number of common differentially expressed genes under salinity stress shared between quinoa and spinach. NDE denotes non-differentially expressed genes.

6.3.4.3 GO enrichment of salt-responsive genes in quinoa and spinach

GO enrichment analysis of up and downregulated genes in quinoa and spinach were applied to identify the over-represented genes involved in the salt response in GCs of quinoa and spinach. In quinoa, a total of 150 and 60 significant GOs (FDR<0.05) were derived from upregulated and downregulated genes, respectively.

Slim GO for both up and down regulated genes is presented in Figure 6.4 and a full list of GOs are provided in Supplementary Table S6.3. Most enriched upregulated biological process GO were response to stimulus (GO:0050896), response to abiotic stimulus (GO:0009628) and response to stress (GO:0006950), homeostatic process (GO:0042592) and ion transport (GO:0006811). In down regulated biological processes GO response to stimulus (GO:0050896), ion transport (GO:0006811) and catabolic process (GO:0009056) were among top enriched GOs. In terms of the molecular function of these genes, they were classified as belonging to catalytic activity (GO:0003824), transmembrane transporter activity (GO:0022857) and hydrolase activity (GO:0016787) (Supplemental Table S6.3).

6.3.4.4 Genes related to response to abscisic acid and stress

A total of 337 and 367 genes related to ABA biosynthesis and signalling were expressed in quinoa and spinach GCs, respectively (Table 6.4). In quinoa, 38 genes were differentially regulated by salt (21 upregulated and 17 downregulated) while only 7 differentially expressed genes were shared between spinach and quinoa.

In spinach, 91 and 19 significant GOs (FDR<0.05) were obtained from upregulated and downregulated genes, respectively (Fig. 6.4). Most enriched upregulated biological process GOs were cell wall organization or biogenesis (GO:0071554) and single-organism metabolic processes (GO:0044710) while in down regulated biological processes GO of ion transport (GO:0006811) and response to stimulus (GO:0050896) were enriched. In molecular function classification of upregulated genes, heme binding (GO:0020037) and in downregulated genes oxidoreductase activity (GO:0016684) were among overexpressed GOs.

bZIP transcription factor gene (*ABI5*), a key transcription factor in ABA signaling, was increased by 3.8-fold in quinoa. Also, expression of *DREBs* (dehydration-responsive element binding factors), which are transcriptional

regulators of responsive element-binding factor (AP2/ERF) family, were induced by salinity in quinoa but not in spinach (Table 6.4). Over expressions of these genes were associated with high sensitivity to ABA (Lee *et al.* 2010). ABA synthesis under limited water availability is regulated by enzyme NCED5 (nine-cis-epoxycarotenoid dioxygenase 5) (Frey *et al.* 2012). In the current study, this gene displayed increased abundance under salt treatment in quinoa GCs. Some other ABA related genes that were highly expressed in quinoa GCs included *annexin 4* (*ANNAT4*), *homeobox 7* (*HB-7*), *lipid transfer protein 3* (*LTP3*), *lipid transfer protein 4* (*LTP4*) and *highly ABA-induced PP2C protein 2* that either not differently expressed in spinach GCs or expressed with a lower degree compared to quinoa. For instance, expression of *LTP3* and *LTP4* in salt-treated GCs were 28- and 9-fold higher than control in quinoa while corresponding values for spinach GCs were 2 and 3-fold in saline conditions (Table 6.4). In contrast, transcript abundance for some genes such as ABA receptor *PYR1-like 4* (*PYL4*) were decreased in salt-grown plants compared to non-stressed quinoa plants (Table 6.4).

6.3.4.5 Salt stress-related genes

In quinoa GCs, 101 genes related to biotic stress (20 genes) and abiotic stresses (81 genes) were upregulated in response to salt stress (Fig. 6.5), of which 77 genes were shared with spinach (17 genes upregulated, 56 not differently expressed and 4 genes were downregulated). Similarly, 77 salt stress genes were downregulated by salt, with 30 genes were shared between two species. This included 9 upregulated, 5 downregulated and 16 not differentially regulated by salt in spinach. The full list of genes has been provided in Supplemental Table S6.4. At the top of this list there were genes encoding *inorganic pyrophosphatase 1 protein*, *AP2/B3-like transcriptional factor family protein*, *HSP20-like chaperones superfamily protein*, and *cystatin* with high expression in quinoa GCs at saline conditions (85-, 79-, 66 and 42-fold respectively). Overexpression of the *inorganic pyrophosphatase 1* was also observed in spinach GCs, although the expression was not high (8-fold) compared to that in quinoa (85-fold). *HSP20-like chaperones superfamily protein* which highly expressed in quinoa GC, was downregulated by salinity in spinach (Supplemental Table S6.4).

As it has been shown in a heatmap (Fig. 6.5), there were few genes that showed induction by salt stress in spinach but suppressed in quinoa. Among them,

peroxidase 27, *L-ascorbate peroxidase 5*, *L-ascorbate peroxidase 3* and *thioredoxin 2* genes are involved in oxidative stress. However, the other isoforms of genes encoding peroxidase superfamily protein (*AT5G05340, AT1G71695, AT5G05340*) were induced by salt in quinoa exclusively. In addition, both isoforms of *L-ascorbate peroxidase* (*APX3* and *APX5*) in quinoa were ranked in topmost 1% abundant transcripts indicating the inherent ability of quinoa in alleviating oxidative stress.

6.3.4.6 Transporters

Salt stress resulted in a differential expression of transporters in GCs of both species (Fig. 6.6 and Supplemental Table S6.5). There were 69 upregulated genes involved in various transporters (ions, lipid, proteins, sugar, and amino acids) in quinoa where 54 transporters were shared between quinoa and spinach which were mostly unaffected by salt stress. Nine transporters genes were upregulated in both species, including *potassium transporter 1* (*KT1*), *HCO3- transporter family* (*BOR4*), *lipid transfer protein 4* (*LTP4*), *lipid transfer protein 2* (*LTP2*) and *germin-like protein 10* (Fig. 6.6 and Supplemental Table S6.5).

Amino acid permease 1 (*AAP1*) and *nitrate transporter 1:2* (also called *ABA-importing transporter 1*) are highly expressed by salt in quinoa while they were downregulated in the spinach.

In quinoa, expression of *high affinity K^+ transporter 5* (*HAK5*) 18.6-fold, *K^+ inward-rectifying channel* (*AKT1*), 6.5-fold, *K^+ transporter 12* (*KT12*), 2-fold and *Trk system K^+ uptake protein* 3.4-fold increased by salinity, while *HAK17* was downregulated (-5.4-fold).

Moreover, salinity stress resulted in overexpression of several isoforms of ABC transporters, water channel (aquaporin), lipid, protein and amino acid transporters in both plants. Salinity also altered the expression of a number of nutrient transporters such as phosphate and nitrates in quinoa and spinach. It is important to highlight that for most transporter groups; higher gene modulation was taken place in quinoa GCs than spinach under salt stress (Fig. 6.6 and Supplemental Table S6.5).

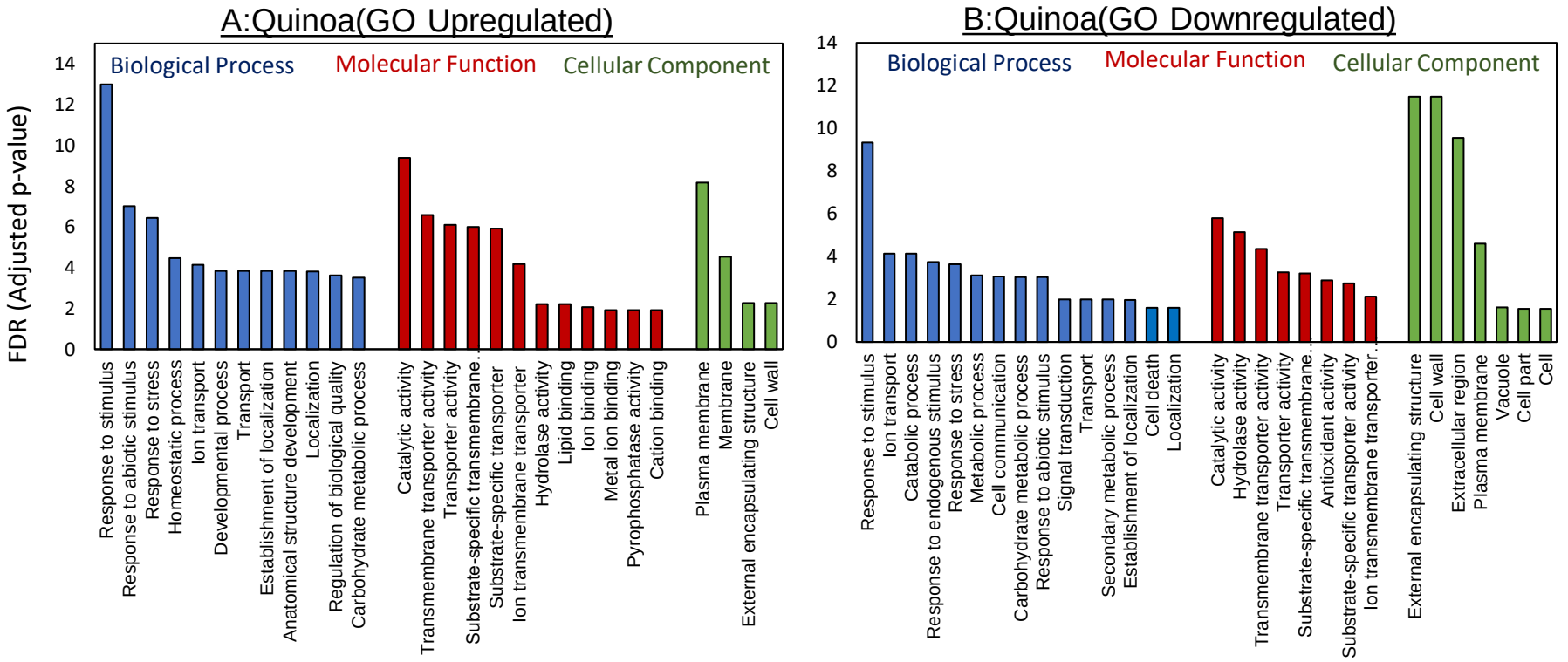
A:Quinoa(GO Upregulated)
FDR (Adjusted p-value)
Biological Process
Molecular Function
Cellular Component
Response to stimulus
Response to abiotic stimulus
Response to stress
Homeostatic process
Ion transport
Developmental process
Transport
Establishment of localization
Anatomical structure development
Localization
Regulation of biological quality
Carbohydrate metabolic process
Catalytic activity
Transmembrane transporter activity
Transporter activity
Substrate-specific transmembrane...
Substrate-specific transporter
Ion transmembrane transporter
Hydrolase activity
Lipid binding
Ion binding
Metal ion binding
Pyrophosphatase activity
Cation binding
Plasma membrane
Membrane
External encapsulating structure
Cell wall
B:Quinoa(GO Downregulated)
Biological Process
Molecular Function
Cellular Component
Response to stimulus
Ion transport
Catabolic process
Response to endogenous stimulus
Response to stress
Metabolic process
Cell communication
Carbohydrate metabolic process
Response to abiotic stimulus
Signal transduction
Transport
Secondary metabolic process
Establishment of localization
Cell death
Localization
Catalytic activity
Hydrolase activity
Transmembrane transporter activity
Transporter activity
Substrate-specific transmembrane...
Antioxidant activity
Substrate-specific transporter activity
Ion transmembrane transporter...
External encapsulating structure
Cell wall
Extracellular region
Plasma membrane
Vacuole
Cell part
Cell

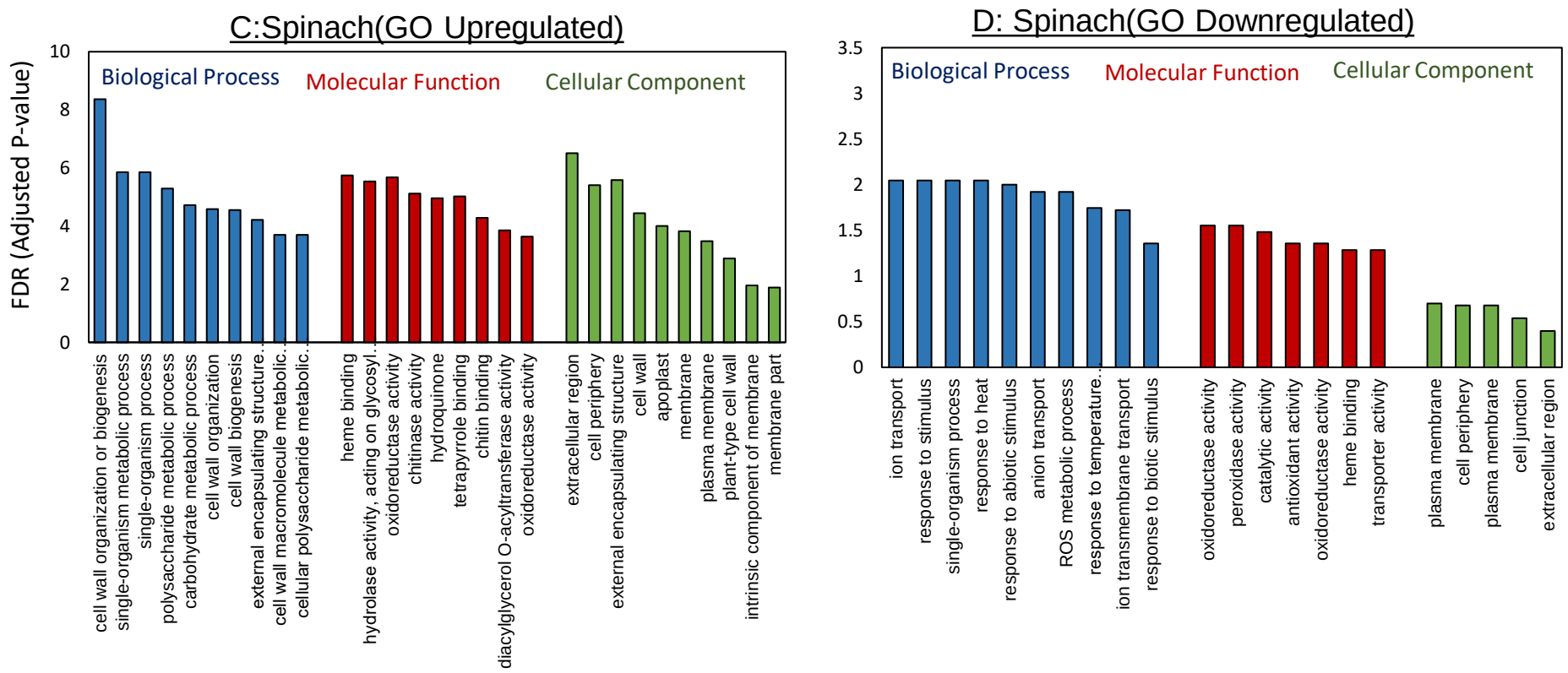

Fig. 6.4 Gene ontology enrichment differentially expressed genes by salt in quinoa (panels A and B) and spinach (panels C and D). In order to study the functions of differentially expressed genes, GO enrichment analysis for Biological Process, Molecular Function and Cellular Component for both upregulated and downregulated genes were performed with Agri GO software with significance threshold of FDR ≤ 0.05.

Table 6.4 The fold change of genes related to ABA biosynthesis and ABA responses in quinoa and spinach.

Gene	Quinoa GC	Spinach GC
Basic-leucine zipper (bZIP) transcription factor (ABI5)	**3.8**	**1.0**
Integrase-type DNA-binding superfamily (DREB2C)	**2.2**	**1.1**
MATE efflux family protein (FRD3)	**4.3**	**1.2**
Uridine diphosphate glycosyltransferase 74E2 (UGT74E2)	**2.6**	**1.3**
Alcohol dehydrogenase 1 (ADH1)	**3.7**	**3.4**
Annexin 4 (ANNAT4)	**6.1**	**1.9**
Galactinol synthase 2 (GolS2)	**4.8**	**0.9**
Homeobox 7 (HB-7)	**4.7**	**1.1**
Lipid transfer protein 3 (LTP3)	**28.4**	**2.1**
Lipid transfer protein 4 (LTP4)	**8.9**	**3.0**
Lipoxygenase 1 (LOX1)	**2.5**	**1.2**
White-brown complex-like protein (ABCG11)	**4.6**	**1.1**
Cellulose synthase family protein (IRX1)	**3.4**	**3.4**
Nine-cis-epoxycarotenoid dioxygenase 5 (NCED5)	**3.8**	**0.9**
Regulatory component of ABA receptor 1 (RCAR1)	**-2.0**	**0.9**
Leucine-rich receptor-like (GHR1)	**-2.0**	**-2.1**
Glycosyl hydrolase family protein with chitinase (ChiC)	**-2.1**	**2.7**
Aldehyde dehydrogenase 7B4 (ALDH7B4)	**-2.1**	**1.1**
ABC-2 and Plant PDR ABC-type transporter (PEN3)	**-2.2**	**1.1**
GAST1 protein homolog 1 (GASA1)	**-2.5**	**1.0**
Calcium-dependent protein kinase 29 (CPK29)	**-2.5**	**1.6**
Dehydrin xero 1 (XERO1)	**-2.7**	**1.0**
GRAS family transcription factor (GAI)	**-6.2**	**0.9**
PYR1-like 4 (PYL4)	**-3.7**	**1.0**
Highly ABA-induced PP2C protein 2	**2.3**	**1.4**
PEBP (phosphatidylethanolamine-binding protein)	**39.0**	**1.9**
G protein coupled receptor	**2.3**	**0.69**
Leucine-rich repeat protein kinase family protein	**2.2**	**0.93**
Regulatory component of ABA receptor 1	**-2.0**	**0.9**
Polyketide cyclase/dehydrase and lipid transport	**-2.6**	**0.9**
Calcium-dependent protein kinase 4	**-4.2**	**0.92**
Leucine-rich receptor-like protein kinase family protein	**-2.0**	**-2.2**
Duplicated homeodomain-like superfamily protein	**-2.1**	**1.6**
Zinc finger protein 7	**-17.5**	**0.85**
Calcium-dependent protein kinase 29	**-2.4**	**1.6**

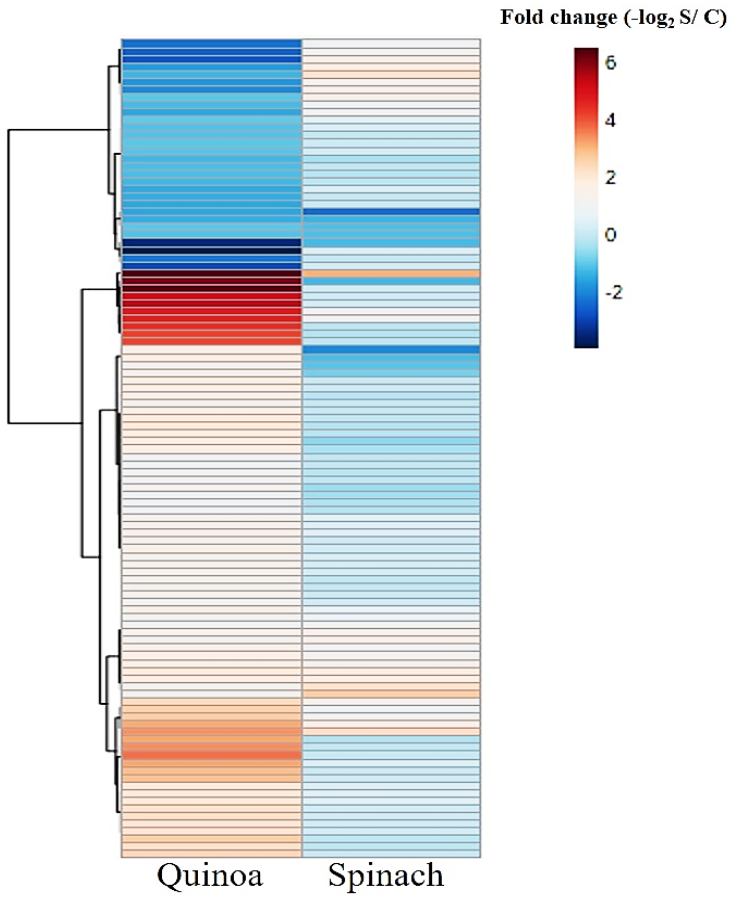

Fig. 6.5 Heatmap showing the mean fold changes (average of 3-4 replicates) of genes involved in "stress" in response to 250 mM salt treatment in quinoa and spinach.

6.3.4.7 Cell wall modification

In spinach, the most enriched GO term in biological process classification for upregulated genes was "cell wall organization" (Supplementary Table S6.3). This GO term contained 39 genes with expression levels between 9.5 and 2-fold higher than control conditions. This GO term in quinoa included 13 genes which 8 of them were common between two species. A total of 9 genes related to cell wall were downregulated in quinoa while none was observed in spinach (Fig. 6.7). Out of 39 upregulated genes in spinach, 10 genes directly were involved in cell wall thickening, cellulose synthase and lignin catabolic process which all could be resulted in stiffness of guard cell wall. To cope with various type of stresses, some species utilise a strategy that consists of reinforcing the cell wall specially secondary cell wall thickening by synthesising cellulose and hemicellulose (Le Gall *et al.* 2015). This process might be linked to a rigidification of the cell wall through

deposition of lignin. In this study, genes encoding laccase/diphenol oxidase family proteins which is involved in lignin synthesis highly upregulated by salt in spinach GCs (9-fold in spinach versus 2-fold in quinoa) (Fig. 6.7). In contrast, in quinoa guard cell *pectin methylesterase* gene which can confer plasticity to cell wall, increased under salt stress by 42-fold.

6.3.4.8 Stomatal development

The results revealed 33 and 37 genes were associated with stomatal development GO in quinoa and spinach (Table 6.3). Among them, 5 genes negatively regulate stomatal complex development including *putative membrane lipoprotein* (*EPF2*), *subtilisin-like serine endopeptidase family protein* (*ATSBT5.2*), *allergen-like protein* (*CHAL*), *carbonic anhydrase 1* (*CA1*) and *epidermal patterning factor 1* (*EPF1*). *CHAL* is similar in sequence to the putative stomatal ligands *EPF1* and *EPF2* and, like the *EPFs*, can reduce or eliminate stomatal production when overexpressed (Abrash and Bergmann 2010). In this study, two genes out of 5 genes responsible for negative regulation of stomatal complex development were induced by salt stress in quinoa (the genes encoding allergen-like protein (*CHAL*) and *EPF1* secreted peptide) while it did not alter in spinach GCs (Fig. 6.8), suggesting that salinity play a role in hampering the formation of stomata in epidermal tissue in quinoa which could confer salt tolerance to plants under limited water availability through reducing transpiration rate.

6.3.5 Validation of the DEGs using RT-qPCR

In order to validate the RNA-sequencing data and to check whether transcriptome data is reproducible, real-time RT-qPCR was performed for 20 differentially expressed genes (Fig. 6.9). Some genes mostly involved in salt stress were selected for this aim. For each gene, the results from RNA-sequencing data were consistent with RT-qPCR analysis, except for *PYR1-like*, a gene that encodes an ABA receptor protein, that was suppressed in RNA-sequencing data while it was weakly induced by salinity in RT-qPCR analysis.

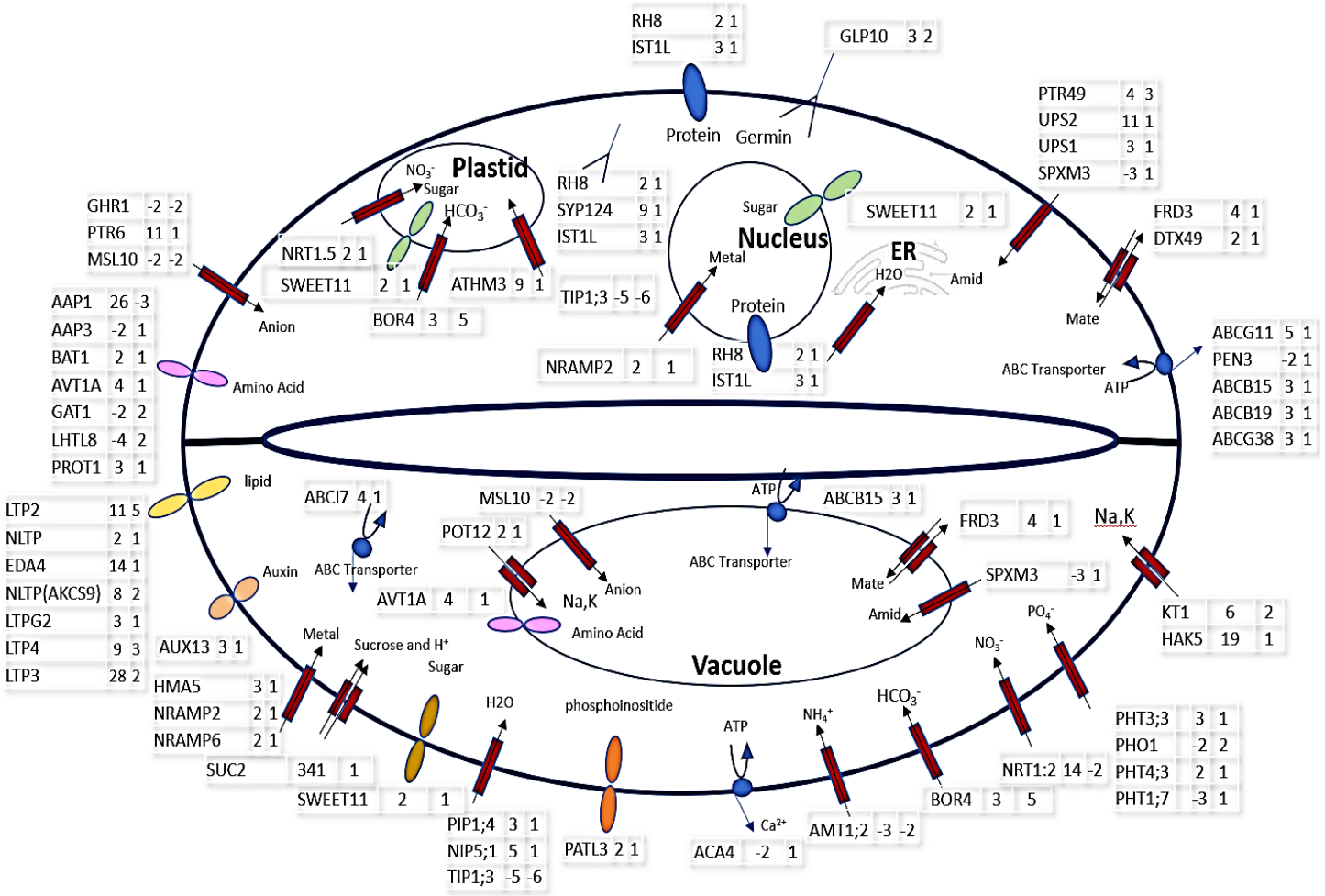

Fig. 6.6 Differentially expressed genes under salinity stress involved in transportation in quinoa and spinach guard cells. The first column is the gene name; the second and third column represent expression values of genes in quinoa and spinach guard cells, respectively. A minus sign of expression value denotes down regulated genes by salt stress.

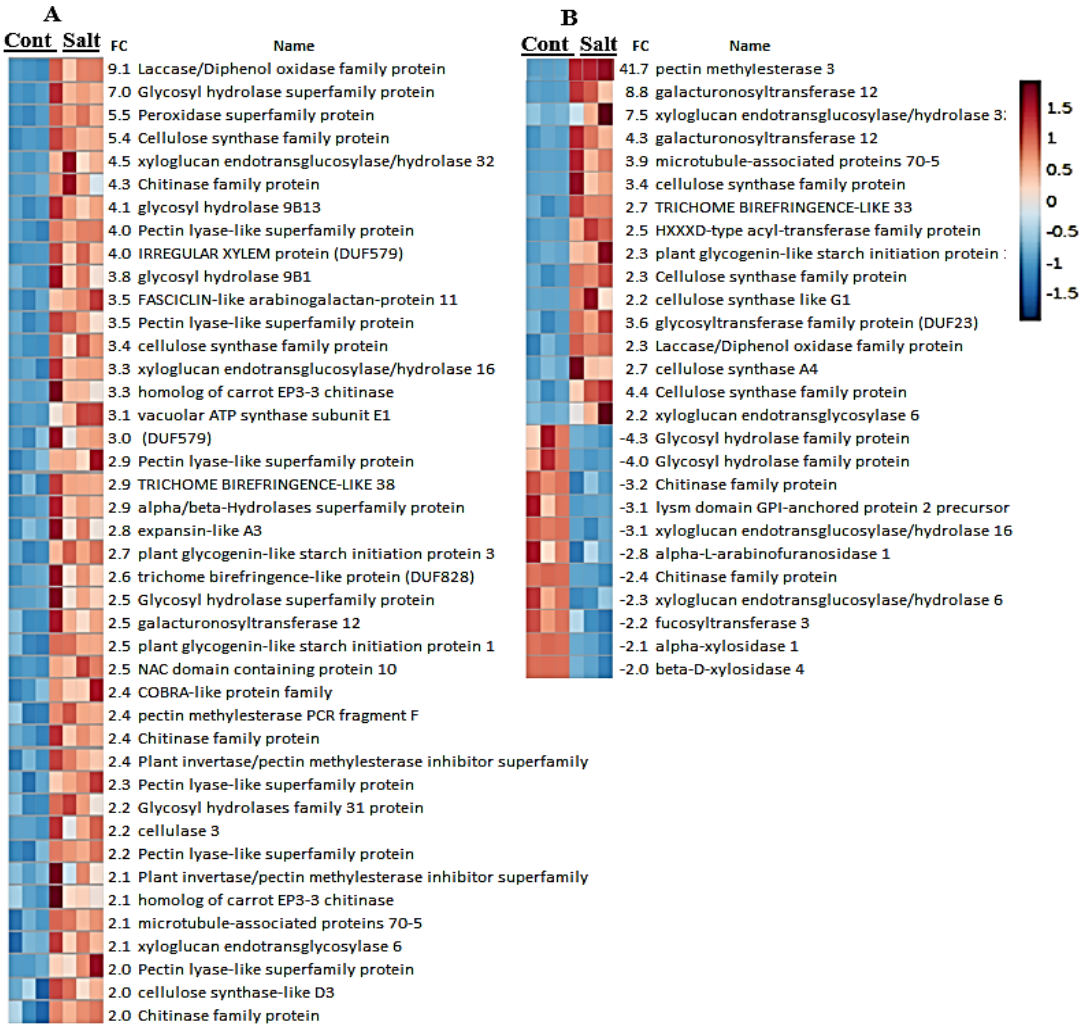

Fig. 6.7 Heatmap analysis of genes involved in guard cell walls in response to 250 mM salt treatment for 39 genes in spinach (Heatmap A) and for 27 genes in quinoa (Heatmap B). The values in the heatmap reflects the fold change of that gene. Negative value shows gene suppression by salinity treatment. FC-fold change; Cont-control conditions

6.3.6. Cell wall rigidity assay

To confirm the effect of salinity in cell wall rigidity in spinach and quinoa, a combination of digestive enzymes was used for dissolving cell wall compositions (Fig. 6.10) and then the time required for 90% digestion of GC walls was recorded. The results revealed that under salt stress conditions, the digestion time for spinach guard cell walls was 24% longer than that for quinoa suggesting the increased cell wall strength in response to salt treatment in spinach.

In the next step, to investigate how the stiffness of guard cell wall affect the dynamics of stomata, modulation of stomatal conductance by light and dark was

monitored in intact leaf in both species grown under saline (Fig. 6.11). Stomatal movements in response to light and darkness followed similar patterns in quinoa and spinach, increasing with the onset of illumination and reaching a maximum value, and then started to decline with darkening of plants and reaching a minimum value.

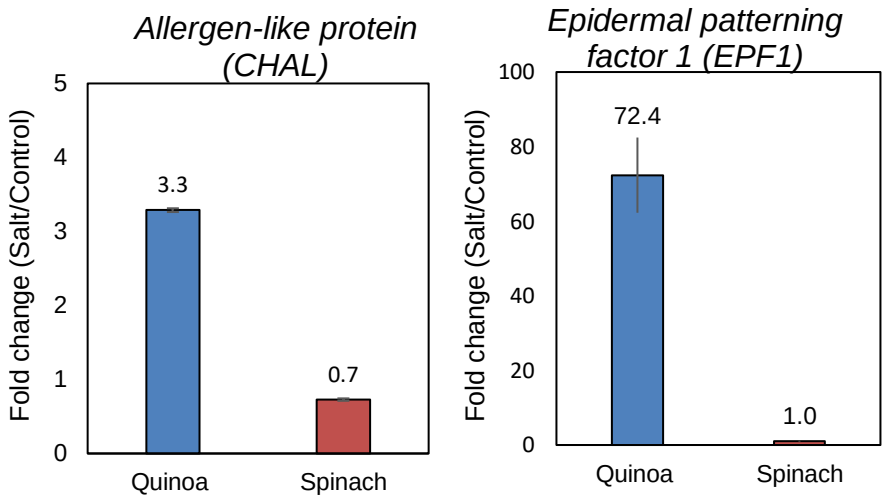

Fig. 6.8 Fold changes of two genes involved in stomatal development in quinoa and spinach guard cell under 250 mM salt stress. Fold changes were calculated by dividing the salt-stress FPKM value by the control value.

6.3.7. Stomatal density and transpiration

In the current study in order to explore the phenotype of *CHAL* and *EPF1* overexpressed in GC of quinoa, stomatal density and transpiration rate were measured under control and salt stress conditions. The results revealed that quinoa had few stomata numbers on leaf epidermis when exposed to salinity treatment while the number of stomata in the epidermal layer of spinach leaf increased under 250 mM salt treatment (Figures 6.12 and 6.13). In addition, lower stomatal index in salt-treated quinoa sample also confirmed that fewer stomata were developed in salt-stressed quinoa. On the contrary, the stomatal index in spinach was not affected by salinity suggesting that stomatal formation and differentiation were not influenced by salt treatment in this species and the increase in the frequency of stomata could be related to smaller-leaf phenotype due to ionic and osmotic effects of salt stress.

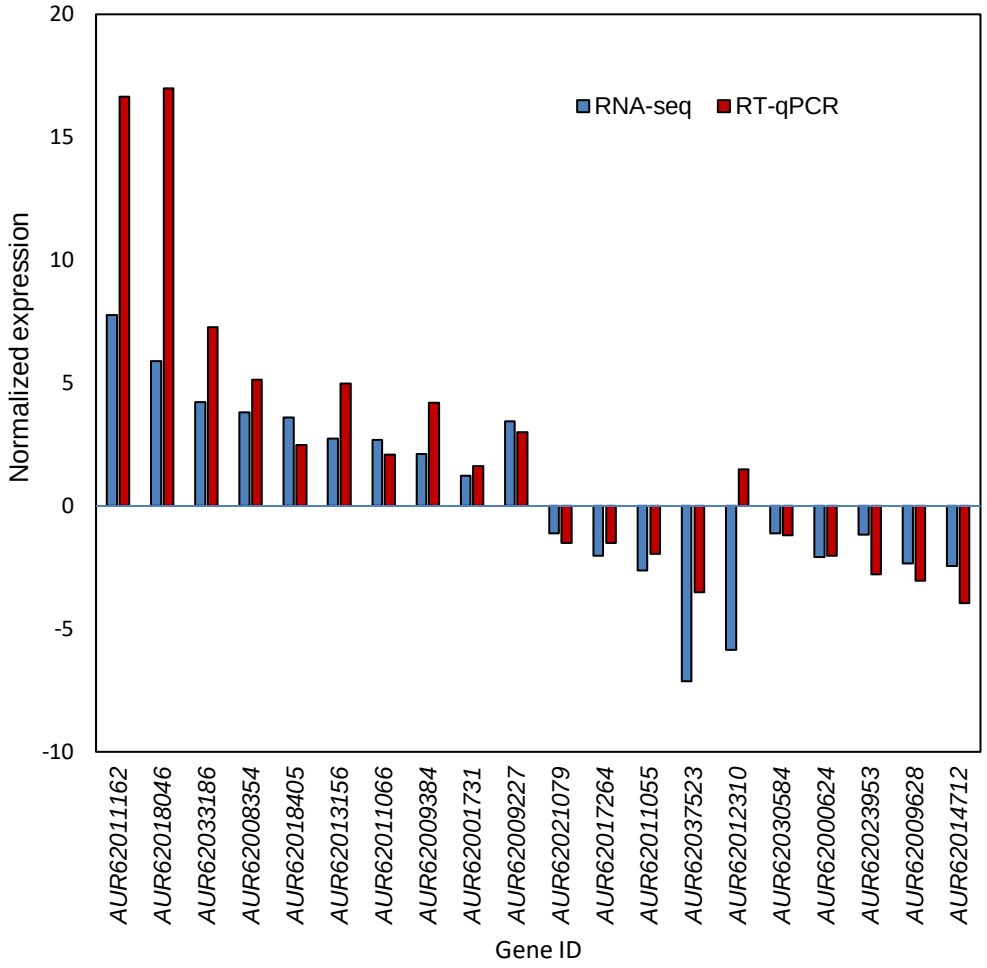

Fig. 6.9 Validation of RNA-sequencing results by RT-qPCR. The log_2-fold-changes and mean normalized expression were calculated from RNA- sequencing data and RT-qPCR analysis respectively. *AUR62011162-epidermal patterning factor 1; AUR62018046-cystatin B; AUR62033186- high affinity K^+ transporter 5*; *AUR62008354-nitrate transporter 1:2*; *AUR62018405-zinc transporter 7 precursor*; *AUR62013156-white-brown complex-like protein*; *AUR62011066-K^+ transporter 1*; *AUR62009384-MATE efflux family protein*; AUR62001731-*highly ABA-induced PP2C protein 2*; *AUR62009227-kinase (leucine-rich repeat domain-containing protein)*; *AUR62021079-SLAC1*; *AUR62017264-osmotin 34*; *AUR62011055-GRAS family transcription factor family protein*; *AUR62037523-AMP-dependent synthetase*; *AUR62012310-PYR1-like 4*; *AUR62030584-serine/threonine protein kinase 2*; *AUR62000624- calcium-dependent protein kinase4*; *AUR62023953- GABA transporter 1-like*; *AUR62009628- tonoplast intrinsic protein*; *AUR62014712- sugar transporter 1*.

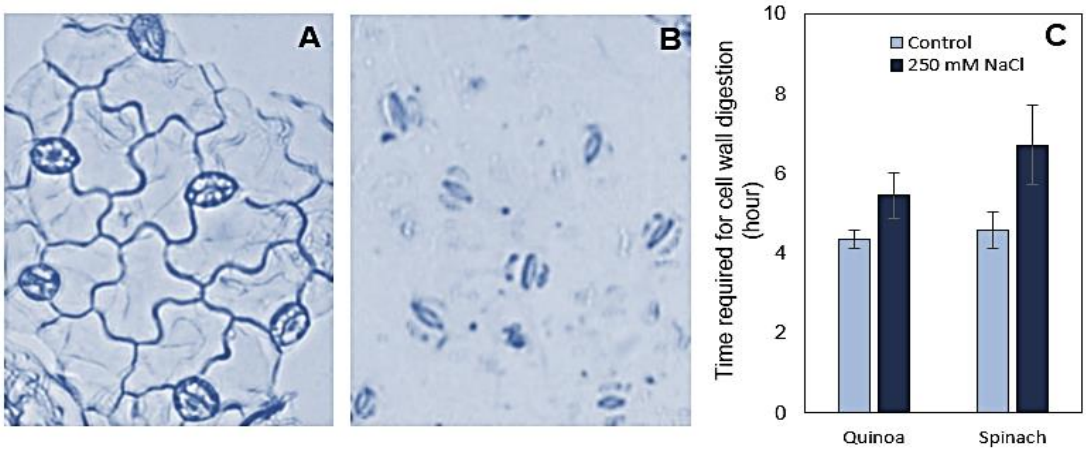

Fig. 6.10 Digestion of cell walls in epidermal strip. Epidermal strip before digestion (A) and after digestion (B), using solution containing 1 % Cellulase R-10, and 0.04 % Macerozyme R-10, 1.1 % (w/v) Onozuka RS cellulase, and 0.03 % (w/v) Pectolyase Y-23. Time required for cell wall digestion for both species under control and salt stressed condition (C).

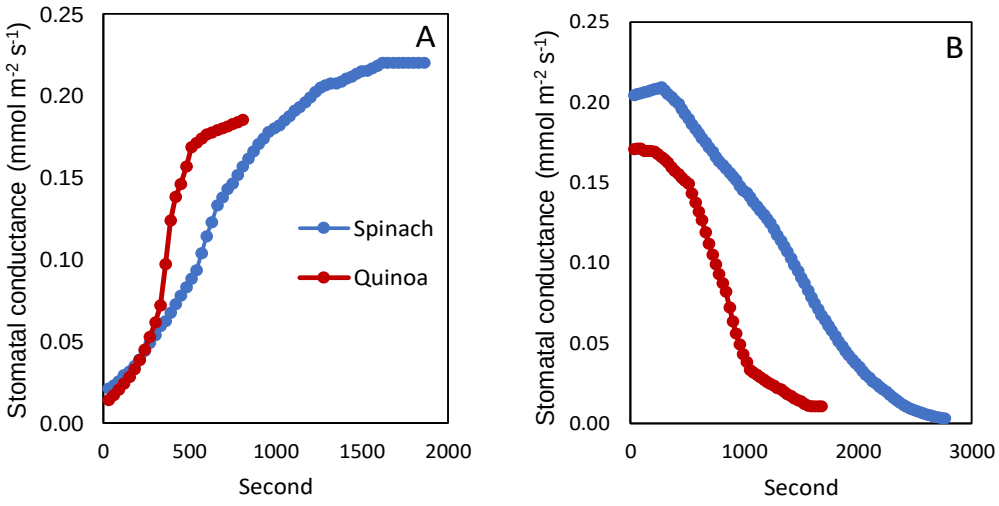

Fig. 6.11 Time-series of stomatal opening (A) and closure (B) in response to illumination and darkening in quinoa and spinach under salt conditions.

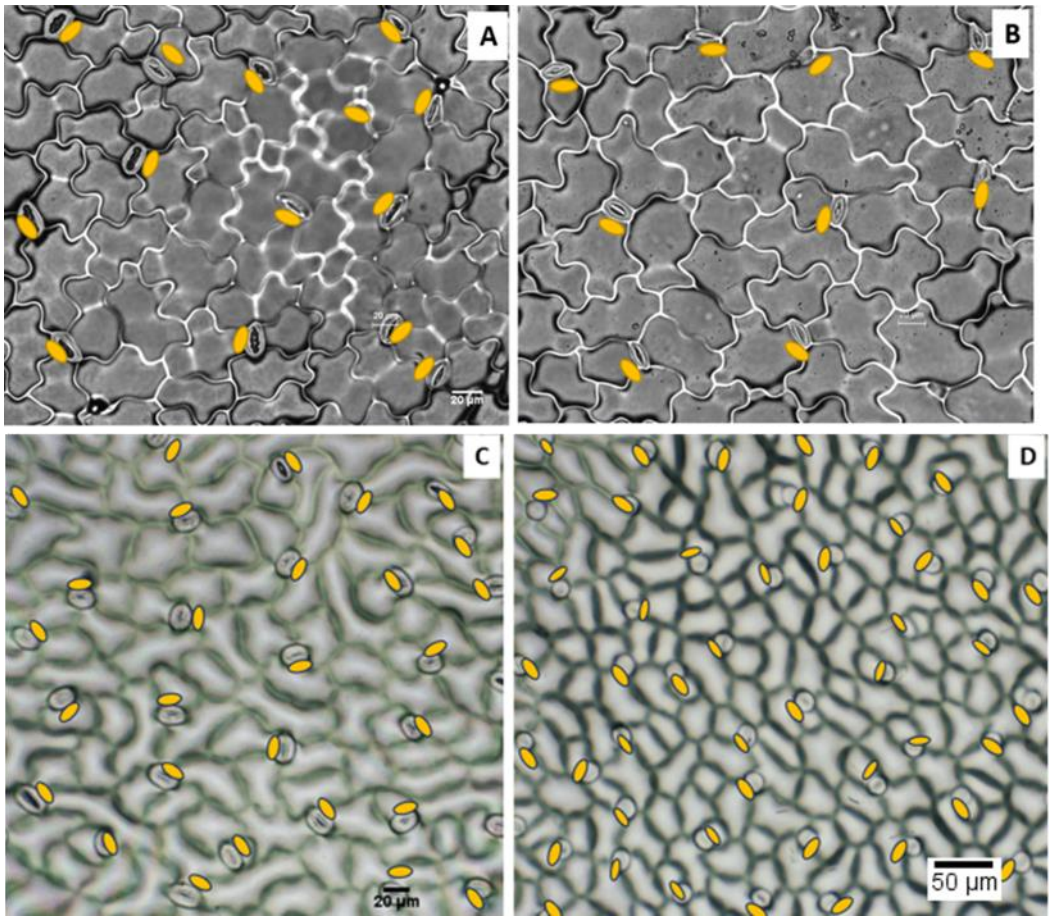

Fig. 6.12 Stomatal size and density in the abaxial leaf surface of quinoa (A and B) and spinach (C and D) grown under non-stress (A and C) and saline conditions (B and D). The yellow ellipses mark the location of stomatal in the epidermis.

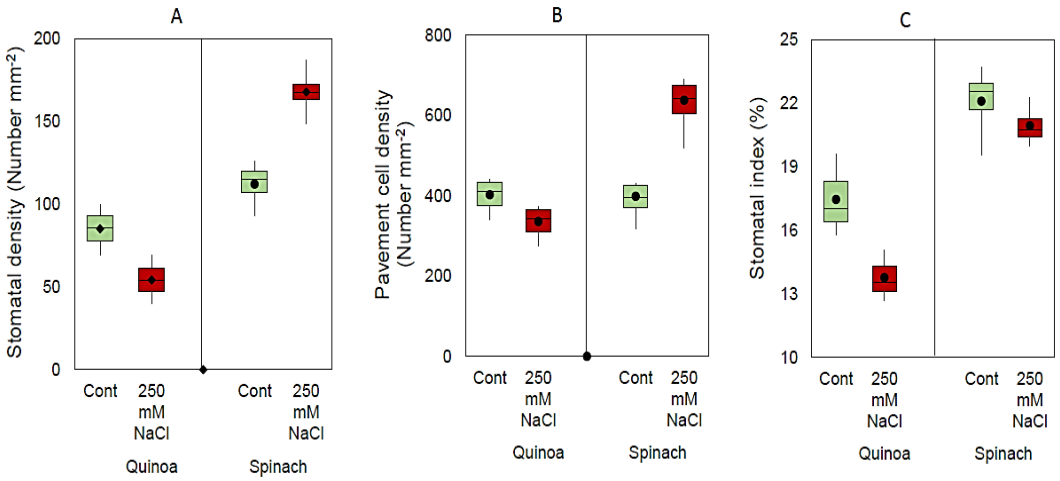

Fig. 6.13 Stomatal density (A), pavement density (B) and stomatal index (C) in quinoa and spinach under control and salt-stressed condition.

In this study, a reduction in a number of stomata was reflected in the reduced transpiration rate measured using a gas exchange system and thermal infrared thermography (Fig. 6.14). Transpiration values obtained from salt-treated plants demonstrated that the maximum water loss through transpiration was much greater in spinach than quinoa (Fig. 6.14).

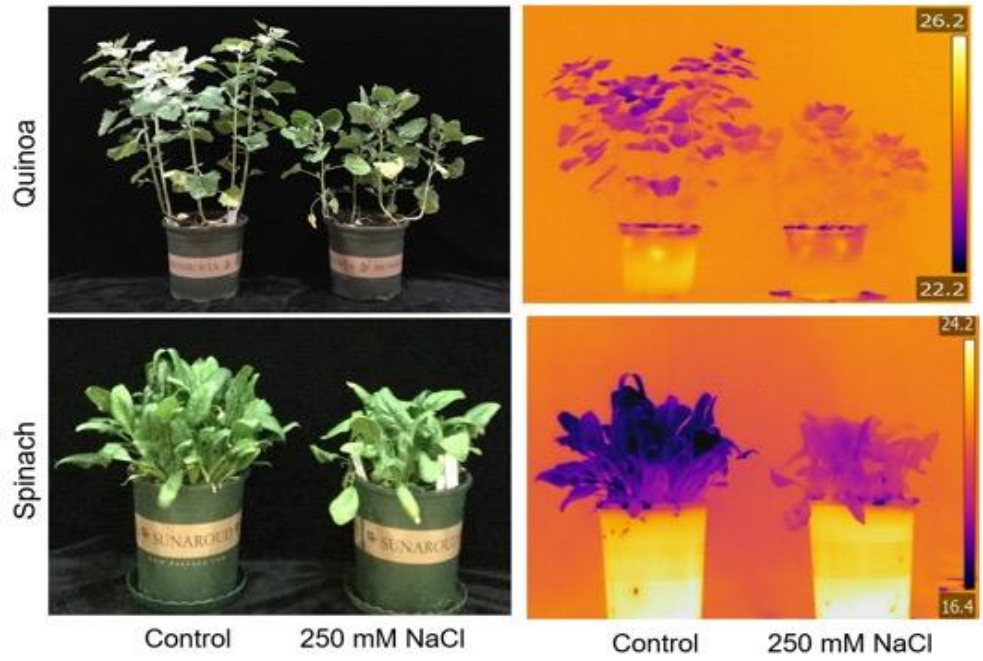

Fig. 6.14 Transpiration rate of quinoa and spinach plants grown under control and 250 mM NaCl for three weeks. Imaging using a normal camera (left panels) and thermal imaging using infrared thermography (right panels). The colour scale shows the change in leaf temperature based on the rate of transpiration ranging from coolest (dark blue) to the warmest (yellow). Both species showed cooler temperature in control conditions however the cool colour in spinach leaf reflected higher rates of evaporative cooling in both control and salt-treated plants as compared to quinoa.

6.4 Discussion

In the present study, the GCs response to salt stress of quinoa as a halophyte and spinach as a glycophyte were evaluated after three weeks of 250 mM NaCl to identify the adaptive responses to salt stress based on transcriptome characterizations. The results showed some dissimilarity in GCs responses to salt stress between quinoa and spinach and the three most pronounced differences between these plants are discussed in the following sections.

6.4.1 More salt-responsive genes are differentially expressed in quinoa GCs than spinach after salt stress induction

Salt stress affected more genes in GCs of quinoa than spinach. For instance, *enzyme pyrophosphatase* (*PPase*) was the most highly up-regulated gene (in stress category) under salt treatment in quinoa; however, in spinach GCs it was manifested at much lower expression level. *PPase* is essential for ion transportation in GCs as it is able to energize the vacuolar membrane for transporting proton across the membrane and knock-out mutant of this gene was accompanied with high susceptibility to drought stress because of delay in stomatal closure (Asaoka *et al.* 2019a).

Amino acid permease 1 (*AAP1*) was highly expressed in quinoa GCs but supressed in spinach. This transporter functions in the uptake of neutral amino acids including proline. Higher accumulation of proline in the cell was correlated with significantly increased expression of *AAP1* (Wang *et al.* 2017). Enhancement of *AAP1* might indicate that more *AAP1* is expressed in the plasma membrane of quinoa GCs to promote proline transport in response to salinity treatment. *NRT1.2*, an ABA importer, showed a 14-fold increase in quinoa with decreased expression level in spinach GCs in response to salt stress. Overexpression of *NRT1.2* resulted in hypersensitivity to exogenous ABA (Kanno *et al.* 2012) while the loss of function of this gene led to excessive transpiration and water loss from open stomata (Kanno *et al.* 2012). This result was confirmed through physiological data where salt-treated spinach plants demonstrated a high rate of transpiration compared to that in quinoa (Fig. 6.14).

Surprisingly, in this study, a member of the inward rectifying potassium channel homolog of the *AKT1* in Arabidopsis was overexpressed in quinoa GCs when plant exposed to salt stress (Fig. 6.6 and Supplemental Table S6.5). Increased expression of *AKT1* in other cell-type than GCs such as root is associated with increased tolerance to desiccation stress (Adrian *et al.* 2015a). However, in the GCs it has been described that *AKT1* activity is down-regulated after ABA exposure, leading to stomatal closure (Leyman *et al.* 1999). Lower water consumption and transpiration rate occurred in *akt1* knock-out mutants, which improved plant response to water stress (Nieves-Cordones *et al.* 2012). Thus, overexpression of *AKT1* in the guard cells in our study may result in higher stomatal conductance and

rate of transpiration under salt stress in quinoa, while our physiological measurements on stomatal conductance and thermal images (Fig. 6.14) proved that less transpiration has occurred in salt-stressed plants. This could be explained by the implication of other signaling molecules that might make the role of this AKT1 pathway much more complex (Nieves-Cordones *et al.* 2012).

Sugars (and, specifically, sucrose) act as a signaling molecule within GCs supporting stomatal closure. In this RNA-seq study, *sucrose transporter* (*SUC3*), which is a guard cell-specific gene, was extremely (340-fold) upregulated by salt in quinoa (Fig. 6.6 and Supplemental Table S6.5). Sugars initiate an ABA pathway that involves the generation of H_2O_2 and NO, consequently inducing stomatal closure (Granot and Kelly 2019). It is important to highlight that sucrose degradation is necessary in both stomatal opening and closure. Daloso and co-workers (Daloso *et al.* 2016b) used isotope techniques to show that during the light-induced stomatal opening, sucrose is broken down and contributed to energy production for stomatal opening. Collectively, the effect of sucrose on stomatal opening or closure depends on environmental factors that affect GC sucrose content and leaf photosynthetic rate (Daloso *et al.* 2016a) and can diminish the effect of upregulated *AKT1* in stomatal opening.

Upregulation of *AKT1 channel* and other potassium transporter genes in response to salt stress in quinoa may be attributed to the essential role of potassium in osmoregulation of GCs in this plant. In quinoa, potassium accumulation in the leaf is correlated with sodium uptake (Kiani-Pouya *et al.* 2019a) suggesting that the presence of Na^+ ions in GC apoplast may stimulate K^+ transporters to take up and accumulate potassium for osmoregulation from a solution containing unfavourable K^+/Na^+ ratio. The significant involvement of potassium transporters in an osmotic adjustment under water and salt stress conditions has been noted in plants and bacteria (Epstein 1986; Li *et al.* 2018b).

In the current study transcript abundance for some genes such as ABA receptor *PYR1-like 4* (*PYL4*) were decreased in salt-grown plants compared to non-stressed quinoa plants (Table 6.4). Downregulation of ABA receptors has been observed in glycophytes (Bauer *et al.* 2013) and halophytes (Ruiz et al., 2019). For example, the down-regulation of ABA receptors in quinoa root and shoot has been reported in an RNA-seq analysis in response to 300 mM NaCl (Ruiz *et al.* 2019).

However, that study did not confirm the results by RT-qPCR. Given that ABA content of halophytes does not change dramatically in response to salt stress (Hedrich and Shabala 2018), it is likely that ABA receptors also remain unchanged.

6.4.2 Cell wall of quinoa was more flexible than spinach in response to salt stress

The bio-mechanical functionality of stomatal highly depends on the nature of guard cell walls (Marom *et al.* 2017). The wall of guard cell needs to be mechanically reinforced to withstand a high tensile strength during turgor pressure and, at the same time, be flexible and extensible to ease stomatal closure. Under saline conditions, the cell walls may stiffen with various degrees depending on species and variety tolerance to salinity. Salt-sensitive species develop a more rigid cell wall compared with salt-tolerant species which may develop a more flexible cell wall under salt stress (Zörb *et al.* 2015).

In this study, many genes related to cell wall stiffness including cellulose and lignin synthesis and peroxidase were induced by salinity in spinach suggesting that GCs where exposure to salt stress caused cell wall tightening in this plant (Fig. 6.10). In quinoa the number of cell wall related genes especially genes responsible for cell wall stiffness is lower than that in spinach and they showed weaker salt-induced increases compared to spinach. Although increasing the cell wall strength is essential under salt stress conditions, the balance between extensibility and strength need to be supported for the well-functioning of the stomata under salt stress.

Several studies have shown that the increase in peroxidase activity was associated with stiffness of the cell wall (Lin and Kao 2002). Cell wall peroxidases mitigate the impact of excess ROS by scavenging hydrogen peroxide molecules to polymerize lignin (Fotopoulos *et al.* 2010). In this case, the transcript levels of cell wall peroxidases gene in spinach increased by 5.5-fold under salt stress.

Cell wall plasticity can be controlled by cell wall-modifying enzymes such as *pectin methylesterase (PME), polygalacturonase, pectin lyase-like* and *pectin acetylesterase* (Le Gall *et al.* 2015). This is consistent with reported 42-fold upregulation of *pectin methylesterase* gene increased in quinoa GCs under salt stress (Fig. 6.7B).

The results also proved that the speed of stomatal opening and closure in both illumination and darkening phases in quinoa were higher compared to spinach

(Fig. 6.11). Fast stomatal responses to environmental cues enable plants to cope with natural dynamic environments and provide superiority with respect to the prevention of losing water and CO_2 uptake (Kubarsepp *et al.* 2020).

Relatively poor sensitivity of stomata to rapid reaction to environmental stimuli such as light and dark conditions can be attributed to less flexibility of the guard cell wall induced by salt stress in spinach.

6.4.3 Quinoa had lower stomatal conductance than spinach under salt stress

As it has been shown in Figure 6.8, *CHAL* and *EPF1* genes were highly induced by salt stress in quinoa but not in spinach. These two genes can effectively control the frequency of stomatal patterning. In barley overexpression of *EPF1* limited the progress of the stomatal formation pathway and reduces stomatal density and leaf gas exchange with no reductions in grain yield (Hughes *et al.* 2017).

Reductions in stomatal density could potentially constrain stomatal conductance and transpiration rate, suggesting a transition to a higher water use efficiency strategy. This mechanism represents an advantage under scenarios of limited water availability if there would be no reduction in the uptake of CO_2 and no penalty in grain yields (Bertolino *et al.* 2019). Decreasing in the stomatal frequency in rice was also associated with maintaining plant productivity (Caine *et al.* 2019). Furthermore, overexpression of *EPF2* in Arabidopsis resulted in reducing stomatal density and maximum stomatal conductance without a significant decline in photosynthetic capacity (Franks *et al.* 2015).

It has been experimentally proved that there is a high correlation between leaf temperature and measurements of stomatal conductance (Qi *et al.* 2018; Yaaran *et al.* 2019). Thus, leaf temperature measurements can be used as an indication of stomatal movements in response to various types of stresses. In the current study, thermal imaging analysis showed that the temperature of quinoa leaf especially under salt stress was higher than those in spinach leaf suggesting that the lower number of stomata resulted in lower stomatal conductance and transpiration rate (Fig. 6.14). This could be beneficial for plants grown under saline conditions, as it might slow down the rate of salt intake from the root media driven by a high transpiration rate. Altogether, reducing stomatal density in quinoa in response to salt treatment can confer enhanced tolerance to plant when subjected to salt stress.

6.5 Conclusion

A comparative RNA-sequencing analysis of quinoa and spinach GCs revealed that the superior ability of quinoa to salt stress as GCs level was obtained through higher salt-adaptability in this halophytic plant. The investigation revealed that quinoa had more salt-responsive genes differentially expressed in GCs than spinach when exposed to salt stress. Also, higher flexibility of cell wall in quinoa than spinach in response to salt stress enables quinoa to have faster stomatal movement and function more efficiently under fluctuating environmental conditions.

6.6 References

Abrash, EB, Bergmann, DC (2010) Regional specification of stomatal production by the putative ligand CHALLAH. *Development* **137**, 447-55.

Adolf, VI, Jacobsen, S-E, Shabala, S (2013) Salt tolerance mechanisms in quinoa (*Chenopodium quinoa* Willd.). *Environmental and Experimental Botany* **92**, 43-54.

Adrian, J, Chang, J, Ballenger, CE, Bargmann, BO, Alassimone, J, Davies, KA, Lau, OS, Matos, JL, Hachez, C, Lanctot, A, Vaten, A, Birnbaum, KD, Bergmann, DC (2015a) Transcriptome dynamics of the stomatal lineage: birth, amplification, and termination of a self-renewing population. *Dev Cell* **33**, 107-18.

Angeli, V, Miguel Silva, P, Crispim Massuela, D, Khan, MW, Hamar, A, Khajehei, F, Graeff-Honninger, S, Piatti, C (2020) Quinoa (*Chenopodium quinoa* Willd.): an overview of the potentials of the "golden grain" and socio-economic and environmental aspects of its cultivation and marketization. *Foods* **9**, 216.

Asaoka, M, Inoue, SI, Gunji, S, Kinoshita, T, Maeshima, M, Tsukaya, H, Ferjani, A (2019) Excess pyrophosphate within guard cells delays stomatal closure. *Plant and Cell Physiology* **60**, 875-887.

Atzori, G, de Vos, AC, van Rijsselberghe, M, Vignolini, P, Rozema, J, Mancuso, S, van Bodegom, PM (2017) Effects of increased seawater salinity irrigation on growth and quality of the edible halophyte *Mesembryanthemum crystallinum* L. under field conditions. *Agricultural Water Management* **187**, 37-46.

Bates, GW, Rosenthal, DM, Sun, J, Chattopadhyay, M, Peffer, E, Yang, J, Ort, DR, Jones, AM (2012) A comparative study of the *Arabidopsis thaliana* guard-cell transcriptome and its modulation by sucrose. *PLoS One* **7**, e49641.

Bauer, H, Ache, P, Lautner, S, Fromm, J, Hartung, W, Al-Rasheid, KAS, Sonnewald, S, Sonnewald, U, Kneitz, S, Lachmann, N, Mendel, RR, Bittner, F, Hetherington, AM, Hedrich, R (2013) The stomatal response to reduced relative humidity requires guard cell-autonomous ABA synthesis. *Current Biology* **23**, 53-57.

Bertolino, LT, Caine, RS, Gray, JE (2019) Impact of stomatal density and morphology on water-use efficiency in a changing world. *Frontiers in Plant Science* **10**, 225.

Butcher, K, Wick, AF, DeSutter, T, Chatterjee, A, Harmon, J (2016) Soil salinity: a threat to global food security. *Agronomy Journal* **108**, 2189-2200.

Caine, RS, Yin, X, Sloan, J, Harrison, EL, Mohammed, U, Fulton, T, et al. (2019) Rice with reduced stomatal density conserves water and has improved drought tolerance under future climate conditions. *New Phytologist* ***221,*** 371-84.

Daloso, DM, Dos Anjos, L, Fernie, AR (2016a) Roles of sucrose in guard cell regulation. *New Phytologist* **211**, 809-18.

Daloso, DM, Williams, TCR, Antunes, WC, Pinheiro, DP, Muller, C, Loureiro, ME, Fernie, AR (2016b) Guard cell-specific upregulation of sucrose synthase 3 reveals that the role of sucrose in stomatal function is primarily energetic. *New Phytologist* **209**, 1470-83.

Diray-Arce, J, Gul, B, Khan, MA, Nielsen, B (2016) Halophyte transcriptomics. In *Halophytes for Food Security in Dry Lands.* (Elsevier Inc.)

Epstein, W (1986) Osmoregulation by potassium transport in *Escherichia coli*. *FEMS Microbiology Reviews* **39**, 73-78.

Fotopoulos, V, Ziogas, V, Tanou, G, Molassiotis, A (2010) Involvement of AsA/DHA and GSH/GSSG ratios in gene and protein expression and in the activation of defence mechanisms under abiotic stress conditions. In *Ascorbate-glutathione pathway and stress tolerance in plants* (Springer Netherlands: Dordrecht)

Franks, PJ, T, WD-A, Britton-Harper, ZJ, Gray, JE (2015) Increasing water-use efficiency directly through genetic manipulation of stomatal density. *New Phytologist* **207**, 188-95.

Frey, A, Effroy, D, Lefebvre, V, Seo, M, Perreau, F, Berger, A, Sechet, J, To, A, North, HM, Marion-Poll, A (2012) Epoxycarotenoid cleavage by NCED5 fine-tunes ABA accumulation and affects seed dormancy and drought tolerance with other NCED family members. *The Plant Journal* **70**, 501-12.

Gharat, SA, Parmar, S, Tambat, S, Vasudevan, M, Shaw, BP (2016) Transcriptome analysis of the response to NaCl in *Suaeda maritima* provides an insight into salt tolerance mechanisms in halophytes. *PLoS One* **11**, e0163485.

Granot, D, Kelly, G (2019) Evolution of guard-cell theories: the story of sugars. *Trends in Plant Science* **24**, 507-518.

Hariadi, Y, Marandon, K, Tian, Y, Jacobsen, SE, Shabala, S (2011) Ionic and osmotic relations in quinoa (*Chenopodium quinoa* Willd.) plants grown at various salinity levels. *Journal of Experimental Botany* **62**, 185-93.

Hedrich, R, Shabala, S (2018) Stomata in a saline world. *Current Opinion in Plant Biology* **46**, 87-95.

Hetherington, AM, Woodward, FI (2003) The role of stomata in sensing and driving environmental change. *Nature* **424**, 901-8.

Huang, J, Lu, X, Yan, H, Chen, S, Zhang, W, Huang, R, Zheng, Y (2012) Transcriptome characterization and sequencing-based identification of salt-responsive genes in *Millettia pinnata*, a semi-mangrove plant. *DNA Research* **19**, 195-207.

Hughes, J, Hepworth, C, Dutton, C, Dunn, JA, Hunt, L, Stephens, J, Waugh, R, Cameron, DD, Gray, JE (2017) Reducing stomatal density in barley improves drought tolerance without impacting on yield. *Plant Physiology* **174**, 776-787.

Jarvis, DE, Ho, YS, Lightfoot, DJ, Schmockel, SM, Li, B, Borm, TJ, Ohyanagi, H, Mineta, K, Michell, CT, Saber, N, Kharbatia, NM, Rupper, RR, Sharp, AR, Dally, N, Boughton, BA, Woo, YH, Gao, G, Schijlen, EG, Guo, X, Momin, AA, Negrao, S, Al-Babili, S, Gehring, C, Roessner, U, Jung, C, Murphy, K, Arold, ST, Gojobori, T, Linden, CG, van Loo, EN, Jellen, EN, Maughan,

PJ, Tester, M (2017) The genome of *Chenopodium quinoa*. *Nature* **542**, 307-312.

Jin, H, Dong, D, Yang, Q, Zhu, D (2016) Salt-responsive transcriptome profiling of *Suaeda glauca* via RNA sequencing. *PLoS One* **11**, e0150504.

Kanno, Y, Hanada, A, Chiba, Y, Ichikawa, T, Nakazawa, M, Matsui, M, Koshiba, T, Kamiya, Y, Seo, M (2012) Identification of an abscisic acid transporter by functional screening using the receptor complex as a sensor. *Proceedings of the National Academy of Sciences of the United States of America* **109**, 9653-8.

Kiani-Pouya, A, Rasouli, F, Bazihizina, N, Zhang, H, Hedrich, R, Shabala, S (2019) A large-scale screening of quinoa accessions reveals an important role of epidermal bladder cells and stomatal patterning in salinity tolerance. *Environmental and Experimental Botany* **168**, 103885.

Kubarsepp, L, Laanisto, L, Niinemets, U, Talts, E, Tosens, T (2020) Are stomata in ferns and allies sluggish? Stomatal responses to CO_2 , humidity and light and their scaling with size and density. *New Phytologist* **225**, 183-195.

Le Gall, H, Philippe, F, Domon, JM, Gillet, F, Pelloux, J, Rayon, C (2015) Cell wall metabolism in response to abiotic stress. *Plants* **4**, 112-66.

Lee, SJ, Kang, JY, Park, HJ, Kim, MD, Bae, MS, Choi, HI, Kim, SY (2010) DREB2C interacts with ABF2, a bZIP protein regulating abscisic acid-responsive gene expression, and its overexpression affects abscisic acid sensitivity. *Plant Physiology* **153**, 716-27.

Leonhardt, N, Kwak, JM, Robert, N, Waner, D, Leonhardt, G, Schroeder, JI (2004) Microarray expression analyses of Arabidopsis guard cells and isolation of a recessive abscisic acid hypersensitive protein phosphatase 2C mutant. *The Plant Cell* **16**, 596-615.

Leyman, B, Geelen, D, Quintero, FJ, Blatt, MR (1999) A tobacco syntaxin with a role in hormonal control of guard cell ion channels. *Science* **283**, 537-40.

Li, W, Xu, G, Alli, A, Yu, L (2018) Plant HAK/KUP/KT K^+ transporters: function and regulation. *Seminars in Cell & Developmental Biology* **74**, 133-141.

Libault, M, Chen, S (2016) Editorial: plant single cell type systems biology. *Frontiers in Plant Science* **7**, 35.

Lin, CC, Kao, CH (2002) Osmotic stress-induced changes in cell wall peroxidase activity and hydrogen peroxide level in roots of rice seedlings. *Plant Growth Regulation* **37**, 177-184.

Livak, KJ, Schmittgen, TD (2001) Analysis of relative gene expression data using real-time quantitative PCR and the 2(T)(-Delta Delta C) method. *Methods* **25**, 402-408.

Love, MI, Huber, W, Anders, S (2014) Moderated estimation of fold change and dispersion for RNA-seq data with DESeq2. *Genome Biology* **15**, 550.

Manaa, A, Goussi, R, Derbali, W, Cantamessa, S, Abdelly, C, Barbatoc, R (2019) Salinity tolerance of quinoa (*Chenopodium quinoa* Willd) as assessed by chloroplast ultrastructure and photosynthetic performance. *Environmental and Experimental Botany* **162**, 103-114.

Marom, Z, Shtein, I, Bar-On, B (2017) Stomatal opening: the role of cell-wall mechanical anisotropy and its analytical relations to the bio-composite characteristics. *Frontiers in Plant Science* **8**, 2061.

Nieves-Cordones, M, Caballero, F, Martinez, V, Rubio, F (2012) Disruption of the *Arabidopsis thaliana* inward-rectifier K^+ channel AKT1 improves plant responses to water stress. *Plant & Cell Physiology* **53**, 423-32.

Obulareddy, N, Panchal, S, Melotto, M (2013) Guard cell purification and RNA isolation suitable for high-throughput transcriptional analysis of cell-type responses to biotic stresses. *Molecular Plant-Microbe Interactions* **26**, 844-849.

Oh, DH, Barkla, BJ, Vera-Estrella, R, Pantoja, O, Lee, SY, Bohnert, HJ, Dassanayake, M (2015) Cell type-specific responses to salinity - The epidermal bladder cell transcriptome of *Mesembryanthemum crystallinum*. *New Phytologist* **207**, 627-44.

Qi, JS, Song, CP, Wang, BS, Zhou, JM, Kangasjarvi, J, Zhu, J-K, Gong, ZZ (2018) Reactive oxygen species signaling and stomatal movement in plant responses to drought stress and pathogen attack. *Journal of Integrative Plant Biology* **60**, 805-826.

Richardson, LG, Torii, KU (2013) Take a deep breath: peptide signalling in stomatal patterning and differentiation. *Journal of Experimental Botany* **64**, 5243-51.

Ruiz, KB, Maldonado, J, Biondi, S, Silva, H (2019) RNA-seq analysis of salt-stressed versus non salt-stressed transcriptomes of *Chenopodium quinoa* Landrace R49. *Genes* **10**, 1042.

Schwacke, R, Ponce-Soto, GY, Krause, K, Bolger, AM, Arsova, B, Hallab, A, Gruden, K, Stitt, M, Bolger, ME, Usadel, B (2019) MapMan4: a refined protein classification and annotation framework applicable to multi-omics data analysis. *Molecular Plant* **12**, 879-892.

Shabala, S (2013) Learning from halophytes: physiological basis and strategies to improve abiotic stress tolerance in crops. *Annals of Botany* **112**, 1209-21.

Tian, T, Liu, Y, Yan, H, You, Q, Yi, X, Du, Z, Xu, W, Su, Z (2017) agriGO v2.0: a GO analysis toolkit for the agricultural community, 2017 update. *Nucleic Acids Research* **45**, 122-129.

Wang, RS, Pandey, S, Li, S, Gookin, TE, Zhao, Z, Albert, R, Assmann, SM (2011) Common and unique elements of the ABA-regulated transcriptome of Arabidopsis guard cells. *BMC Genomics* **12**, 216.

Wang, T, Chen, Y, Zhang, M, Chen, J, Liu, J, Han, H, Hua, X (2017) Arabidopsis amino acid permease1 contributes to salt stress-induced proline uptake from exogenous sources. *Frontiers in Plant Science* **8**, 2182.

Wilson, RS, Nairn, AC (2018) Cell-type-specific proteomics: a neuroscience perspective. *Proteomes* **6**, 51.

Xu, C, Jiao, C, Sun, H, Cai, X, Wang, X, Ge, C, Zheng, Y, Liu, W, Sun, X, Xu, Y, Deng, J, Zhang, Z, Huang, S, Dai, S, Mou, B, Wang, Q, ., Fei, Z, Wang, Q (2017) Draft genome of spinach and transcriptome diversity of 120 Spinacia accessions. *Nature Communications* **8**, 15275

Yaaran, A, Negin, B, Moshelion, M (2019) Role of guard-cell ABA in determining steady-state stomatal aperture and prompt vapor-pressure-deficit response. *Plant Science* **281**, 31-40.

Zhang, FY, Lu, X, Lv, ZY, Zhang, L, Zhu, MM, Jiang, WM, Wang, GF, Sun, XF, Tang, KX (2013) Overexpression of the Artemisia orthologue of ABA receptor, AaPYL9, enhances ABA sensitivity and improves artemisinin content in *Artemisia annua* L. *PLoS One* **8**, e56697.

Zhu, M, Jeon, BW, Geng, S, Yu, Y, Balmant, K, Chen, S, Assmann, SM (2016) Preparation of epidermal peels and guard cell protoplasts for cellular,

electrophysiological, and -Omics assays of guard cell function. *Methods in Molecular Biology* **1363**, 89-121.

Zörb, C, Mühling, KH, Kutschera, U, Geilfus, CM (2015) Salinity stiffens the epidermal cell walls of salt-stressed maize leaves: is the epidermis growth-restricting? *PLoS One* **10,** e0118406.

Chapter 7: General Discussion

Stomata are mediators of gas exchange between the plant and atmosphere. While representing only between 0.5 to 5% of total leaf surface, they are responsible for over 95% of all water loss by the leaf (Hetherington and Woodward 2003a). This important role in water loss make stomata key players in water use efficiency and global water cycle. Thus, functions and physical attributes of stomata and the impacts of environmental factors on stomata are very important.

Salinity is a major abiotic stress that affects crop productivity globally (Golldack *et al.* 2011) through ion imbalance, hyperosmotic stress and oxidative damage (Flowers and Colmer 2008). The above constraints affect stomata operation (Yu and Assmann 2016). In this context, the effects of salt stress on traditional plants may be different from their halophytic counterparts. It has been argued that halophytes have evolved numerous adaptation characteristics that enable then to efficiently deal with saline conditions (Flowers and Colmer 2008; Hedrich and Shabala 2018). For example, salinity stress reduces stomatal conductance that in turn results in reduction of photosynthesis and transpiration rates in glycophytes, while these parameters are less affected by salt stress in halophytes, and the latter have shown better stomatal performance when grown in saline soils (Shabala 2013; Chaves *et al.* 2016; Hedrich and Shabala 2018)

During the past decades, significant advances have been made in our understanding of stomata operation in glycophytes however, less information is available about mechanisms underlying stomatal kinetics in halophytes, particularly under salinity stress (Hedrich and Shabala 2018). Hence, a comparative analysis of effects of salt stress in glycophytes and halophytes may improve our understanding of adaptive strategies of halophytes and be an important step in improving abiotic stress tolerance in traditional crops.

The comparative physiological study of glycophytes and halophytes has revealed that there were significant differences between these plant species. Reduction in stomatal conductance in halophytes occurred in a dose-dependent manner; nevertheless, photosynthetic rates remained constant or were higher at the medium levels of salinities. This study showed that the superiority of halophytes in

terms of stomatal function may be partly due to the faster stomatal movements in these species. The results of this investigation showed that the speed of stomatal response to light and dark was species-specific, with the highest values in the cultivated barley and sea barley and the lowest in sugar beet and sea beet. Halophytes exhibited a higher speed of stomatal opening and closure in response to light or dark fluctuations. Fast stomatal responses to internal signals and environmental factors may be essential for synchronization of photosynthetic and stomatal conductance responses, thus optimizing water use efficiency under changing conditions. The summary of some important differences identified between halophytes and glycophytes is demonstrated in Figure 7.1.

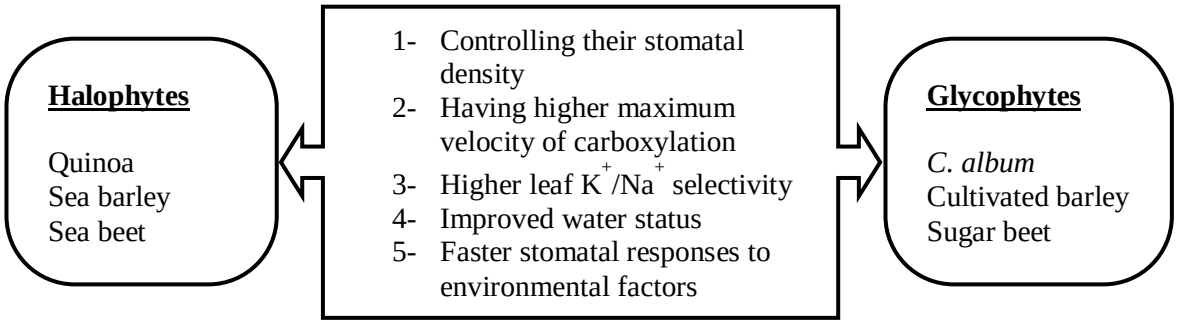

Fig. 7.1 The summary of differences between halophytes and glycophyes based on several physiological measurements

Given the fact that omics studies provide a comprehensive picture of the biological molecules that form an organism, tissue or cell (Horgan and Kenny 2011), application of these technologies at single-cell-type level could provide some valuable information. However, single cells are not easily available in higher plants and obtaining sufficient quantities of high-quality cells such as GCs could be a challenge for omics analysis. In this study, to be able to apply omics-based approaches in stomatal function studies, we developed protocols for mechanical isolation of GC-enriched epidermal peels. Although available GC-enriched epidermal fragments method has been applied in a few previous studies, these protocols were not successful under saline conditions requiring appropriate changes to generalise this method for diverse growth conditions as well as plant species. In this work, some important modifications were devised based on the GC-enriched

epidermal fragments method of Arabidopsis involving mesh size, blending time, number of runs and basic solution.

Also, no direct experimental evidence has yet been provided to test the quality and purity of GC epidermal fragments until now. Our work provides such evidence for the suitability of mechanically isolated GC epidermal fragments method for omics studies. The results proved a wide range of proteins as well as suitability of RNA integrity for gene expression analysis. For example, transcriptional levels of several GC-specific genes such as *MYB60*, *FAMA*, *ICE1*, *SLAC1* and *PP2CA* were quantified in both leaf and GC samples. A high abundance of transcripts of these genes was observed in GCs compared with those in the leaf. Thus, isolated GCs were enriched in GC specific genes suggesting suitability of this isolation approach for molecular studies. Given the importance of the GC protoplast isolation method as the most practiced approach to study GC biology (Yao *et al.* 2018a) our evaluation shows that the GC-enriched epidermis method has more advantages than "protoplasting" for GC isolation and stomatal studies.

After successful validation of our GC isolation method and given the importance of proteomics approach in understanding of molecular mechanisms underlying stomatal function under saline conditions, a proteomics investigation was undertaken to analyse protein profile of sugar beet GC under saline and non-saline conditions. The results revealed that of the 2088 proteins identified in sugar beet GCs, 82 were differentially regulated by salt treatment. Based on GO enrichment analysis and protein classification, these proteins were involved in lipid metabolism, cell wall modification, ATP biosynthesis, and signalling. Among the significant differentially abundant proteins, several proteins classified as "stress proteins" were upregulated, including non-specific lipid transfer protein, chaperone proteins, heat shock proteins, inorganic pyrophosphatase 2, responsible for energized vacuole membrane for ion transportation. Moreover, several antioxidant enzymes such as peroxide, superoxidase dismutase were highly upregulated. Our studies also revealed that cell wall proteins play important role in stomata function. Cell wall proteins detected in GCs in this study provided some evidence that GC walls were more flexible in response to salt stress. As an example of this finding, proteins such as L-ascorbate oxidase that were constitutively high under both

control and high salinity conditions may contribute to the ability of sugar beet GCs to adapt to salinity by mitigating salinity-induced oxidative stress.

We then applied proteomics analyses to epidermal fragments enriched in GCs isolated from the halophytic *Chenopodium quinoa* (Wild.) species grown under saline conditions. In this investigation 2471 proteins were identified in total, of which 36% were differentially regulated by salinity stress in GC. These differently expressed proteins belong to various biological functions such as signalling molecules, enzyme modulators, transcription factors and oxidoreductases. In addition, several proteins involved in responses were found to be highly abundant in GC following salinity treatment, including protein desiccation-responsive protein 29B (50-fold), osmotin-like protein OSML13 (13-fold), PLAT domain-containing protein 3-like (8-fold), and dehydrin ERD14 (8-fold). These findings point out at quinoa as a halophyte employing specific modes of responses to salt at the GC level. The results also revealed ten upregulated proteins related to GO of response to ABA such as, aspartic protease in guard cell1, phospholipase D, plastid-lipid-associated protein. In addition, seven proteins in sucrose-starch pathway were upregulated in the GC in response to salinity stress. Furthermore, accumulation of amino acids tryptophan and L-methionine synthase was observed in the GC under salt stress. Exogenous application of tryptophan, L-methionine and sucrose resulted in reduction in stomatal aperture and conductance, which could be advantageous for plants under salt stress.

We found 20 common differentially abundant protein between sugar been and quinoa (10 proteins upregulated and 10 down regulated). Proteins aspartic protease in guard cell 1, and non-specific lipid-transfer showed enhanced abundance while catalase and cationic peroxidase showed lower abundances in GCs of both salt-treated plants. Lower levels of catalase may be necessary in the guard in saline conditions as H_2O_2 functions as a signalling molecule in the guard cell and induces stomatal closure in response to high salinity stress. Moreover, some proteins involved in mitigation of oxidative stress such L-ascorbate oxidase were presented at elevated levels under non-stress conditions in both species suggesting the constitutive accumulation of those proteins in the guard cells of the halophyte quinoa and the salt-tolerant sugar beet that can confer augmented tolerance to GCs of both species when exposed to salt stress. The salinity treatment

in quinoa exhibited the larger number of differentially abundant proteins compared with sugar beet suggesting that modulation of more proteins is required for conferring salt-tolerance in quinoa. Comparison of differentially expressed proteins in salt-responsive proteomes of guard cells of quinoa and sugar beet based on their biological function revealed that in quinoa consistent with sugar beet the largest single group of proteins included those involved in protein biogenesis and disposal (e.g. ribosomal subunits, molecular chaperones, and proteasomal subunits) and the next most abundant protein categories were identified as "stress". However, the top proteins according to overall abundance in sugar beet and quinoa GCs were dissimilar and they were different from what is previously reported in the other species such as Arabidopsis (Zhao et al, 2008). Further research is required to obtain insight into role of those top proteins in guard cells of quinoa and sugar beet. Mutations in the genes encoding those proteins can confirm their essential roles in the guard cells.

Although stomata are the main gaseous gates in plants, very few transcriptome studies have been conducted on GCs. Due to the presence of large number of gene families in plants, a single cell-level gene expression analysis provides an effective approach to identify the gene families and pathways that are probably specific to that individual cells (Leonhardt *et al.* 2004a). For this reason, this project then applied transcriptome analysis to decipher more molecular analysis of stomatal function.

The RNA-sequencing analysis of mechanically prepared guard cell-enriched epidermal fragments of quinoa and spinach demonstrated that these two plant species had similar responses where in both plants salt-responsive genes were mainly related to biological processes such as protein metabolism, secondary metabolites, signal transduction, and transportation system. On the other hand, genes related to ABA signalling and ABA biosynthesis were strongly induced in quinoa GCs. Furthermore, GCs in quinoa as a halophytic plant showed higher expression levels of amino acids, proline, sugars, sucrose and potassium transporters under saline condition.

This study also shown that one of the main transcriptomic differences between quinoa and spinach was occurred at the cell wall where spinach as a traditional crop plant developed more rigid guard cell wall while quinoa as a

halophyte had flexible cell wall upon exposure to salt stress. These differences resulted in higher stomatal movements in response to light and dark in quinoa. Furthermore, genes involving in inhibition of stomata development and differentiation were highly expressed by salt in quinoa but not in spinach. This resulted in lesser stomatal density and index in quinoa leaf while salinity did not alter stomatal formation in the epidermal tissue in spinach (Figure 7.2). Overall, this comparative transcriptomic analysis revealed that quinoa GCs had better salt-adaptability responses compared to spinach. Thus, it could be concluded from this investigation that the superior GC function in quinoa was achieved through fine modulation of transporters, cell wall modification and control of stomatal development which were resulted in high K^+/Na^+ balance, smaller stomatal conductance and more resilience of stomata in response to environmental stimuli.

Omics technologies such as transcriptomics and proteomics studies provide a global and comprehensive picture of biological molecules of a cell, tissue or organism of purpose (Horgan and Kenny 2011). These technologies could be used for detection of genes, proteins and peptides in a specific biological sample making this possibility to exploring proteins and genes involved in various biological processes (Wang *et al.* 2009a; Urano *et al.* 2010). Thus, such analyses are considered to be ideal tools to discover mechanisms that controls biological process at molecular level (Wang *et al.* 2009a; Guo *et al.* 2019).

Following the generation of numerous genetic resources and the application of proteomics and RNA-sequencing analysis, knowledge of guard cell metabolism has improved considerably, nevertheless, several basic questions concerning how guard cells metabolism tune in response to environmental conditions such as salinity stress have remained unanswered. In proteomics and transcriptomic studies of quinoa, seven proteins in the sucrose-starch pathway were upregulated in the guard cells in response to salinity stress, sucrose transporter (SUC3) and sugar transporters are also highly upregulated by salt in guard cells. Information regarding kinetics, regulation and expression of sugar transporters in guard cells is still limited while the role of sugars in stomata regulations have been matter of debates (Granot and Kelly, 2019; Lawson and Matthews, 2020). In our study exogenous sucrose induced stomata closure. However, there is evidence showing that sucrose and other sugars supported stomatal opening. The null mutants of

sucrose transporter, sugar transporters and genes in sucrose/starch pathway will provide critical information of sucrose and sugars functions in the stomatal movement under salt stress. To achieve insight into the function of different genes expression in the guard cells, that would be useful to create transgenic plants that overexpress sugars under control of guard cell- specific promoters and comprehensive study of associated phenotypes in guard cells and whole plant. Source of sugars in the guar cells and the mechanisms by which sucrose and other sugars enter guard cells are also important and require to be explored in future experiments.

With the increasing water deficiency, breeding crops with reduced stomatal density is one of the top priorities in agriculture. In our study, exposure to 250 mM NaCl, stimulates the activity of EPF1 (Chapter 6) and causes the reduction of stomatal density in halophyte quinoa, thus reducing stomatal conductance. However, this strategy is not common in all halophytic species. As we observed that stomatal density in halophyte sea beet (Chapter 2) did not change dramatically with imposing salinity. Moreover, reducing stomatal density is often associated with a penalty in carbon assimilation. Thus, this approach that pose a trade-off between carbon uptake and water saving creates a greater challenge but is still favourable under saline conditions. Accelerating the kinetics of stomatal reaction to internal and external stimuli could be used to promote carbon uptake and maintain plant water status when a demand for carbon is relatively at lower level (Papanatsiou *et al.* 2019). In our study, stomatal speed in response to light and darkness were higher in halophytes than glycophytes. Comparative transcriptomic of quinoa and spinach demonstrated that genes involved in guard cell wall are important in speed of stomatal reactions. Stomata movements require rapid uptake and efflux of inorganic ions such as K^+ and Cl^- that is mediated by a range of plasma membrane and tonoplast-based channels and transporters. In our proteomics analysis on quinoa, we found out that a *pyrophosphatase-driven proton pump* gene, capable of energizing the vacuolar membrane, was upregulated 85-fold by salt stress in quinoa guard cells.

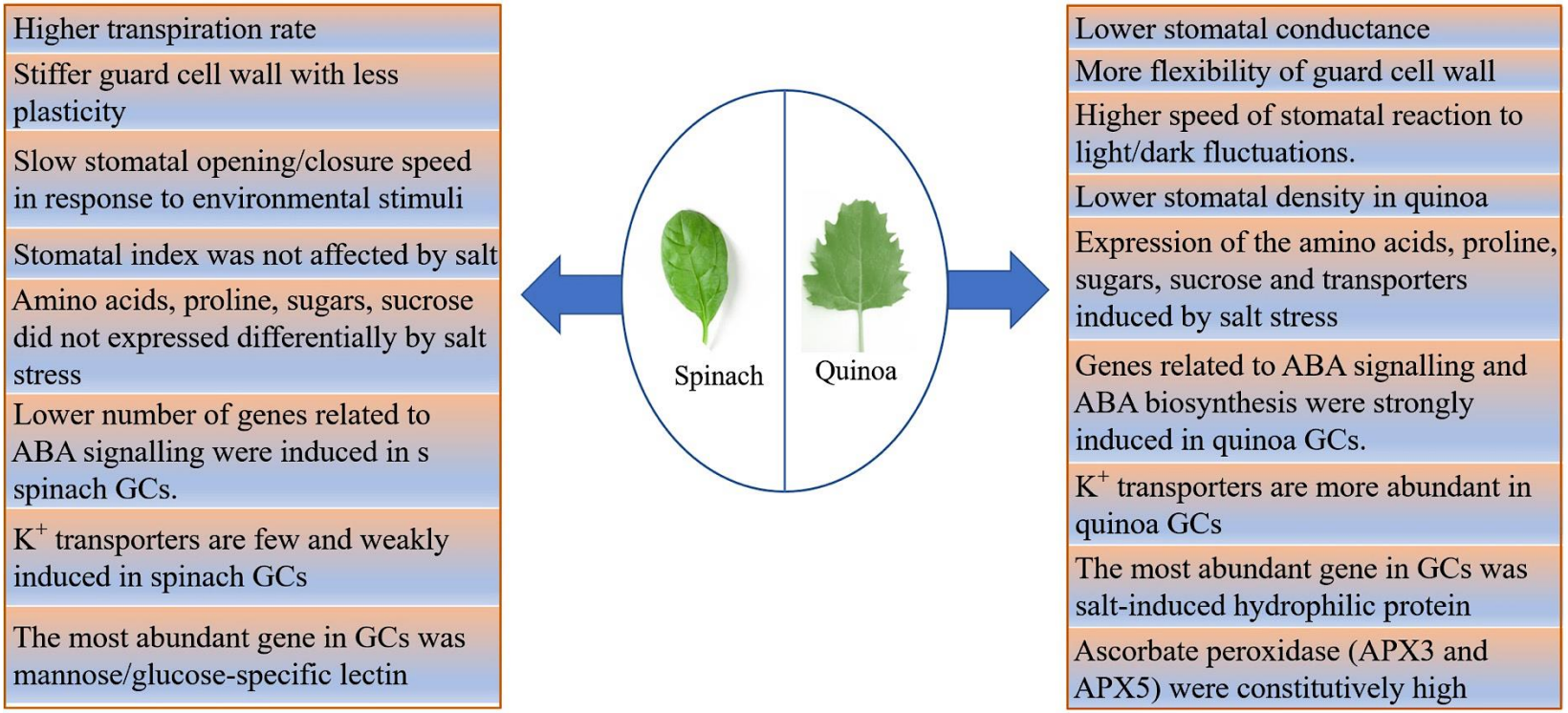

Fig. 7.2 The summary of differences between quinoa guard cells and spinach guard cells based on transcriptome analysis and physiological parameters

Recent literature reports suggested that overexpression of halophytic PPase in Arabidopsis have accelerated stomatal movement. Rapid stomatal movement in response to stimuli can result in more than 2-fold increase in biomass without cost in water use by the plant (Papanatsiou *et al.* 2019). Therefore, *PPase* can potentially be used in gene editing programs for improving stomatal kinetics to increase WUE without penalty in CO_2 assimilation.

Manipulating the native pumps and ion channels in guard cell using optogenetics (use of light-sensitive ion channels) could affect both photosynthesis and stomatal conductance. Recently, a synthetic channel (BLINK1) was expressed in the guard cells to increase ion flux to drive turgor. BLINK1 enhanced stomatal kinetics and produced a greater biomass without cost in water (Papanatsiou *et al.* 2019). It is noteworthy to mention that application of omics studies such as proteomics and transcriptome analysis which may result in identification of new genes or proteins in stomata function can be further investigated using optogenetics technology. This technique could be used as a tool for manipulating channels in the guard cells to promote plant tolerance to salinity stress in future study on stomata operations in different crops.

On the other hand, genome editing, and synthetic biology approaches have now become a routine procedure in many research projects. Genome editing technologies that enable scientists to change an organism's DNA, provide this opportunity to add, remove, or altered genetic material at particular locations in the genome. By applying omics approach and identification of new genes or proteins in stomata function and then changing the responsive genes with the aim of producing plants with higher stomata function there would be opportunity to make better crop plants that resist environmental stresses such as salinity.

For cell specific expression analysis such as our guard cells study, a rich research platform is required. In our study, an obstacle to progress with quinoa was the poor availability of functional genomics tools. Genome sequences of quinoa has been recently published (Jarvis *et al.* 2017) which is a large step in plant molecular biology study but there are just limited available mutant populations for detailed study of individual genes and no transgenic lines for analysing cell specific expression. CRISPR-Cas9 techniques could be used as a powerful tool for gene editing and generating transgenic quinoa for further salinity research; however, this

technique is efficient for model plant Arabidopsis but has to be optimized for quinoa. Alternatively, some other techniques such as RNA silencing can be used to regulate gene expression, thus giving an opportunity to explore the role of some genes in the guard cells.

Identifying shared differentially expressed genes between two various species in response to abiotic stress facilitate the understanding of evolutionarily conserved transcriptional responses and could identify polymorphisms responsible for phenotypic variations across species (Zhang *et al.* 2017). RNA sequencing techniques has overcome the challenges associated with traditional microarray approaches. RNA-seq techniques allow us to quantify and to compare gene expression levels among any combination of species (Romero *et al.* 2012). However, identifying interspecies changes in gene regulation is still challenging specially when they are not closely relatives. Currently, there is no advanced methods for a comprehensive comparison between species. The available approaches are far less developed. One approach is mapping RNA-seq data from both species to a common reference genome (Burkart-Waco *et al.* 2015).

In our study for quinoa and spinach comparison in transcriptomic analysis of GCs, protein BLAST analysis was performed using the top hit (e-value < 10^{-5}) from each species against the Arabidopsis. Genomes of quinoa and spinach have been sequenced but their genomes have not been well-annotated. Therefore, we relied on Arabidopsis as to its genome comprehensively has been annotated. This model plant could be used as reference for obtaining insight into function of genes in other plant species (Oh *et al.* 2015) as well as interspecies comparisons in gene regulation. Identifying syntenic orthologs between species is another approach that has also been employed for cross-species comparisons of cold-responsive transcriptional regulation between maize and sorghum, two species which are closely related (Zhang *et al.* 2017). One of the challenges associated with comparing multiple species with independently sequenced and assembled references genome is the baseline expression levels of orthologous genes can diverge significantly which creates a statistical challenge (Zhang *et al.* 2017). Normalization of RNA-seq data with different species is more complex than that with same species. In the process of detecting differentially expressed genes, the expression levels of orthologous genes must be comparable between different

species, and a robust approach is required to make the normalized (Zhou *et al.* 2019).

Given the fact that cellular responses to environmental factors are regulated by a complex interplay of proteins, RNA and DNA, we used differentially regulated mRNA and proteins to analyse the correlation between protein abundances and cellular mRNA levels in response to salt stress. We found low correlation when we compared proteins abundance and mRNA expressions (RNA-sequencing) for quinoa GC. This low correlation made it difficult to integrate RNA-seq and protein data obtained from quinoa GC. Recent studies have shown that the correlation between protein and mRNA expressions has been low mainly due to post-translational regulation (Koussounadis *et al.* 2015).

In our study, we exposed plants to moderate salinity stress (250 mM NaCl) for three weeks which is considered long-term stress in proteomics and transcriptome studies. Prolonged exposure of plants to salinity stress gives us insight into understanding pathways, genes and proteins which are important in acclimation process of plants to salt stress. Nevertheless, short-term salt stress that involve multiple time points, provide a comprehensive picture on the modulation in the expression profiles of early and late responsive genes in saline conditions (Liu *et al.* 2019) and enables one to identify important pathways and connections of gene expressions. Protein turnover and degradation in specific proteins of interest can also be navigated over the timeframe of measurements (Li *et al.* 2017). Moreover, some cellular reactions such as phosphorylation in response to a stimulus occurs quite fast (in the second-to-minute time regime) (Blazek, *et al.* 2015). Therefore, a time resolution of a few seconds for investigating cell-signaling events is required. Phosphorylation plays critical roles in the signal transduction pathways in guard cells (Zhang *et al.* 2014) and could become a target of investigation on guard cells in future studies through phosphoproteomics analysis of guard cells in response to various stimuli including salt stress.

7.1 References

Blazek, M, Santisteban, TS, Zengerle, R, Meier, M (2015) Analysis of fast protein phosphorylation kinetics in single cells on a microfluidic chip. *Lab Chip* **15**, 726-34.

Burkart-Waco, D, Ngo, K, Lieberman, M, Comai, L (2015) Perturbation of parentally biased gene expression during interspecific hybridization. *PLoS One* **10**, e0117293.

Chaves, MM, Costa, JM, Zarrouk, O, Pinheiro, C, Lopes, CM, Pereira, JS (2016) Controlling stomatal aperture in semi-arid regions-The dilemma of saving water or being cool? *Plant Science* **251**, 54-64.

Flowers, TJ, Colmer, TD (2008) Salinity tolerance in halophytes. *New Phytologist* **179**, 945-63.

Golldack, D, Luking, I, Yang, O (2011) Plant tolerance to drought and salinity: stress regulating transcription factors and their functional significance in the cellular transcriptional network. *Plant Cell Reports* **30**, 1383-91.

Guo, SM, Tan, Y, Chu, HJ, Sun, MX, Xing, JC (2019) Transcriptome sequencing revealed molecular mechanisms underlying tolerance of *Suaeda salsa* to saline stress. *PLoS One* **14**, e0219979.

Granot, D, Kelly, G (2019) Evolution of guard-cell theories: The story of sugars. *Trends in Plant Science* **24**, 507-518.

Hedrich, R, Shabala, S (2018) Stomata in a saline world. *Current Opinion in Plant Biology* **46**, 87-95.

Hetherington, AM, Woodward, FI (2003) The role of stomata in sensing and driving environmental change. *Nature* **424**, 901-8.

Horgan, R, Kenny, LC (2011) Omic technologies: genomics, transcriptomics, proteomics and metabolomics. *The Obstetrician & Gynaecologist* **13**, 189-195.

Jarvis, DE, Ho, YS, Lightfoot, DJ, Schmockel, SM, Li, B, Borm, TJ, Ohyanagi, H, Mineta, K, Michell, CT, Saber, N, Kharbatia, NM, Rupper, RR, Sharp, AR, Dally, N, Boughton, BA, Woo, YH, Gao, G, Schijlen, EG, Guo, X, Momin, AA, Negrao, S, Al-Babili, S, Gehring, C, Roessner, U, Jung, C, Murphy, K, Arold, ST, Gojobori, T, Linden, CG, van Loo, EN, Jellen, EN,

Maughan, PJ, Tester, M (2017) The genome of *Chenopodium quinoa*. *Nature* **542**, 307-312.

Koussounadis, A, Langdon, SP, Um, IH, Harrison, DJ, Smith, VA (2015) Relationship between differentially expressed mRNA and mRNA-protein correlations in a xenograft model system. *Scientific Reports* **5**, 10775.

Lawson, T, Matthews, J (2020) Guard cell metabolism and stomatal function. *Annual Review of Plant Biology* PP71CH22.

Leonhardt, N, Kwak, JM, Robert, N, Waner, D, Leonhardt, G, Schroeder, JI (2004) Microarray expression analyses of Arabidopsis guard cells and isolation of a recessive abscisic acid hypersensitive protein phosphatase 2C mutant. *The Plant Cell* **16**, 596-615.

Li, L, Nelson, CJ, Trosch, J, Castleden, I, Huang, S, Millar, AH (2017) Protein Degradation Rate in Arabidopsis thaliana Leaf Growth and Development. *Plant Cell* **29**, 207-228.

Liu, A, Xiao, Z, Li, MW, Wong, FL, Yung, WS, Ku, YS, Wang, Q, Wang, X, Xie, M, Yim, AK, Chan, TF, Lam, HM (2019) Transcriptomic reprogramming in soybean seedlings under salt stress. *Plant Cell Environ* **42**, 98-114.

Oh, DH, Barkla, BJ, Vera-Estrella, R, Pantoja, O, Lee, SY, Bohnert, HJ, Dassanayake, M (2015) Cell type-specific responses to salinity - the epidermal bladder cell transcriptome of *Mesembryanthemum crystallinum*. *New Phytologist* **207**, 627-44.

Papanatsiou, M, Petersen, J, Henderson, L, Wang, Y, Christie, JM, Blatt, MR (2019) Optogenetic manipulation of stomatal kinetics improves carbon assimilation, water use, and growth. *Science* **363**, 1456-1459.

Romero, IG, Ruvinsky, I, Gilad, Y (2012) Comparative studies of gene expression and the evolution of gene regulation. *Nat Rev Genet* **13**, 505-16.

Shabala, S (2013) Learning from halophytes: physiological basis and strategies to improve abiotic stress tolerance in crops. *Annals of Botany* **112**, 1209-21.

Urano, K, Kurihara, Y, Seki, M, Shinozaki, K (2010) 'Omics' analyses of regulatory networks in plant abiotic stress responses. *Current Opinion in Plant Biology* **13**, 132-8.

Wang, XC, Fan, PX, Song, HM, Chen, XY, Lil, XF, Li, YX (2009) Comparative proteomic analysis of differentially expressed proteins in shoots of *Salicornia europaea* under different salinity. *Journal of Proteome Research* **8**, 3331-3345.

Yao, XH, Zhao, WC, Yang, R, Wang, JL, Zhao, FK, Wang, SH (2018) Preparation and applications of guard cell protoplasts from the leaf epidermis of *Solanum lycopersicum*. *Plant Methods* **14**, 26.

Yu, Y, Assmann, SM (2016) The effect of NaCl on stomatal opening in Arabidopsis wild type and agb1 heterotrimeric G-protein mutant plants. *Plant Signaling & Behavior* **11**, e1085275.

Zhang, Y, Ngu, DW, Carvalho, D, Liang, Z, Qiu, Y, Roston, RL, Schnable, JC (2017) Differentially Regulated Orthologs in Sorghum and the Subgenomes of Maize. *The Plant Cell* **29**, 1938-1951.

Zhou, Y, Zhu, J, Tong, T, Wang, J, Lin, B, Zhang, J (2019) A statistical normalization method and differential expression analysis for RNA-seq data between different species. *BMC Bioinformatics* **20**, 163.

Supplemental Figures

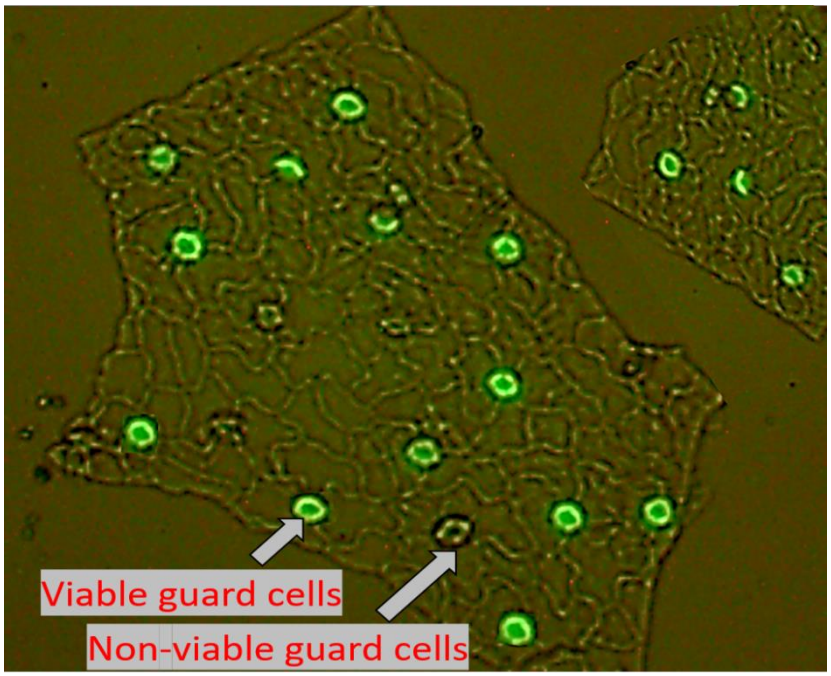

Supplemental Fig. S3.1 Fluorescent signal only detectable in viable GCs, not in remaining pavement and non-viable guard cells.

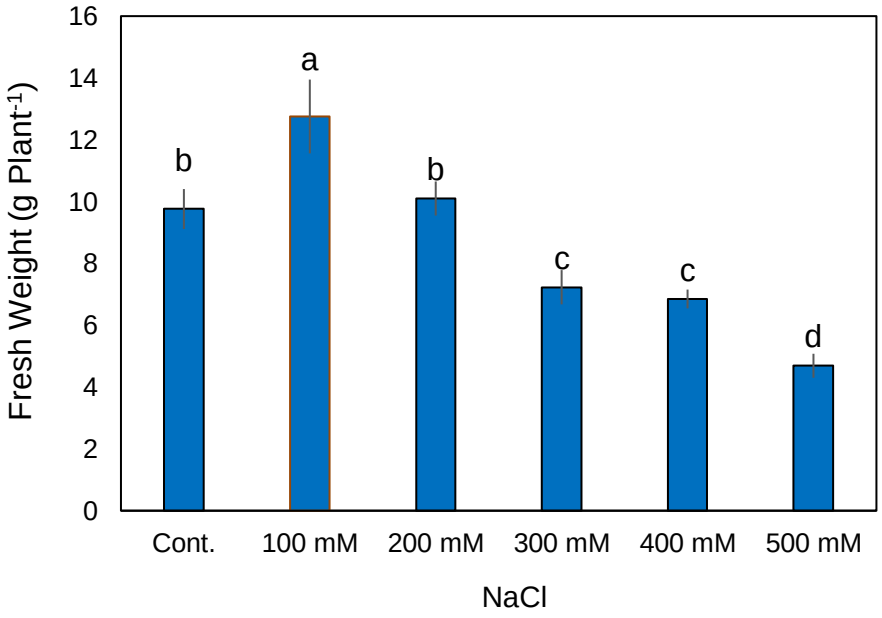

Supplemental Fig. S4.1 The fresh weight response of sugar beet to varying external concentration of NaCl. Plants were grown under control and saline (100, 200, 300, 400, and 500 NaCl) conditions. Mean ± SE (n = 5). Data labelled with different lower-case letters are significantly different at $P < 0.05$.

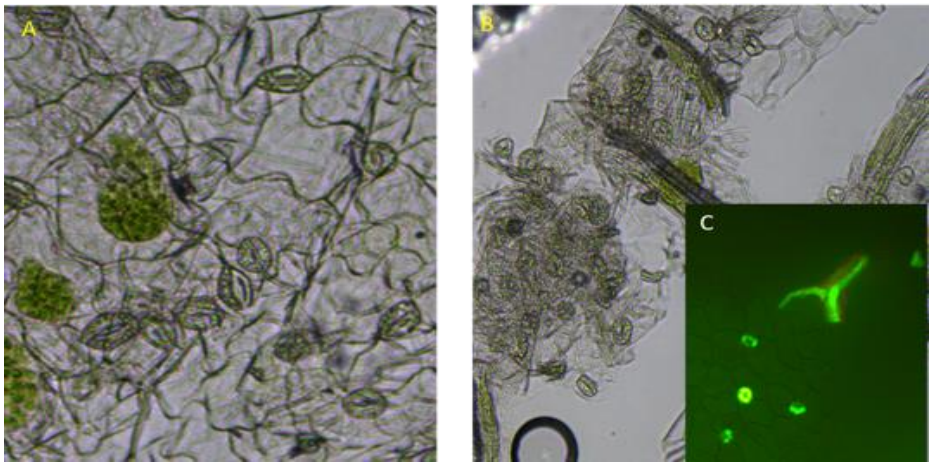

Supplemental Fig. S4.2 Typical examples of contaminated GC samples with mesophyll (A) and vascular tissue (B and C).

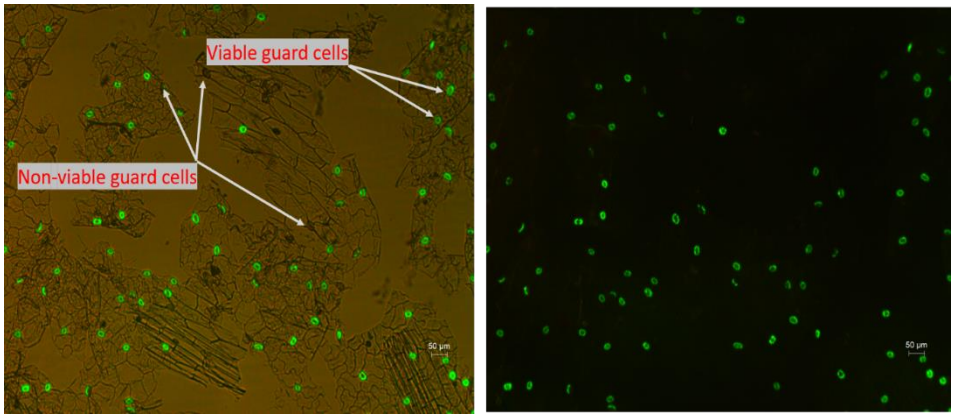

Supplemental Fig. S4.3 Viability test for Guard cell-enriched epidermal peels. Fluorescein diacetate (FDA) staining assay was used for measuring the cell viability. Epidermal peels collected after grinding process show the fluorescent signal only detectable in guard cells, not in remaining pavement or mesophyll cells.

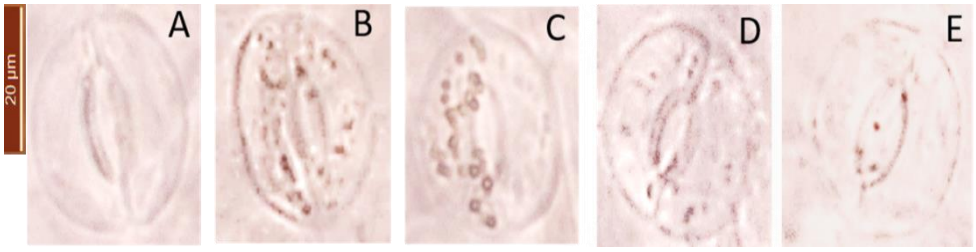

Supplemental Fig. S4.4 DAB staining (raw images) for detection of H_2O_2 in guard cell under control (A) and 300 mM NaCl (B-E). B: control (zero ascorbic acid, AsA); C: 150 mg L^{-1} AsA; D: 300 mg L^{-1} AsA; E: 450 mg L^{-1} AsA. Formation of brown precipitates showed the generation of H_2O_2 by guard cells. One (of 15) typical images is shown.

Supplemental Tables

Supplemental Table S3.1 Primers used in quantitative RT-PCR in quinoa, sugar beet and spinach guard cells.

Gene name	Gene ID	Forward primer	Reverse primer
ABI5	AUR62028537	GCAGGCCCTGGATGAAATTG	CTTGAGCTCTCTGTGCCCTG
DREB2C	AUR62030763	ACATGCAACCAACAGCTTCC	GCTCCCATTACTCGAATGTGTC
NCED5	AUR62002735	CTTCACGGACATTCGGGGAT	ATGTTAGCTGACCTTGGTAGGG
LTI65	Bv3_055530_kzfa	TGCGTCAGATGTTACATGGGT	GTTGAAAATCGAGTCGGGCG
PS2	Spo26520	ATCAGCTTACGATGCTGGGT	TGTGTTGTCCCCTTCATTGGT

Supplemental Table S4.3 Primer pairs for quantitative RT-PCR for sugar beet guard cells

Name of protein		Primer sequence
Actin (Reference gene)	F*	TAAACCGAGATGGCTGATGC
	R*	ATACTTGGGAAGACAGCCCT
XP_010690044.1: inorganic pyrophosphatase 2	F	TGATGCCGGGTGTGATTTGC
	R	TCGCAACCATGAGGAGTAGTTGT
XP_010685378.1: cell wall / vacuolar inhibitor of fructosidase 1	F	AGCTCCAAGGCTGCTGACTC
	R	GGGTCTTCCGGGTCAAGTCC
XP_010682183.1: choline monooxygenase	F	TCGAGATGGTCAGGGCGAAC
	R	TTGCTTTGCTGGCTTTGGCG
XP_010673593.1: transcription factor bHLH130	F	TGAGGACTGGTGGTGGTGTG
	R	TGGCGAAAAATCCAGCAGGG
XP_010675238.1: sucrose synthase 7 isoform X3	F	GACAACAGTAAGACCGCAGCC
	R	TTAAGCCCCGAACCACCTCTG
XP_010686277.1: sugar carrier protein C	F	TGGGGTCGTAGGTTCCTTTTCC
	R	TGACCATGCAAAGGCCGAGA
XP_010680669.1: protein SPIRAL1-like 1	F	CCAGTTGCAGATTCCCAGCC
	R	GTTGAGGGTCGATCCGTGATG

*F -forward primer; R- reverse primer

Supplemental Table S6.1 Primer pairs for quantitative RT-PCR for quinoa guard cells.

Gene ID	Gene Name	**Forward primer**	**Reverse primer**
AUR62011162	Epidermal patterning factor 1	ACACCGTTGAAATCGCGGGT	GCCTACATGGTGAGCATGAACC
AUR62018046	Cystatin B	CAAGAGGTTGCTGCTTGGGC	TCTTCATATTGCCGTCGGAAACG
AUR62033186	High affinity K+ transporter 5	TGGGTTCATGGGAACGATGCT	TAACGCGTCCTCCTTAGCCC
AUR62008354	Nitrate transporter 1:2	ACGGAGCCGAGCAGTTTGAT	TCCGAATCCCCATTGCCAGC
AUR62018405	Zinc transporter 7 precursor	TGCGCTACACCCCGATAAGG	GGCTTTTCAGGCAGACACGG
AUR62013156	White-brown complex-like protein	CGGAGATGATGACGGTGTGTG	TCACCAGGGCAGGCATAACC
AUR62011066	K^+ transporter 1	TCATCAGGAGAACCATGTCGCT	TCAACTCTCAAAGGGAAAATTCCGA
AUR62009384	MATE efflux family protein	CGCGATTGCAAGCATTGGAT	ATGGTCCGGTTCCAGTTCCC
AUR62001731	Highly ABA-induced PP2C protein 2	TTCCCTCTTTCCGACGACCAC	ACCTCTGGCTCACAGCTCAC
AUR62009227	Kinase family with leucine-rich repeat domain-containing protein	ACGGGAAGCTGTTAGGTGTTGT	CCCTGCAAAGACCACATCCC
AUR62021079	SLAC1 homologue 3	CATTGGCGTGGTGGGCTTAC	TCAAGGCCAAGGTCCGTGTT
AUR62017264	Osmotin 34	CCTATCTCCTTCAGCCCCACT	TTGGGTCGTGCAAGGGTTGTG
AUR62011055	GRAS family transcription factor	TCCGGTATCCGATATGGACGAGT	GACCCGGGCCCTAGAATATGT
AUR62037523	AMP-dependent synthetase	TGCCAAACCCCTGACAAAACC	TTAACCACCAACCCACCCGT
AUR62012310	PYR1-like 4	ACGCCATAGGGTTTCGGGTT	AGCTGCTGCATTATTATTGTCCTCT
AUR62030584	Serine/threonine protein kinase 2	GAAGCCATAAATGGTTCAAGTGCAT	GAGATTTTCACTCTCCTCCCTTGAT
AUR62000624	Calcium-dependent protein kinase 4	GAACTCCAGCAAGCCTGCATC	CCTCCCACCTTTTCCATTGCC
AUR62023953	GABA transporter 1-like	GCTCAATTAGGTCGCCGCC	TAGCCAGACAAGCGCCAAC
AUR62009628	Tonoplast intrinsic protein 1%3B3	AACATCTTGGCTGGTGGTGCC	GCAGTGGTAGACGAGGGCAG
AUR62014712	Sugar transporter 1	ATCAGTGTGGGCGCGTTACT	TCACTGGCAGCCACAAGGTC